



UNIVERSITY OF STRATHCLYDE
DEPARTMENT OF BIOMEDICAL ENGINEERING

A study on the tolerance of intermittent
hypoxia training and its effect on sensory
and motor spinal pathways

Agioula Anna Toli

2021

This thesis is submitted in fulfilment of the requirements for
the degree of Doctor of Philosophy in the Biomedical
Engineering Department, University of Strathclyde,
Glasgow.

Copyright

'This thesis is the result of the author's original research. It has been composed by the author and has not been previously submitted for examination which has led to the award of a degree.'

'The copyright of this thesis belongs to the author under the terms of the United Kingdom Copyright Acts as qualified by University of Strathclyde Regulation 3.50. Due acknowledgement must always be made of the use of any material contained in, or derived from, this thesis.'

Signed:

Date:

Art and the spinal cord

Below is a section of the Assyrian lion-hunting scenes that decorated the walls of the North Palace of the Assyrian king. This is an early illustration of spinal cord injury. It is dated 650 B.C. and portrays a dying lioness with hindlimb paralysis as a result of arrows piercing the spinal cord. It is available to see at the British Museum.



This is the spinal cord created using 21 K and 12 K gold leaf, ink and dye on stainless steel, created by Greg Dunn and Dr. Brian Edwards. It uses microetchings which are handmade lithographs that reflect light in a specific way. More on microetching fabrication can be found here: <http://www.brian-edwards.com/microetching-fabrication>



(permission to use this image from the website (<https://www.gregadunn.com/>) was granted by Greg Dunn)

Acknowledgements

I would like to express my deep sense of gratitude to my Masters and PhD supervisor, Professor Bernard Conway, for his valuable supervision and mentoring. I would also like to thank you for the wonderful experience we had at the intermittent hypoxia conference.

An utmost appreciation to the Postdoc and good friend Doctor Danial Kahani for his guidance, assistance during experiments and programming, as well as for his words of encouragement and valuable advice on professional growth.

Lastly, I would like to thank both, Professor Conway and Doctor Kahani, for your support during the COVID-19 pandemic.

Additionally, I would like to thank Stephen Murray for his advice on the design of the experimental rigs as well as for taking the time to build them and Doctor Helen Berry for sharing her knowledge on TMS.

Many thanks to Professor Philip Rowe and Doctor Craig Childs for sharing their expertise on the Vicon system and for their help with the navigation system. Also, a massive thank you to Professor Philip Rowe, Professor Jonathan Delafield-Butt and the wonderful staff at the Laboratory for Innovation in Autism for allowing me to use their Vicon laboratory.

Also, I would like to thank Magstim for sending a TMS coil for a short-term lend. Their service was very quick and helpful!

A debt of gratitude to all PhD students at the Department of Biomedical Engineering for volunteering to take part in my lengthy experiments. I very much appreciate your time, patience and contribution.

Lastly, but most importantly, a very special thank you to my incredible family and friends for their endless support.

Abstract

Intermittent hypoxia is defined as brief exposures of low oxygen concentration. It is commonly associated with a disease state known as obstructive sleep apnoea, however, a mild to moderate form can benefit patients with spinal cord injury. Studies have shown that a single exposure of intermittent hypoxia enhances the excitability of spinal connections spared following a cord injury. The enhanced excitability may last for more than an hour and during this time medical professionals can use conventional rehabilitation therapies and offer a heightened rehabilitation outcome and perhaps even speed up recovery. Nevertheless, there is a limited understanding in the tolerance of the intermittent hypoxia protocol given to spinal cord injury patients and its effects on spinal pathways. The purpose of this thesis was to go back to the basics and study intermittent hypoxia on healthy volunteers. To examine the tolerance, and to also find an appropriate IHT intervention that challenged the homeostasis of healthy volunteers, measurements of heart rate, saturation of oxygen in the blood, and blood pressure were taken. To analyse the response of the autonomic nervous system, heart rate variability was analysed. Regarding the investigation on spinal pathways, the effect on the sensory and motor pathways was examined by recording somatosensory evoked potentials and motor evoked potentials. These measurements were taken prior, during and up to 30 minutes following the IHT intervention. Results showed that a single exposure of IHT given to healthy young volunteers was well tolerated and its effects were long lasting and localised on the corticospinal tract following a stimulus on the motor cortex. Yet, to know the true potential of its ability to alter corticospinal excitability it is also essential to study its effect on skeletal muscle metabolism and as a result on force.

Key abbreviations

ANS- Autonomic nervous system

ASIA- American spinal injury association

BDNF- Brain-derived neurotrophic factor

CNS- Central nervous system

COPD- Chronic obstructive pulmonary disease

CST- Corticospinal tract

DCML- Dorsal column medial lemniscus pathway

EEG- Electroencephalography

EMG- Electromyography

FES- Functional electrical stimulation

FiO₂- Fraction of inspired oxygen

IHT- Intermittent hypoxia training

iSCI- Incomplete SCI

LTF- Long term facilitation

MEP- Motor evoked potentials

nTMS- Navigated TMS

OSA- Obstructive sleep apnoea

pLTF- Phrenic long term facilitation

SCI- Spinal cord injury

SEPs- Somatosensory evoked potentials

SpO₂- Pulse oximeter blood oxygen measurements

TrkB- Tropomyosin receptor kinase B

5-HT- Serotonin

Table of Contents

Copyright.....	i
Art and the spinal cord	ii
Acknowledgements.....	iii
Abstract.....	iv
Key abbreviations.....	v
Chapter.1. Literature review.....	1-76
1.1. Introduction.....	1
1.2. Demographics of SCI in Scotland.....	3
1.3. The spinal cord.....	4
1.4. What happens to the spinal cord following injury?.....	8
1.5. Causes of SCI.....	10
1.6. Types of SCI.....	11
1.7. The impact of SCI.....	13
1.8. Assessing SCI in the clinic.....	14
1.9. Spontaneous recovery following traumatic SCI and SCI prognosis.....	16
1.10. Neurophysiological techniques.....	17
1.10.1. Electroencephalogram (EEG).....	19
1.10.2. Somatosensory evoked potentials (SEPs).....	22
1.10.3. Transcranial magnetic stimulation (TMS).....	25
1.10.3.1. Reliability of MEPs.....	30
1.10.3.2. Navigated TMS.....	33
1.11. Ways to induce neuroplasticity in SCI.....	36
1.12. Rehabilitation methods.....	37
1.12.1. Gait training.....	39
1.12.2. Electrical stimulation.....	41
1.13. Common tests to study recovery.....	42
1.14. Changing demographics directs research to new rehabilitation approaches.....	43
Intermittent hypoxia: A new rehabilitation method for SCI?.....	43-76
1.15. Intermittent hypoxia: Severe to mild.....	43
1.16. Delivery methods: IHT.....	45
1.17. Importance of spared serotonergic innervations.....	46
1.18. The mechanism of action.....	47
1.19. Respiratory plasticity: Expression of TrkB and adenosine 2 _A receptor.....	49
1.20. BDNF and spinal cord.....	50
1.21. BDNF, IHT and the spinal cord.....	50
1.22. BDNF missense polymorphism.....	51
1.23. Important aspects of IHT protocol.....	52
1.24. iSCI patients with cardiopulmonary complications.....	52
1.25. IHT induces motor facilitation in animal models of SCI.....	53
1.26. IHT induces motor facilitation in SCI patients.....	54
1.27. IHT coupled with task specific training (TST).....	57
1.28. IHT coupled with anti-inflammatory drugs.....	58
1.29. Study design limitations.....	64
1.30. Factors that may influence neuroplasticity induced by IHT.....	65
1.31. Potential side effects or potential benefits?.....	68
1.32. Safety monitoring when investigating IHT on SCI patients.....	70
1.33. Tolerance of IHT by healthy elderly individuals.....	73
1.34. Aims and objectives.....	74
Chapter.2. Examining the tolerance of moderate intermittent hypoxia in healthy subjects.....	77-121
2.1. Introduction.....	77
2.1.1. Mild intermittent hypoxia versus OSA.....	77
2.1.2. Tolerance of IHT.....	79
2.1.3. Safety of the IHT protocol given to SCI.....	79
2.1.4. Heart rate variability (HRV).....	79
2.1.5. Improving cardiovascular health by increasing HRV with intermittent hypoxia... ..	83
2.1.6. Aims and objectives.....	84
2.2. Methodology.....	85

2.2.1. Subjects.....	85
2.2.2. Experimental design.....	86
2.3. Preliminary GO2Altitude hypoxia test.....	88
2.3.1. Methodology.....	88
2.3.2. Results.....	89
2.4. Comparing IHT with Hyperoxia versus Room Air breathing during recovery periods...	91
2.4.1. Methodology.....	91
2.4.2. Results.....	91
2.5. Exploring IHT intervention to study participant tolerance when extending hypoxia interval from 1 minute to 2 minutes while keeping hyperoxia interval at 1 minute.....	93
2.5.1. Methodology.....	93
2.5.2. Results.....	94
2.6. The IHT intervention adopted involved 1 minute hypoxia (at $FiO_2= 9.00\%$) interspersed with 1 minute hyperoxia (at FiO_2 between 21.00% and 40.00%).....	95
2.6.1. Intermittent Hypoxia training (IHT).....	95
2.6.2. Vital Sign Measurements (blood pressure, saturation of oxygen and heart rate)...	96
2.6.3. Analysis.....	96
2.6.4. Results.....	98
2.6.4.1. Blood Pressure.....	98
2.6.4.2. Saturation of oxygen.....	99
2.6.4.3. Time shift and rate of rise and drop analysis on the grand average SpO_2	104
2.6.4.4. Average rate of recovery and drop in SpO_2 across all participants and time shift.....	108
2.6.4.5. Heart rate.....	112
2.6.4.6. Heart rate variability (HRV).....	115
2.7. Discussion.....	117
2.7.1. Results from pilot studies on the IHT intervention.....	118
2.7.2. Blood pressure and heart rate.....	119
2.7.3. HRV.....	120
2.7.4. SpO_2	120
2.7.8. Conclusion.....	121
Chapter.3. Studying the effects of IHT on cortical SEPs in health subjects.....	122-160
3.1. Introduction.....	122
3.1.1. Intermittent hypoxia and iSCI.....	122
3.1.2. Investigating the mechanism of action.....	122
3.1.3. Somatosensory evoked potentials (SEPs).....	123
3.1.4. Recording SEPs.....	124
3.1.5. Monopolar and bipolar SEP recordings.....	124
3.1.6. Nomenclature of SEPs.....	125
3.1.7. SEP: Frequency of stimulation.....	126
3.1.8. SEP: Filters.....	126
3.1.9. Difficulties recording evoked potentials.....	126
3.1.10. SEP analysis.....	127
3.1.11. Median nerve SEP waveform meanings.....	128
3.1.12. SEPs and neuroplasticity.....	129
3.1.13. Abnormal cortical SEPs.....	129
3.1.14. Continuous hypoxia and SEPs.....	130
3.1.15. Aims and objectives.....	131
3.2. Methodology.....	132
3.2.1. Subjects.....	132
3.2.2. Experimental design.....	132
3.2.3. Peripheral stimulation: Median nerve.....	133
3.2.3.1. Skin impedance.....	133
3.2.3.2. Site of stimulation.....	133
3.2.3.3. Ring electrode placement.....	134
3.2.3.4. Sensation threshold.....	134
3.2.4. Electroencephalography (EEG).....	134
3.2.4.1. Scalp preparation.....	134
3.2.4.2. EEG recording of SEPs.....	134
3.2.4.3. Montage of electrodes.....	134
3.2.5. Components of SEP waveform.....	135

3.2.6. Signal processing.....	135
3.2.7. Analysis: SEPs.....	136
3.2.8. Analysis: SpO ₂ and heart rate.....	138
3.3. Results.....	138
3.3.1. Participant details.....	138
3.3.2. Onset latency analysis during IHT.....	139
3.3.2.1. Cc and Cc-FPz.....	139
3.3.2.2. FCc.....	140
3.3.2.3. CPc-FPz.....	140
3.3.3. Peak-to-peak latency.....	141
3.3.3.1. Cc and Cc-FPz.....	141
3.3.3.2. FCc.....	141
3.3.3.3. CPc-FPz.....	142
3.3.4. Peak-to-peak amplitude: IHT1.....	142
3.3.4.1. SEP amplitude histogram distributions.....	142
3.3.4.2. Peak-to-peak amplitude.....	148
3.3.4.2.1. Cc and Cc-FPz.....	148
3.3.4.3.2. FCc.....	150
3.3.4.3.3. CPc-FPz.....	150
3.3.5. Individual responses: Peak-to-peak amplitude.....	151
3.3.6. Peak-to-peak amplitude: Grand average.....	151
3.3.6.1. Reliability of pre-IHT data.....	151
3.3.6.2. Histogram distribution.....	152
3.3.6.3. Peak-to-peak amplitude.....	157
3.3.6.3.1. Cc and Cc-FPz.....	157
3.3.6.3.2. FCc.....	158
3.3.6.3.3. CPc-FPz.....	159
3.4. Discussion.....	159
3.4.1. SEPs and MEPs.....	160
3.4.2. Conclusion.....	160
Chapter.4. Creating a manual navigated coil placement system for TMS.....	161-176
4.1. Introduction.....	161
4.1.1. Reliability of TMS coil placement.....	161
4.1.2. Navigated systems.....	162
4.1.3. StimTrack.....	164
4.1.4. Coil tracking using two webcams.....	165
4.1.5. Aims and objectives.....	165
4.2. Methodology.....	166
4.2.1. Manual coil placement for TMS.....	166
4.2.2. Calibration of cameras.....	168
4.2.3. Matlab code.....	168
4.2.4. Key calculations.....	170
4.3. Discussion.....	175
Chapter.5. Studying the effects of IHT on the corticospinal pathway in healthy subjects.....	177- 239
5.1. Introduction.....	177
5.1.1. Intermittent hypoxia.....	177
5.1.2. Assessing sensory and motor pathways.....	177
5.1.3. TMS and MEPs.....	178
5.1.4. TMS coils.....	179
5.1.5. Accuracy of TMS stimulation.....	179
5.1.6. MEP waveform analysis.....	181
5.1.7. Corticospinal function in healthy subjects.....	181
5.1.8. Aims and objectives.....	183
5.1.9. Summary of findings.....	184
5.2. Methodology.....	186
5.2.1. Subjects.....	186
5.2.2. Experimental design.....	186
5.2.3. Transcranial magnetic stimulation (TMS).....	188
5.2.3.1. Double-cone coil.....	188
5.2.3.2. Stimulation ‘hotspot’.....	189

5.2.3.3. Stimulation intensity.....	189
5.2.4. Electromyography (EMG).....	189
5.2.4.1. Skin preparation.....	189
5.2.4.2. EMG setup.....	190
5.2.4.3. Maximum voluntary contraction.....	190
5.2.4.4. Motor evoked potentials (MEPs).....	190
5.2.5. Signal processing: MEPs.....	191
5.2.6. Analysis: MEPs.....	191
5.2.9. Analysis: SpO ₂ and heart rate.....	194
5.3. Results.....	194
5.3.1. Participant details.....	195
5.3.2. Participant IHT13.....	195
5.3.2.1. Peak and trough variability in baseline measurements of the target muscle (TA R) in subject IHT13.....	195
5.3.2.2. Reliability of pre-IHT peak-to-peak amplitude.....	197
5.3.2.3. Peak-to-peak amplitude.....	198
5.3.2.4. Group responses: Peak-to-peak amplitude.....	204
5.3.2.5. Reliability of pre-IHT AUC.....	207
5.3.2.6. AUC.....	208
5.3.2.7. Group responses: AUC.....	212
5.3.3. Grand average of all subjects.....	216
5.3.3.1. Peak-to-peak analysis.....	216
5.3.3.2. AUC.....	223
5.3.4. MEPs success rate for each muscle following TMS.....	229
5.4. Discussion.....	235
5.4.1. Reliability of pre-IHT MEP measurements.....	235
5.4.2. Improving the variability in MEP measurements.....	236
5.4.3. Corticospinal excitability following IHT.....	236
5.4.4. Individual differences.....	237
5.4.5. Success rate of MEPs following IHT.....	238
5.4.6. Limitations of the study.....	239
5.4.7. Conclusion.....	239
Chapter.6. Investigating the effects of IHT on muscle metabolic/contractile properties.....	240-251
6.1. Introduction.....	240
6.1.1. Skeletal muscle and intermittent hypoxia.....	240
6.1.2. Aims and objectives.....	241
6.1.3. Summary of studies.....	242
6.2. Methodology: Grip strength.....	242
6.2.1. Subjects.....	242
6.2.2. Protocol and analysis.....	243
6.3. Results: Grip strength.....	243
6.4. Methodology: FDI force measurements.....	246
6.4.1. Subjects.....	246
6.4.2. Protocol and analysis.....	246
6.4.3. AirFilm cooling coil (70 mm) experimental protocol and analysis.....	248
6.5. Results: FDI force measurements.....	248
6.6. Discussion.....	249
6.7. Future study.....	250
Chapter.7. IHT's mechanism of action and thoughts on implementing IHT in rehabilitation training.....	252-267
7.1. The impact of SCI to the individual and current needs in rehabilitation.....	252
7.2. What may be required in incorporating IHT during rehabilitation training.....	252
7.3. Key findings from this project.....	254
7.4. Current knowledge on the safety of the IHT protocol by Trumbower et al. (2012) and thoughts on iSCI patient tolerance.....	255
7.5. Results from the thesis on the safety and tolerance of the IHT intervention by Trumbower et al. (2012) and considerations for patients.....	256
7.6. Functional benefits in iSCI following IHT.....	258
7.7. Current knowledge of IHT's mechanism of action.....	260

7.8. Possible uses of TMS in clinical setting.....	263
7.9. Future study: Studying skeletal muscle contractile activity following IHT.....	265
7.10. Thoughts on the use of IHT to treat other neurological conditions.....	266
7.11. Conclusion.....	266
References.....	268-284
Appendices.....	285-320
Appendix. I. (Chapter.2.).....	285
Appendix. II. (Chapter.5.).....	289
Appendix. III. (Ethics Application).....	309
Appendix. IV. (Participant Information Sheet and Consent form).....	310
Appendix. V. (Hashemirad et al. 2017 Figure).....	317

Chapter.1. Literature review.

1.1. Introduction

A common rehabilitation therapy that is currently being used to promote functional recovery in patients with spinal cord injury (SCI) is body weight supported treadmill training (BWSTT). But this is an intensive training programme and is not suitable for frail elderly spinal cord injured patients. Laboratories, mainly in the United States, have recently begun investigations on a potential novel treatment, known as intermittent hypoxia training (IHT) for its promising ability to enhance motor function in patients with incomplete spinal cord injury (iSCI) (Trumbower et al., 2012; Trumbower et al., 2018; Sandhu et al., 2019; Naidu et al., 2020; Hayes et al., 2014; Navarrete-Opazo et al., 2016b; Navarrete-Opazo et al., 2017; Lynch et al., 2016). IHT provides an alternative or adjunct treatment that is attractive to clinical populations that cannot tolerate the current vigorous and intensive rehabilitation associated with BWSTT. These are usually elderly individuals who now, compared to the past, make up the majority of SCI patients (McCaughey et al., 2016; Scivoletto et al., 2008). Hence, IHT may be considered a novel rehabilitation approach that is suited for the rehabilitation treatment of the growing population of elderly SCI patients as well as young cases.

IHT seems to provide functional benefits when used on its own or in combination with rehabilitation. First of all, it is important to highlight that IHT alone enhances fitness by improving respiratory function and cardiovascular health. This is supported by studies on altitude training in athletes (Terrados et al., 1998, Casas et al., 2000) and in the elderly population. It is important to highlight here the study by Burtscher et al. in 2004 that reported improvements in exercise tolerance in elderly patients with and without coronary artery disease following IHT. IHT as a rehabilitation aid takes advantage of physiology and incorporating it in rehab programmes is highly likely to be beneficial in improving general fitness levels of patients and especially advantageous when dealing with elderly patients that are likely to be less fit. Age related differences in walking prognosis in incomplete spinal cord injury have been reported in the United States (Burns et al., 2012) and partly, it may be associated by the inability of elderly patients to undergo intensive rehabilitation sessions. Overall, there is a significantly lower percentage of elderly patients with functional ambulation at

rehabilitation discharge compared to young patients (Burns et al., 2012). Secondly, given the increasing evidence for IHT to bring about long lasting neuromodulatory effects on non-respiratory motor pathways, the potential facilitatory effects of IHT as a promotor for recovery at low cost makes it an attractive adjunct therapy. Small scale trials with iSCI patients have highlighted that when IHT is administered, without additional training, lasting improvements in ankle plantar flexion torque and walking speed, can be measured (Trumbower et al., 2012; Hayes et al., 2014). These functional gains are further enhanced when IHT is coupled with a task specific training (TST) (Navarrete-Opazo, 2017; Navarrete-Opazo 2016; Trumbower et al., 2017 and Hayes et al., 2014). Accordingly, further research is required, preferably based on large scale clinical trials, to gain a deeper understanding of the benefits and level of response to IHT when given alone as well as when paired with a task specific training.

IHT involves the breathing of hypoxic air sustained for several seconds and interrupted by several seconds of normoxia. It is believed that IHT causes a release of serotonin in the central nervous system (CNS) that ultimately strengthens the spared connections between the brain and spinal cord. A facilitatory effect has been reported to last up to around 120 minutes (Christiansen et al., 2017) and during this time window medical professionals are encouraged to perform conventional rehabilitation therapies. Currently, in the United States clinical trials are being conducted on combining IHT with rehabilitation (<https://clinicaltrials.gov/ct2/show/NCT03644277>).

After reviewing the literature, studies administering IHT on iSCI patients report an improvement in motor function; however, the mechanisms of action, safety with respect to dose and exclusion criteria to date is not well developed. Consequently, the purpose of this research was to explore the influence of IHT on sensory and motor performance in healthy individuals to better understand the underlying central mechanism of action of a single dose of IHT, as well as examine its safety by monitoring key vital signs. Ideally, the investigation would have progressed into studying IHT on patients with iSCI, however, during the course of this three-year project a significant part of the experimental programme was affected by the impact of the COVID pandemic on face-to-face research thus curtailing some of the planned work.

The principal reason for examining IHT intervention in healthy subjects before moving to patients is to acquire baseline data free from the complications that normally occur in patients in addition to paralysis; these are related to cardiovascular and respiratory debilities. Furthermore, it is also essential to acquire knowledge on neurophysiological assessment procedures, recordings and analysis methodologies before moving into patient tests and clinical trials. Accordingly, the work reported here is focussed on key questions relating to the effect of single session IHT on sensory pathways as measured by somatosensory evoked potentials (SEPs) and corticospinal excitability as measured using transcranial magnetic stimulation (TMS).

The review that will follow will cover the organisation of the spinal cord and what occurs following injury as well as the types, causes, impact and demographics of SCI. Furthermore, the assessments and rehabilitation methods available will be discussed as well as the necessity of introducing a different rehabilitation approach for the growing elderly population with iSCI and how intermittent hypoxia comes into play as an attractive potential treatment. In addition, information on specific techniques and concepts will be elaborated as they will arise in individual chapters of this report.

1.2. Demographics of SCI in Scotland

According to the World Health Organization (2013) the global incidence of traumatic and non-traumatic SCI is around 40 to 80 cases per million of the population. Generally, the life expectancy of the SCI population is lower compared to the general population and the leading cause of death in high income countries are respiratory problems (WHO, 2013).

A retrospective review of the Queen Elizabeth National Spinal Cord Injury Unit (QUENSIU) database in Scotland was performed over 20-years, 1994-2013, to investigate how the demographics of SCI changed over this period. Between 1994 and 2013, 1,638 patients with traumatic SCI were admitted to QENSIU (McCaughey et al., 2016). The incidence rate for traumatic SCI between 1994 and 2013 was 15.9 per million (McCaughey et al., 2016). The main findings of this review are the following:

- 1) The most common cause of traumatic SCI is falls (51.7%). Incidence rate significantly increased from 41.6% between 1994 and 1998 to 60.0% between 2009 and 2013 for traumatic SCI caused by falls.
- 2) There was a significant increase in mean age at the time of injury from 44.1 years between 1994 and 1998 to 52.6 years between 2009 and 2013.
- 3) There was a marked increase of patients with traumatic SCI at the cervical level and it was mainly due to an increase in C1-C4 lesions. (McCaughey et al., 2016)

Compared to the past, there are now more elderly patients in Scotland with upper cervical traumatic SCI resulting from a domestic fall (McCaughey et al., 2016). This stems from the elderly living longer and being more socially and economically active but also from higher risk of falling as we age. It has been estimated that by 2034, 23% of the population will be aged 65 years and above (MASCIP, 2010). Therefore, researchers interested in SCI are now focusing on treatments that take account the physical capabilities of the patient population. It is evident that we need a different model of SCI care pathway and this is not only reported in Scotland but across all developed economies where an increased life expectancy exists (Jackson et al., 2004; Wirz and Dietz, 2012; Scivoletto et al., 2008). For instance, Jackson et al. (2004) reported that over 30 years from 1973 to 2003 in the United States a significant increase in mean age at the time of injury for each following decade.

1.3. The spinal cord

The spinal cord serves as a medium of communication between the peripheral nervous system and the brain to control motor, sensory and autonomic functions. The information is relayed via spinal nerves or tracts.

The peripheral nervous system carries information to and from the spinal cord via the 31 pairs of spinal nerves (8 cervical, 12 thoracic, 5 lumbar, 5 sacral and 1 coccygeal) that arise from the spinal vertebrae. A nerve is a bundle of axons (or projections of neurons) that carry motor, sensory (pain, temperature, vibration, pressure or proprioception) and autonomic signals from and to peripheral receptors that are found on the skin, muscles, tendons, joints and viscera (Cramer, Darby and Cramer, 2014, p.65).

In the central nervous system (CNS), the bundles of axons are referred to as tracts and they are located in the white matter of the spinal cord. The white matter is divided into the dorsal columns that carry sensory information, the lateral columns where the information travels from the cerebral cortex to spinal motor neurons and the ventral columns that carries sensory ascending information as well as motor descending information (Cramer, Darby and Cramer, 2014 p.82; Weidner, Rupp and Tansey, 2017, p.30-34; Purves and Williams, 2001).

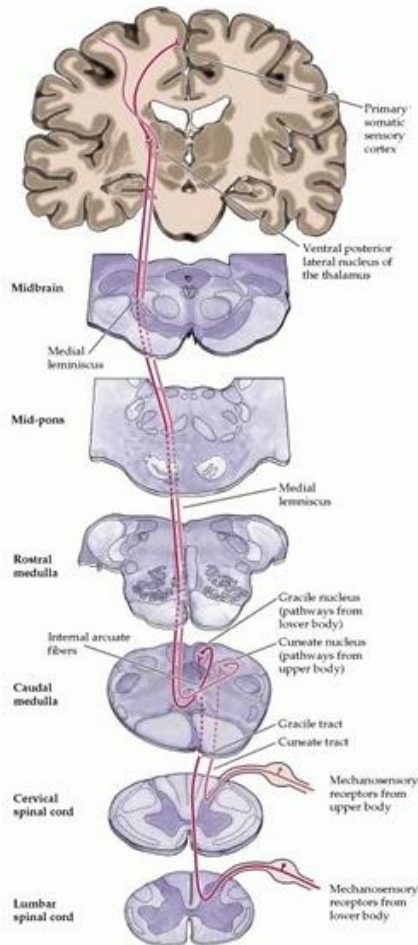


Figure.1.1. DCML is an ascending pathway that conveys discriminatory touch, proprioception, vibration and pressure. Peripheral mechanoreceptors afferent fibers enter the dorsal root and at this stage some branches descend, and they are involved in mediating reflex responses, while the rest ascend, cross at the medulla and terminate at the postcentral gyrus and posterior paracentral lobule. The pathway is clearly displayed in red. (diagram used with permission from Purves and Williams, 2001)

The ascending tracts convey sensory information from skin, muscles, tendons, joints or viscera to the brain and between spinal cord segments. All spinal sensory information that travels via the dorsal column pathways, synapse in thalamic nuclei

where information is processed and then transmitted on to cortical areas of the primary sensory cortex (Weidner, Rupp and Tansey, 2017, p.34-39). The primary somatosensory cortex is found in the postcentral gyrus or Brodmann area 1-3. Some of the ascending sensory information is integrated in the brain and used by autonomic centres to maintain homeostasis or by motor centres to control movement (Weidner, Rupp and Tansey, 2017, p.34-39). Here it is worth mentioning the dorsal column-medial lemniscus pathway (DCLM) that conveys fine touch, two-point discrimination, vibration and proprioception (sensing the position of limbs into space). As illustrated in Figure.1.1, these inputs ascend to the primary somatosensory cortex where they are processed and form a somatotopic map of the body regions within the primary sensory cortex. This gives different areas functional specificity related to different body regions and structures.

Descending tracts, as shown in Figure.1.2, originate in the brain and convey motor information to the spinal cord. An important descending tract responsible for all voluntary movements, especially skilled movements of the hands and fingers, is the corticospinal tract (CST) (Cramer, Darby and Cramer, 2014 p. 362). Most of the fibres originate from pyramidal neurons in the primary motor cortex known as the upper motor neurons and unlike other descending cortical tracts these cells make monosynaptic and polysynaptic synapse connections to the spinal motor neurons that innervate skeletal muscles (Cramer, Darby and Cramer, 2014 p. 375-376).

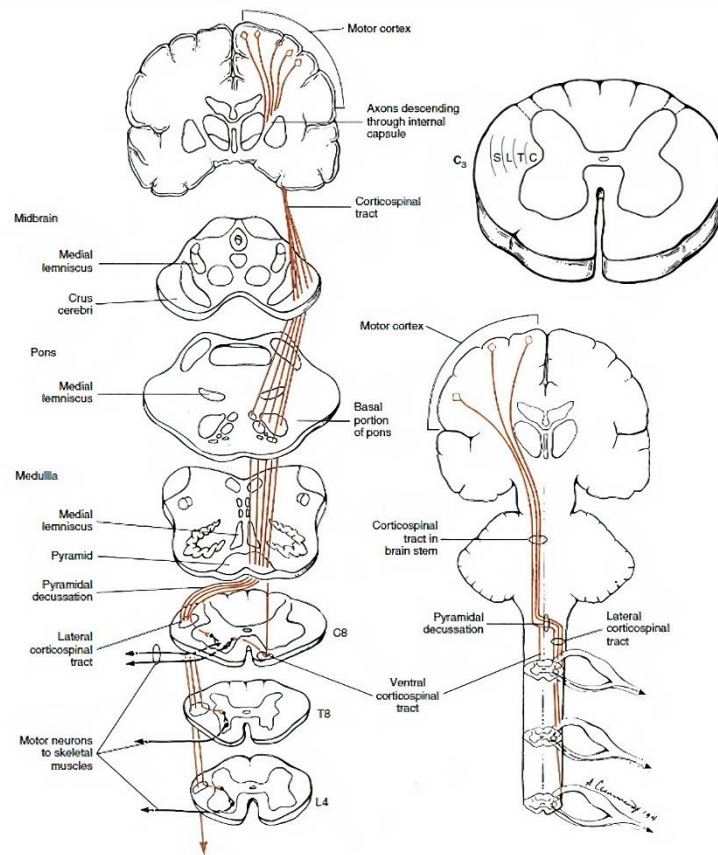


Figure.1.2. Corticospinal Tract (CST): Most fibers (lateral CST) cross in the caudal medulla and descend in the lateral funiculus of the cord. The uncrossed fibers descend in the ventral funiculus. The axons terminate in the intermediate gray matter and the ventral horn. (diagram used with permission from Cramer, Darby and Cramer, 2014).

The primary motor cortex is found in the precentral gyrus or Brodmann area 4 in the frontal lobe and body part representation area in this region is related to the level of control the brain devotes to it. Penfield and Boldrey found that larger areas of the cortex are responsible for areas of the body that are involved in precision tasks and fine control of movement (Penfield and Boldrey et al., 1937). As mentioned, most fibres originate from the primary motor cortex, however, some also originate from the postcentral gyrus or sensory cortex and the parietal lobe. Around 80 % to 90 % of the fibres cross at the level of the pyramid, known as pyramidal decussation providing contralateral control of motor function (Cramer, Darby and Cramer, 2014 p. 377). The remaining descend ipsilaterally with some fibres making ipsilateral connections to motor pools.

As mentioned, the spinal cord allows communication between the peripheral nervous system and the brain. Following spinal cord injury, this communication is disrupted resulting to loss of motor, sensory and autonomic functions below the innervation level of injury. The ability for the CNS to repair itself is limited, however, there are interventions that encourage plasticity which ‘*is the quality of being plastic; specifically, the ability to be easily moulded or to undergo a permanent change in shape*’ (Oxford English dictionary, 2021).

1.4. What happens to the spinal cord following injury?

The CNS ability to regenerate changes from development into adulthood. In the adult CNS there is limited availability for morphological changes in neurons and strengthening of synapses following an injury (Quraishie, Forbes and Andrews, 2018). These changes are referred to as neuroplasticity and defined by the Oxford English dictionary as ‘*the ability of the nervous system to form and reorganize connections and pathways, as during development and learning or following injury*’ (Oxford English dictionary, 2021).

In the developing CNS, neurons express growth-promoting proteins and create a favourable environment for neuronal growth (Maier and Schwab, 2006; Quraishie, Forbes and Andrews, 2018). In the adult CNS, however, synapses are stabilised and synaptic plasticity is controlled mainly by the presence of perineuronal nets which are

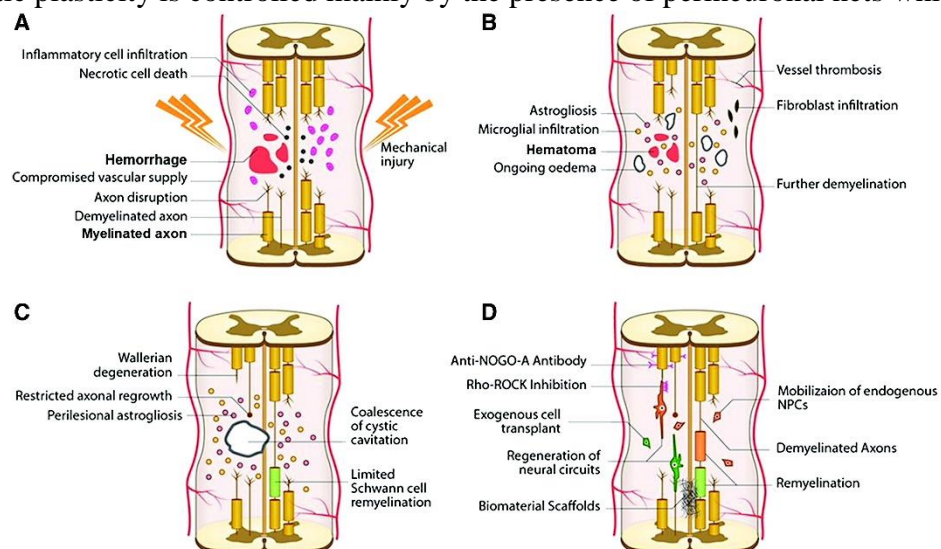


Figure.1.3. Pathophysiology following SCI. **A)** acute phase (0-48h), **B)** late subacute, **C)** intermediate and **D)** chronic (diagram used with permission from Ashammakhi et al.,2019). NPCs: neuroprogenitor cells.

extracellular matrix structures (ECM) (Quraishe, Forbes and Andrews, 2018). In addition, neurite outgrowth inhibitors (chondroitin sulphate proteoglycans and semaphorins) and myelin-associated inhibitors (Nogo-A) are present and tenascin glycoprotein growth-promoting factors are downregulated (Quraishe, Forbes and Andrews, 2018).

Yet, the CNS has the inherent (but latent) ability to recover and following several decades of research we now have a good understanding of how the environment at the site of injury may limit or hinder this. This has directed scientists to focus on manipulating the environment at the site of injury to be more favourable for plasticity. For instance, damage may be prevented close to the time of injury by the use of neuroprotective agents such as corticosteroid (Maier and Schwab, 2006).

Following injury, the stable environment for neuronal growth and repair is disrupted by the upregulation of growth-inhibitory factors. Initially, SCI leads to haemorrhage, ischemia at the site of injury causing necrotic cell death, an immune response, and disruption of ionic homeostasis (Oyinbo, 2011; Quraishe, Forbes and Andrews, 2018). At this point acute care is needed to reduce inflammation and stabilise the patient. This is considered the first phase or also known as the initial mechanical damage. The next phase is associated with the formation of the glial scar and Wallerian degeneration (Oyinbo, 2011). In summary, the secondary phase includes a cascade of events that leads to neurodegeneration and creates a hostile and negative environment for growth and repair. Some of these events include the upregulation of neurite outgrowth inhibitors creating retraction bulbs, the formation of glial scar by astrocytes at the site of injury, the secretion of myelin-associated inhibitors from injured myelin sheaths, the release of pro-inflammatory cytokines and ECM proteins that encourage inflammation and tissue damage, the formation of reactive oxygen and reactive nitrogen species leading to protein damage, apoptotic cell death and the increase in glutamate neurotransmitter release causing demyelination of oligodendrocytes (Oyinbo, 2011; Quraishe et al., 2018). Please refer to Figure.1.3 a diagram from Ashammakhi et al. in 2019 which illustrates in detail the phases of SCI.

Understanding the phases following injury has facilitated neuroscientists to explore a variety of possible interventions targeting different cellular and molecular

factors. Some examples are the use of methylprednisolone steroid to reduce inflammation in the acute phase, the use of agmatine NMDA receptor antagonist to inhibit glutamate induced neurotoxicity and the oral administration of fast voltage-sensitive potassium channel blocker 4-aminopyridine that is capable to improve gait by reducing demyelination of axons, among many other interventions that are being researched (Bracken et al., 1992; Segal et al., 1998).

1.5.Causes of SCI

Following the summary of the destructive cascades of events after injury, the discussion will proceed with the most probable causes of injury. SCI is a loss of motor and/or sensory function from traumatic (89.6 million in Scotland) or non-traumatic causes (14 million in Scotland) (McCaughey et al, 2016). Traumatic SCI results from falls (42%), vehicle crashes (37%), acts of violence (4%), sports or recreational activities (12 %), assault (3%) and other unspecified causes resulting from trauma (3%) (these percentages are for UK in 2015) (Statista, 2021). Non-traumatic SCI occurs from compression of the cord due to degenerative conditions affecting the spinal column, vascular disorders and viral infections (Hatanpaa and Kim,2014; Kalsi-Ryan, Karadimas and Fehlings, 2013). For instance, vascular disorders include spinal vascular malformations where spinal dural arteriovenous fistula and type I arteriovenous malformations are the most common (Weidner, Rupp, and Tansey, 2017, p.107). These malformations cause a congestion within the veins from blood being shunted in the perimedullar veins, triggering inflammation within the spinal cord and ultimately causing myelopathy (Weidner, Rupp, and Tansey, 2017, p.107). Myelitis can be caused by systemic autoimmune diseases, such as sarcoidosis, Sjögren's syndrome and systemic lupus erythematosus, or by pathogens such as herpes simplex virus, varicella zoster virus and retrovirus or by bacterial infections such as mycobacteria, brucella and chlamydia (Sawaya and Radwan, 2013; Kim et al., 2009; Weidner, Rupp, and Tansey, 2017). Other causes of non-traumatic SCI that compresses the cord include: degenerative spinal diseases (i.e. spondylotic myelopathy and compression of cauda equine), neoplastic diseases (i.e. haemangioma), spinal hematoma (i.e. spinal epidural or subdural hematoma), infectious lesions (i.e. spinal

epidural abscess) and other aetiologies (i.e. meningeal or arachnoid cysts) (Dey, Landrum and Oaklander, 2005; Weidner, Rupp, and Tansey, 2017).

1.6. Types of SCI

The extent of lost function depends on the number of tracts damaged and on the location of the injury. If no tracts are preserved, there is a lack of sensory and motor function below the level of the injury resulting to complete SCI. If some ascending and descending tracts are preserved, then there are some motor and sensory function below the level of injury and this is known as incomplete SCI (iSCI).

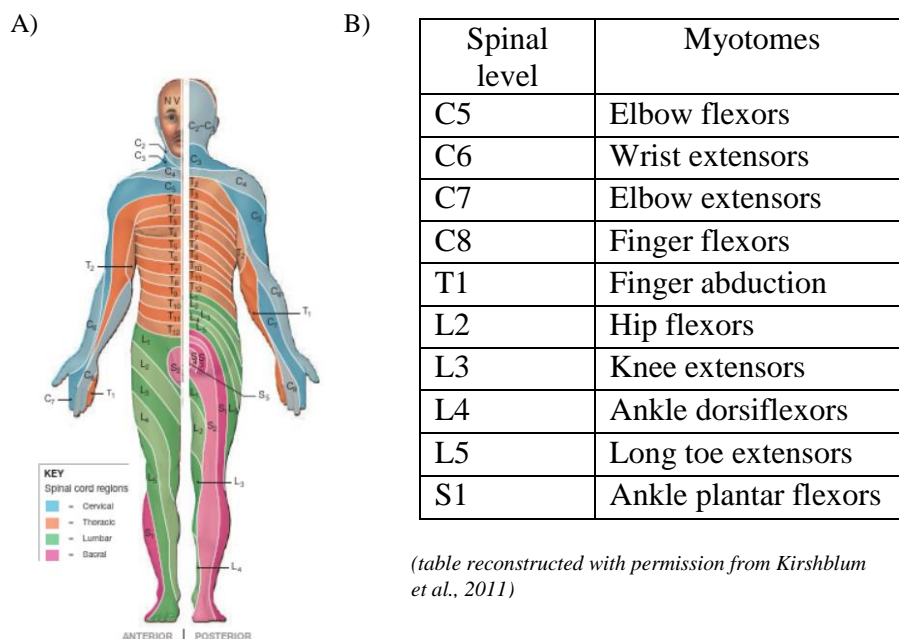


(table reconstructed with permission from Kirshblum et al., 2011)

(diagram used with permission from Martini, Nath and Batholomew, 2018)

Figure.1.4. A) Anterior and posterior distributions of dermatomes. NV= cranial nerve five (trigeminal nerve). B) Spinal level and myotomes.

The injury can cause either tetraplegia, resulting from lesions in the cervical level, where all limbs are affected or paraplegia, resulting from lesions in the thoracic level (Marino et al., 2003). Incomplete tetraplegia was the most frequent type of SCI in Scotland with an incident rate of 66.3% between 2009 and 2013 (McCaughey et al., 2016).

The level of the injury is an important factor on the extent of function retained and lost. The spinal cord is organised into cervical, thoracic, lumbar and sacral levels along with a coccygeal spinal segment. In between the vertebra, spinal nerves enter and exit

from the spinal cord. They innervate a different dermatome, myotome and visceral organ (Figure.1.4; Figure.1.5). A dermatome is defined as a discrete skin area innervated by sensory axons that the spinal cord receives sensory information from and a myotome is a group of fibres within the muscles innervated by motor axons from specific spinal nerves (Figure.1.4) (Martini, Nath and Batholomew, 2018). Therefore, functional loss following a SCI is associated with the segmental level of injury.

High cervical lesions at C1 to C4 spinal vertebrae are the most severe and sometimes fatal due to respiratory paralysis unless the patient can be ventilated quickly following the injury but these are also very rare (Wong, Shem and Crew 2012). Cervical SCI leads to full paralysis below the neck and also leads to autonomic dysfunction (Krassioukov and Claydon, 2006). The patients require ventilation and they are totally dependent on a caregiver for all daily living activities (Wong, Shem and Crew 2012). Ventilator support is also critical as post management can cause complications such as pneumonia (Wong, Shem and Crew 2012).

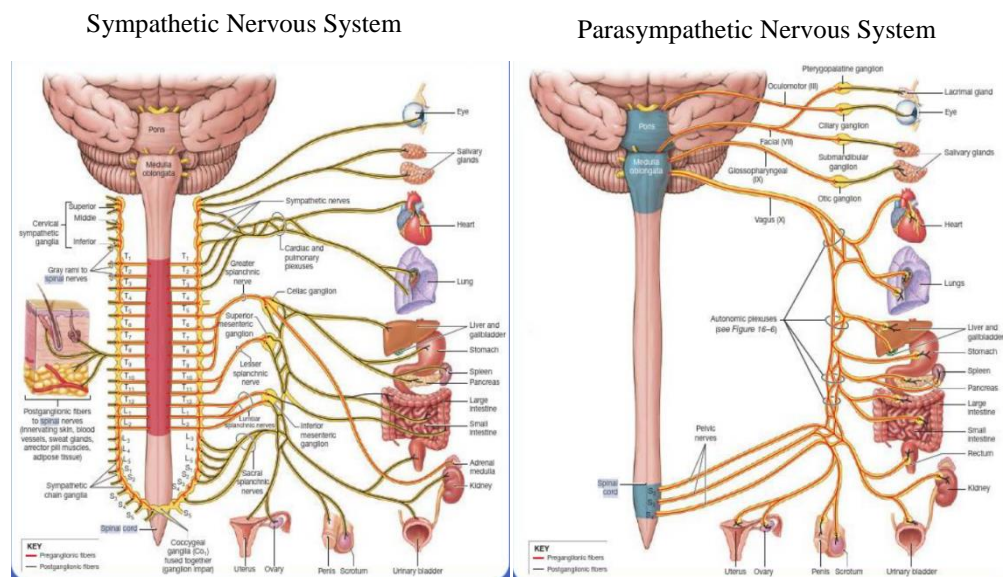


Figure.1.5. Sympathetic and parasympathetic nervous system (illustrations used with permission from Martini, Nath and Batholomew, 2018).

For lesions at C5 to C8 vertebrae, patients must retain some residual hand function and many learn to use a battery powered wheelchairs. They may even have sufficient dexterity to complete some daily activities such as eating unaided (Nas et al., 2015). Lesions in the thoracic, lumbar and sacral vertebrae result in paraplegia where there is paralysis in the lower limbs and part of the trunk or abdomen. Moreover, they also can

commonly suffer from sensory loss and poor to no voluntary control of bowel, bladder or sexual function (Nas et al., 2015).

1.7. The impact of SCI

SCI is a major life event as the individual needs to learn what it means to live with SCI and losing independence. Lost independence means that the patient needs to rely on a caregiver. SCI results to a serious physical disability and secondary medical issues that negatively impact the quality of life of the individual, friends and family members. The secondary medical issues include: problems with pressure sores, bowel and/or bladder control, respiratory problems, cardiovascular issues and a negative impact in sexual and reproductive function (Nas et al., 2015). According to a community-based rehabilitation programme in the United States with 56 participants that had either tetraplegia (32.1 %) or paraplegia (64%), they identified bladder issues as the most problematic (30.4%) (Piatt et al., 2016).

For a SCI patient, mental health issues are a normal reaction until the individual adjusts and creates a meaningful life with their disability. It is especially debilitating for patients that once lived an active life. In some cases, though, the individual cannot accept their condition and they may develop clinical depression as well as substance abuse and in extreme cases the individual may have suicidal thoughts (Kolakowsky-Hayner et al., 2002, Giannini et al., 2010). According to the WHO (2013) 20% to 30% of SCI individuals have clinical depression. Moreover, mental health problems negatively impact the overall health and rehabilitation progression of the patient.

Furthermore, living with SCI is a financial burden. The average yearly expenses that include health care costs and living expenses but not indirect costs such as lost earnings is \$1, 064, 716 for the first year and \$ 184, 891 each subsequent year for a high tetraplegic patient (C1-C4). For low tetraplegic (C5-C8) is \$ 769, 351 the first year and \$ 68, 739 each subsequent year (Reeve Foundation, 2020). This information is available for the United States, but the current healthcare costs for UK based patients have not been updated. Even though there is no current analysis reporting the estimate of healthcare costs in the UK, it is not expected to mirror those in the US to a large extend.

Furthermore, there are significant financial implications that also depend on the severity of the injury, the age at which the injury occurred and the prospect of employment. Unemployment affects most SCI patients and this places an economic burden on the state and family. In the United Kingdom employment rate decreased from 86.5% in individuals prior to suffering a SCI to 37.2% following SCI and 45.5% of the subjects in the study reported a lower gross household income and 19.5% reported a 50% fall in earnings (NSCISC, 2019; Savic et al., 2000).

1.8. Assessing SCI in the clinic

To determine the prognosis following a spinal injury, clinicians complete a standard clinical assessment validated and produced by the International Standards for Neurological Classification of Spinal Cord Injury (ISNCSCI). The assessments are advised to be performed at least 72 hours post-injury (Herbison et al., 1992) and thereafter at intervals to chart progression toward discharge. Current evaluations of SCI in the clinic involves categorising the patient according to the severity of symptoms and performing neurophysiological assessments.

Figure.1.6. Standard neurological classification of SCI used by clinicians (figure used with permission from Kirshblum et al., 2011)

In SCI the conduction of sensory and motor information is disrupted by the lesion (Marino et al., 2003). By examining the dermatomes and myotomes well trained clinicians can determine the extent and level of the injury. The globally recognised impairment scale used by clinicians was published by the American Spinal Injury

Association (ASIA) in collaboration with the International Standards for Neurological Classification of Spinal Cord Injury (ISICOS) and it is known as the ASIA Impairment Classification (Alexander et al., 2010). This impairment classification tool is used to classify SCI but also to evaluate the rehabilitation progress (Kirshblum et al., 2011). It assesses 28 dermatomes and 10 paired myotome functions around the suspected injury level and it also grades the completeness of SCI (Kirshblum et al., 2011). The ASIA scale ranges from A to E where A is assigned to complete loss of sensory and motor function and E is assigned to normal sensory and motor function (Kirshblum et al., 2011).

During the sensory examination, sensitivity is assessed using the pin prick test and light touch. The pin prick test examines the spinothalamic pathway, and the light touch is used to examine the DCML pathway (Vasquez et al., 2013). For the duration of the pin prick test the clinician uses a disposable safety pin and during the light touch the clinician uses a cotton bud. Sensation is scaled according to a three-point scale system (0=absent, 1=impaired, 2=normal, NT= not testable) (Marino et al., 2003) (Figure.1.6). During the motor examination muscles are examined in a rostral to caudal sequence and graded according to a six-point scale (Table.1.1).

Table.1.1. Six-point scale (table used with permission from Kirshblum et al., 2011)

0	Total paralysis
1	Palpable or visible contraction
2	Active movement, full range of motion (ROM) with gravity eliminated
3	Active movement, full ROM against gravity
4	Active movement, full ROM against moderate resistance
5	Normal active movement, full ROM against full resistance
5*	Normal active movement, full ROM against sufficient resistance to be considered normal if identified inhibiting factors were not present
NT	Not testable as a result of immobilisation or severe pain

The muscles of the upper limb that are tested are: elbow flexors, wrist extensors, elbow extensors, finger flexors and finger abductors. For the lower limb the muscles that are tested are: hip flexors, knee extensors, ankle dorsiflexors, long toe extensors and ankle plantar flexors (Figure.1.6).

1.9. Spontaneous recovery following traumatic SCI and prognostic factor

Following a traumatic SCI, there is often some spontaneous recovery, such as axonal sprouting and synaptic rearrangement. In animal models of SCI axonal sprouting is observed by the formation of new intra-spinal circuits (Bareyre et al., 2004). However, spontaneous plasticity is limited by a decrease in growth factors, the release of inhibitory molecules and the overall formation of a hostile environment for regeneration of axons following injury, as further described in the previous section, Chapter 1 Section.1.4 (Fawcett et al., 2007).

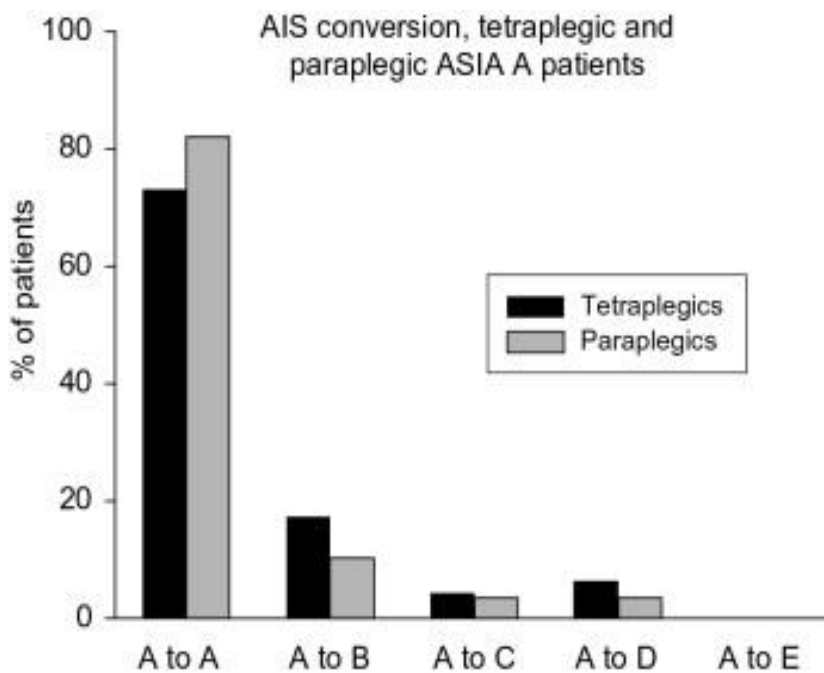


Figure.1.7. Percentage conversion of AIS grade in tetraplegics and paraplegics AIS A patients from the European Multicenter Study about SCI (EMSCI) database (figure use with permission from Fawcett et al., 2007).

In SCI patients the spontaneous recovery process takes place within the first 6 to 9 months following the injury and often plateaus at 12 to 18 months, but this recovery depends heavily on the level and the completeness of the injury (Onifer, Smith and Fouad, 2011; Burns et al., 2012). According to Fawcett et al. (2007) who reviewed several SCI studies, patients with iSCI had a significantly higher degree of spontaneous recovery compared to complete SCI patients. In complete SCI patients (AIS A), only 20% converted either to AIS B or C. Following 1-year post injury AIS B to AIS C was around 15 % to 40 % and from AIS B to AIS D was as high as 40 %

(Fawcett et al., 2007). Figure.1.7 demonstrates the percentage of patients AIS conversion in both tetraplegic and paraplegic patients (Fawcett et al., 2007; Burns et al., 2012).

Furthermore, the prognosis of walking following SCI depends on the severity of the injury. Table.1.2 demonstrates the prognostic factor, the AIS grade and the anticipated outcome (Burns et al., 2012). It is important to mention that age affects the prognosis for functional recovery following SCI (Penrod, Hegde and Ditunno, 1990; Stevenson et al., 2016). Functional ambulation for discharge following a rehabilitation programme was 52% for younger patients whereas only 23% for elderly patients (Burns et al., 2012).

Table.1.2. Prognostic factor and anticipated outcomes (table used with permission from Burns et al., 2012)

Prognostic factor	grade	Anticipated outcome
Absence of sacral sparing	A	Clinically complete. Functional motor recovery distal to lesion rare, although ~ 10–20% convert to incomplete
Delayed plantar response > 7 days post injury	A	Remain clinically complete
Intramedullary hemorrhage > 10 mm	A	Remain clinically complete
MMT grade for individual muscle \geq 1/5 by 1 week to 1 month post injury	A, B, C, D	\geq 85% of these muscles regain functional, antigravity strength (\geq 3/5) by 1 year post injury
LEMS \geq 10 by 1 month post injury	C, D	\geq 85% are community ambulators 1 year post injury

MMT, manual muscle testing; LEMS, lower extremity motor scores.

1.10. Neurophysiological techniques

There may be some spontaneous recovery in the first few months following a SCI again depending on the severity of injury. Neurophysiological techniques complement clinical evaluation of SCI using the ASIA scale. In Figure.1.8 a list of neurophysiological techniques is displayed, including motor evoked potentials (MEPs), somatosensory evoked potentials (SEPs), sympathetic skin response (SSR), laser evoked potentials (LEPs), galvanic vestibular stimulation (GVS) and nerve conduction tests. These techniques assess the functional integrity of different pathways

and systems of the CNS. The pathways and systems assessed are the following: corticospinal, dorsal column, spinothalamic, vestibulospinal and peripheral system (Dietz and Curt, 2006). Some of the neurophysiological measurements will be described more in depth in the following paragraphs as they will be referred to again later in the thesis while others will be just briefly mentioned.

The two neurophysiological techniques that will be described in detail are the MEPs and SSEPs. MEPs are responses evoked by transcranial magnetic stimulation (TMS) and is used to analyse the corticospinal pathway by activating fast-conducting corticospinal fibres that synapse with spinal alpha motor neurons. Following stimulation of the motor cortex there is a muscular response which is measured using electromyography (EMG) electrodes placed on the muscle belly. EMG electrodes record the electrical activity of the muscle (Hallett, 2000; Ginhoux et al., 2013; Merton and Morton, 1980).

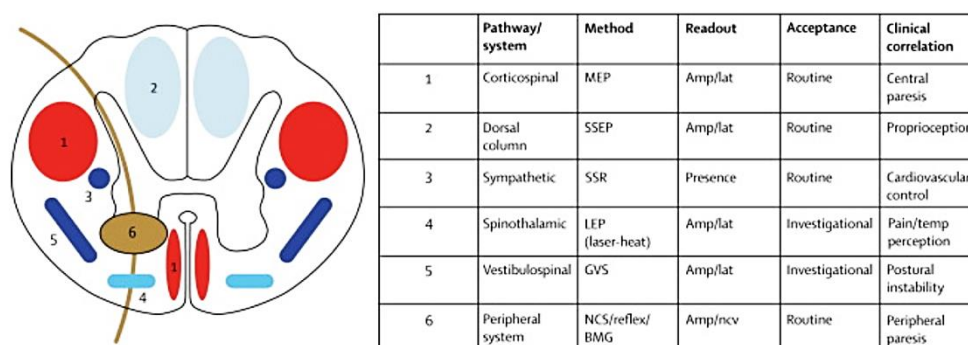


Figure.1.8. Neurophysiological techniques assessing function of the spinal cord (figure used with permission from Dietz and Curt, 2006)

Usually, the latency and amplitude of MEPs are studied and any deviation from the norm indicates an underlying condition. The amplitude of MEP reflects the level of corticospinal excitability while the latency reflects the conduction time from the stimulation at the motor cortex all the way to the peripheral muscles (Bestmann and Krakauer et al., 2015). In contrast, SSEPs evaluate the somatosensory pathways and the spinal subcortical and cortical nervous system (Norbert Weidner, Neurological Aspects of Spinal Cord Injury). Usually, they are evoked by stimulating the tibial, median, ulnar or pudendal nerves and measured using electroencephalography (EEG),

a non-invasive technique that is used to study the electrical activity of the brain. Analysis mainly involves looking at latency and amplitude of the early components of the waveform.

Other methods include SSR, LEP, GVS and nerve conduction measurements (Figure.1.8). SSR is used to assess sympathetic fibres by recording the change in potentials generated in the skin sweat glands. This response results from polysynaptic reflex activation and it usually involves electrical stimulation of a peripheral nerve while measuring the response using electrodes placed over a dermatome of interest (Kucera, Goldnberg and Kurca, 2004). LEPs are used to evaluate the function of A δ and C sensory fibres to study lesions in the spinothalamic tract (Treede, Lorenz and Baumgärtner 2003). They are usually recorded at stimulus intensity of 1.5-2 times the pain threshold and the analysis involves studying changes in latency and amplitude of LEP (Treede, Lorenz and Baumgärtner 2003). GVS activates fibres of the vestibular nerve pathways and evokes a biphasic EMG response (Liechti et al., 2008). Nerve conduction studies investigate how well the nerves and muscles are functioning by stimulating the nerve and recording EMG activity from the muscle (Chung, Prasad and Lloyd, 2014).

To conclude, neurophysiological techniques are used to better evaluate the condition and to assess treatment progress. For SCI, clinicians and scientists use neurophysiological techniques to evaluate the connectivity between the brain and the periphery following an injury on the spinal cord. In the subsections below the main neurophysiological techniques that are used to assess SCI will be explained in depth.

1.10.1. Electroencephalogram (EEG)

Before describing the neurophysiological technique known as SEPs it is essential to first introduce EEG. EEG, according to Piotr Olejniczak, is a graphical representation that measures voltage generated by cerebral neurons over time (Olejniczak, 2006). In SCI and for many other neurological diseases, EEG is used to measure SEPs from the brain following a peripheral stimulus.

EEG is a non-invasive measurement that involves placing surface scalp electrodes according to a standard positioning system (the international 10-20 system)

and recording electrical activity of the brain while the participants sits comfortably in a quiet and relaxed environment (Aminoff, 2012; Ozkul and Uckardes, 2002). The international 10-20 system defines the placement of electrodes referred to four standard positions: nasion, inion and right and left preauricular points (Aminoff, 2012) (Figure.1.9).

EEG is also commonly used to monitor brain states for seizures, sleep disorders or following a head injury. EEG signals is recorded in microvolts with an amplitude of around 100 μ V. Monitoring brain states involves five frequency bands (alpha (8-13 Hz), beta (13-30 Hz), gamma (>30 Hz), delta (0.5-4 Hz) and theta (4-8 Hz)) (Valipour, Shaligram and Kulkarni, 2014). Alpha, beta and gamma are usually observed during consciousness whereas delta and theta are observed during unconsciousness (Valipour, Shaligram and Kulkarni, 2014).

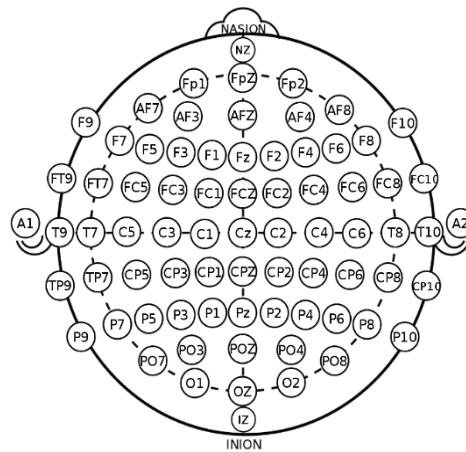


Figure.1.9. Internationally recognised electrode placement 10-20 system where '10' and '20' represent the distance between the neighbouring electrodes. The position of the electrodes is determined by two anatomical positions the nasion, found between the eyebrows and the inion, a protuberance at the occipital lobe of the scalp. F, T, C, P and O refer to the lobes of the brain: Frontal, Temporal, Central, Parietal and Occipital. The number following the brain location is the hemispheric location. Even numbers refer to positions in the right hemisphere while odd numbers refer to the electrodes in the left hemisphere. The 'z' refers to the electrodes down the midline.

(image used with permission from https://commons.wikimedia.org/wiki/File:International_10-20_system_for_EEG-MCN.svg) [Accessed 3 April 2021]

Of importance for this work, EEG is also used to measure SEPs which are produced following a stimulation of a neural tract (Valipour, Shaligram and Kulkarni, 2014). These measurements evaluate SCI sensory impairment neurophysiologically.

The amplitude of the SEP peak amplitude is around 10 μV , therefore, it is essential to ensure high quality low noise data capture and the use of signal averaging (Valipour, Shaligram and Kulkarni, 2014; Markand, 2020; Aminoff, 2012). Care also needs to be taken on what recording format is used as SEP amplitude will vary depending on whether it is recorded between an electrode and a common reference or between two pairs of electrodes, these are known as monopolar and bipolar, respectively (Aminoff, 2012). The common reference point usually is placed on the ear but it can also be placed on the head (Aminoff, 2012).

Moreover, in order to achieve good quality signals from the scalp the electrode impedance needs to be below 5 $\text{k}\Omega$ (Ferree et al., 2001). If the impedance of the electrode is high, then the resistance of current flow is high. This leads to a low signal/noise ratio in the EEG signal. Therefore, properly cleaning the scalp with abrasive gels to remove the dead skin cells and then using electrolyte conductive gel is an essential procedure to lower the impedance (Ferree et al., 2001). This cleaning technique allows to electrically bridge the scalp and the electrode (Ferree et al., 2001). It is time consuming and uncomfortable for the patient, especially when recording from many channels (Taheri, Knight and Smith 1994).

There are also dry active electrodes that do not need any skin preparation or conductive gels (Taheri, Knight and Smith 1994). These electrodes are much faster to set up and have a better signal/noise ratio (Taheri, Knight and Smith 1994). They are beneficial to use for long-term continuous recording. However, active electrodes in general do not perform better than passive electrodes based on current technology.

Also, for EEG recordings it is important to be aware of the two main sources of noise: noise from the environment or physiological noise and noise within the brain from various other processes taking place. Physiological noise includes: blinking, facial muscle movements and swallowing. Environmental noise originates from electrical equipment generating 50 Hz or 60 Hz noise. To manage external noise, it is best to eliminate these sources of noise from the recording area such as cell phones, laptops, transformers or other equipment. Furthermore, electrostatic potentials can arise when moving in the area where recordings are being taken (Mathewson, Harrison and Kizuk 2017; Aminoff, 2012). To control internal noise, it is essential to ask the

participant to remain relaxed while recordings are being taken (Ozkul and Uckardes, 2002).

1.10.2. Somatosensory evoked potentials (SEPs)

Electrical activity in the brain can either be measured using continuous EEG or as a form of an evoked potential in response to a triggered event. The evoked potential is time-locked and occurs following a sensory peripheral stimulus which may repeat to allow signal averaging. The amplitude of the evoked potential is very low around $0.1 \mu\text{V}$ to $10 \mu\text{V}$ and requires for the signal to be amplified and processed (Markand, 2020). Figure.1.10 displays a diagram of the equipment used to record and

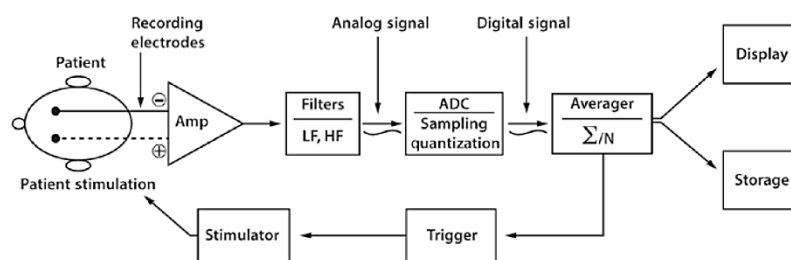


Figure.1.10. Equipment used to record evoked potentials. The data is recorded using recording scalp electrodes. Then the recordings are amplified and filtered. The ADC converts the signal to a digital signal and then several signals are averaged. The averaged signal is then converted to an analog waveform to be visualised on the monitor. The analysis of the evoked potential can then be performed. Amplifier (Amp); LF (low-frequency); HF (high-frequency); ADC (analogue-to-digital converter). (diagram used with permission from Markand, 2020)

process evoked potentials. The main challenge of evoked potential recordings, also mentioned above, is the signal/noise ratio which is further reduced by averaging several evoked potentials with respect to the stimulus on set times (Markand, 2020). It is important to keep in mind that the evoked potential waveform is time-locked to the stimulus while noise is random (Markand, 2020). The noise decreases proportional to the number of epochs in an average (Markand, 2020). Furthermore, there may be artefacts such as blinking, muscular movement or swallowing as they are not time-locked to the stimulus their effect is diminished with averaging. Nevertheless, it is good practice to scan through the data and reject any epochs with artefacts prior to averaging.

In SCI, SEPs are a non-invasive neurophysiological assessment tool that allows scientists and clinical professionals to study the functional integrity of CNS pathways that carry sensory information from periphery to the cortex (Macerollo et al., 2018).

Sensory fibres carry information of light touch, vibration and proprioception. The information ascends via the dorsal column of the spinal cord following the presentation of a peripheral stimulus (Macerollo et al., 2018). Usually the median nerve and posterior tibial nerve are stimulated. Other nerves include: the ulnar, radial and peroneal (Macerollo et al., 2018).

SEPs have been recommended to be used in the clinic as a neuronal processing tool throughout the recovery stages following a SCI but only a small number of international centres with clinical neurophysiology expertise do this test regularly. There is a close clinical collaboration among several spinal cord injury centres in Europe (EMSCI) that work together to standardise the use of a wide-range of assessment tools to evaluate SCI and monitor recovery. EMSCI highlighted the importance of including functional tests that evaluate endurance, gait speed, functional mobility and the amount of assistance required from devices as well as the use of neurophysiological tools (SEPs, MEPs and nerve conduction studies) to study ascending and descending spinal pathways when assessing and monitoring SCI (Curt, Schwab and Dietz, 2004).

Before taking SEP measurements, age, height, , upper limb length and weight are parameters considered in research studies as they can influence SEP components (Poornima et al., 2013). SEPs involve repetitive transcutaneous stimulation of a sensory or mixed sensory/motor peripheral nerves. If the nerve is both sensory and motor the stimulation should be calibrated to the motor threshold. Motor threshold is the minimum stimulation strength that causes a visible muscle twitch. In contrast, for pure sensory nerve the stimulus intensity needs to be around 2 to 3 times the sensory threshold, a parameter that is difficult to obtain in patients with sensory loss (Kalogianni et al., 2018). Generally, mixed nerves are preferred because they trigger a reproducible muscle twitch response that can be quantified and controlled (Macerollo et al., 2018).

While stimulating the periphery, changes in voltage are recorded using non-invasive surface scalp electrodes placed on the corresponding brain area. Recording sites for median SEPs are found on the contralateral side of the brain, either around the C3 area or C4 area of the international recognised 10-20 system (Poornima et al., 2013). For median nerve stimulation, the anode is placed proximal to the palmar crease and the cathode 3 cm proximal to the anode between the tendons of the palmaris longus. Monophasic square waves are delivered at a sufficient intensity in order to produce a visible muscle twitch of the thumb (Poornima et al., 2013). The SEP waveform occurs within 50 and 1000 ms or more. Epochs are averaged to increase the signal/noise ratio and reveal the phase locked components in the EEG signal (Poornima et al, 2013). The components of an evoked potential are designated either as P or N waves and these denote a positive or a negative polarity, respectively. As you can see from Figure.1.11, the negative wave is usually plotted upwards and the positive wave downwards. The number following the P or N is the latency of the wave peak measured in msec. The Figure.1.11, demonstrates several median nerve SEPs recorded at different recording derivations (i.e. CPc-CPi) and the associated

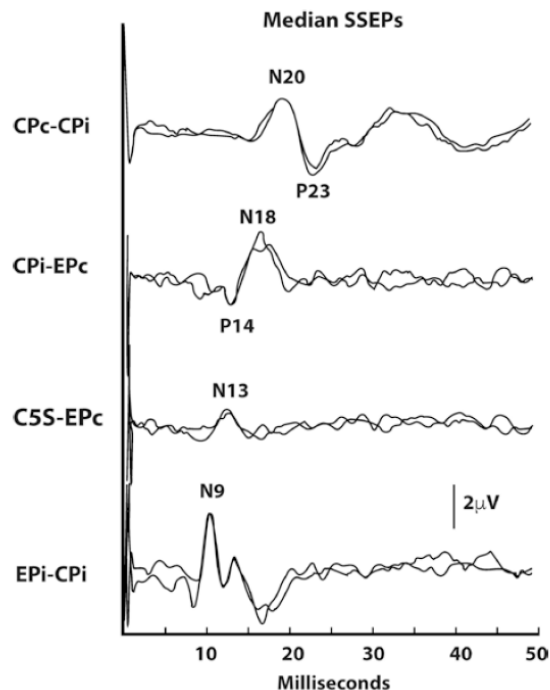


Figure.1.11. Normal median SSEPs indicating certain components (N9, N13, N18, N20, P23). N9 is the brachial plexus potential, N13 is the cervical cord potential, P14 and N18 are subcortical potentials and N20 and P23 are cortical potentials. (graph used with permission from Markand, 2020, p. 156)

components (i.e. N20). For standardisation purposes it is important to stimulate at the same anatomical position when repeating SEP measures or if making comparisons between patients. Example sites include the finger where the anode is placed at most distal phalange of the finger, the cathode at the second most distal phalange and the inter- electrode distance is approximately 1 cm (Kalogianni et al., 2018). If the lower limb is studied usually the posterior tibial nerve is stimulated. For posterior tibial nerve stimulation, the cathode is placed between the Achilles tendon and the medial malleolus while the anode is placed 3cm distal to the cathode (Cruse et al.,1982). Recording sites are found at Cz, CPz and Fz area of the 10-20 system (Tzvetanov, Rousseff and Milanov, 2003).

SEPs are used to evaluate the peripheral nervous system and localise the anatomical site of somatosensory pathway lesions. Short latency SEPs (SSEPs) refers to the portion of SEP that occur within 25 ms for median nerve stimulation and 50 ms for posterior tibial nerve stimulation (Tzvetanov, Rousseff and Milanov, 2003). The recording is composed of peaks and troughs (Figure.1.11). There are several parameters of the waveform that can be analysed such as latency, peak to peak amplitude and peripheral or central conduction time (Macerollo et al., 2018). These measurements are used to examine changes in neural activity (Poornima et al., 2012). More information on this will be provided in Chapter 3.

1.10.3. Transcranial magnetic stimulation (TMS)

SEPs are useful in assessing the conduction and excitability of the DCML ascending sensory tract. In contrast, TMS provides information on the conduction and excitability of the CST in healthy subjects and patients with neurological conditions including SCI. In complete SCIs, MEPs are abolished below the level of the lesion while for incomplete injuries it disturbs the conduction of the signal through the CST resulting to slow and/or reduced amplitude MEPs. TMS also has many other applications. For instance, it is used as a treatment for major depressive disorders and bipolar disorder (O'Reardon et al., 2007; Agarkar et al., 2011). In addition, it may be used for its potential to alleviate neuropathic pain (Klein et al., 2015).

TMS is a non-invasive neurophysiological technique that is commonly used to activate motor areas of the brain. It involves stimulating the motor cortex either with a single pulse or repetitive pulses. Brain stimulation with the magnetic coil results in a muscle twitch at the corresponding muscle innervated by the activated brain region (Figure.1.12). The muscle twitch or its EMG recoding known as the MEP is measured by surface adhesive EMG electrodes placed over the muscle belly (Hallett, 2000; Groppa et al., 2012). The MEP is a measure of cortical and corticospinal excitability (Eldaief, Press and Pascual-Leone 2013).

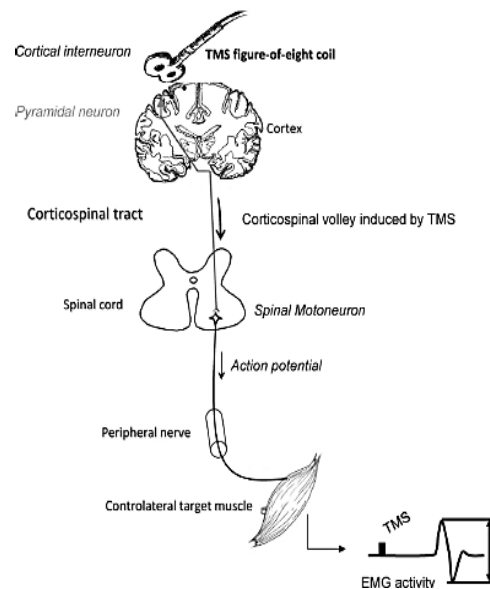


Figure.1.12. Transcranial magnetic stimulation (TMS). The coil is placed over the motor cortex and it produces an electric current that penetrates the brain and activates pyramidal neurons. These neurones evoke descending volleys through the corticospinal tract to the motoneurons where surface electrodes on the muscle belly measure muscle activity. The response that is measured is called a MEP. (reproduced with permission from Klomjai, W., Katz, R. and Lackmy-Vallée, A. (2015). Basic principles of transcranial magnetic stimulation (TMS) and repetitive TMS (rTMS), Annals of Physical and Rehabilitation Medicine, 58(4), pp. 208–213. Copyright © 2015. Elsevier Masson SAS. All rights reserved.).

The pioneers of MEPs are Penfield and Boldrey who localised motor function in the cerebral cortex in 1937 by opening the skull and directly stimulating the brain in conscious patients. In 1980, Merton and Morton were the first to measure non-invasive MEPs from conscious patients by using surface scalp electrodes that delivered electrical stimulation to the brain (Merton and Morton, 1980). This technique is referred to as transcranial electrical stimulation (TES), and provides direct stimulation of neurons also known as direct waves (D-waves) (Nakamura et al.,1996). TES requires electrodes being placed directly on the skin and is both uncomfortable and

painful for subjects as it requires a high intensity of stimulation since the current flow is attenuated by tissue (Ellaway, Davey and Ljubisavljevic, 1999). Furthermore, it activates local small myelinated axons and unmyelinated axons of free nerve endings in the skin resulting in pain (Ellaway, Davey and Ljubisavljevic, 1999; Hallett, 2000; Rossini et al., 2015; Merton and Morton, 1980).

Baker et al. at the University of Sheffield in 1985 developed the world's first TMS, creating a non-invasive and painless test that is used today in the clinic to assess CST excitability (Hallett, 2000; Rothwell et al., 1991). The TMS copper coil is well insulated using plastic and it is placed on the scalp at the region where the brain motor area is located, which is near Cz (Groppa et al., 2012). For stimulation, the experimenter selects the strength of the stimulus and presses a switch to discharge the capacitors (Ellaway, Davey and Ljubisavljevic, 1999). The advantage of TMS is that it can penetrate tissues regardless of their electrical resistance. The stimulation uses the same mechanism as electrical stimulation. They both induce an electrical current in neuronal tissue (Groppa et al., 2012). Furthermore, the magnetic coil does not need to touch the scalp and thus, preparation of the skin is not required. However, it is recommended to place the coil directly on the scalp since any increase in distance decreases exponentially the electromagnetic field induced in the brain (Groppa et al., 2012). A limitation is that the current produced by the coil also heats it up, which can degrade coil performance during repetitive TMS stimulations (Rossi et al., 2009). To combat this problem, coils with cooling systems have been developed.

As mentioned, during stimulation the device discharges a capacitance through the coil (Rothwell et al., 1991). TMS works by Faraday's law of induction where the rapidly changing magnetic field from the coil, which reaches an electric current of 2 Tesla in less than 1ms, induces an electric field in the brain (Ginhoux et al., 2013; Hallett, 2000; Rothwell et al., 1991; Groppa et al., 2012). As a result of the electromagnetic field individuals with metal fragments or electronic device implants should not be exposed to TMS (Fang et al., 2019).

Following stimulation, the electric field in the brain leads to either the depolarization or hyperpolarization of neurons. When these neurons are depolarised it either causes anterograde or retrograde propagation of action potentials. The action

potential induced in cortical axons is propagated to cortical and subcortical areas, travelling along the CST and the peripheral motor nerve (Groppa et al., 2012). More information is available in Chapter 5.

The TMS stimulus pulse can be monophasic which involves a strong current flow with a magnetic field of 1 to 2.5 Tesla at around 50 μ s and the return of a dampened current that has no effect in the brain or biphasic which is similar to the cosine wave, a rise followed by the reverse current and a rise again (Groppa et al., 2012). The monophasic pulse activates one type of neuron whereas the biphasic is capable of activating both inhibitory and facilitatory neuronal populations (Arai et al., 2005). Furthermore, having a fixed stimulating intensity, a biphasic single stimulus creates a larger peak-to-peak amplitude compared to monophasic (Arai et al., 2005; Di Lazzaro et al., 2001).

The intensity of the TMS pulse can affect the focality of stimulation. For instance, a stronger TMS pulse activates a greater area of neuronal tissue compared to a weak pulse. This means higher stimulation intensities are less region specific (Knecht et al., 2005). It is important to mention that a lower stimulus intensity is needed to activate the hand area, whereas a higher intensity is required to activate leg area. This is because the latter is found deeper in the brain at the interhemispheric fissure which is 3 cm in distance from the scalp where the coil is placed (Groppa et al., 2012). As the distance between the coil and the target area increases the intensity of stimulation also needs to increase because the strength of the electric field in the brain is attenuated with an increase in distance and this in turn affects the focality of stimulation (Deng, Lisanby and Peterchev, 2013; Groppa et al., 2012; Knecht et al., 2005).

There is a range of coil shapes available giving scientists a choice depending on whether they desire depth of penetration or focality (Deng, Lisanby and Peterchev, 2013). Available coils include: round coil of variable diameter, figure-of-eight coils and the double-cone coil (Figure.1.13). The round coil was the first non-focal coil manufactured (Ellaway, Davey and Ljubisavljevic, 1999; Deng, Lisanby and Peterchev, 2013). In this coil, coil orientation changes the magnetic stimulation from clockwise to anticlockwise. A clockwise current favours the activation of muscles on

the left side of the body whereas anticlockwise current activates better muscles on the right (Figure.1.14) (Rothwell et al., 1991).

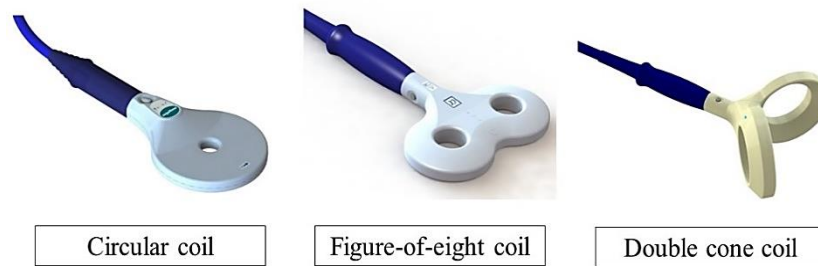


Figure.1.13. TMS coils. (images taken from the Magstim website with permission from <https://www.magstim.com/row-en/product-category/coils/>) [Accessed on 18 January 2021]

A focal coil design was first developed by Ueno et al. in 1988, which involved a pair of circular coils with time-varying magnetic fields where their current travels in opposite directions. The largest current is located at the intersection of the two circular coils (Ueno, Tashiro and Harada, 1988). Then Yunokuchi, Cohen and Cuffin improved the figure-of-eight coil design by making it more focal and smaller (Cohen and Cuffin, 1991; Yunokuchi and Cohen, 1991; Ellaway, Davey and Ljubisavljevic, 1999). Furthermore, rotation of this coil by 180° changes the current direction at the stimulating site (Figure.1.14) (Groppa et al., 2012). The double-cone coil is specifically used to stimulate deeper in the cortex at the central sulcus and thus an attractive coil for lower limb muscle activation. It is similar to the figure-of-eight coil but the windings are angled by 100 degrees (Ellaway, Davey and Ljubisavljevic, 1999). It is placed to encompass the participants head between the two coils (Terao and Ugawa, 2002). To stimulate the hand area, the juncture of the figure-of-eight coil is placed 5 cm lateral and around 1 cm anterior to the vertex (Groppa et al., 2001). It is important to angle the coil 45 degrees to the parasagittal plane so the electrical current runs perpendicular to the motor area in the precentral sulcus (Groppa et al., 2001). Figure.1.14 provides a diagram for stimulating the first dorsal interosseous muscle of the hand using either the round coil or figure-of-eight coil. Other common muscles studied on the upper limbs are abductor pollicis brevis, abductor digiti minimi, flexor carpi radialis, extensor carpi radialis, biceps and deltoid (Groppa et al., 2001).

As mentioned earlier MEPs in leg muscles are challenging to obtain because of their representation in the brain, deep in the cortex. The motor area for the leg is around 1cm to 2 cm to the midline posterior to the vertex (Groppa et al., 2001). The stimulation threshold is higher compared to the upper limb in order to reach the cortex area assigned to lower limb muscles. A good muscle to target in the leg is the tibialis anterior because of its larger representation in the motor cortex compared to other leg muscles (Groppa et al., 2001). For lower limb activation, the double-cone coil is most frequently used (Kesar, Stinear and Wolf, 2018).

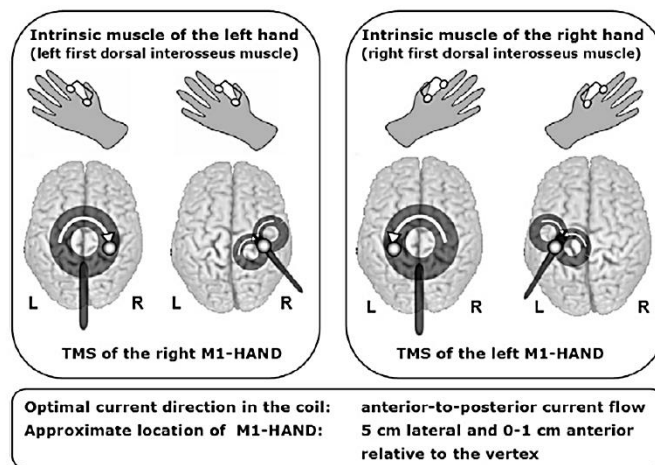


Figure.1.14. TMS to activate the first dorsal interosseus muscle (FDI) using either the round coil or figure-of-eight coil on the left hand and right hand. The arrows show the direction of current flow. Primary motor cortex (M1). (illustration used with permission from Groppa et al., 2001)

1.10.3.1. Reliability of MEPs

The reliability of TMS evoked responses is affected by many factors including: background activation of muscles, error in coil positioning, habituation effect (a decrease in response to the stimulus resulting from repetitive stimulations) and constant fluctuations in neuronal excitability at the time of stimulation (Kesar, Stinear and Wolf, 2018; Darling, Wolf and Butler, 2006; Kiers et al., 1993). Reliability has been tested by the test-retest method and assessed using the intra-class correlation coefficient (ICC) (Ngomo et al., 2012; Carroll, Riek and Carson, 2001; Malcolm et al., 2006).

Overall, reliability estimates of experimental data are very important for research as it allows the experimenter to decide if the measurements have value, by determining instrumental and/or rater reliability (Bruton, Conway and Holgate, 2000).

To accurately describe reliability, included here is the definition from Oxford English dictionary: reliability is *'the degree to which the result of a measurement, calculation, or specification can be dependent on to be accurate.'* (Oxford English dictionary, 2021). Reliability is mathematically calculated as follows: $reliability = \frac{\sigma_s^2}{\sigma_s^2 + \sigma_e^2}$ where σ^2 = variance, s= subject, e= error (Streiner, Norman and Cairney, 2015, p.159).

The ICC index measures reliability by taking into consideration both the degree of consistency and agreement among ratings (Streiner, Norman and Cairney, 2015, p.9-10; Burton, Conway and Holgate, 2000). It is different to the Pearson correlation that only considers the degree of covariance. ICC is a statistical tool that measures the reliability in test-retest intrarater and interrater reliability within a class of data and has a value between 0 to 1 where 1 relates to excellent reliability (Koo and Li, 2016). Please refer to Figure.1.15 from Koo and Li (2016) that uses a flowchart to nicely describe the process of choosing the best-suited ICC model for analysis.

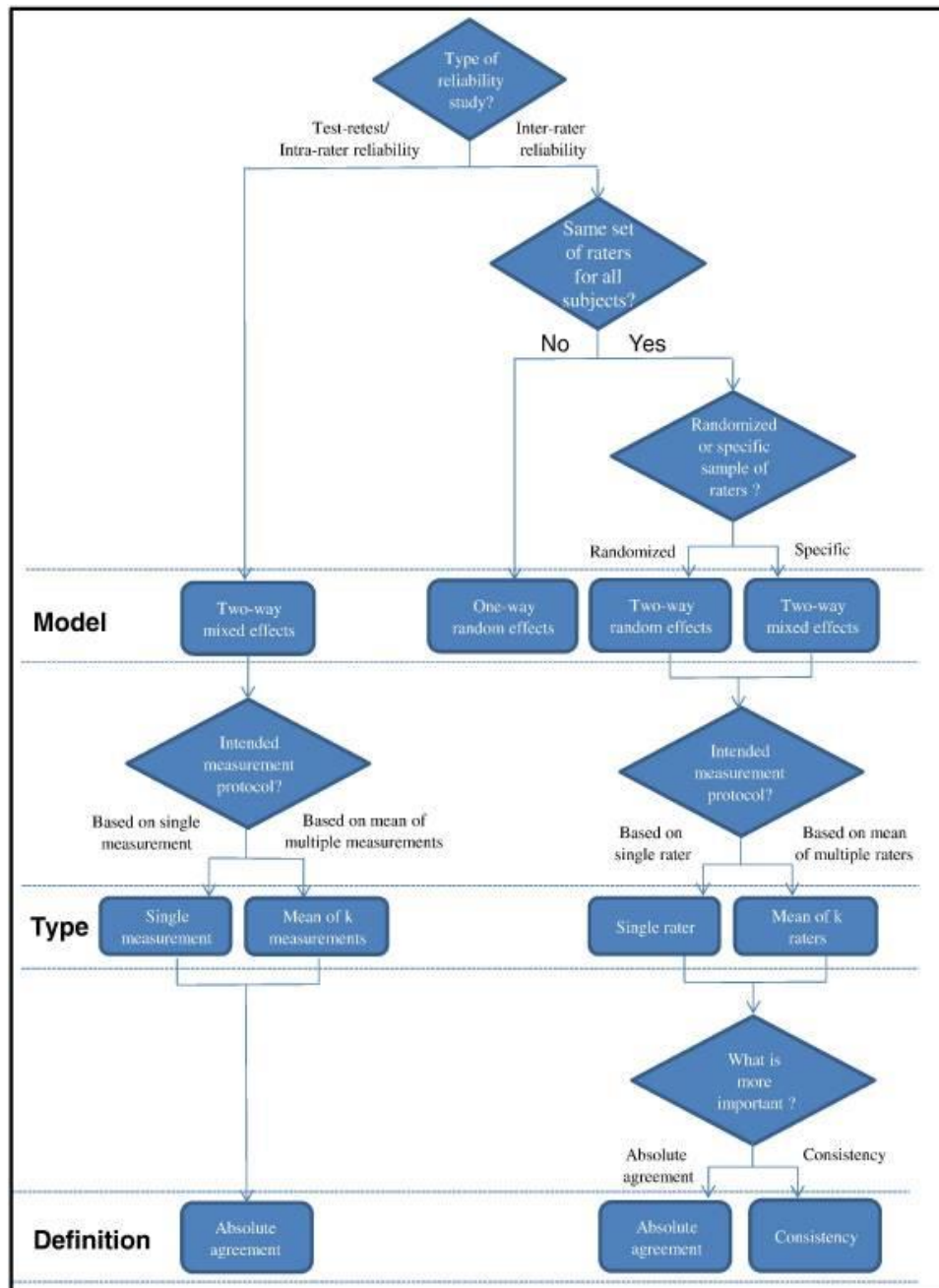


Figure.1.15. Flowchart for choosing the intra-class correlation coefficient (ICC) model suitable for your analysis. (diagram used with permission from Koo and Li, 2016)

ICC was developed by Fisher in 1954 (Fisher, 1954; Koo and Li, 2016). Generally speaking, in ICC, random errors needs to be small enough, so that the experimental results are not masked (Liljequist, Elfving and Roaldsen, 2019; Bruton, Conway and Holgate, 2000). When unwanted variance is large the ICC value will be

below 0.5 which means that the study has poor reliability (Liljequist, Elfving and Roaldsen, 2019; Koo and Li, 2016). When reporting ICC usually studies report the ICC value along with the 95% confidence interval (Koo and Li, 2016).

Malcolm et al. in 2006 observed that size, location and excitability of MEPs are overall reliable measures (also suggested by other studies) but they are directly affected by the muscle being studied (Ngomo et al., 2012; Carroll, Riek and Carson, 2001; Malcolm et al., 2006). Furthermore, to obtain scientifically reliable TMS data, studies need to take into consideration the unique size and shape of the cranium and the location and orientation of the anatomical structures in the brain of the individual (Ginhoux et al., 2013; Ruohonen and Karhu, 2010; Fang et al., 2019). Usually, the positioning of the coil is based on external landmarks on the head and by trying to find the best coil position using trial and error (Fang et al., 2019). This technique is restricted to a two-dimensional grid of its bony landmarks, and this causes a distortion when a three-dimensional map is embodied on a two-dimensional coordinate system (Krings et al., 2001). The variability of structural anatomy among subjects makes it challenging to compare subjects and establish structure to function correlation (Krings et al., 2001). Furthermore, a small change in the location, orientation or angling of the coil on the scalp can lead to significant changes in the electric field produced in the brain up to a factor of two (Danner et al., 2008; Knecht et al., 2005). The following section will discuss advantage of using navigated TMS systems (nTMS).

1.10.3.2. Navigated TMS

In clinical applications it is important for TMS stimulation to be accurate and reproducible. nTMS is an attractive option which guides the magnetic coil position with respect to the cortex in real time (Ginhoux et al., 2013; Ruohonen and Karhu et al., 2010; Hannula et al., 2005; Harquel et al., 2017). It commonly uses magnetic resonance images (MRI) and considers the geometry of the head to create a 3D cortex mapping model. The head geometry is obtained using a digitised pen to identify and mark out specific landmarks (Fang et al., 2019). Then the MRI image is aligned with the head geometry (Fang et al., 2019). Head location and movement as well as the location, orientation and angling of the coil are monitored using markers that are tracked using motion capture equipment (Ruohonen and Karhu, 2010; Sandro, 2017,

p. 4). This allow for a graphical interface of the position of the coil with respect to the participant's cortex to be created and visualised. In addition to these parameters, it also considers the shape and wiring of the copper coil. With this information the distribution and strength of the intracranial stimulating field can be calculated in real time (Hannula et al., 2005). Furthermore, this navigated system can save the desired location of the coil and thus, stimulation can be made reproducible (Harquel et al., 2017; Hannula et al., 2005). Figure.1.16 nicely illustrates what has been explained above regarding nTMS.

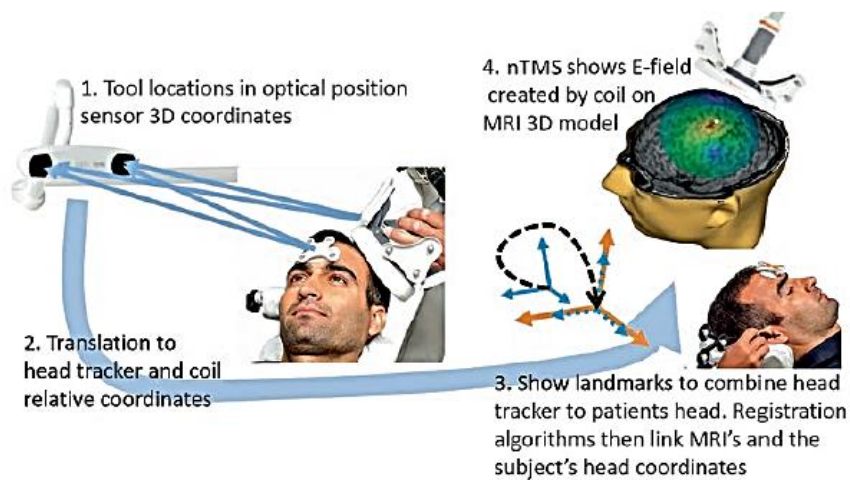


Figure.1.16. Navigated TMS (diagram used with permission from Sandro, 2017)

Motor mapping using nTMS can be used prior to surgery has shown to produce higher survival rates in patients with brain tumours and can be paired with diffusion tensor imaging fibre tracking (DTI-FT), a technique that is able to show white matter subcortical pathways (Raffa et al., 2016; Rizzo et al., 2014; Picht et al., 2013; Fang et al., 2019). The next step in innovation is the TMS coil controlled by a robotic arm such as the one seen in Figure.1.17 by Axilum robotics.



Figure.1.17. Axilum Robot. (image used with permission from <http://www.axilumrobotics.com/en/tms-robot-features/>) [Accessed on 10 March 2020].

An alternative navigation system for TMS, is known as StimTrack, an open-source software written in C++ language, and used for manual TMS coil positioning within and between sessions (Ambrosini et al., 2015). Moreover, it is compatible with all types of coils (Ambrosini et al., 2015). It uses an optical tracking system called Polaris Vicra and reflective markers. Reflective markers are placed on the participant's forehead and the stimulating coil to monitor the position of the coil relative to the head (Ambrosini et al., 2015). The accuracy of the coil is around 0.7 mm for translation and $<1^\circ$ for rotation which is similar to the manual navigation systems that are available, such as Brainsight (Ambrosini et al., 2015). Furthermore, this software responded with an ICC value of 0.9 for intra- and inter-session reliability (Ambrosini et al., 2015). Furthermore, Peri et al. (2017) used this system to study the intra- and inter-session reliability of rapid TMS stimulation. The study was conducted on 24 healthy participants and measured the motor threshold, area under the stimulus response curve, the maximum MEP, stimulation intensity midway MEP max and MEP min (I50), the slope in I50, MEP latency and silent period. For these measurements the study reported an ICC value of around 0.8 to 0.9 (Peri et al., 2017).

To conclude, neurophysiological tests are adjacent assessments above physical examination for clinical prediction and monitoring of functional recovery following SCI. Neurophysiological tests can be used even within 2 weeks following SCI and can give useful information regarding the completeness of injury that cannot be judged simply by manual muscle testing. Also, they provide means to study plasticity during recovery or rehabilitation.

1.11. Ways to induce neuroplasticity in SCI

The consequences and degree of recovery following SCI is dependent on the site of injury, the extent of the insult (incomplete or complete SCI), the age of the patient as well as access to appropriate rehabilitation training. SCI disrupts axonal pathways causing impairments in sensory, motor and autonomic functions below the site of insult. The focus of rehabilitation is on the recovery of circuits that were lost following SCI (Fawcett et al., 2006). The CNS is capable of plastic changes or structural remodelling such as normalization of reflexes, axonal/dendritic sprouting, neurogenesis, synaptogenesis, upregulation of neurotransmitters/neurotrophic factors and alterations in gene expression (Lynskey, Belanger and Jung, 2008).

Exercise, cell transplantation, anti-inflammatory drugs and electrical stimulation are some of the methods that encourage neuroplasticity (Lynskey, Belanger and Jung, 2008). Exercise promotes recovery in motor function for both SCI and stroke patients (Sandrow-Feinberg and Houlé, 2015; Langhammer et al., 2014). Animal models of SCI have implied that brain-derived neurotrophic factor (BDNF) is upregulated following exercise. This is a neurotrophic factor that binds to tyrosine kinase B receptor (TrkB) and is associated with encouraging neuroplasticity, neuroprotection and neuronal growth (Garraway and Huie, 2016). BDNF may also be associated with the IHT and more on this will be discussed later in the report. Other means of promoting recovery is the use of functional electrical stimulation (FES) which has been shown to improve intralimb coordination in overground gait training (Lynskey, Belanger and Jung, 2008). It triggers a variety of cellular and molecular pathways and there is evidence that it may also upregulate of BDNF and TrkB expression (Al-Majed, Brushart and Gordon, 2004).

Other possible approaches for rehabilitation of the elderly group of patients are cell transplantation and pharmacological interventions. Cell transplantation approach focuses on replacing lost or damaged cells following the injury or enhancing regeneration at the site of injury by secreting high concentrations of neurotrophic factors (Li and Lepski, 2013; Dasari, 2014). This is accomplished by transplanting a wide variety of stem cells, neural progenitors and glial cells (Li and Lepski, 2013; Dasari, 2014). Embryonic stem cell-derived neural stem/progenitor cells (NS/PC)

have shown to replenish lost neurons and glia, but an immune response can reject the graft. However, there are also ethical concerns with the use of embryonic stem cells. In contrast, pluripotent stem cell-derived NS/PC may that are generated from adult somatic cells and then differentiated to NS/PC lead to tumour formation due to their proliferation capacity (Deng et al., 2018). Overall, despite the promise of future treatments there is currently no effective and safe treatment using stem cells for SCI recovery.

In terms of pharmacological interventions, there are currently no drugs available that facilitates sprouting of severed axons but researchers are studying potential drug targets. For instance, the use of epothilone D has been shown to promote regrowth of severed axons by reducing the production of inhibitory factors at the lesion scar (Tica, Bradury and Didangelos, 2018). Another example is the use of the chondroitinase ABC enzyme that degrades inhibitory chondroitin sulphate proteoglycans (CSPGs) (Rosenzweig et al., 2019). CSPGs affects negatively the repair process of the SCI lesion scar by affecting processes such as neural survival and synaptogenesis (Karimi-Abdolrezaee et al., 2010). Furthermore, the combination of transcriptomics, proteomics and bioinformatics have been used to identify possible drug candidates for SCI therapy (Tica, Bradury and Didangelos, 2018). Another way to encourage plastic changes, without the need of vigorous rehabilitation, is potentially IHT. During this treatment, the patient sits comfortably while they breathe, through a mask, various concentrations of oxygen provided by a normobaric hypoxia machine.

1.12. Rehabilitation methods

Rehabilitation for SCI patients is vital since paralysed muscles and bones undergo atrophy (Hamid and Hayek, 2008). As a result of osteoporosis, fractures occur during bed transfer and falls increasing morbidity and mortality rates causing high healthcare costs (Jiang, Dai and Jiang, 2006). Furthermore, a sedentary lifestyle increases the likelihood of the patient developing hyperlipidaemia, obesity and diabetes. This can result in cardiovascular disease (Myers, Lee and Kiratli, 2007).

Following SCI, the functions below the level of injury are disrupted. The amount of residual function that remains depends on the level of injury and whether it is complete or incomplete. For instance, a lesion in the cervical level leads to tetraplegia while a lesion in the thoracic level leads to paraplegia (Marino et al., 2003; Wong, Shem and Crew, 2012). For more detailed examples please refer to Chapter 1 Section 1.6. where it explains different levels of spinal lesions and the associated complications.

Table.1.3. Spinal cord injury rehabilitation approaches (table used with permission from Pons, Raya, González, 2016, p.70)

Severity	Treatment	Goal	Current state
Complete SCI (AIS A)	Compensation by assistive devices (such as BCI)	ADL independence	Established
	Neural repair	Low level of motor function (hand or locomotor)	Still in translation to human
Incomplete SCI (AIS B/C)	Epidural electrical or pharmacological stimulation.	Low level of motor function (hand or locomotor)	Still in translation to human
	FES (Functional Electrical Stimulation) and orthosis	Tenodesis grasp	Established
		Assisted stepping	Established
	ISMS (Intraspinal Microstimulation)	Restore limb function	Still in research
	Intracortical Microstimulation	Restore sensation	Still in research
Incomplete SCI (AIS C/D)	Functional training	Active hand function	Established
		Restricted locomotor function	Established

Activities of daily living, ADL; Brain-Computer Interphase (BCI)

The priority needs of a tetraplegic patient are different to a paraplegic patient, one is interested in recovering upper limb function so they can perform basic tasks required for daily living while the other is interested in recovering lower limb function and becoming independent (Pons, Raya, González 2016). Therefore, rehabilitation is focussed on recovering function of upper and lower extremities but tailored to the needs of the patient. Restoration of mobility improves performance of daily living activities and most importantly the quality of life. As explained above the severity of injury governs the rehabilitation approaches that are applicable for the patient. For instance, a patient with AIS A, refers to complete SCI. Therefore, assistive devices such as wheelchairs and exoskeletons can be used to help with activities required for

daily living. In contrast, rehabilitation for a patient with incomplete SCI (AIS B/C) will focus on motor function, grasping and restoring sensation (Pons, Raya, González, 2016, p.70). Please refer to Table.1.3 where Pons, Raya, González (2016) clearly list the severity of SCI and treatment methods applicable for each in order to achieve specific functional requirements. The following paragraphs will discuss two treatments available which are: gait training and electrical stimulation.

1.12.1 Gait training

The main form of rehabilitation for SCI is gait training or locomotor training and it is believed that repetitive and intense training can lead to functional recovery (Lam et al., 2012; Harkema et al., 2012). There are a variety of gait training rehabilitation methods for SCI patients such as assisted over-ground training or treadmill training, but these are costly in terms of staff numbers and time. Usually in the clinic, assisted over-ground training is performed requiring staff to provide postural support and assist in guiding the patient's legs during each step. This is difficult and tiring work for both staff and patient, and in those individuals with poor postural control and walking ability multiple therapists may be required to attend in a single therapy session with relatively few steps attained (Swinnen et al., 2010). Overall, intensive gait training incorporating a high number of steps improves posture, balance, standing, and walking (Harkema et al., 2012). Gait training successfully utilises patterned sensory feedback from limb proprioceptors during stepping motion to entrain elements of spinal locomotor central pattern generators (CPGs) even in the absence of corticospinal drive. The CPGs is an intrinsic system of neural networks within the spinal cord that allows autonomous gait-like rhythmogenic activity. In gait training, the patterned rhythmic proprioceptive feedback from limb movement raises the excitability of these networks which over a prolonged period of intensive training (daily for 1 hour over 8-10 weeks) can lead to the improved walking capability (Harkema, 2012, Harkema, 2008, Duysens and Van de Crommert, 1998). Furthermore, gait training improves glucose homeostasis, as glucose is fuel for contracting muscles, and as mentioned earlier diabetes is a risk factor for SCI patients (Phillips et al., 2004).



Figure.1.18. Lokomat device by Hocoma. (image used with permission from [hocoma.com/solutions/lokomat-2/](https://www.hocoma.com/solutions/lokomat-2/)) [Accessed on 19 January 2021]

An example of this form of gait training is body weight-supported treadmill training (BWSTT) which has shown to provide functional recovery in SCI patients (Wessels et al., 2010; Lam et al., 2012). The patient can start this rehabilitation before they can fully bear their weight. It requires therapists to guide their legs in a walking pattern on the treadmill while a harness holds the patient in an upright position (Wessels et al., 2010; Harkema et al., 2012). In a systemic review by Lam et al. 2012, which examined seven articles that used therapist- and robot- assisted BWSTT on iSCI patients, they summarised that the treatment intensity ranged from 60 to 300 minutes per week and the duration of the treatment ranged from 3 to 23 weeks (Lam et al., 2007). In a systematic review by Santo et al. 2015 it was suggested that BWSTT may improve musculoskeletal system function in both acute and chronic stages of SCI patients. BWSTT has been shown to provoke an increase in cross-sectional area of leg muscles by 2.3% to 16.8 % by increasing trophism of type IIa and IIx fast twitch muscle fibres (Santo et al., 2015). These improvements in musculoskeletal system are directly correlated to the enhancement in treadmill performance and walking speed (Santo et al., 2015).

Another form of body supported training is performed in the water, known as hydrotherapy or aquatic/water therapy, and it can be beneficial for spasticity (Zamparo and Pagliaro, 1998; Kesiktas et al., 2004). In addition to reducing spasticity, it has been reported that it improves gait kinematics underwater and cardiorespiratory capacity (Ellapen et al., 2018). In terms of treadmill training, robotic-assisted gait training

devices (RAGT) have been developed. For instance, ‘Lokomat’, an exoskeleton that helps guide the legs during treadmill training (Figure.1.18). It reduces workload on therapist, provides synchronised movement and it is used to assess the progression of motor recovery (Jezernik et al., 2003; Banala et al., 2008).

1.12.2. Electrical stimulation

Other devices that assist in rehabilitation are the wearable electrical stimulation devices. Examples of this are FES devices and their controllers bypasses the spinal cord circuitry by stimulating peripheral nerves to generate a muscle contraction of paralysed muscles. FES is used to stimulate nerves noninvasively rather than directly stimulating muscles because less current is required for nerve stimulation to generate an action potential (Rushton, 2003). Therapeutic benefits of FES include: the ability to provide assistance during standing or walking, improving muscle strength, enhancing flexibility, increasing range of motion and in some cases improving spasticity (Rushton, 2003). Furthermore, it can assist with respiration and bowel or bladder voiding and long-term FES coupled with rowing in chronic complete SCI patients has shown to attenuate bone loss as well as improving cardiac function and fitness (Hamid and Hayek, 2008; Gibbons et al., 2016; Gibbons, Beaupre and Kazakia, 2016). Therefore, there are many applications and benefits of FES. There are also FES robot assisted devices that focus on restoring fine motor skills for tetraplegics. An example includes the Freehand System, initially manufactured by NeuroControl Corporation in USA, that was designed to stimulate muscles of the hand and arm to assist tetraplegic SCI patients with an injury at C5-C6 (Mulcahey et al., 2004).

Another way to deliver electrical stimulation is via an implantable device that sits over the spinal cord itself and can drive locomotor activity, this device is called epidural stimulation. Epidural stimulation activates spinal circuits without the need for direct brain control. For a 23-year-old man with paraplegia from a C7-T1 subluxation, epidural stimulation enabled him to bear his weight and facilitated stepping (Harkema et al., 2011). There is also an option of transcutaneous stimulation that does not require surgery and the complications that may arise. It is important to mention that locomotion is controlled by the central pattern generators whose rhythm generation circuits are located in the lumbosacral spinal cord. Central pattern generators are neural

circuits that have potential to generate rhythmic movements such as walking without the need of a sensory or cortical input. Transcutaneous electrodes are placed on the skin over the lower thoracic and/or lumbosacral vertebrae (Gerasimenko et al., 2015). Similar to epidural stimulation, transcutaneous stimulation leads to rhythmic stepping movements. Furthermore, it has also been shown to be effective in improving spasticity (Sivaramakrishnan, Solomon and Manikandan, 2018). However, this approach to rehabilitation remains experimental and considerable development remains to be done before such devices become part of standard SCI rehabilitation.

1.13. Common tests to study recovery

This section will provide a brief explanation on measurements commonly used in SCI studies to investigate ambulation in SCI patients following an intervention such as electrical stimulation and gait training. They include the six-minute walk test (6MWT) and ten-metre walk test (10MWT) (Alexander et al., 2010). The 6MWT was standardised by the American Thoracic Society Pulmonary Function Standards Committee and measures the distance the patient can cover walking fast for 6 minutes (ATS board of Directors). In contrast, the 10MWT is timed for 6 metres using a stopwatch, two meters before and two meters after are used for acceleration and deceleration (Hirsch et al., 2014).

To study static and dynamic balance in SCI patients, studies use the time up and go test (TUG) (Zakaria et al., 2015; Van Middendorp et al., 2009). This test requires the patient to rise from a chair, walk for 3 meters, turn around, walk back and sit down while measuring the time it takes for the patient to complete this task. This test allows patients to use their assistive walking aids. Furthermore, studies also investigate muscle strength. A type of muscle strength measurement of the lower limbs is the ASIA lower extremity motor scores (LEMs) and these measures have been shown to correlate with ambulatory capacity (Shin et al., 2011). These tests are mentioned here because they have shown to have a good validity and reliability and provide a way to compare autonomy from clinical trials focussed on lower limb recovery of function (Van Middendorp et al., 2009).

1.14. Changing demographics directs research to new rehabilitation approaches

SCI is an irreversible condition that impacts 250,000 to 500,000 individuals annually around the world (WHO, 2013). Several rehabilitation methods were mentioned above and they are pathways for SCI patients to regain mobility and to improve their quality of life. The main treatments available are exercise based, such as locomotor training, BWSTT and resistance training (Gregory et al., 2007; Wessels et al., 2010; Behrman and Harkema, 2000). These forms of rehabilitation are high in intensity, expensive and require dedicated trained staff to get a significant functional improvement (Carpino et al., 2018). Robotic assisting devices have been developed and they do reduce therapist time commitment from therapists as well as their number of therapists required for rehabilitation training. They are therefore more cost-effective than conventional rehabilitation, but they require high levels of activity (Carpino et al., 2018). However, investments in such devices by non-research active clinics remains low meaning that relatively few SCI gain exposure to the best advances in rehabilitation medicine.

As mentioned in Chapter 1 Section 1.2, over the past few years the demographic trend for SCI has changed and predominantly elderly patients with SCI are admitted to hospitals where once were young adults (WHO, 2013; Jackson et al., 2004; Wirz and Dietz, 2012). This has been reported across all developed economies where there has been increased life expectancy and demographic change. Therefore, it is evident that we need a different model of SCI care pathway. A treatment method that has the potential to change SCI care is IHT but even though it has shown to improve motor function in iSCI patients, there is little known about its mechanism of action or its safety.

Intermittent hypoxia: A new rehabilitation method for SCI?

1.15. Intermittent hypoxia: Severe to mild

Intermittent hypoxia is not a new concept. Hypoxia training arose before World War II in the Soviet Union to acclimatise Soviet pilots (Serebrovskaya et al., 2002). However, it is most often associated with a serious medical condition known as obstructive sleep apnea (OSA) (Mahamed and Mitchell, 2007). This syndrome is

described as severe exposures to intermittent hypoxia. According to a review by Dale, Mabrouk and Mitchell (2014) OSA is characterised as 5 to 100 episodes per hour with 10 to 100 s exposures of hypoxia. In contrast, a mild to moderate IHT used to treat iSCI patients involves 15 cycles of repetitive alternating exposures of 1 to 1.5 min of hypoxic ($FiO_2 = 0.09$) and 1 to 1.5 min of normoxic ($FiO_2 = 0.21$) air (Trumbower et al., 2012; Trumbower et al., 2017; Navarrete-Opazo et al., 2017; Hayes et al., 2014).

In OSA the upper airway dimension narrows during sleep leading to frequent pauses in breathing, snoring and several awakenings during the night (Levy et al., 2015). Frequent pauses of breathing causes frequent drops in arterial oxygen. This drop in oxygen damages blood vessels, increases heart rate and increases blood pressure. Medical complications associated with OSA include hypertension, arrhythmias, coronary heart disease, atherosclerosis and stroke (Levy et al., 2015). Treatments for OSA consists of mandibular advancement device that is worn in the mouth during sleep or a continuous positive airway pressure (CPAP) device that pumps air under pressure through a mask to maintain airway patency. Both of these treatment options aim to stop the airway from collapsing during sleep and they can help resolve or ameliorate cardiovascular complications associated with OSA. However, they do not treat the underlying condition which is often linked to obesity and lifestyle.

Unlike the prolonged hypoxia experienced by OSA sufferers, a mild to moderate form of IHT is recently being explored for its potential in inducing plasticity in somatic motor pathways (Mahamed and Mitchell, 2007; Golder and Mitchell, 2005; Mitchell and Terada, 2011; Trumbower et al., 2012). As defined earlier, plasticity is the ability of the CNS to make some adaptive changes in response to a stimulus, such as intermittent hypoxia. The idea to explore the benefits of IHT on motor function in iSCI patients arose following extensive research on IHT's ability to strengthen synaptic inputs to phrenic motor neurons (Trumbower et al., 2012). Subsequently, scientists noticed that IHT provided functional benefits on iSCI patients and assumed that a similar cascade of events that induced respiratory facilitation in animal studies may also stimulate plasticity on somatic motor pathways (Trumbower et al., 2012; Trumbower et al., 2018; Sandhu et al., 2019; Naidu et al., 2020; Hayes et al., 2014;

Navarrete-Opazo et al., 2016b; Navarrete-Opazo et al., 2017; Lynch et al., 2016). The studies, however, have used slightly different IHT protocols as well as different delivering methods of IHT which have made comparisons of results challenging.

1.16. Delivery methods: IHT

Studies either use commercially available automated machines or manual switched pressurised gas cylinder systems to deliver the treatment (Navarrete-Opazo et al., 2017; Tan et al., 2020). The automated device that provides the alternating concentrations of inspired oxygen is known as a hypoxicator. This device delivers breathable hypoxic air with adjustable oxygen concentration, it monitors saturation of oxygen in the blood and ventilation rate and can incorporate a safety cut-off mechanism. The experimenter can also adjust the exposure time to the treatment and level of inspired O₂ prior to training sessions. Automated machines are preferred over manual systems because manual systems have inefficiencies in dose timing, flow rate and fractional inspired oxygen (FiO₂) (Tan et al., 2020).

Some devices have an inbuilt hypoxic test that can evaluate the response of the individual to hypoxia. During the hypoxia test the individual is provided with low oxygen level via a breathing mask connected to the device that provides various concentrations of oxygen (Bassovitch and Serebrovskaya, 2009). The individual breaths through the mask for several minutes until they reach a baseline SpO₂ level, usually around 85% SpO₂, thereafter the inspired O₂ level is returned to normal and the time for the recovery period is recorded. This measure of recovery rate gives the experimenter an idea of the individual's tolerance and reaction to hypoxic air breathing (Bassovitch and Serebrovskaya, 2009). Such methods can be used in clinical assessments in order to adapt the IHT treatment according to subject tolerance to hypoxic exposure.

Tan et al. (2020) completed a study to examine whether the performance of an automated hypoxia machine while controlling the intervals of intermittent hypoxia using a microcontroller is better when compared to a manual system. This study examined the dose timing, flow rate and variation of fraction of inspired oxygen (FiO₂). The manual system requires switching of gas chambers and this can make the

treatment dose inconsistent. This inconsistency affects the ability to compare results between labs (Tan et al., 2020). The overall findings of this study are listed below:

- 1) Less accuracy in dose timing with the manual system because of errors during the switch of gasses. The automated machine had a 63.3% higher IHT dose delivery timing.
- 2) Automated system provided 62.7% greater flow than manual system ($p < 0.001$).
- 3) Variation in FiO_2 was significantly reduced in automated systems that incorporate a mixing chamber as this stabilises the delivery of oxygen during hypoxia and during normoxia.
- 4) Depletion of reservoir bags was observed in the manual system following deep breathing. The automated machine, however, was able to combat this problem by reducing the variation in FiO_2 as gas supply is not limited by bag volumes.
- 5) It may seem that manual systems have no benefit over the automated systems but they have one major advantage which is delivering high precision air mixtures (Navarrete-Opazo et al., 2017; Tan et al., 2020).

Using these methods of delivering IHT, scientists have begun to examine the functional benefits this treatment has on iSCI patients. The mechanism of action on somatic motor pathways, however, is not well understood. Scientists believe it is similar to IHT's effects on respiratory motor neurons.

1.17. Importance of spared serotonergic innervations

Respiratory plasticity, associated with long term facilitation (LTF), was first described by Millhorn and Eldridge (1986). Following repeated stimulation of the carotid body afferents in anaesthetised vagotomised and paralysed cats, Millhorn and Eldridge (1986) observed a long-lasting enhancement of phrenic inspiratory activity that lasted 90 min post-stimulation. Moreover, this long-lasting facilitation in respiration was directly correlated with serotonergic activation (Millhorn and Eldridge, 1986). Therefore, the mechanism for the LTF described by Millhorn and Eldridge (1986) is serotonin-dependent.

Serotonergic neurons or otherwise referred as raphe neurons within the brainstem and their fibres innervate medullary respiratory neurons, phrenic motoneurons in the spinal cord as well as the intercostal, laryngeal and hypoglossal motoneurons (Kinkead et al., 2001). The raphe neurons, once activated, release a neuromodulator serotonin and this neurotransmitter is believed to be essential for respiratory facilitation (Kinkead et al., 2001).

It is suggested by the literature that IHT's mechanism of action is dependent on spared serotonergic innervations but not the maintenance of LTF (Baker-Herman and Mitchell, 2002; Bach and Mitchell, 1996; Lynch et al., 2001; Hoffman et al., 2010; Golder and Mitchell, 2005). To confirm that serotonin innervation is essential Golder and Mithcell (2005) tested a serotonin receptor antagonist (5-HT₂), ketanserin, which abolished LTF in C2 hemisected rats when administered before IHT. Furthermore, Tadjalli and Mitchell (2019) concluded that both 5-HT_{2A} and 5-HT_{2B} subtypes expressed in the cervical spinal cord are essential for phrenic LTF (pLTF) induced by IHT. Moreover, Wu et al. (2020) established that inhibiting 5-HT₇ action potentiates the effect of IHT. This is because 5-IHT₂ receptors activate a different cellular cascade compared to 5-HT₇ (Figure.1.19).

1.18. The mechanism of action

Information on the mechanism of action of IHT originate from studies on rat models that look at the effects of this treatment on respiratory plasticity. The effects of IHT depends on the balance between the G_q and G_s protein receptors for serotonin (Figure.1.19). The Q and S pathways interact by cross-talk inhibition. A moderate level of IHT favours the Q pathway leading to pLTF while a severe dose favours the S pathway. Please refer to Figure.1.19 for more details on these pathways.

In summary, a mild to moderate dose of IHT activates medullary raphe nuclei serotonergic neurons, raises the levels of brain-derived neurotrophic factor (BDNF) and activates tropomyosin-regulated kinase B (TrkB) receptor (Baker-Herman et al., 2004). TrkB is a G-protein coupled receptor that works via phospholipase C pathway and upon activation via mature BDNF, it dimerises and autophosphorylates.

Downstream signaling cascades leads to the synaptic modulation, neuroplasticity, cell survival, axonal elongation and neurite growth (Garraway and Huie, 2016).

Overall, as clearly described, IHT's mechanism of action are dependent on spared serotonergic innervations and the normal role of this transmitter as a neuromodulator of motoneuron activity (Hounsgaard et al., 1987), the production of mature BDNF and the expression of TrkB receptors. The importance of spared serotonergic innervations was previously discussed. In the following section the value of TrkB and BDNF will be considered as well as adenosine 2_A that is capable in trans-activating TrkB.

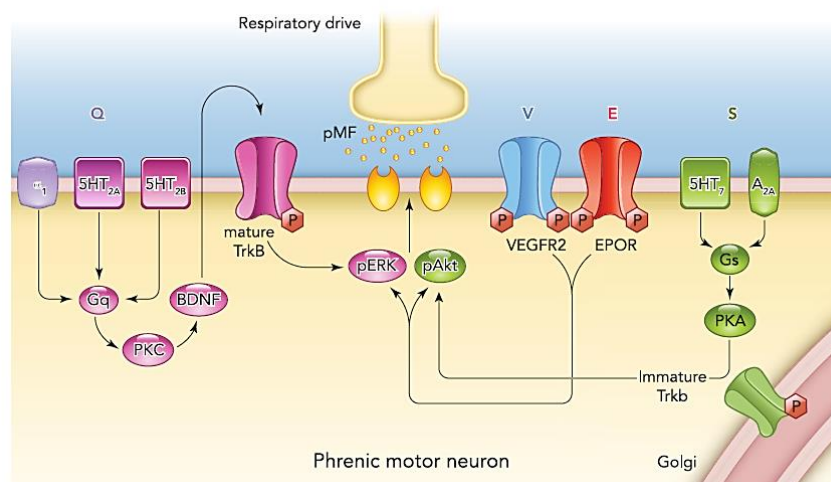


Figure.1.19. These are the cellular mechanisms that are activated by intermittent hypoxia. The Q and S pathways are named after the G-protein couple receptor they are using, G_q and G_s, respectively. In the Q pathway phrenic LTF depends on 5-HT₂ receptors that leads to new synthesis of BDNF and activation of protein kinase C, the increased expression of TrkB receptor and signaling to ERK/MAPK kinases (Dale, Mabrouk and Mitchell, 2014; Kim et al., 2016). Then downstream signaling cascades leads to an enhancement in glutamatergic transmission in the phrenic motor neurons. The S pathway involves the activation of G_s by 5-HT₇ or adenosine 2_A receptors (A_{2A}). This activates protein kinase A (PKA), generates immature TrkB receptors and leads to downstream signaling cascades associated with phosphorylated- AKT (pAkt) (Dale, Mabrouk and Mitchell, 2014; Kim et al., 2016). The Q and S pathways interact by cross-talk inhibition where moderate IHT favors the Q pathway, leading to respiratory pLTF, and severe IHT favors the S pathway, leading to deleterious effects (Hoffman and Mitchell 2013; Fields, Springborn and Mitchell, 2015; Welch et al., 2020). Intermediate IHT dose cancels the two pathways out and does not elicit plasticity (Welch et al., 2020). Another receptor that activates the S pathway is 5-HT₇ and inhibits the activation of the Q pathway by 5-HT₂ receptor (Wu et al., 2020). Inhibiting 5-HT₇ and A_{2A} receptors using an antagonist significantly enhances IHT's respiratory plasticity and further investigations are needed to report whether it enhances non-respiratory motor function (Hoffman et al., 2010; Wu et al., 2020; Welch et al., 2020). (diagram used with permission from Dale, Mabrouk and Mitchell, 2014)

1.19. Respiratory plasticity: Expression of TrkB, BDNF and adenosine 2_A receptor

Expression of TrkB is critical for respiratory plasticity. For instance, selective inhibition of TrkB affects recovery of rhythmic diaphragm muscle activity in adult cervical hemisectioned rats (Mantilla et al., 2014). Furthermore, Martinez-Galvez et al. (2016) used adeno-associated virus (AAV) to locally deliver TrkB to phrenic motoneurons in adult cervical hemisectioned rats and reported recovery of ipsilateral diaphragm muscle. Repetitive exposures of intermittent hypoxia enhance levels of trophic factors, mainly BDNF and vascular endothelial growth factor (VEGF), in respiratory motor neurons promoting LFT and respiratory motor neuron plasticity (Mitchell et al., 2001; Dale-Nagle et al., 2010). It has been shown that the rise in BDNF is dependent on IHT since its effects were inhibited after intrathecal administration of a protein synthesis inhibitor (Baker-Herman et al., 2004). Furthermore, a rat model study found that the highest expression of BDNF mRNA was observed after 2 hours of a hypoxic exposure. The increase in BDNF mRNA was 316% compared to sham (Lindvall et al., 1992). Other studies have also reported an increase in BDNF levels following hypoxia. For instance, Wilkerson and Mitchell et al (2009) reported a 25% rise in BDNF and a 18% rise in phrenic burst amplitude while Baker-Herman et al. (2004) reported 60% and 54%, respectively.

There has also been a focus on adenosine 2_A. This receptor activation mimics the effects of neurotrophins effects on respiratory motor output by transactivating TrkB in the cervical ventral horn (Golder et al., 2008). Golder et al. 2008 reported that transactivation of TrkB receptors with A_{2A} receptor agonists in rat models of cervical SCI resulted into pLTF. However, Hoffman et al. (2010) subsequently reported that while inhibition of this receptor enhances phrenic LTF, suggesting that both serotonin and adenosine pathways, G_q and G_s, respectively, induce phrenic motor facilitation but the serotonin G_q pathway predominates. Furthermore, A_{2A} receptor via cross-talk inhibition restricts serotonin-dependent pLTF following a severe dose of IHT (Golder et al., 2008; Hoffman et al., 2010; Wu et al., 2020; Welch et al., 2020). Refer to Figure.1.19 to view the pathways that are involved.

Following our understanding of some important factors on IHT's mechanism of action for respiratory plasticity the next section will review the BDNF expression in the spinal cord. This will provide a link associated with the functional improvements observed in iSCI following the administration of IHT.

1.20. BDNF and the spinal cord

Following injury of the spinal cord, as described in Chapter 1 Section 1.4, there are a number of factors that inhibit regeneration, one of them being the absence of neurotrophic factors (Jones et al., 2001). BDNF neurotrophic factor is widely studied in SCI models and it is known to be a neuroprotective agent in both the central and peripheral nervous system. BDNF is associated with neuronal development, synaptic transmission and synaptic plasticity (Garraway and Huie, 2016). For instance, Ruitenberget al. (2004) showed in rats that a viral vector-mediated gene transfer of BDNF can reverse atrophy of lesioned neurons in both acute and chronic stages of SCI. In addition, Ji et al. (2015) showed that high levels of BDNF at the SCI lesion declined the immune response by reducing the concentration of proinflammatory cytokines and increasing the expression of anti-inflammatory factors.

Benefits of BDNF have been observed following cervical lesions. For example, Weishaupt et al. (2013) showed that administration of BDNF enhance motor performance in unilateral cervical spinal cord injured rats when combined with rehabilitative training. Significant improvement in corticospinal innervation have also been observed. BDNF delivery into cell bodies of lesioned corticospinal neurons significantly increased collateral sprouting and propriospinal interneuron innervations in the spinal cord (Vavrek et al., 2006). Furthermore, implanting collagen scaffolds with collagen binding BDNF in completely transected spinal cord dogs reported improvement in unassisted standing, locomotion and functional sensory recovery (Han et al., 2015).

1.21. BDNF, IHT and the spinal cord

Satriotomo et al. (2016) used immunohistochemistry and immunofluorescence in spinal sectioned rats that were exposed to acute intermittent hypoxia for 10 weeks and reported an increase in BDNF and TrkB in alpha motor neurons in cervical and

lumbar spinal cord and pyramidal neurons of the primary motor cortex. Similar results were also observed with vascular endothelial growth factor (VEGF). As suggested by Satriotomo et al. (2016) both BDNF and VEGF are regulated by reduction in oxygen levels and their physiological action on central nervous system neurons promotes neuroplasticity, neuroprotection and synaptogenesis.

Furthermore, IHT in combination with motor training in cervical SCI rats resulted in an increase in hypoxia inducible factor-1a (HIF-1a), a hypoxia sensing factor, in spinal neurons of both the cervical and lumbar segments after only one day of IHT treatment with motor training. Similar results were also observed after 7 days of treatment when combined with motor training (Hassan et al., 2018). In addition, both VEGF and BDNF expression were also significantly higher following 7 days (Hassan et al., 2018).

1.22. BDNF missense polymorphism

It is interesting to also mention that around 25% of the human population show a Val66Met missense polymorphism in BDNF (Duman et al., 2016). This polymorphism does not encourage the formation of new neuronal pathways. In clinical research some invasive stimulation protocols work in some SCI patients and not others. There is the possibility that individuals who carry different BDNF allele may influence the IHT responsiveness. For instance, BDNF homozygotes show significantly higher spinal plasticity following direct current stimulation in comparison with BDNF Met carriers (Lamy and Boakye, 2013). However, intensity of training has been shown to overcome the effects of this BDNF mutation (McHughen et al., 2011). Furthermore, it is known that rehabilitation training methods increased levels of BDNF in the spinal cord and in combination with IHT has an additive effect suggesting this combination therapy could possibly also overcome the effects of BDNF mutation in Val66Met polymorphism (Gómez-Pinilla et al, 2002; Navarrete-Opazo et al., 2017). Moreover, researchers have shown that carriers of the Met BDNF allele responded to jump fatigue differently compared to Val66Val carriers following trans-spinal anodal direct current stimulation. These researchers have previously shown that trans-spinal anodal direct current stimulation at the lumbosacral cord induced fatigue-resistance probably through neuromodulation promoting plasticity (Berry et al., 2017).

1.23. Important aspects of IHT protocol

As mentioned IHT actions depend on spared serotonergic innervation, TrkB and BDNF. Furthermore, respiratory plasticity is pattern sensitive, thus, the intermittent aspect is essential as LTF is not observed following continuous exposure to low oxygen levels (Baker and Mitchell, 2000; Millhorn, Eldridge and Waldrop, 1980). Also, the exposure needs to be repetitive over a long period of time in order to result in a long-lasting effect (Fuller et al., 2000). Factors that can affect respiratory plasticity are as follows: age, as younger rats show a greater LTF compared to older rats, and sex hormones, since gonadectomy has shown to attenuate LTF (Zabka et al., 2005).

1.24. iSCI patients with cardiopulmonary complications

Currently, there are several slightly different protocols for IHT interventions that are being investigated by neurophysiology labs. Ultimately, it is essential to explore neural mechanism underpinning the effects seen in order to optimize treatment effect and minimize the risk of adverse events (Trumbower et al., 2012; Hayes et al., 2014; Tan et al., 2020). To create an optimised treatment, we need to consider the above information, but it is also important to take into account that patients with SCI have other underlying conditions.

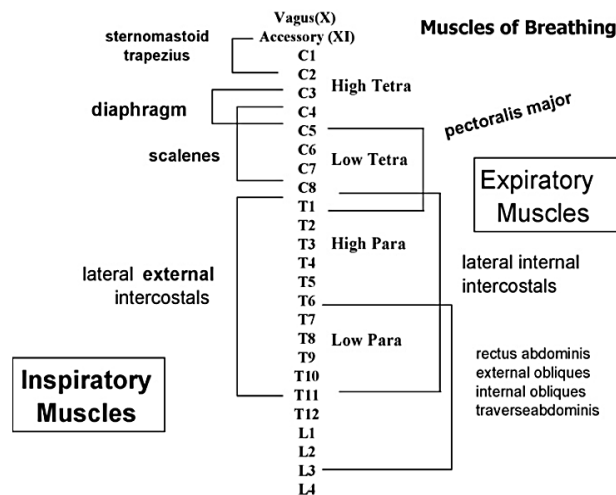


Figure.1.20. Spinal vertebrae and their innervation to inspiratory and expiratory muscles (diagram used with permission from Schilero et al., 2009)

Respiratory complications are the main cause of mortality and morbidity in SCI patients (Zimmer, Nantwi and Goshgarian, 2007; NSCISC, 2019). In a study 68% of subjects with chronic SCI reported respiratory symptoms such as breathlessness, cough, phlegm and wheeze (Spungen et al., 1997). Moreover, according to a review by Schilero et al. (2009) tetraplegic patients have a high prevalence to developing OSA accompanied by secondary cardiovascular complications. Also, patients with cervical and upper thoracic SCI have impaired diaphragmatic, intercostal, accessory respiratory and abdominal muscle function, Figure.1.20 (Schilero et al., 2009). The figure shows the respiratory muscles involved at each spinal level and provides information on the complications that may arise in different levels of SCI (Schilero et al., 2009). Keeping this in mind, studies investigating IHT in SCI patients routinely exclude participants with cardiopulmonary complications (Trumbower et al., 2012; Hayes et al., 2014; Trumbower et al., 2017; Navarrete-Opazo et al., 2017; Lynch et al., 2017). However, in some cases IHT may improve both respiratory insufficiencies and somatic motor function in SCI (Tan, Barth and Trumbower, 2020).

Overall, the mechanism of action underlying the effects of IHT in patients with iSCI is not yet fully understood and there is still progress in research to be made (Navarrete-Opazo et al., 2016b). There is enough information in the literature suggesting that the mechanism of action establishes a link between IHT and the cascade of events in respiratory motor neurons. However, the link between IHT and somatic motor plasticity is still not investigated as thoroughly.

1.25. IHT induces motor facilitation in animal models of SCI

From animal models we have a basic understanding of how IHT induces neuroplasticity in motoneurons (Mabrouk and Mitchell, 2014). The effects of IHT, however, are not just localised in motoneurons (Streeter et al., 2017). Streeter et al. (2017) observed in adult rats that IHT is capable in strengthening excitatory and decreasing inhibitory connections in between mid-cervical propriospinal interneurons. As these neurons are synaptically coupled to respiratory and somatic motoneurons, they may be responsible for the increase in motor output observed following IHT (Streeter et al., 2017). Further information gathered from animal studies is the

importance of spared serotonergic innervations, an increase in BDNF and TrkB expression, which has already been discussed (Golder et al., 2005).

Studies in animal models of SCI have also shown to improve grasping and locomotion when combining IHT with a task-specific training (TST). For instance, Lovett-Barr et al. (2012) reported that four days of daily IHT and ladder walking in C2 hemisectioned rats had significantly fewer foot-slip errors compared to before IHT and sham treated animals. The improved skilled forelimb function in horizontal-ladder walking was apparent even at 3 weeks following daily acute IHT (Lovett-Bar et al., 2012). Furthermore, this finding coincides with the immunohistochemistry which showed an increase of BDNF, TrkB and phosphorylated TrkB in motor nuclei (Lovett-Barr et al., 2012). This study demonstrates that functional improvement is persistent and coincides with changes in proteins that are believed to be involved in respiratory and non-respiratory motor function. Furthermore, animal models suggest that perhaps IHT alone may not be enough to significantly restore function and it may be essential to be combined with a TST (Prosser-Loose et al., 2015). For instance, Prosser-Loose et al. (2015) completed a study where rats post-4 weeks of cervical iSCI received seven days of daily IHT which reduced foot-slips only when combined with a ladder-walking task.

1.26. IHT induces motor facilitation in SCI patients

Studies that investigate IHT in patients with SCI have looked at ankle plantar flexion, agonist/antagonist activation, standing and dynamic balance, consecutive days of treatment, task-specific combination therapies, combination with anti-inflammatory drugs, walking speed and endurance, and hand dexterity.

Trumbower et al. (2012) recruited C5 to T7, AIS C and D iSCI patients who retained residual ankle plantarflexion and reported an 82% increase in ankle plantar flexion torque immediately following IHT, an observation reproduced to a lesser extent observed by Lynch et al. (2017) and Sandhu et al. (2020) who followed the same methodology. Moreover, Trumbower et al. (2012) reported that this increase in maximum voluntary torque (MVT) was correlated with an increase in gastrocnemius agonist muscle activation (Table.1.4). However, Lynch et al. (2017) found no

significant increase in EMG activity or median firing frequency in the gastrocnemius or soleus muscle. Furthermore, Lynch et al. (2017) concluded that the lower increase of ankle plantar flexion torque reported in their study, 30% increase, is as a result of recruiting stronger patients, where baseline MVT was 48 Nm higher than the those recruited by Trumbower et al. (2012). Sandhu et al. (2020) using the same IHT protocol reported an ankle plantarflexion torque increase of 29% that persisted for three hours post-IHT (Sandhu et al., 2019; Tan, Barth and Trumbower, 2020). Furthermore, in the Trumbower et al. (2012) study four out of the ten subjects showed a 50% increase in maximum voluntary ankle plantar flexion that maintained for more than 4 hours post-IHT, suggesting the effects of the treatment is consistent with long-lasting plastic effects (Table.1.4).

Trumbower et al (2012) recommends that more exposures of IHT are needed over a period of time. Results from a thematic poster session which reported the effects of IHT on iSCI with sleep-disordered breathing (SDB) concluded that those with moderate sleep apnea had an enhanced motor improvement compared to healthy or those with mild sleep apnea (Vivodtzev et al.,2020). This suggest that more frequent exposures to hypoxia are beneficial on motor function but the safety of more exposures needs to be studied (Vivodtzev et al.,2020).

In addition, Trumbower et al (2012) suggested that combination treatments with physical rehabilitation such as a TST should be considered because it can potentially have an additive effect. But elderly patients or patients with severe motor impairments could still benefit from repetitive IHT alone (Trumbower et al., 2012). However, we need to keep in mind that IHT responsiveness may be dependent on spared serotonergic innervations following the injury meaning that not all patients with SCI will respond to the treatment (Golder and Mitchell, 2005).

Furthermore, more studies need to be conducted to examine the benefits of IHT treatment alone and in combination with activity-based training. Naidu et al. (2020) published a study protocol and are conducting a randomised clinical study involving 85 subacute SCI patients with a variety of walking abilities. It aims to study the effects of IHT or sham treatment coupled with or without 60-minute walking practice on walking ability in patients with subacute SCI. Moreover, the study will monitor the

safety of IHT, hypertension and autonomic dysreflexia as well as neuropathic pain and spasticity. It is anticipated that this study will report in 2022 or 2023.

Hayes et al. (2014) reported that daily IHT combined with walking increased walking endurance while daily IHT alone improved walking speed by 18% and these effects persisted for more than three days in eighteen out of the nineteen subjects (Table.1.4). The effects on speed and endurance was clinically meaningful in 30% and 70% of patients, respectively (Hayes et al., 2014). Furthermore, according to Hayes et al. (2014) daily IHT attained almost double the effect for speed and endurance when compared with results from studies looking at overground walking training alone and this effect was larger when daily IHT was combined with walking. Hayes et al. (2014) mentioned that respiratory plasticity resulting from IHT could be a factor in the endurance improvement observed in patients. Navarrete-Opazo et al. (2016) confirmed these findings, where walking speed in iSCI patients was enhanced following daily IHT in combination with locomotor training but the effect on endurance was not clinically relevant in this study (Table.1.4). This study consisted of two groups one receiving IHT with BWSTT and the other group receiving normoxia with BWSTT. For the IHT group walking speed increased from a baseline of 0.54 ± 0.11 m/sec to 0.74 ± 0.14 m/sec following five consecutive days of treatment and BWSTT (Navarrete-Opazo et al., 2016b). In contrast, five consecutive days of normoxia with BWSTT increased the walking speed from 0.53 ± 0.12 m/s at baseline to 0.69 ± 0.15 m/s in this group (Navarrete-Opazo et al., 2016b). Furthermore, this study showed that following five consecutive days of training followed by repetitive IHT three times a week, maintained walking speed to the level observed following 5 days of IHT and had a beneficial effect on walking endurance (Navarrete-Opazo et al., 2016b). In addition, four weeks following the study, in the IHT group, three out of the seventeen subjects reported that they could walk without canes and such outcomes were not seen within the sham group (Navarrete-Opazo et al., 2016b). Furthermore, one patient in the IHT group discontinued use of his ankle-foot orthosis (Navarrete-Opazo et al., 2016b). However, the TUG test did not show any significant change following combination treatment with IHT and BWSTT (Table.1.4).

Navarrete-Opazo et al., (2017) also studied standing and dynamic balance in iSCI patients following a combination treatment of IHT with BWSTT. The findings of this study showed that there was no improvement in standing balance and suggested that it could be the case of not performing TST balance training because neuroplasticity in animal models have shown to be task specific (Navarrete-Opazo et al., 2016b; Navarrete-Opazo et al., 2017). In terms of dynamic balance, which was significantly enhanced following IHT, Navarrete-Opazo et al. (2017) suggested that this could be somewhat explained by greater walking speed. An increase in walking speed was also reported in Hayes et al. (2014) study and Navarrete-Opazo et al. (2016) (Table.1.4). Improving walking speed is a positive outcome for SCI patients but also important to improve coordinated movement and balance to minimize risk from falls and potential hospitalisation.

1.27. IHT coupled with task specific training (TST)

Trumbower et al. (2017) reported that a combination of IHT and hand opening for five consecutive days improved hand dexterity in patients with residual hand function (Table.1.4). This suggests the potential benefit of combining IHT with a form of TST rehabilitation training (Trumbower et al., 2017; Hayes et al., 2014). As mentioned above, IHT may need to be combined with a TST (Lovett-Bar et al., 2012; Hayes et al., 2014; Posser-Loose et al., 2015; Navarrete-Opazo et al., 2017; Trumbower et al., 2017). A working hypothesis is that IHT increases BDNF synthesis throughout the body, bringing the concentration to a much higher levels and subsequently TST further elevates BDNF levels specifically in spinal neural circuits that are activated by the task used (Welch et al., 2020).

For instance, standing balance was not improved following administration of IHT combined with BWSTT and the case could be that BWSTT with IHT was not specifically engaging pathways to improve standing balance (Navarrete-Opazo et al., 2017). Welch et al. (2020) in a review suggested a neural and cellular mechanism for IHT combined with TST. Please refer to Figure.1.21 that describes the pathways suggested by Welch et al. (2020). It is important to mention that this is a suggested working hypothesis and requires further investigation (Welch et al., 2020).

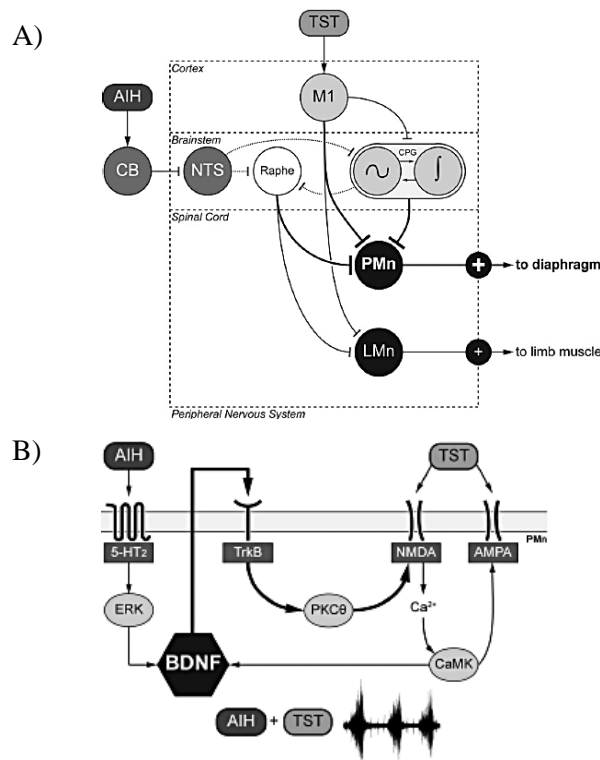


Figure.1.21. Neural and chemical pathways proposed by Welch et al. (2020) for the combination treatment of IHT with TST. **A)** Describes the neural pathway which involves IHT and TST. IHT activates the carotid body chemoreceptors and the secondary-order neurons in the brainstem, the nucleus tractus solitarius (NTS), and subsequent activation of raphe neurons that project to respiratory and non-respiratory motor neurons. NTS also activates raphe neurons indirectly via the central pattern generators (CPGs). CPGs are associated in autonomous rhythmogenic activity of walking and other functions such as breathing and swimming. Then raphe neurons and CPGs both project to motoneurons (phrenic motor neurons, PMn; limb motor neurons, LMn). TST activates the primary motor cortex which directly activates motoneurons or acts on CPGs. **B)** Describes the cellular cascade where IHT activates the 5-HT₂ serotonin receptors, the subsequent increase in BDNF synthesis and the activation of TrkB receptor. The TrkB receptors via the PKC acts on NMDA receptors which also increases BDNF synthesis. In contrast, TST increases the concentration of BDNF by activating NMDA and AMPA receptors which leads to calcium influx and the activation of calcium/ calmodulin-dependent protein kinase (CaMK) which increases BDNF synthesis. (diagram used with permission from Welch et al., 2020)

1.28. IHT coupled with anti-inflammatory drugs

Combination therapies apart from locomotor training and hand opening task have also been investigated. Lynch et al. (2017) studied IHT in patients following pre-treatment with an anti-inflammatory drug, ibuprofen, to observe whether it would enhance the ability of IHT to induce spinal motor plasticity in chronic SCI patients. As mentioned in Chapter 1 Section 1.4. inflammation in chronic SCI patients forms a

barrier for plasticity. Following administration of an anti-inflammatory agent, cyclooxygenase inhibition may be able to increase the motor facilitation observed with IHT. However, this study reported no significant difference in maximum voluntary torque measurements between ibuprofen and the placebo condition which may be simply due to the dose of ibuprofen studied which was the highest dose approved by the FDA (Lynch et al., 2017). Furthermore, the study did not consider the bodyweight of participants, so dosage was poorly controlled (Lynch et al., 2017). Another essential limitation of this study was that it did not recruit y patients with high serum levels of pro-inflammatory cytokines (Lynch et al., 2017). In contrast, Sandhu et al. (2019) administered 60 mg of a prednisolone, a potent anti-inflammatory drug, or a placebo prior using the same IHT protocol as Lynch et al. (2017) in AIS C or D SCI patients and reported that prednisolone prior to IHT showed a 12% higher improvement in ankle torque and soleus muscle EMG activity as well as increasing IL-10 anti-inflammatory agent (Sandhu et al., 2019; Tan, Barth and Trumbower, 2020). It is important to mention that SCI patients exhibit chronic elevated levels of inflammatory factors (da Silva Alves et al., 2013). Sandhu et al. (2019) highlighted that corticosteroids have also been linked with neuroplasticity and the selective increase in TrkB receptor expression, thus the enhanced improvement in ankle strength by prednisolone may not be related to its anti-inflammatory effects.

Table.1.4. Protocol and findings from studies that investigated IHT on SCI patients

Author	Year	Subjects	Protocol	Measurements	Findings
Trumbower <i>et al.</i>	2012	13 subj.; chronic iSCI; AIS C or D; volitional plantar flexion strength	Single treatment IHT Protocol A (8 subj.): One treatment of 30 min IHT (60 sec hypoxia (FiO ₂ 0.094) and 60 sec normoxia) IHT Protocol B (5 original subj.+ 5 new subj.): One treatment of 37.5 min IHT (90 sec hypoxia (FiO ₂ 0.094) and 60 sec normoxia) SHAM Protocol: normoxic air Minimum 2 weeks washout period between IHT and SHAM	Agonist and antagonist EMG during ankle isometric plantar flexion torque Average MVT and EMG of dominant ankle	IHT Protocol A: In all subjects that received IHT isometric plantar flexion strength increased (p<0.002) and this was not observed in SHAM. Increase in agonist EMG (p=0.04) immediately after the treatment which overlapped with an increase in maximum plantar flexion torque (p<0.03). MVT elevated after 30 min of IHT. IHT Protocol B: Increase in plantar flexion MVT up to an hour post- IHT. 4 hours post IHT a 50% increase in MVT was observed in all subjects. Significant correlation between agonist EMG and MVT (p<0.001). A negative correlation was observed in antagonist muscle but not significant (p=0.2).

Hayes <i>et al.</i> 2014	19 subj.; chronic iSCI	<p>Five consecutive days of daily IHT or SHAM +/- overground walking</p> <p>IHT Protocol: 37.5 min of IHT (90 sec hypoxia (FiO₂ 0.090) and 60 sec normoxia)</p> <p>SHAM Protocol: normoxic air</p> <p>9 subj.: daily IHT or daily SHAM (normoxic air)</p> <p>10 subj.: daily IHT or daily SHAM (normoxic air) + 60 min overground walking</p> <p>Minimum 2 weeks washout period</p> <p>Block design and randomisation</p>	Walking speed was measured using a 10MWT	Walking endurance was measured using a 6MWT	<p>Daily IHT significantly enhanced walking speed (p<0.05).</p> <p>Enhanced endurance was observed but not significant (p>0.05).</p> <p>Endurance increased in daily IHT following one IHT session and persisted after second week follow-up.</p> <p>Daily IHT +walking significant enhanced walking endurance (p<0.05) that continued after one-week follow-up (p=0.011). No significant change observed in speed (p>0.05).</p> <p>Daily IHT+ walking improved endurance more compared to daily IHT alone which was around twice higher after one-week follow-up.</p> <p>Walking speed enhanced by 0.09 m/s for 30% of patients and endurance >100 m for 70% of patients.</p>
Lynch <i>et al.</i> 2016	9 subjects; chronic iSCI; AIS C or D; volitional ankle plantar flexion strength	<p>Single treatment</p> <p>IHT Protocol: 45 min IHT (90 sec hypoxia (FiO₂ 0.090) and 60 sec normoxia)</p> <p>Combined treatment with ibuprofen (800 mg) or placebo</p> <p>Minimum 1-week washout period</p> <p>Double-blinded randomised placebo-controlled, crossover study design</p>	Same experimental design as Trumbower <i>et al.</i> (2012)	<p>Calculated LEMS</p> <p>Ankle plantar flexion strength studied by measuring MVT and EMG recorded from agonist and antagonist muscles</p>	<p>Maximum MVT increased with time (p=0.006).</p> <p>No significant difference in MVT between ibuprofen and placebo (p >0.05).</p> <p>No significant difference between IHT or ibuprofen on EMG muscle activity (p >0.05).</p> <p>Significant correlation between EMG of gastrocnemius (p<0.005) and soleus (p<0.005) muscle activity and MVT while no significant difference in antagonist muscle tibialis anterior (p >0.05).</p>

Navarrete-Opazo <i>et al.</i>	2016	33 subj.; chronic iSCI; AIS C or D	Five consecutive days followed by 3 times a week for 3 more weeks IHT or SHAM + BWSTT	Walking speed was measured using a 10MWT	IHT had a greater impact on walking speed compared to SHAM group which was observed after 5 days and maintained up to week 3.
			IHT Protocol: 45 min IHT (90 sec hypoxia (FiO ₂ 0.090) and 90 sec normoxia)	Walking endurance was measured using a 6MWT	A follow-up after 2 weeks both groups displayed an increase in walking speed (p<0.05).
			SHAM Protocol: normoxic air	TUG test	Comparing the two groups there is a decrease in TUG time for IH group but not significant (p>0.05).
			BWSTT: training begun with 30% body weight support and speed at 0.6 km/h		Within-group assessments displayed that IHT decreased TUG time from day 5 and preserved up to week 3 and this result was statistically significant (p<0.05).
			17 subj.: IHT + 45 min of BWSTT		Significant improvement in walking endurance observed in IHT group up to week 4 and follow-up (p<0.05).
			16 subj.: SHAM+ 45 min of BWSTT		Within-groups the IHT group showed an increase in walking distance from day 5 up to week 4.
			Randomised, triple-blind, placebo controlled, two-arm parallel clinical trial		

Navarrete-Opazo <i>et al.</i>	2017	35 subj.; chronic iSCI; AIS C and D	Five consecutive days followed by 3 times a week for 3 weeks IHT or SHAM + BWSTT	Measured standing and dynamic balance	Standing balance was not improved with the treatment of IHT in combination with BWSTT as there was no significant difference in jerkiness between IHT+BWSTT and SHAM group (p>0.05).
			IHT Protocol: 45 min IHT (1.5 min of hypoxia (FiO ₂ 0.090) interspersed with normoxia	Standing balance was measured by normalizing jerk and root-mean-square of sway	Significant change was observed between IHT+BWSTT and SHAM group in turning duration (p<0.01).
			SHAM Protocol: normoxic air	Dynamic balance was measured by studying turning duration, number of steps during turn and turn- to-sit duration	Furthermore, in the IHT participants significantly decreased their median number of steps compared to baseline (p<0.001) and the turn-to-sit duration compared to baseline (p<0.001) and had a significantly faster turn-to-sit duration compared with SHAM (p=0.001).
			18 subj.: IHT + BWSTT		
			17 subj.: SHAM + BWSTT		
Trumbower <i>et al.</i>	2017	6 subj.; chronic iSCI; AIS C or D; residual finger movements	Five consecutive treatments IHT or SHAM + opening hand task	Box and Block Test (BBT) for hand dexterity	IHT with hand opening enhanced hand dexterity (BBT scores) (p=0.057) in 5 participants while SHAM with hand opening improved dexterity in all participants (p=0.016).
			IHT Protocol: 37.5 min of IHT (90 sec hypoxia (FiO ₂ 0.090) and 60 sec normoxia)	Jebesen-Taylor Hand Function Test (JTHFT) for hand use in daily-living activities	JTHFT was improved in all participants (p=0.078).
			SHAM Protocol: normoxic air	Maximum hand opening studied using kinematics and surface EMG data gathered from extensor digitorum and extrinsic hand muscles involved in hand opening	IHT with hand opening increased maximum hand aperture in 5 participants (p=0.018), similar results observed with SHAM (p=0.030). This result correlated with an enhanced EMG activity (p=0.029) for IHT while SHAM showed no significant difference (p=0.606).
			Minimum 2 weeks washout period between IHT and SHAM		
			Post-treatment 20 repetitions of hand opening		

Sandhu <i>et al.</i>	2019	14 subj.; chronic iSCI; AIS C or D; volitional plantar flexion strength	Single treatment IHT Protocol: 30 min IHT (60 sec hypoxia (FiO ₂ 0.090) and 60 sec normoxia) Prednisolone or placebo pre-treatment 1 hour before IHT Randomised, double-blinded, crossover study	Isometric ankle torque and EMG of quadriceps, medial gastrocnemius, soleus and tibialis anterior	Ankle plantarflexion torque was significantly enhanced at 30, 60, and 120 minutes post-IHT (p=0.0012, p=0.0004, p=0.0067, respectively) Biggest difference in torque was observed post-IHT at 60 min with a value of 21.8 % ± 4.4 % EMG activity of soleus muscle was significantly higher at 60 minute post-IHT following prednisolone +IHT (p=0.0918). However, no significant difference was observed in tibialis anterior (p>0.190, medial gastrocnemius (p>0.19) and quadriceps (p>0.17).
----------------------	------	---	--	--	--

Maximum voluntary torque (MVT); fraction of inspired oxygen (FiO₂); intermittent hypoxia training (IHT); Electromyography (EMG); incomplete SCI (iSCI); lower extremity motor score (LEMS); body weight-supported treadmill training (BWSST); 10 meter walk test (10MWT); 6 meter walk test (6MWT); time up and go (TUG). Refer to Chapter 1 Section 1.13 to obtain information on the tests mentioned here.

1.29. Study design limitations

There are limitations on the design of the studies mentioned above, that need to be considered. Several studies reported that their experiments included a small sample size (<15 subjects) (Table.1.4), patients had a variable post injury time, level of injury, and continued taking prescribed medications some of which could interfere with neuromodulatory effects (Hayes et al., 2014; Trumbower et al., 2017; Lynch et al., 2017; Navarrete-Opazo et al., 2016b; Navarrete-Opazo et al., 2017; Sandhu et al., 2019).

A large sample size for these studies is very difficult to achieve because of the natural history of SCI, its incidence and variation in level and completeness (Navarrete-Opazo et al., 2016b). Also, studies may be biased toward using a combination treatment with locomotor training where the intensity of training is not standardised to the patient's capability limits (Navarrete-Opazo et al., 2017). Furthermore, several of the studies reported a washout period of minimum 1- 2 weeks between the IHT and sham treatments. It is unknown if this is enough time for the

effects of IHT to diminish, especially following a repetitive administration of the treatment protocol over several days (Trumbower et al., 2012; Trumbower et al., 2017; Hayes et al., 2014; Lynch et al., 2017; Sandhu et al., 2019). Furthermore, Sandhu et al. (2019) reported large variability in the response to IHT following both the anti-inflammatory drug and the placebo. Sandhu et al. (2019) concluded that it could be due to genetic variability between participants, gender, age, assessment tools or the time post injury.

To conclude, even though these studies have several limitations they show significant functional benefits following IHT. The section below will discuss some factors that can affect IHT's ability to induce neuroplasticity.

1.30. Factors that may influence neuroplasticity induced by IHT

As with all neuroplasticity rehabilitation methods some patients are responsive while others are not and as Tan, Barth and Trumbower (2020) highlighted in the review, it is important to identify biomarkers that affect IHT's responsiveness. Some factors include:

- 1) Inflammatory factors which are elevated in SCI patients may limit plasticity (Tan, Barth and Trumbower, 2020). However, as already mentioned BDNF levels have shown to reduce the concentration of pro-inflammatory cytokines and increase the expression of anti-inflammatory factors (Ji et al., 2015). Therefore, with the appropriate personalised IHT treatment for this limiting factor could be investigated. Moreover, administering an anti-inflammatory drug, such as prednisolone, prior to the treatment may be beneficial (Sandhu et al., 2019; Tan, Barth and Trumbower, 2020).
- 2) Also it is required to consider Val66Met mutation in BDNF gene, which occurs in 25% of the population, as its expression decreases the secretion of BDNF (Duman et al., 2016; Tan, Barth and Trumbower, 2020). As it has already been mentioned, high intensity training was able to overcome the effects of BDNF mutation (McHughen et al., 2011). This needs to be considered and perhaps for patients with this mutation we may need to

include a combination treatment with a higher intensity activity-based training to further elevate BDNF levels or increasing the number of intervals or frequency of IHT treatments.

- 3) SDB is frequent in SCI patients and as we know a severe dose of IHT leads to an inflammation and detrimental effects. However, Vivodtzev et al. (2020) reported that moderate SDB was an advantageous preconditioning factor on IHT since these patients were associated with more significant therapeutic benefits following IHT compared to patients that exhibit mild to no SDB (Tan, Barth and Trumbower, 2020).
- 4) Another factor is the extent of preserved connections following injury and corticospinal tract drive to motor neurons (Tan, Barth and Trumbower, 2020).
- 5) Lastly, best results are observed when combining IHT with activity-based training, especially with TST (Tan, Barth and Trumbower, 2020).

Other factors that could influence neuroplasticity are: aging, stress and hormones. In the respiratory system, hormones and aging play an important role in influencing serotonin-dependent plasticity and LTF (Behan, Zabka and Mitchell, 2002). The number of serotonergic neurons in raphe nuclei appear not to be affected by aging, however, the concentration of serotonin, binding characteristics, serotonin reuptake and serotonin receptor density seems to be altered (Behan, Zabka and Mitchell, 2002). It is important to mention that age related changes in regard to serotonin do not necessarily occur in all brain regions (Behan, Zabka and Mitchell, 2002). Furthermore, according to a review by Behan, Zabka and Mitchell, 2002, levels of serotonin and its receptor are higher in females compared to males in all brain regions. Moreover, serotonin concentration changes during the estrus cycle probably due to changes in hormone levels (Behan, Zabka and Mitchell, 2002). Hormones that have been reported to affect serotonin levels in the brain are: estrogen, progesterone, testosterone and cortisol (Long, Youngblood and Kizer, 1983; Genazzani et al., 2000; Cowen et al., 2002; Behan, Zabka and Mitchell, 2002).

In terms of BDNF, aging causes a decline in circulating and stored BDNF concentration in the brain (Lommatzsch et al., 2005). Furthermore, it has been shown

that BDNF is regulated by glucocorticoids, estrogen, progesterone and testosterone and affects the cell survival and function of the CNS (Numakawa et al., 2010). It is also important to mention that BDNF and testosterone work synergistically for the maintenance of motoneurons and testosterone regulates the expression of TrkB in motoneurons (Osborne et al., 2007; Verhovshek et al., 2010).

An example where aging affects the plasticity induced by IHT in rats was mentioned by Navarret- Opazo et al. (2006). The study was conducted by McGuire and Ling (2005) and showed that respiratory plasticity was significantly higher in younger compared to older rats following intermittent hypoxia. Furthermore, Navarret-Opazo et al. (2016) investigated the effect of IHT in combination with BWSTT in patients with iSCI reported no significant difference in walking speed between patients that were younger than 35 and patients older than 35. However, they did report higher walking endurance in younger patients that received the combination treatment and concluded possible influences of hormones and aging (Navarret-Opazo et al., 2016b).

As discussed, IHT may have beneficial effects on patients with iSCI (Tan, Barth and Trumbower, 2020). However, there are factors such as the natural process of aging, having the BDNF Val66Met mutation, high levels of inflammatory factors, the extend of preserved connections following injury, stress, gender and hormones that may influence the neuroplasticity induced by IHT and other rehabilitation methods. As already mentioned, the primary patient group for SCI across all developed economies are elderly patients. Aging may sabotage the potential benefits of IHT and thus it may cause a diversity in results if studies are recruiting patients between the age of 20 and 70. Nevertheless, it is important to take into account that the diversity in responsiveness is likely to be attributed to a combination of factors. In the next section potential benefits of IHT will be discuss along with the importance of avoiding a IHT overdose.

1.31. Potential side effects or potential benefits?

Cardiovascular and respiratory effects by IHT are controversial but it seems to depend on dose severity. A severe form of IHT, as mentioned earlier, can lead to deleterious medical conditions such as hypertension, stroke, cognitive impairments and respiratory complications that are associated with OSA (Levy et al., 2015). In contrast, there is evidence in the literature that a mild form of intermittent hypoxia improves cardiovascular and respiratory function (Kim et al., 2016; Navarrete-Opazo et al., 2015; Hoffman et al., 2010; Casas et al., 2000; Béguin et al., 2005). Please refer to Figure.1.22 that was created to provide a summary of the different IHT doses given to humans and the benefits and side effects.

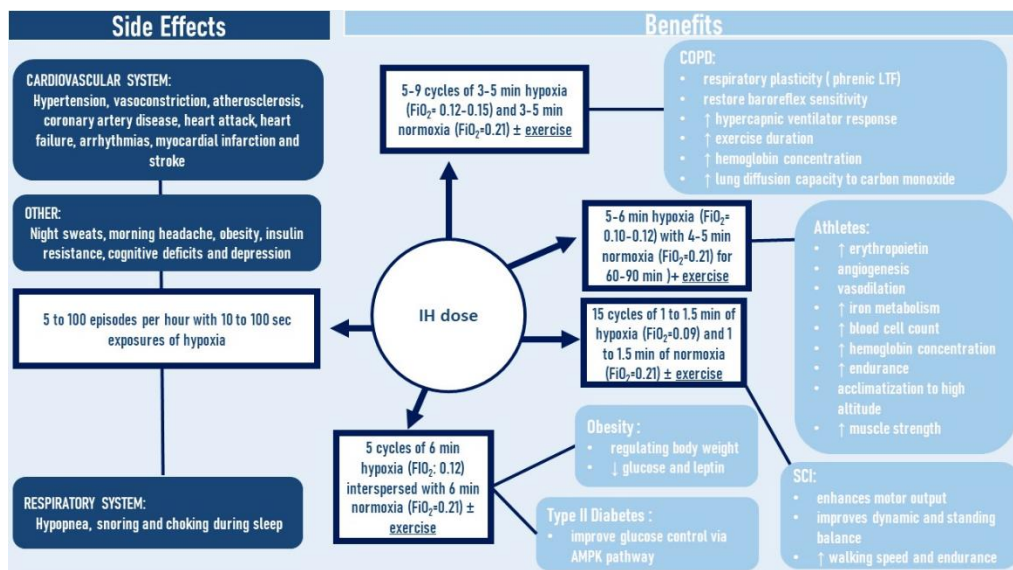


Figure.1.22. Intermittent hypoxia (IH) dose and the associated benefits and side effect. In dark blue the side effects are described when the intermittent hypoxia dose is severe, often observed in OSA. In light blue the benefits in COPD, athletes, SCI patients, obesity and type II diabetics are described and accompanied by the IHT dose mentioned in the literature. IH dose (Intermittent hypoxia dose)

Vogtel and Michels (2010) in a review summarised that IHT can increase baroreflex sensitivity to normal levels as well as increase hypercapnic ventilator response, exercise duration, hemoglobin concentration and lung diffusion capacity of carbon monoxide in patients with chronic obstructive pulmonary disease (COPD), a lung disease that includes emphysema and chronic bronchitis (Vogtel and Michels, 2010). The physiological changes that benefit patients with COPD are related to hypoxia-inducible factor (HIF).

Hypoxia-inducible factor-1 α/β (HIF-1 α/β) is an important transcription factor that upregulates several genes to support survival during hypoxic events (Semenza and Wang, 1992; Jelkmann and Hellwig-Bürgel, 2001). Overall, HIF transcripts several genes which are involved in hematological and ventilation responses to hypoxia. For instance, it increases gene transcription of glycolic enzymes that are important for anaerobic metabolism as well as VEGF which may be involved in increasing airway vascularity and airway remodeling by thickening the basement membrane in COPD patients (Vogtel and Michels, 2010). Furthermore, it increases gene transcription of other genes to augment the production of vasodilators, increase iron metabolism, an important co-factor for hemoglobin oxygen binding, and raise ventilation (Vogtel and Michels, 2010; Weidemann and Johnson, 2008; Peyssonnaud, Nizet and Johnson, 2008; Semenza, 2008).

Furthermore, IHT is used in sports medicine to enhance aerobic performance of athletes by producing hematological and ventilatory adaptations (Casas et al., 2000; Knaupp et al., 1992). For instance, combination of IHT and low-intensity exercise increased red blood cell count, hemoglobin concentration, decreased heart rate and induced ventilator adaptive changes. This process is known as acclimatization and is a response to IHT exploited by athletes (Casas et al., 2000).

Knaupp et al. (1992), reported that IHT increased erythropoietin (EPO) concentration by 52% in healthy subjects. EPO is produced in the kidneys by specialised cells which sense changes in oxygen levels (Jelkmann and Hellwig-Bürgel, 2001). EPO hormone activates the synthesis of new red blood cells in the bone marrow. The increased concentration of red blood cells or erythrocytes allows humans to adapt at low oxygen partial pressures. Interestingly, EPO changes depend on repetition of the IHT protocol. For instance, Burtscher et al. (2004) repeated IHT 15 times and found that in the 4th session there was a significant change in EPO levels.

In terms of cardiovascular protection and improvement, Béguin et al. (2005) investigated the effect of brief periods of IHT (10% O₂) on the infarct size development in isolated rat heart and found that it induced protection against myocardial infarction. Furthermore, moderate IHT reduced cardiac arrhythmias during ischemia and decreased infarct size by 43% in rats with myocardial ischemia/reperfusion

(Manukhina et al., 2013). Similar results have also been observed in dogs (Zong et al, 2004). The protection of IHT against myocardial ischemia/reperfusion results from a decrease in myocardial apoptosis (Wen Dong et al., 2003). Furthermore, Mallet et al. (2018) in their review reported that IHT reduces infarct size, enhances coronary blood flow and reduces hypertension.

In a study with an IHT treatment that comprised of 15 sessions over 3 weeks with 3-5 minutes intervals of 14.00% to 10.00% FiO₂ and 3 minute intervals of recovery was well tolerated by elderly subjects with coronary artery disease and the results showed a 4% increase in red blood cell count and 4.2% increase in haemoglobin concentration improving oxygen carrying capacity. Furthermore, they observed an 8.3% decrease in heart rate during the sub-maximal cycle test following IHT (Burtscher et al., 2004). Furthermore, after 3 weeks of IHT, systolic blood pressure had decreased by 5.5% in the sub-maximal cycle test (Burtscher et al., 2004). In addition, a combination of IHT with antihypertensives has an additive beneficial effect on blood pressure and heart rate in patients with cardiovascular disease (Simonenko et al, 2003). Therefore, a mild to moderate IHT appears to have no cardiovascular risks and it could be considered as a therapeutic option.

1.32. Safety monitoring when investigating IHT on SCI patients

A mild to moderate concentration of IHT seems to have many beneficial effects. Table.1.5. provides a summary of the safety monitoring in studies that investigate IHT in SCI patients. Generally, blood pressure, heart rate and oxyhemoglobin saturation (SpO₂) were monitored. These studies did not report any adverse effects and some mentioned that the treatment was well tolerated by the participants (Hayes et al., 2014; Trumbower et al., 2012; Lych et al., 2016; Navarrete-Opazo et al., 2016b). However, many of these studies excluded participants with cardiopulmonary complications (Trumbower et al., 2012; Trumbower et al., 2017; Navarrete-Opazo et al., 2016b; Navarrete-Opazo et al., 2017; Lynch et al., 2016; Hayes et al., 2014).

As mentioned above, it seems that IHT has beneficial effects in a variety of systems and perhaps SCI patients with other underlining complications may gain

benefits from this treatment. However, it is important to investigate further if iSCI patients with underlining cardiopulmonary complications can tolerate this IHT protocol and whether the treatment dose and frequency need to be modified.

Table.1.5. IHT experiments on SCI patients: IHT protocol, SpO₂, safety monitoring and effects

Author	Year	IHT Protocol	SpO ₂ level (%)	Safety Monitoring Measurements	Effects
Trumbower <i>et al.</i>	2012	One treatment of 30 min IHT (60 sec hypoxia (FiO ₂ 0.094) and 60 sec normoxia)	~ 81.0 ± 1	Heart rate, oxyhemoglobin saturation and blood pressure	Hypoxic exposures changed heart and oxyhemoglobin saturation. The oxyhemoglobin saturation after 60 sec of hypoxia dropped to around 81%. No changes in systolic and diastolic blood pressure when comparing before and immediately after IHT
Trumbower <i>et al</i>	2012 & 2017	One treatment of 37.5 min IHT (90 sec hypoxia (FiO ₂ 0.090) and 60 sec normoxia) (Trumbower et al., 2012) Five consecutive treatments of 37.5 min of IHT (90 sec hypoxia (FiO ₂ 0.090) and 60 sec normoxia) (Trumbower et al, 2017)	<75.0	Heart rate, systolic blood pressure and oxyhemoglobin saturation	No difference in heart rate, blood pressure and oxyhemoglobin saturation when comparing before and after five consecutive days of IHT
Tester <i>et al.</i>	2014	Ten days of 32 min IHT (120 sec of hypoxia (FiO ₂ 0.080) and 120 sec of normoxia)	~ 97.4	Heart rate and oxyhemoglobin saturation	<i>Nothing reported</i>

Hayes <i>et al.</i>	2014	Five consecutive treatments of 37.5 min of IHT (90 sec hypoxia (FiO ₂ 0.090) and 60 sec normoxia)	78.0± 1.5 IH 81.9± 1.0 IH + walking	Heart rate, systolic blood pressure and oxyhemoglobin saturation	No changes in heart rate and blood pressure. Heart rate between 40-160 bpm, systolic blood pressure between 85-160 mmHg and oxyhemoglobin saturation around 75%.
Navarrete-Opazo <i>et al.</i>	2016	Fourteen treatments in 24 days of 45 min IHT (90 sec hypoxia (FiO ₂ 0.090) and 90 sec normoxia)	80.0-83.5%	Respiratory distress, cyanosis, saturation of oxygen and autonomic disreflexia Oxygen saturation was kept around 80% and not below during the hypoxic episodes.	The oxyhemoglobin saturation dropped around 80-83 %.
Lynch <i>et al.</i>	2017	One treatment of 45 min IHT (90 sec hypoxia (FiO ₂ 0.090) and 60 sec normoxia)	~ 84.0	Heart rate and oxyhemoglobin saturation.	No changes in heart rate and oxygen saturation.
Navarrete-Opazo <i>et al.</i>	2017	Fourteen treatments in 24 days of 45 min IHT (90 sec hypoxia (FiO ₂ 0.090) and 90 sec normoxia)	80.0-85.0	Respiratory distress, cyanosis, saturation of oxygen and autonomic disreflexia Oxygen saturation was kept around 80% and not below during the hypoxic episodes.	The oxyhemoglobin saturation dropped around 80-85 %.
Christiansen <i>et al.</i>	2018	One treatment of 30 min IHT (60 sec hypoxia (FiO ₂ 0.094) and 60 sec normoxia)	81.3± 1.2	Oxyhemoglobin saturation and heart rate	<i>Nothing reported</i>

Sandhu <i>et al.</i> 2019	One treatment of 30 min IHT (60 sec hypoxia (FiO ₂ 0.090) and 60 sec normoxia)	82-85 %	Oxyhemoglobin saturation, heart rate and blood pressure	<i>Nothing reported</i>
---------------------------	---	---------	---	-------------------------

Other factors investigated in studies that completed research on SCI patients are cognition and spasticity. Navarrete- Opazo et al. (2016a) observed no impact on cognition in iSCI patients following a month of mild repetitive IHT in combination with BWSTT. The study used complutense verbal learning test (TAVEC) and the Rey-Osterrieth Complex Figure Test (ROCF) to examine episodic verbal and visual memory, respectively (Navarrete- Opazo et al., 2016a). The TAVEC involves immediate recall, short-term free recall, long-term free recall and recognition while the ROCF tests involves recalling a complex line drawing from memory (Navarrete- Opazo et al., 2016a).

Hayes et al. (2014) investigated IHT ability to induce spasticity in SCI patients, because BDNF and serotonin have been linked with spasticity. The study reported no spasticity following IHT. In addition, Tan, Barth and Trumbower’s (2010) review highlighted that IHT may be able to reduce spasticity by upregulating potassium chloride cotransporter 2 (KCC2) expression. It has been reported that activation of 5-HT_{2A} which is essential for pLTF induced by IHT, upregulates KCC2 (Bos et al., 2013). Also BDNF has been observed not only to upregulate the expression of this chloride transporter and suppress spasticity but also suppress allodynia (Tashiro et al., 2015; Schulze et al., 2018). In conclusion, IHT may potentially have far more beneficial effects on iSCI patients that currently reported.

1.33. Tolerance of IHT by healthy elderly individuals

As highlighted throughout the report, elderly individuals make up the majority of SCI patients. Liu et al. (2017) study, provided us with essential information on various cardiovascular and respiratory measurements on the elderly (71 ±2 years). The study monitored heart rate (HR), systolic blood pressure (SBP), diastolic blood pressure (DBP), SpO₂, middle cerebral arterial blood flow velocity (MVA), cerebral vascular conductance (CVC), cerebral tissue oxygen saturation (ScO₂), breathing

frequency (f_{Br}), tidal volume (V_T), ventilation (VENT), partial pressure of end tidal oxygen ($P_{ET}O_2$) and partial pressure of end tidal carbon dioxide ($P_{ET}CO_2$) (Liu et al., 2017). Table.1.6 provides the change (Δ) from baseline to post-IHT measurements at the start and end of IHT. Liu et al. (2017) concluded that 5 minutes of acute 10% intermittent hypoxia was tolerated well by elderly subjects and the SpO_2 levels reduced to 25% without resulting in adverse effects. The subjects excluded from this study were: smokers, those with sleep problems or those that in the past 3 months prior to volunteering for the study lived at altitudes ≥ 2000 m.

Table.1.6. Cardiovascular and respiratory measurements at the first and last exposure of hypoxia. (table used with permission from Liu et al., 2017)

	Group	Bout	Min 1	Min 2	Min 3	Min 4	Min 5	ANOVA Outcome	
ΔHR (bpm)	Elderly	1	+2.1 \pm 0.9	+4.7 \pm 1.0*	+6.6 \pm 1.2* [†]	+8.2 \pm 1.4* [†]	+7.8 \pm 1.2* [†]	Bout P = 0.005	
		5	+2.9 \pm 0.8	+5.7 \pm 1.1*	+8.5 \pm 1.3* [†]	+11.9 \pm 1.5* [†]	+13.9 \pm 1.8* [†]	Age P = 0.001	
	Young	1	+6.5 \pm 1.9	+12.2 \pm 1.6 [†]	+13.8 \pm 1.6 [†]	+16.8 \pm 1.6 [†]	+18.1 \pm 1.4 [†]	Min P = 0.001	
		5	+4.1 \pm 1.1	+10.9 \pm 1.8 [†]	+17.1 \pm 1.9 [†]	+19.4 \pm 1.5 [†]	+22.0 \pm 1.7 [†]		
	ΔSBP (mmHg)	Elderly	1	+0.8 \pm 0.9	-1.8 \pm 0.9	-3.8 \pm 1.1 [†]	-3.8 \pm 0.7 [†]	-3.9 \pm 1.1 [†]	Bout P = 0.449
			5	-1.4 \pm 0.5	-3.0 \pm 0.9	-5.9 \pm 1.0 [†]	-4.5 \pm 1.5	-3.6 \pm 1.8	Age P = 0.016
Young		1	-2.9 \pm 2.8	-3.4 \pm 2.4	-5.9 \pm 2.9	-6.4 \pm 2.6	-6.7 \pm 2.3	Min P = 0.008	
		5	-1.8 \pm 0.8	-4.9 \pm 1.1	-6.2 \pm 1.1	-5.3 \pm 2.5	-4.6 \pm 2.7		
ΔDBP (mmHg)		Elderly	1	+0.7 \pm 0.6	-1.2 \pm 0.7	-2.3 \pm 0.8	-2.1 \pm 0.7	-2.6 \pm 1.0 [†]	Age P = 0.281
			5	-0.3 \pm 0.3	-1.3 \pm 0.5	-3.3 \pm 0.6 [†]	-2.3 \pm 0.7	-2.4 \pm 0.7 [†]	Min P = 0.001
	Young	1	-1.4 \pm 1.3	-1.3 \pm 1.3	-3.3 \pm 1.4	-3.3 \pm 1.1	-4.2 \pm 1.2	Bout P = 0.639	
		5	-0.8 \pm 0.7	-1.5 \pm 0.7	-2.0 \pm 0.8	-1.6 \pm 0.9	-1.9 \pm 1.0		
	ΔV_{MCA} (cm/s)	Elderly	1	+0.12 \pm 0.35	+1.64 \pm 0.44	+3.46 \pm 1.07	+4.55 \pm 1.13 [†]	+5.38 \pm 1.13 [†]	Age P = 0.012
			5	+1.23 \pm 0.53	+3.27 \pm 1.32	+4.53 \pm 1.39	+7.15 \pm 1.89 [†]	+8.05 \pm 1.80 [†]	Min P = 0.001
Young		1	+1.15 \pm 0.49	+2.09 \pm 0.65	+4.79 \pm 1.11 [†]	+7.11 \pm 1.61 [†]	+7.98 \pm 1.31 [†]	Bout P = 0.001	
		5	+1.44 \pm 0.86	+4.17 \pm 2.13 [†]	+7.67 \pm 2.81 [†]	+10.09 \pm 2.70 [†]	+10.73 \pm 3.02 [†]		
ΔCVC (unit)		Elderly	1	+0.005 \pm 0.005*	+0.025 \pm 0.006	+0.056 \pm 0.017 [†]	+0.065 \pm 0.014 [†]	+0.082 \pm 0.015 [†]	Age P < 0.001
			5	+0.018 \pm 0.006	+0.049 \pm 0.015	+0.077 \pm 0.014 [†]	+0.100 \pm 0.020 [†]	+0.106 \pm 0.020 [†]	Min P < 0.001
	Young	1	+0.030 \pm 0.015	+0.042 \pm 0.016	+0.092 \pm 0.019 [†]	+0.120 \pm 0.023 [†]	+0.137 \pm 0.022 [†]	Bout P = 0.001	
		5	+0.026 \pm 0.011	+0.069 \pm 0.022	+0.119 \pm 0.025 [†]	+0.141 \pm 0.033 [†]	+0.149 \pm 0.038 [†]		
	ΔSaO_2 (%)	Elderly	1	-5.8 \pm 0.6	-11.2 \pm 0.9 [†]	-15.0 \pm 1.2 [†]	-17.9 \pm 1.5 [†]	-20.2 \pm 1.7 [†]	Age P < 0.001
			5	-7.4 \pm 0.9	-15.4 \pm 1.1* [†]	-19.7 \pm 1.1 [†]	-22.9 \pm 1.6* [†]	-25.6 \pm 1.9 [†]	Min P < 0.001
Young		1	-7.7 \pm 1.3	-14.7 \pm 1.4 [†]	-17.5 \pm 1.3 [†]	-20.7 \pm 1.3 [†]	-22.7 \pm 1.4 [†]	Bout P < 0.001	
		5	-9.7 \pm 1.3	-18.6 \pm 1.5 [†]	-23.7 \pm 1.5 [†]	-26.6 \pm 1.7 [†]	-28.7 \pm 1.9 [†]		
ΔScO_2 (%)		Elderly	1	-4.1 \pm 0.4	-7.6 \pm 0.7* [†]	-9.9 \pm 0.7* [†]	-12.1 \pm 0.8* [†]	-13.9 \pm 0.9* [†]	Age P < 0.001
			5	-5.3 \pm 0.7	-10.2 \pm 0.8 [†]	-13.4 \pm 0.9 [†]	-15.3 \pm 0.9 [†]	-17.3 \pm 1.1 [†]	Min P = 0.001
	Young	1	-4.9 \pm 0.6	-10.0 \pm 0.7 [†]	-13.3 \pm 0.8 [†]	-15.8 \pm 0.9 [†]	-18.0 \pm 0.9 [†]	Bout P = 0.001	
		5	-5.8 \pm 0.8	-11.0 \pm 0.9 [†]	-14.2 \pm 1.3 [†]	-16.5 \pm 1.4 [†]	-18.2 \pm 1.7 [†]		
	Δf_{br} (br/min)	Elderly	1	-0.308 \pm 0.496	0.025 \pm 0.435	-0.383 \pm 0.580	+0.033 \pm 0.277	-0.350 \pm 0.414	Age P = 0.001
			5	-0.350 \pm 0.439	-0.133 \pm 0.464	-0.008 \pm 0.587	-0.183 \pm 0.592	-0.017 \pm 0.708	Min P = 0.781
Young		1	+0.262 \pm 0.419	+0.092 \pm 0.713	+0.131 \pm 0.673	+0.546 \pm 0.751	-0.238 \pm 0.829	Bout P = 0.019	
		5	+1.031 \pm 0.586	+1.569 \pm 0.703	+1.700 \pm 0.699	+1.685 \pm 0.747	+0.715 \pm 0.709		
ΔV_T (L/br)		Elderly	1	+0.181 \pm 0.067	+0.186 \pm 0.070	+0.228 \pm 0.062	+0.225 \pm 0.066	+0.315 \pm 0.135	Age P = 0.911
			5	+0.151 \pm 0.068	+0.166 \pm 0.068	+0.189 \pm 0.080	+0.275 \pm 0.083	+0.225 \pm 0.058	Min P = 0.439
	Young	1	+0.254 \pm 0.103	+0.241 \pm 0.073	+0.223 \pm 0.067	+0.270 \pm 0.101	+0.286 \pm 0.102	Bout P = 0.137	
		5	+0.134 \pm 0.048	+0.155 \pm 0.060	+0.166 \pm 0.037	+0.269 \pm 0.092	+0.180 \pm 0.051		
	$\Delta Vent$ (L/min)	Elderly	1	+2.61 \pm 0.55	+2.69 \pm 0.77	+3.14 \pm 0.84	+3.19 \pm 0.73	+3.86 \pm 1.19	Age P = 0.032
			5	+1.57 \pm 0.55	+1.79 \pm 0.42	+2.07 \pm 0.61	+2.89 \pm 0.65	+2.65 \pm 0.49	Min P = 0.189
Young		1	+2.75 \pm 0.75	+3.15 \pm 0.72	+3.55 \pm 0.82	+4.08 \pm 1.16	+3.69 \pm 1.30	Bout P = 0.121	
		5	+2.60 \pm 0.58	+3.16 \pm 0.57	+3.56 \pm 0.45	+3.78 \pm 0.61	+3.32 \pm 0.58		
$\Delta P_{ET}O_2$ (mmHg)		Elderly	1	-44.2 \pm 1.9	-54.1 \pm 1.0 [†]	-58.3 \pm 0.8 [†]	-60.1 \pm 0.9 [†]	-62.7 \pm 0.8 [†]	Age P = 0.018
			5	-42.2 \pm 2.6	-52.9 \pm 1.9 [†]	-56.2 \pm 1.9 [†]	-57.4 \pm 1.9 [†]	-59.1 \pm 2.0 [†]	Min P = 0.001
	Young	1	-41.5 \pm 2.0	-55.2 \pm 1.3 [†]	-59.0 \pm 1.1 [†]	-61.2 \pm 1.1 [†]	-62.8 \pm 0.9 [†]	Bout P = 0.001	
		5	-39.4 \pm 2.0	-49.3 \pm 2.4 [†]	-51.5 \pm 2.5 [†]	-53.4 \pm 2.6 [†]	-54.2 \pm 2.6 [†]		
	$\Delta P_{ET}CO_2$ (mmHg)	Elderly	1	-2.5 \pm 0.3	-3.3 \pm 0.5	-3.4 \pm 0.6	-3.8 \pm 0.5	-3.5 \pm 0.6	Age P = 0.255
			5	-2.8 \pm 0.5	-3.3 \pm 0.5	-3.3 \pm 0.6	-3.7 \pm 0.6	-3.3 \pm 0.7	Min P = 0.001
Young		1	-1.8 \pm 0.4	-2.8 \pm 0.3 [†]	-3.4 \pm 0.3 [†]	-4.0 \pm 0.3 [†]	-4.4 \pm 0.4 [†]	Bout P = 0.308	
		5	-2.6 \pm 0.3	-3.5 \pm 0.3	-3.9 \pm 0.4 [†]	-4.2 \pm 0.5 [†]	-4.5 \pm 0.5 [†]		

1.34. Aims and objectives

There has been considerable focus on understanding the adaptations that our bodies go through under hypoxic stress and potentially IHT can be used as an intervention to treat a variety of diseases. The attractiveness of using IHT as a

treatment for elderly iSCI patients who cannot tolerate vigorous and intensive rehabilitation methods has been highlighted in this report as well as IHT's ability to enhance the beneficial outcomes of current rehabilitation methods. However, there is inadequate knowledge in the literature on the neurological mechanism of IHT's actions and its tolerance.

The aim of this research was to investigate the underlying mechanism of action of the IHT protocol suggested by Trumbower et al. (2012). But before completing this research it was essential to study the tolerance of this IHT protocol and finding an appropriate intervention that challenged the homeostasis of healthy volunteers.

The tolerance of IHT was studied by monitoring heart rate, blood pressure and saturation of oxygen. Moreover, its effect on the autonomic nervous system was examined by analysing heart rate variability. The hypothesis states that since the exposures of hypoxia in this protocol were very short and lead to a brief decrease in SpO₂, of around 20%, there would be no significant atypical variations in blood pressure, heart rate and heart rate variability.

Subsequently, the research focussed on examining the sensory and motor performance of the CNS in healthy individuals before, during and following a single exposure of IHT, while monitoring the safety of the participants. To study the integrity of sensory and motor pathways, common neurophysiological tools were used to record SEP and MEP measurements, respectively. These measurements provided information on IHT's ability to modulate neural activity in the spinal cord. SEPs were measured by stimulating the median nerve. The stimulus ascended via sensory pathways to the somatosensory cortex and EEG scalp surface electrodes were used to record the waveform. MEPs were measured by stimulating the motor cortex at an area targeting the innervation to the tibialis anterior muscle. This stimulus descended through the CST to the corresponding muscle where MEP waveforms were recorded using EMG electrodes placed on the muscle belly.

The hypothesis was that the functional motor improvements reported in the literature should show some degree of correlation with changes in CNS motor and sensory responses. The literature has demonstrated that even a single exposure of IHT

is capable in improving motor function in iSCI patients. That has led to the hypothesis states that IHT enhances the neural activity of spinal pathways that translates to an increase in SEP and MEP amplitude. Furthermore, if there is a significant detectable effect resulting from IHT the results from SEPs and TMS will co-vary. The null hypothesis states that there will be no detectable difference in SEP and MEP amplitude following a single exposure to IHT.

To detect even small changes in SEP and MEP amplitude following a single exposure of IHT, it was essential to analyse the reliability of baseline measurements. In addition, there was an experimental challenge in using TMS to take MEP measurements which was to accurately control the placement of the coil for subsequent repeat stimulation sessions. To overcome this problem, a novel manual navigation system was developed for TMS coil placement and triggering to minimise variability in stimulation targeting.

Moreover, since this study aimed to test IHT's effects on motor function, we required to investigate the possibility that IHT may also cause changes in skeletal muscle metabolism and consequently force. Understanding the peripheral effects of IHT on muscle function is important in order to evaluate the true potential of IHT to change neural pathways. There were two experimental designs proposed for the study of IHT on muscle force, one for the upper limb and the other for the lower limb. To study the upper limb, the first dorsal interosseous (FDI) muscle of the hand was stimulated and the generated force exerted by the index finger is measured using a transducer. To study the lower limb, the peroneal nerve that supplies the tibialis anterior muscle of the lower leg was targeted to evoke dorsiflexion of the ankle. Outcome measures were the force generated by activity of tibialis anterior together with the evoked EMG responses. As intermittent hypoxia has been shown to affect many systems it may also cause direct adaptations in muscle. The null hypothesis states that detectable changes in force would not be observed following a single exposure to IHT.

Chapter.2. Examining the tolerance of moderate intermittent hypoxia in healthy subjects.

2.1. Introduction

2.1.1. Mild intermittent hypoxia versus OSA

Intermittent hypoxia is most commonly experienced in people with OSA, however, with mild controlled exposure scientists have identified many potential benefits that may result from IHT in an assortment of conditions. It appears that it all depends on the dose, intervals and duration of intermittent hypoxia which separates morbid and therapeutic properties (Clanton and Klawitter, 2001).

With severe chronic OSA creating intermittent hypoxia, the airway narrows during sleep because pharyngeal muscles relax causing the upper airway to collapse (Malhotra and White, 2002). When the oxygen level in the blood drops significantly, brief periods of reawakening occur allowing airway recovery (Serebrovskaya et al., 2008; Dale, Mabrouk and Mitchell, 2014). Recurrent hypoxic episodes alter autonomic nervous system (ANS) activity and it can lead to cardiovascular morbidity in OSA patients (Abboud and Kumar, 2014; Bisogni et al., 2016; Malhorta and White, 2002; Sequeira, Bandeira and Azevedo, 2019). To assess this imbalance in sympathetic and parasympathetic activity, studies have used heart rate variability (HRV) and recent work, reports sustained high sympathetic responsiveness in OSA patients compared to controls (Sequeira, Bandeira and Azevedo, 2019).

At the cellular level oxygen delivery and the clearance of carbon dioxide is compromised during hypoxic episodes because of the obstruction to respiratory flow in the upper airway. Peripheral chemoreceptors known as glomus cells in the carotid and aortic bodies detect fluctuations in the partial pressure of oxygen, partial pressure of carbon dioxide and pH in arterial blood (Martini, Nath and Batholomew, 2018). Significant blood gas disturbances cause the depolarisation of the glomus cells and the release of neurotransmitters. This sensory response is then conveyed by afferents in the vagus nerve in the aortic arch and the glossopharyngeal nerve near the carotid bodies which subsequently transmit this information to respiratory centres located in the medulla oblongata. In addition, central chemoreceptors that indirectly detect the build-up of carbon dioxide in the blood are also activated and provide feedback on pH

levels to the respiratory centres. Collectively, the respiratory centres of the medulla oblongata respond to direct increased neuronal drive to respiratory muscles (diaphragm and intercostal muscles) to enhance tidal volume and ventilation rate as part of the homeostatic control mechanisms (Martini, Nath and Batholomew, 2018).

In addition to the above respiratory response, sympathetic activation promotes vasoconstriction to direct blood flow to vital (Abboud and Kumar, 2014; Bisogni et al., 2016). At the end of each recurrent apnoeic episode, the peripheral vasculature is still constricted when the cardiac output increases contributing to an increase in blood pressure (Bisogni et al., 2016). Haemodynamic variations can manifest in chronic OSA through hypertension, myocardial infraction, arrhythmias, heart failure, heart attack and coronary artery disease (Malhotra and White, 2002; Serebrovskaya et al, 2008).

Furthermore, OSA triggers oxidative stress, defined as an imbalance in free radicals and antioxidants in the body which elicits tissue damage. Oxidative stress encourages the manifestation of metabolic syndrome comprising of abnormal cholesterol levels, an increase in β -cell death in pancreatic islets leading to insulin resistance, and high glucose levels. Moreover, it amplifies the risk of cardiovascular diseases, atherosclerosis and type II diabetes (Tahrani et al., 2013; Malhotra and White, 2002; Serebrovskaya et al, 2008; Cohen, Riahi and Sasson, 2012).

In contrast, it seems both counter intuitive and surprising that intermittent hypoxia could serve as a therapeutic tool with beneficial cardiovascular, respiratory, neuromuscular and metabolic adaptations, but only if the dose is mild to moderate (Chacaroun et al, 2017; Trumbower et al., 2012; Vogtel and Michels, 2010; Mackenzie et al., 2011). Studies are investigating the benefits of a moderate IHT intervention in a variety of areas such as exercise tolerance, cognitive performance, respiratory facilitation, endurance training and glucose control (Vogtel and Michels, 2010; Casas et al., 2000; Knaup et al., 1992; Mallet et al., 2018; Chacaroun et al., 2017; Trumbower et al., 2012; Lynch et al., 2017; Trumbower et al., 2017; Navarrete-Opazo et al., 2016b; Hayes et al., 2013; Tester et al., 2014; Schega et al., 2013; Burtscher et al., 2004; Workman et al., 2012; Mackenzie et al., 2011). (Please refer to Chapter 1 Section 1.31 which provides details on beneficial effects of IHT in COPD, sports medicine, and cardiovascular protection.)

Table 2.1 lists a range of studies reporting positive effects of IHT together with the lowest SpO₂ levels that the hypoxia induced in these studies. Please keep in mind that the intervention dose of IHT is different for each application. However, the table supports the view that an intermittent drop of 25% in SpO₂ due to breathing a reduced level of oxygen is well tolerated without presenting acute or lasting adverse effects (Table.2.1) and for the studies on motor function following SCI the results are highly suggestive that IHT promotes a degree of functional neuroplasticity (Trumbower et al., 2012; Trumbower et al., 2018; Hayes et al., 2014).

Table.2.1. SpO₂ levels reported in studies using intermittent hypoxia

Author	Year	Application	SpO ₂ level (%)
Sandhu <i>et al.</i>	2019	SCI	82.0 - 85.0%
Chacaroun <i>et al.</i>	2017	Healthy	~ 74.6
Lynch <i>et al.</i>	2017	SCI	~ 84.0
Trumbower <i>et al.</i>	2017	SCI	>75.0
Navarrete-Opazo <i>et al.</i>	2017	SCI	>80.0
Christiansen <i>et al.</i>	2018	Healthy	81.3± 1.2
Navarrete-Opazo <i>et al.</i>	2016	SCI	80.0 - 83.5%
Hayes <i>et al.</i>	2014	SCI	78.0± 1.5 IHT 81.9± 1.0 IHT + walking
Tester <i>et al.</i>	2014	SCI	~ 97.4
Schega <i>et al.</i>	2013	Elderly	90-80
Trumbower <i>et al.</i>	2012	SCI	~ 81.0 ± 1
Workman <i>et al.</i>	2012	Obese	~80
Mackenzie <i>et al.</i>	2011	Type II diabetes	92
Burtscher <i>et al.</i>	2004	Coronary heart disease	~ 76

2.1.2. Tolerance of IHT

Even though everyone initially responds to low oxygen breathing by an increase in heart rate and a drop in arterial saturation of oxygen, the tolerance to hypoxia varies (Bassovitch and Serebrovskaya et al, 2009). As Chacaroun et al (2017) suggested, it may be valuable to examine each individual's response to brief periods of low oxygen and adapt the intervention to receive the favourable effects it can result in while avoiding a severe dose which encourages deleterious side effects (Chacaroun

et al., 2017). This is the reason why a hypoxia test has been suggested as a measure of the reaction to hypoxic air breathing (Bassovitch and Serebrovskaya et al, 2009). The hypoxia test measures:

- 1) the time an individual tolerates hypoxic air breathing of around 11.00% FiO_2 before the SpO_2 reaches a safety baseline of 85% and
- 2) the time it takes for the individual to recover to a normal SpO_2 level of 95% or greater when returned to breathing ambient sea level air (Bassovitch and Serebrovskaya et al, 2009).

2.1.3. Safety of the IHT protocol given to SCI

The focus of this thesis was to investigate the intervention protocol used in iSCI patients to improve motor function. The IHT protocol involved 15 cycles of repetitive alternating exposures of 1 to 1.5 min of hypoxic ($FiO_2=9.00\%$) and 1 to 1.5 min of normoxic ($FiO_2=21.00\%$) air (Trumbower et al., 2012; Trumbower et al., 2017; Navarrete-Opazo et al, 2017; Hayes et al., 2014). These studies monitored heart rate, SpO_2 and blood pressure and reported an SpO_2 drop of 15% to 25% with no adverse effects following IHT (Trumbower et al., 2012; Trumbower et al., 2017; Hayes et al., 2014; Navarrete-Opazo et al., 2016b; Lynch et al., 2017; Sandhu et al., 2019; Hayes et al., 2014; Navarrete-Opazo et al., 2017). Navarrete-Opazo (2016 and 2017) also observed no signs of respiratory distress, cyanosis or autonomic dysreflexia. Lastly, Hayes et al. (2014) reported that the heart rate in their study was maintained between 40 to 160 bpm, the systolic blood pressure between 85 to 160 mmHg and the SpO_2 remained at levels greater than 75%. However, these studies have not investigated HRV, which is a useful measure of ANS function.

2.1.4. Heart rate variability (HRV)

The ANS consists of the sympathetic and parasympathetic branches that reciprocally interact in the control of heart rate and other aspects of cardiovascular function according to changes in the external and internal environments. The variability in heart rate can therefore be interpreted to reflect a changing equilibrium

between the sympathetic and parasympathetic branches acting on the heart's pacemaker (sinoatrial node (SAN)).

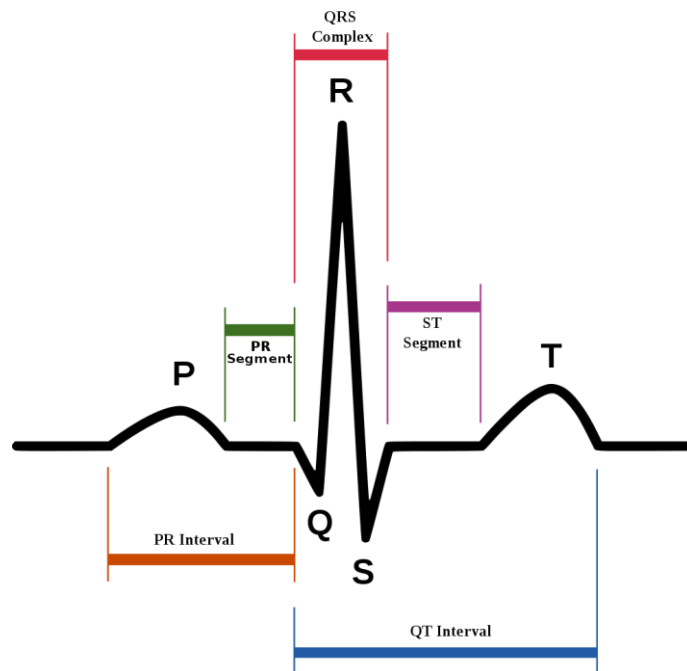


Figure.2.1. Normal ECG. (image used with permission from <https://upload.wikimedia.org/wikipedia/commons/9/9e/SinusRhythmLabels.svg>) [Accessed on 20 March 2021]

HRV defined as the variability in consecutive heartbeat intervals or RR intervals when measured from the electrocardiogram (ECG) (Lizamore et al.,2016; Bobyleva and Glazachev, 2007). The ECG signal consists of three waveforms the p-wave that reflects the depolarization of the atria, the QRS complex that reflects the depolarization of the ventricles and the T-wave that reflects the repolarization of the ventricles (Figure.2.1). These waveforms occur in a repeating pattern known as the sinus rhythm.

Usually, 5 minute recordings of ECG are used to calculate RR interval but studies have also taken briefer measurements lasting only 10 seconds (Salahuddin et al., 2007). HRV analysis exists in the time-domain and frequency-domain. The time-domain analysis involves studying the variation of RR intervals (Task force, 1996). Examples of common time-domain measurements are stated in Table.2.2.

The most frequently used measure in the time-domain to study RR interval differences is the root mean square of successive heartbeat interval differences (rMSSD). rMSSD is measured by first calculating the successive time difference between heartbeat intervals in milliseconds, squaring the values, then taking an average and lastly the square root (Shaffer and Ginsberg, 2017; Task Force, 1996, p.355).

Table.2.2. Time-domain analysis of HRV (table used with permission from Schumacher, 2004)

Variable	Description	Normal Values
Mean R-R interval	The average time interval between heartbeats within a data set. R-R intervals are measured in milliseconds (ms) and are also called heart periods.	> 750 ms
SDNN (standard deviation of normal-to-normal beats)	The calculated standard deviation for all R-R intervals within a data set. SDNN estimates overall HRV and is dependent on length of ECG recording. In 24-h electrocardiographic (ECG) recordings, values below 50 ms are considered too low.	141 ± 39 ms
SDANN (standard deviation of average normal-to-normal beats)	The standard deviation of mean R-R interval times for all 5-min segments of an entire ECG recording. 24-h ECG recordings are divided into 5-min data sets, 12 per hour. SDANN estimates long-term HRV and allows for comparisons over time.	127 ± 35 ms
RMSSD (root mean square of squared differences)	The time difference between consecutive R-R intervals is calculated. The value is then squared and averaged, and the square root value is obtained. The RMSSD estimates short-term HRV and accounts for sequential order of R-R intervals.	27 ± 12 ms

NOTE: This information is summarized from Berntson and others (1997), Crawford and others (1999), and Task Force (1996). Normal values given are for human adults.

The frequency-domain provides information on the distribution of the signal across frequency bands and in HRV it can provide insight on ANS. Power spectral analysis (PSA) was first introduced by Akselrod et al. (1981) who studied mid- and high-frequency peaks following the administration of an anticholinergic drug to block the PNS and studied the low frequency peaks following the administration of a beta blocker to inhibit the sympathetic nervous system.

The PSA involves three main frequency components: high frequency (HF) (0.15 to 0.40 Hz range) indicative of RR interval modulation between 2.5 and 7 seconds, low frequency (LF) (0.04 to 0.15 Hz range) indicative slower RR interval modulation between 7 and 25 seconds and very low frequency (VLF) modulation of intervals occurring over long intervals (25 seconds and 5 minutes) (Task Force, 1996) (Table.2.3). The power of the band is quantified using area under the curve. Experts consider the HF to reflect vagal activity and is dependent on respiratory pattern while the LF is influenced by both branches of the ANS but predominantly the sympathetic

branch. For instance, an increase in LF is observed during mental stress and moderate exercise (Martinez et al., 2017 p.38). Normal values for frequency-domain analysis of HRV are provided in Table.2.3.

Table.2.3. Frequency-domain analysis of HRV (table used with permission from Schumacher, 2004)

Variable (Unit)	Description	Normal Values
Total power (ms ² /Hz)	The total area under the curve in a power spectrum plot. The ms ² /Hz unit is considered an absolute unit of measure.	3466 ± 1018 ms ² /Hz
ULF (ultra low frequency)	The peak frequency found in this defined range; obtained from 24-h recordings and may be a graphical representation of direct current (DC).	0.00-0.003 Hz
VLF (very low frequency)	The peak frequency found in this defined range. The physiological significance is unknown but may correspond to thermoregulation. VLF power affected by mathematical algorithms of trend (baseline) removal.	0.003-0.04 Hz
LF (low frequency)	The peak frequency found in this defined range. Both parasympathetic and sympathetic activity influences this component, which may reflect baroreflex-mediated modulatory activity.	0.04-0.15 Hz
LF power (ms ² /Hz)	The area under the spectral curve within this frequency range.	1170 ± 416 ms ² /Hz
LF power (nu)	Measure represents relative proportional value of LF power to total power; calculated as (LF power/(total power – VLF power)) × 100. Power in normalized units should be reported in conjunction with absolute units. Normalization minimizes the effect of change in total power dependent on the individual frequency components.	54 ± 4 nu
HF (high frequency)	The peak frequency found in this defined range, which is influenced by both respiratory and parasympathetic activity.	0.15-0.4 Hz
HF power (ms ² /Hz)	The area under the spectral curve within this frequency range.	975 ± 203 ms ² /Hz
HF power (nu)	Measure represents relative proportional value of HF power to total power; calculated as (HF power/(total power – VLF power)) × 100.	29 ± 3 nu
LF/HF ratio	Calculated as LF power/HF power. This controversial measure is considered an assessment of sympathovagal balance.	1.5-2.0

NOTE: nu = normalized unit. This information is summarized from Berntson and others (1997), Crawford and others (1999), and Task Force (1996). Normal values given are for human adults for stable 5-min electrocardiographic recordings, which is the recommended data set/time series length for power spectrum analysis.

2.1.5. Improving cardiovascular health by increasing HRV with intermittent hypoxia

A reduced HRV is linked to poorer coronary health and perhaps an intervention such as IHT can increase HRV and restore cardiac health (Lizamore et al., 2016). Lizamore et al. (2016) studied whether 4 weeks of IHT affected HRV in healthy sedentary elderly participants aged between 45 to 60 years. The intervention involved alternating exposure of six 5 minute intervals of hypoxia (FiO₂ 16% to 12%) and six 5 minute intervals of normoxia. They investigated changes in HRV by measuring rMSSD and RR interval which are resistant to breathing artefact.

The study reported that in the fourth week of the hypoxia exposure intervention there was a 15% decrease in rMSSD, a 10% decrease in RR interval with a 9% increase in heart rate when an individual transitioned from breathing normoxia to hypoxia (Lizamore et al., 2016).

In contrast, there were no apparent fluctuations in rMSSD and heart rate in the group that was exposed to normoxia. Moreover, the study reported that the ANS adapted to repeated intermittent hypoxic exposures. After 4 weeks of hypoxic exposure there was a 16% increase in rMSSD compared to baseline (Lizamore et al., 2016). For the sham group they reported a 6% decrease in rMSSD. Knowing that reduced HRV is linked to poorer cardiovascular health this increase in rMSSD may serve as a beneficial intervention for those that are unable to exercise and live a sedentary lifestyle (Lizamore et al., 2016).

2.1.6. Aims and objectives

The aim of this chapter was to explore the IHT intervention and document its safety by monitoring blood pressure, SpO₂, heart rate and HRV. HRV was used to study changes in the autonomic nervous system activity.

There were several stages to the investigation:

- 1) Primarily, the study investigated each participants' tolerance to hypoxia using the hypoxia test that was integrated in the hypoxia machine (OnePlus R3 GO2Altitude) used in the study.
- 2) After knowing that participants could tolerate low oxygen levels the effect of the IHT intervention delivered by our hypoxia machine were examined. The literature reports that during recovery, normoxia is delivered to participants. However, the hypoxicator used here automatically delivered hyperoxia during the recovery period. Therefore, one aim was also to explore whether there was a difference between the results of recovery during normoxia or hyperoxia.

As the intervention was given to healthy subjects, it was expected that there will be no difference administering hyperoxia instead of normoxia in the recovery intervals of IHT. The rationale for breathing hyperoxic air rather than normoxic air during the recovery period, was that it would assist recovery from hypoxia without potential ventilation/perfusions restriction limiting oxygen saturation of venous blood passing through the lungs.

3) Lastly, unpublished pilot studies conducted by the author, using the Trumbower et al. (2012) IHT protocol, showed that the intervention did not sufficiently challenge the homeostasis of our healthy subjects. A potential confounding factor that was considered was that the OnePlus R3 GO2Altitude hypoxicator device cycled between hypoxia and hyperoxia during IHT sessions. Accordingly, to increase the homeostatic challenge to subjects the IHT cycle duration was increased from 1 min to 2 min intervals. Therefore, the resulting protocol adopted here involved an IHT dose of alternating intervals of 2 minutes hypoxia ($FiO_2 = 9.00\%$) interspersed with 1 minute recovery periods (hyperoxia $FiO_2 > 20\%$).

To summarise, this chapter serves as an initial assessment on the safe use of the OnePlus R3 GO2Altitude hypoxicator and to establish an effective IHT intervention. The outcome from this chapter was to provide an IHT protocol to use in assessment of effects on sensory and motor pathways via SEP and MEP measurements, respectively.

2.2.Methodology

2.2.1. Subjects

Ethics approval was obtained from the ethics committee of the University of Strathclyde. Fourteen healthy adults (9 men and 5 women; mean age, 27; range, 26 to 36 years) were recruited from staff and students of the University of Strathclyde. Please note that all subjects were pseudo-anonymised by allocating a study ID-number that begins with IHT followed by an integer (ex: IHT1). The purpose of this was to maintain confidentiality and protect the participant's identity. Exclusion criteria included any participant with pre-existing high blood pressure conditions, a history of blood clots or cardiovascular disease including narrowing of arteries, angina/chest pain on exertion, congenital heart disease or respiratory conditions including upper respiratory tract infections, asthma, chronic bronchitis, emphysema or tuberculosis. Please refer to the Activity and Health Questionnaire in Appendix.I.1).

2.2.2. Experimental design

Prior to investigating the safety of the IHT intervention, by monitoring blood pressure, SpO₂, heart rate and HRV, participants were required to complete a preliminary GO2Altitude Hypoxia test to ensure that they can tolerate low oxygen levels. This primary exposure to hypoxia eases the participant into the IHT intervention and reduces the initial anguish associated with the concept of breathing air with low O₂ content.

Before exposing participants to the IHT intervention, two preliminary experiments were completed to explore the intervention and make sure that it challenges the homeostasis of the healthy participants to a level reported in the literature. The preliminary experiments include:

- 1) Comparing IHT with Hyperoxia versus Room Air breathing during recovery periods

It was identified from previous pilot studies, that the hypoxia machine delivers hyperoxia rather than normoxia in the recovery intervals of the IHT intervention. Therefore, it was decided to study the difference in SpO₂ levels when administering hyperoxia or normoxia during recovery intervals. When the participant was exposed to hyperoxic intervals they were asked to keep the mask on for the entire intervention while during normoxic intervals the participant was asked to remove the mask. The later, disrupted the hypoxia interval and made participants very anxious. Two participants were studied and it is believed that proceeding with removing the mask every recovery interval was not an effective method of delivering the intervention.

- 2) Exploratory IHT intervention to study participant tolerance when extending the hypoxia interval from 1 minute to 2 minutes while keeping the hyperoxia interval at 1 minute

As mentioned, previous pilot studies showed that the intervention of 1-minute hypoxia interspersed with 1 minute recovery did not sufficiently challenge the homeostasis of healthy subjects. Accordingly, a protocol with

a longer duration of hypoxia was essential to investigate, and to be safe 5 rather than 15 intervals of 2 minutes hypoxia ($FiO_2=9.00\%$) paired with 1 minute of recovery at FiO_2 levels of 21.00% to 40.00% was delivered to the participants. The purpose of exposing participants to a shorter IHT intervention was for safety as a 2 minute hypoxia interval has not yet been documented in the literature. The aim of this study was to judge if any adverse vital sign events accompanied this pattern of stimulation with an additional aim that was to observe whether the hypoxia stimulus in healthy young participants resulted in an SpO_2 level equivalent to those reported in the literature in patient studies (approximately 80%). Four participants were initially recruited. At some point during the intervention, all participants reached an unsafe level of SpO_2 that required the interruption of the intervention until their SpO_2 reached 78% or above. Moreover, participants reported breathlessness and slight dizziness with this dose of hypoxia.

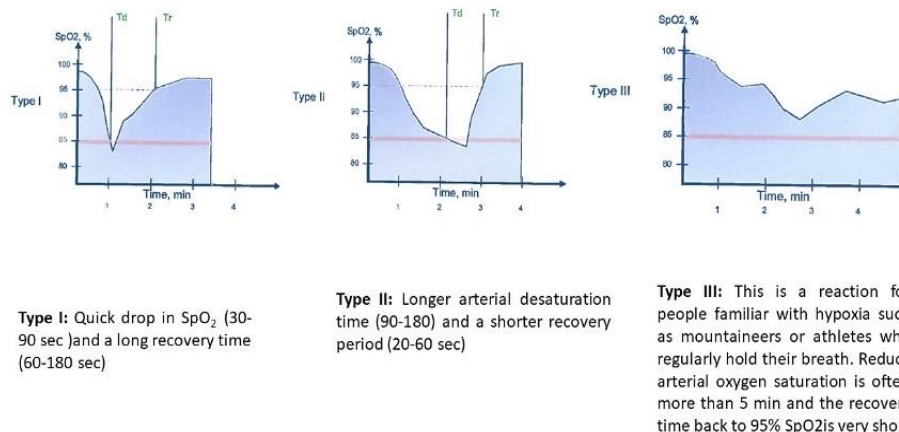
Following these investigations, the initial IHT protocol that involved 1 minute of hypoxia ($FiO_2=9.00\%$) paired with 1 minute of recovery at FiO_2 levels of 21.00% to 40.00% was adopted as it was impossible to study a duration of hypoxia between 1 and 2 minutes. The issue was that the hypoxia machine used in the study constrained the increase in interval duration of hypoxia and normoxia by a factor of 1. With this protocol the SpO_2 , heart rate, blood pressure and HRV were studied. Moreover, measurements of rate of recovery and drop of SpO_2 and the time shift of SpO_2 from the O_2 intervention were also studied. These measurements provided information on the tolerance of the intervention and whether there was a physiological adaptation to low oxygen.

To keep the flow of the report simple the methodology for each study will be followed by the relevant results section. To summarise, firstly participants were exposed to the hypoxia test; this was followed by two preliminary experiments were completed to study the IHT intervention; and lastly, the duration of hypoxia was finalised to one that challenged the homeostasis of the participants enough where their SpO_2 level was dropped to approximately 80%, as reported in the literature.

2.3. Preliminary GO2Altitude hypoxia test

2.3.1. Methodology

The hypoxia test is a programme available in the OnePlus R3 GO2Altitude; (Melbourne, Australia). Participant responsiveness to hypoxic air breathing was studied using this programme (Bassovitch and Serebrovskaya, 2009). It involved inspiring 11% oxygen through a face mask whilst monitoring the time for SpO₂ to fall to 85% and thereafter measuring the SpO₂ recovery period when the mask was removed, and the participant resumed breathing ambient air. The device instructed the participants to remove their face mask when the SpO₂ reached the target safety baseline of 85%. SpO₂ was logged by the hypoxicator device continuously and a chart recording the time it takes for the SpO₂ to drop to 85%, and the time it takes for the SpO₂ to recover to normal levels was produced to determine the individual's reaction to hypoxic breathing.



Td: time to descend
Tr: time to recover

Figure.2.2. Three categories for hypoxia response (graphs of each response are used with permission and created into one figure where a summary of each response is added; Bassovitch and Serebrovskaya, 2009)

According to Bassovitch and Serebrovskaya (2009) an individual response to this test was assignable to one of three categories. A Type I response shows a 30-90 sec drop in SpO₂ with long recovery time of 60-180s, a Type II response shows a 90-180 sec drop in SpO₂ with a short recovery time of 20-60s while the Type III responder shows prolonged (> 5 min) time for SpO₂ to reach 85% and recovery is very rapid (<20s) (see Figure.2.2 for illustration of responder Types I to III). All of the

participants performed this test and based on their response times were allocated to one of the three types. The results were analysed offline in Matlab.

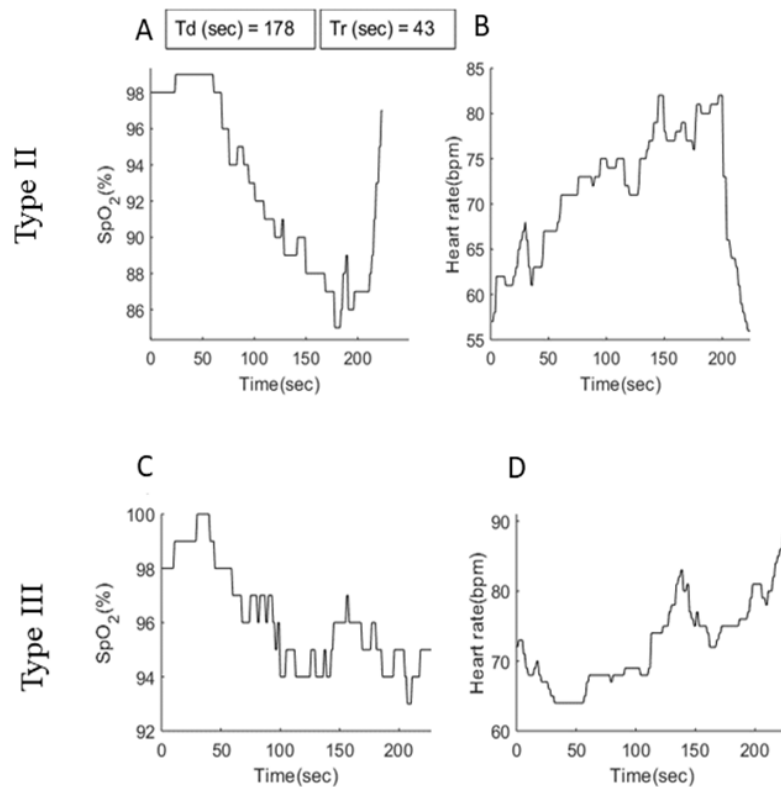
2.3.2. Results

The hypoxia test studied subjects' tolerance to hypoxia, and acted to provide a familiarisation to the basic equipment set-up allowing subjects to gain experience of breathing hypoxic air prior to continuing to full participation in the experimental study.

Figure 2.4 displays an example of a Type II and Type III hypoxia test response recorded during these experiments and Table 2.4 collates the classification type of all the participants recruited in the study (n=14). Please refer to Appendix.I.2) to view all the individual graphs.

All participants recruited for this study showed good resistance to the hypoxia stimulus with rapid recovery and with no reported adverse effects. As seen in Table.2.4, 11 participants were allocated in Type II (90-180 sec drop in SpO₂ with short recovery of 20-60 sec) and 3 participants in Type III (> 5 min for SpO₂ drop and recovery was very short).

The hypoxia test demonstrated that all subjects were considered suitable recruits for the study and no volunteers were excluded from further participation.



Td: time to descend; *Tr*: time to recover

Figure.2.3. Example of a Type II and Type III SpO₂ response. A) and C) show the SpO₂ response and B) and D) heart rate. On the top of the SpO₂ graph the Td and Tr values are reported in seconds. In Type III, because the participant did not drop below 85%, measurements of Td and Tr are not provided. Measurements of SpO₂ and heart rate were taken every second.

Table.2.4. The response to hypoxia for each healthy participant

Participant Code	Hypoxia Test Type
IHT1	Type II
IHT2	Type II
IHT3	Type II
IHT4	Type II
IHT5	Type III
IHT6	Type II
IHT7	Type II
IHT8	Type II
IHT10	Type III
IHT11	Type II
IHT12	Type II
IHT13	Type II
IHT14	Type II
IHT15	Type II
IHT16	Type III

2.4. Comparing IHT with Hyperoxia versus Room Air breathing during recovery periods

2.4.1. Methodology

In the literature, during the recovery period the participant breaths room air at sea level (21.00% FiO₂), however, as mentioned above the device used here delivers higher oxygen concentrations during the recovery period. Therefore, it was considered important to study the logistics of removing the mask during the recovery interval and to then also investigate whether breathing room air (referred to as ‘mask off’ experiment) challenged the homeostasis of the participant more compared to being connected to the hypoxia machine, with hyperoxia breathing (approximately 40% FiO₂) during the recovery interval (referred as the ‘mask on’ experiment). Moreover, it was essential to record the participant’s experience of removing the mask every interval as making the participant anxious could interfere with measurements of SEPs and MEPs.

Two participants, IHT1 and IHT2, were recruited for this study and because this was a preliminary experiment, the intervention lasted 15 minutes rather than 30 minutes (the usual duration reported in the literature). The IHT protocol involved 1 minute of hypoxia (FiO₂= 9.00%) interspersed with 1 minute of normoxia (FiO₂= 21.00%) in the ‘mask off’ experiment or hyperoxia (> 21.00%) in the ‘mask on’ experiment. The ‘mask on’ experiment was conducted prior to the ‘mask off’ experiment with two-week gap (washout) between sessions.

To show each participant’s response to IHT with or without a mask during the recovery interval, the SpO₂ values were graphed over time and a box plot of the SpO₂ response was produced to show the spread of the data. The analysis and graphs were completed in Matlab.

2.4.2. Results

These preliminary measurements from two participants (IHT1 and IHT2) are showing the timing control and dosage of IHT when keeping the mask on throughout the intervention and when removing the mask every recovery interval. The latter allows the participant to breath room air rather than hyperoxia.

Figure.2.5. B summarises the SpO₂ data using a boxplot for participant IHT1 and IHT2. For participant IHT1 the median, shown in red, has a slightly higher SpO₂ for the ‘mask off’ experiment at 95% while the ‘mask on’ experiment has an SpO₂ median of 91%. The 25th and 75th percentiles, displayed in blue, are 85% and 99% for the ‘mask on’ experiment and 88% and 99% for the ‘mask off’ experiment. The whiskers display the range of SpO₂ which is 72% to 100% for the ‘mask on’ experiment and 63% to 100% for the ‘mask off’ experiment.

For IHT2 the median is 92% for the ‘mask on’ experiment and 93% for the ‘mask off’ experiment. The 25th percentile is 87% for the ‘mask on’ experiment and 86% for the ‘mask off’ experiment and the 75th percentile is 98% in both cases. The range of SpO₂ was 74% to 100% for the ‘mask on’ experiment and 68% to 99% for the ‘mask off’ experiment.

In the ‘mask off’ experiment the subjects reached a lower SpO₂ level. In participant IHT1 the SpO₂ was 9% lower in the ‘mask off’ experiment and for participant IHT2 6% lower. However, the process of putting on and off the mask every minute was stressful for the participant and precise control over the initiation of the hypoxia intervals was lost.

Moreover, it is important to mention that the SpO₂ level reached by the participants in the ‘mask on’ and ‘mask off’ interventions were much lower compared to previous pilot studies. The participants reached a level of SpO₂ below 80%. Therefore, responses to IHT vary from individual to individual.

It was also clear that when breathing room air the minimum SpO₂ levels were experienced at the end of the hypoxia episodes suggesting that during hyperoxia an effect is to reduce the extent of the SpO₂ fall within hypoxic intervals. Due to this and the better control of timing measurements a decision was taken to retain the use of hyperoxia during the recovery phases of IHT and for subjects to retain mask breathing throughout IHT sessions.

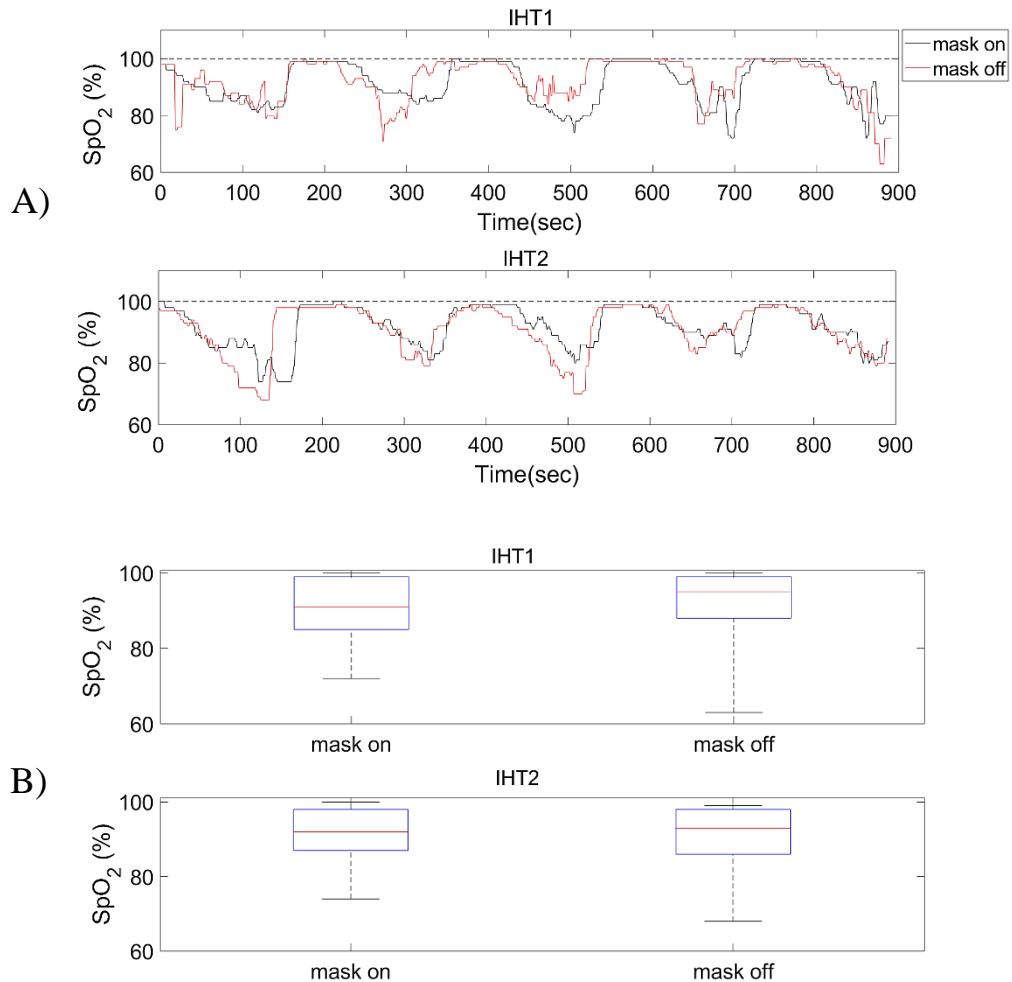


Figure.2.5. A) The SpO₂ response of two participants IHT1 and IHT2 with or without wearing the hypoxia machine mask during the recovery period. Wearing the mask provided higher levels of SpO₂ in order to ensure the participant recovers back to 100% SpO₂ before hypoxia. B) A box plot showing the spread of the data in the ‘mask on’ and ‘mask off’ experiments for each participant (IHT1 and IHT2). The box plot displays the median in red and the bottom and top edges show the 25th and 75th percentiles in blue. The whiskers show the minimum and maximum SpO₂ (%).

2.5. Exploratory IHT intervention to study participant tolerance when extending the hypoxia interval from 1 minute to 2 minutes while keeping the hyperoxia interval at 1 minute

2.5.1. Methodology

Since previous preliminary experiments (Toli, 2017) showed that the IHT intervention only weakly challenged the homeostasis of healthy participants, experiments exploring an IHT intervention with a longer hypoxia interval were carried out. Due to timing control limitations of the GO2Altitude hypoxia machine, the IHT

interval examined included a 2-minute hypoxia period paired with 1 minute of hyperoxia recovery.

As a precaution we began our investigation delivering only 5 cycles of IHT compared to 15 cycles that are usually given to SCI patients (Hayes et al., 2014; Trumbower et al., 2017). The intervention exposed participants to five intervals of 2 minutes of hypoxia ($FiO_2=9.00\%$) paired with 1 minute of recovery at FiO_2 levels of 21.00% to 40.00%. A safety SpO_2 baseline level was set at 78% that warned the experimenter to remove the participant's mask if the SpO_2 level decreased below this value.

Four subjects volunteered for the experiment investigating the latency (lag time) of their SpO_2 response and recovery to this IHT protocol. For individual analysis, the average SpO_2 response from each IHT cycle was produced and graphed. Thereafter, a grand average for all subjects was calculated and plotted using Matlab.

2.5.2. Results

The results generated from the four participants are shown in Figure 2.6. The Figure illustrates the cycle averages calculated from the time of onset of each hypoxia interval. Due to the long latency of the respiratory response to hypoxia the minimum SpO_2 is only reached during the hyperoxia breathing periods, making it difficult for the experimenter to predict the participant's final SpO_2 level when breathing in at low oxygen levels (Figure.2.6). The timing and level of SpO_2 drop is variable for each participant (IHT3: 80%, IHT4: 84%, IHT5: 77% and IHT6: 86%) with the minimum average (all subjects) SpO_2 level reaching 82%.

Moreover, Figure.2.6 clearly shows the delayed response of all subjects to hypoxia with IHT5 showing the longest delay of approximately 40s before SpO_2 falls. IHT5 was the only participant in this experiment that was allocated to Type III during the hypoxia test.

Lastly, it is important to mention that all four participants reported breathlessness and slight dizziness with this dose of hypoxia as the experiment progressed and, in all cases, the SpO_2 cut off at 78% was reached at some point during the intervention. Accordingly, a decision to maintain a 1 minute hypoxia period was taken to avoid potential adverse events and interruptions to experiments due to a need to terminate sessions where SpO_2 fell below thresholds.

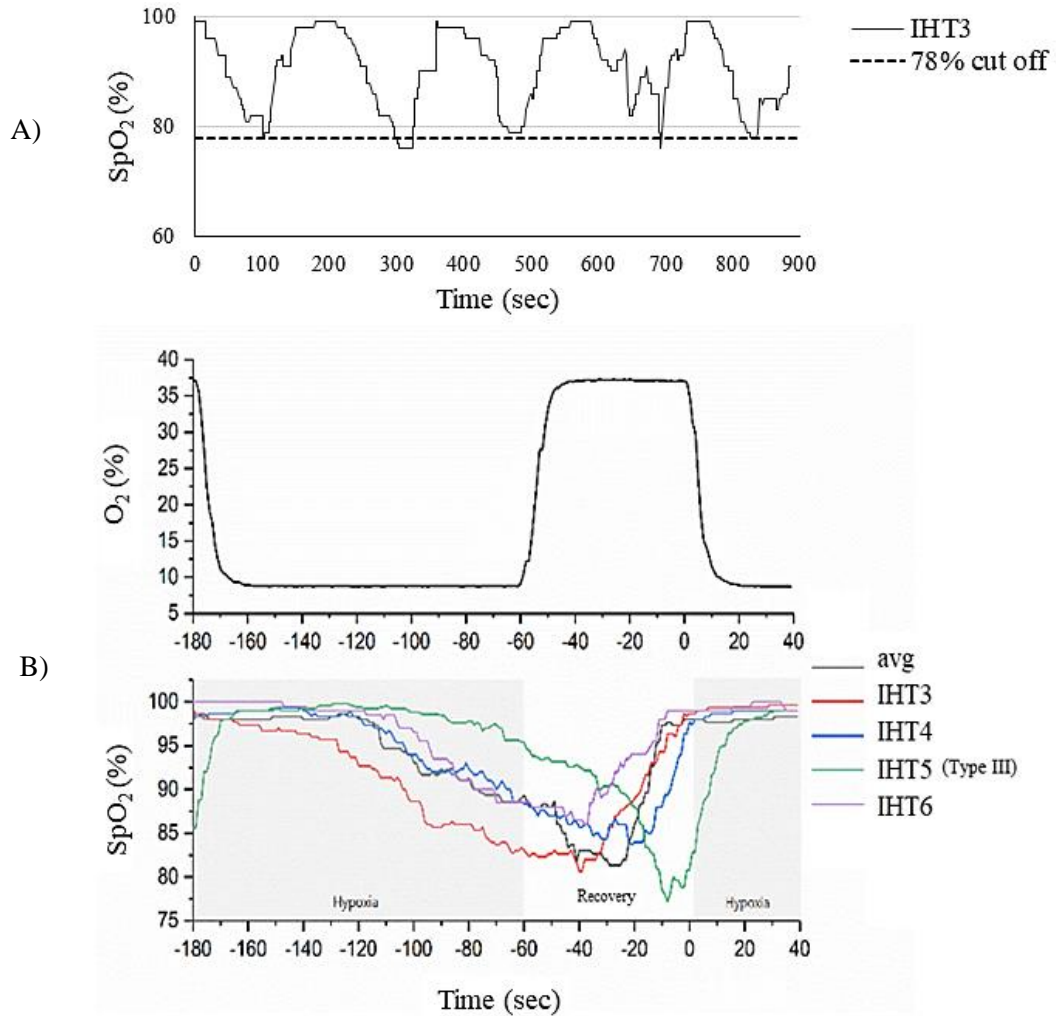


Figure.2.6. Shows the IHT given to four healthy participants (IHT3, IHT4, IHT5, and IHT6). **A)** Is an example of the SpO₂ response (participant IHT3). **B)** Shows the O₂ (%) over time (sec) in the top panel and in the bottom panel it shows the O₂ (%) event dependent averaging of the SpO₂ (%) responses to the IHT intervention. The graph displays the average of all IHT cycles for each participant as well as the grand average. The grand average is displayed in black.

2.6. The IHT intervention adopted involved 1 minute hypoxia (at FiO₂= 9.00%) interspersed with 1 minute hyperoxia (at FiO₂ between 21.00% and 40.00%)

2.6.1. Intermittent hypoxia training (IHT)

As the protocol with a longer hypoxia dose period was not well tolerated it was concluded that the intervention by Trumbower et al. (2012) described below was best suited in terms of maintaining subject compliance and safety over the duration of experiments to be performed in this thesis and would provide a more direct comparison to be drawn with prior published work. Measurements on key vital signs are reported

here for volunteers undergoing this IHT protocol consisting of one-minute intervals of repeated exposures of hypoxic ($\text{FiO}_2 = 9.00\%$) and normoxic/hyperoxic ($\text{FiO}_2 \sim 21.00$ to 40.00%) air. The participant was asked to sit comfortably and breathe normally through a mask connected to the air outflow of the GO2Altitude hypoxicator. The SpO_2 safety baseline level was set to 78% as in the previous section. This safety mechanism works by warning the experimenter to remove the mask when the participant's SpO_2 level decreases and remains below 78% SpO_2 level.

2.6.2. Vital Sign Measurements (blood pressure, saturation of oxygen and heart rate)

To study the safety and tolerance of this IHT intervention in healthy subjects we monitored blood pressure, saturation of oxygen and heart rate.

Blood pressure measurements were taken manually with an Omron M10-IT blood pressure measurement device using standard methods. Two recordings, 10 minutes apart, were taken before the IHT intervention. Further recordings were taken approximately 15 minutes into the intervention and at 10 and 30 minutes following cessation of IHT. The blood pressure measurements were taken from 7 participants (5 men and 2 women; mean age, 28; range, 24 to 36 years).

Arterial oxygen saturation (SpO_2 %) and heart rate was measured continuously for the entire 30 min of the IHT intervention through a pulse oximeter sensor whose output was connected to the hypoxicator which also stored the SpO_2 data in digital form. The SpO_2 and heart rate measurements were taken from 14 healthy adults (9 men and 5 women; mean age, 27; range, 26 to 36 years).

2.6.3. Analysis

As mentioned earlier the participants recruited in this study were allocated into two groups (Type II and Type III) depending on their response to the hypoxia test. In the previous preliminary experiment where the 2 minutes of hypoxia was studied, the participant that was allocated in Type III had a longer lag time compared to the participants allocated in Type II (Figure.2.6). Therefore, it was decided that the blood pressure, SpO_2 , heart rate and HRV would be shown separately for each type as well as together, so the reader has the chance to visually compare the results. Eleven participants were allocated to Type II and only three in Type III, making it impossible to complete an accurate comparison between the types using statistical methods.

Blood pressure measurements were recorded at pre-, during and post-IHT. The raw data of each participant's measurements were graphed as well as the mean± standard deviation. The average measurements across all participants at pre-IHT, during IHT and post-HT were submitted for One-way repeated measures ANOVA ($p < 0.05$) to study if a significant change occurred over time ($n=7$). The analysis was completed in SPSS and the graph in Matlab.

For the SpO₂ the raw data of each participant and the grand average is displayed on a graph. A box plot was also constructed to show the spread of the data. Moreover, the study reports measurements of time shift in the SpO₂ when compared to the intervention (the O₂ concentration given at each interval) were reported as well as the rate of drop in SpO₂ and the rate of recovery in SpO₂. The time shift was calculated from the minimum SpO₂ to the minimum O₂ and the rate of drop and rate of recovery were measured by calculating the slope. These measurements were taken for each cycle of each participant's response as well as from the grand average SpO₂ waveform. They provide insight into the subjects' experience during this IHT intervention dose. In the results section the grand average SpO₂ waveform was analysed first. Images displaying the shift in the grand average SpO₂ waveform compared to O₂ are shown in this section too. Subsequently, the mean and standard deviation across all participants for time shift, rate of drop and rate of recovery is displayed on a graph. The analysis and graphs were completed in Matlab and Excel.

To illustrate the heart rate, a moving average was calculated over a sliding window of 30 RR intervals. Additionally, as in the SpO₂ data a box plot was constructed to show the spread of the data. The graph was constructed in Matlab.

To measure HRV, the heart rate (bpm) was converted into RR intervals measured in ms ($\frac{60}{heart\ rate} \times 1000$). Then rMSSD was calculated using RR (please refer to Table.2.2 for how rMSSD was calculated) and both RR and rMSSD were graphed every 20 seconds. Therefore, during the 1-minute intervals we provide 3 measurements of RR and rMSSD. It is important to mention that a PSA analysis was not used because we believe it was not an appropriate measure for cyclical hypoxia with a lag time. The analysis was completed in Matlab and the graphs in Excel.

2.6.4. Results

In the results section the data is presented in the following order:

- 1) blood pressure results before, during and following IHT recorded from 7 healthy participants
- 2) SpO₂ measurements during the IHT intervention recorded from 14 healthy participants
- 3) SpO₂ time shift when comparing it to the IHT intervention, rate of drop in SpO₂ and rate of recovery in SpO₂ (these measurements were taken from each participant's response and from the grand average SpO₂ waveform)
- 4) heart rate measurements during the IHT intervention recorded from 14 healthy participants and
- 5) HRV measurements of RR and rMSSD calculated using the heart rate (bpm) measurements recorded during IHT from 14 healthy participants.

Blood pressure measurements were recorded while exploring the IHT intervention. There are more measurements of SpO₂ and heart rate because they were gathered during the SEPs and TMS experiments that will be discussed in the following chapters of the thesis.

2.6.4.1. Blood pressure

The blood pressure measurements of each participant is displayed in the Figure 2.7. In panel A) the figure displays all the participants except IHT5 who was allocated in Type III while B) displays all the participants together. The mean and standard deviation across all subjects (Figure.2.7.B) at each stage of the intervention (pre, during and post-IHT) was calculated and a One-way repeated measures ANOVA showed no significant difference in the mean systolic and diastolic blood pressure, Wilks' Lambda=0.177, $F(4,3)=3.497$, $p=0.166$ and Wilks' Lambda=0.591, $F(4,3)=0.519$, $p=0.733$, respectively at the different measurement times relative to IHT exposure despite what appears a trend for a decrease in systolic pressure immediately after IHT (post IHT₀).

In Figure.2.7.A, the graph displays the average excluding participant IHT5. The One-way repeated measures ANOVA showed no significant difference in the mean systolic and diastolic blood pressure, Wilks' Lambda= 0.143, $F(4,3) = 3.971$, $p=0.143$ and Wilks' Lambda= 0.495, $F(4,2) = 0.511$, $p=0.745$, respectively.

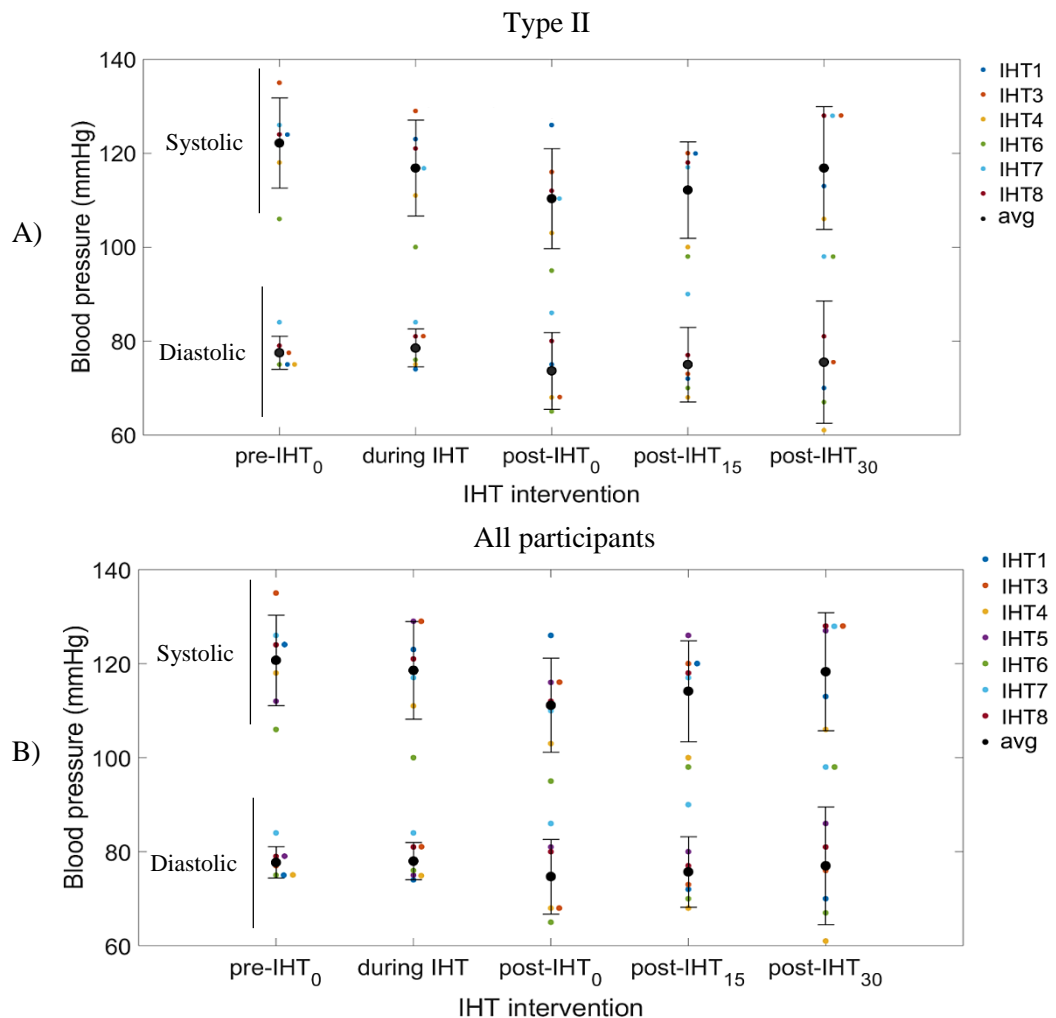


Figure.2.7. Blood pressure measurements (mmHg), systolic and diastolic, displayed for each participant (IHT1, IHT3, IHT4, IHT5, IHT6, IHT7 and IHT8) and the mean with the standard deviation in black. One-way repeated measures ANOVA was used to examine if there was a significant difference in blood pressure over time. $p < 0.05$ is displayed with an *. A) excludes participant IHT5 that was allocated in Type III according to the hypoxia test while B) includes the entire pool of participants.

2.6.4.2. Saturation of oxygen

Figure.2.8, displays the SpO₂ response of each participant in Type II (A), each participant in Type III (B) and all the participants (C). The average measures are displayed in black. Looking at the results in Figure.2.8 and the box plots in Figure.2.10

it was concluded that there were no clear differences in the responses between participants in Type II and Type III. However, a statistical analysis could not be completed as there were only 3 participants allocated in Type III while there were 11 participants in Type II.

In Figure.2.8.A we can see from the individual responses that following the first exposure to hypoxia there was a higher level of variability in SpO₂ and most participants displayed the highest drop in SpO₂ in the first hypoxia cycle. Out of 13 participants 9 subjects (IHT1, IHT3, IHT4, IHT7, IHT10, IHT11, IHT12, IHT14 and IHT15) showed this behavior during the first exposure to hypoxia. This was expected as it was the first exposure to low oxygen.

The lowest SpO₂ level reached by each participant is displayed in Table.2.5 with IHT6 demonstrating a sudden drop in SpO₂ to 68% that triggered an alarm resulting in face mask removal and allowing the participant to breathe room air. Once normal breathing was re-established (62 seconds) and the subject's comfort and willingness to proceed was determined, the face mask was refitted and intervention resumed (Figure.2.8.A). This adverse incident occurred only once during the intervention and the participant did not report any concerning adverse effects during and following IHT. It is believed that this occurred because the sensor was not in good contact with the skin. A supplementary graph was created, Figure.2.9, to show how this drop in SpO₂ by participant IHT6 affected the average response. As clearly displayed the effect was minimal (Figure.2.9).

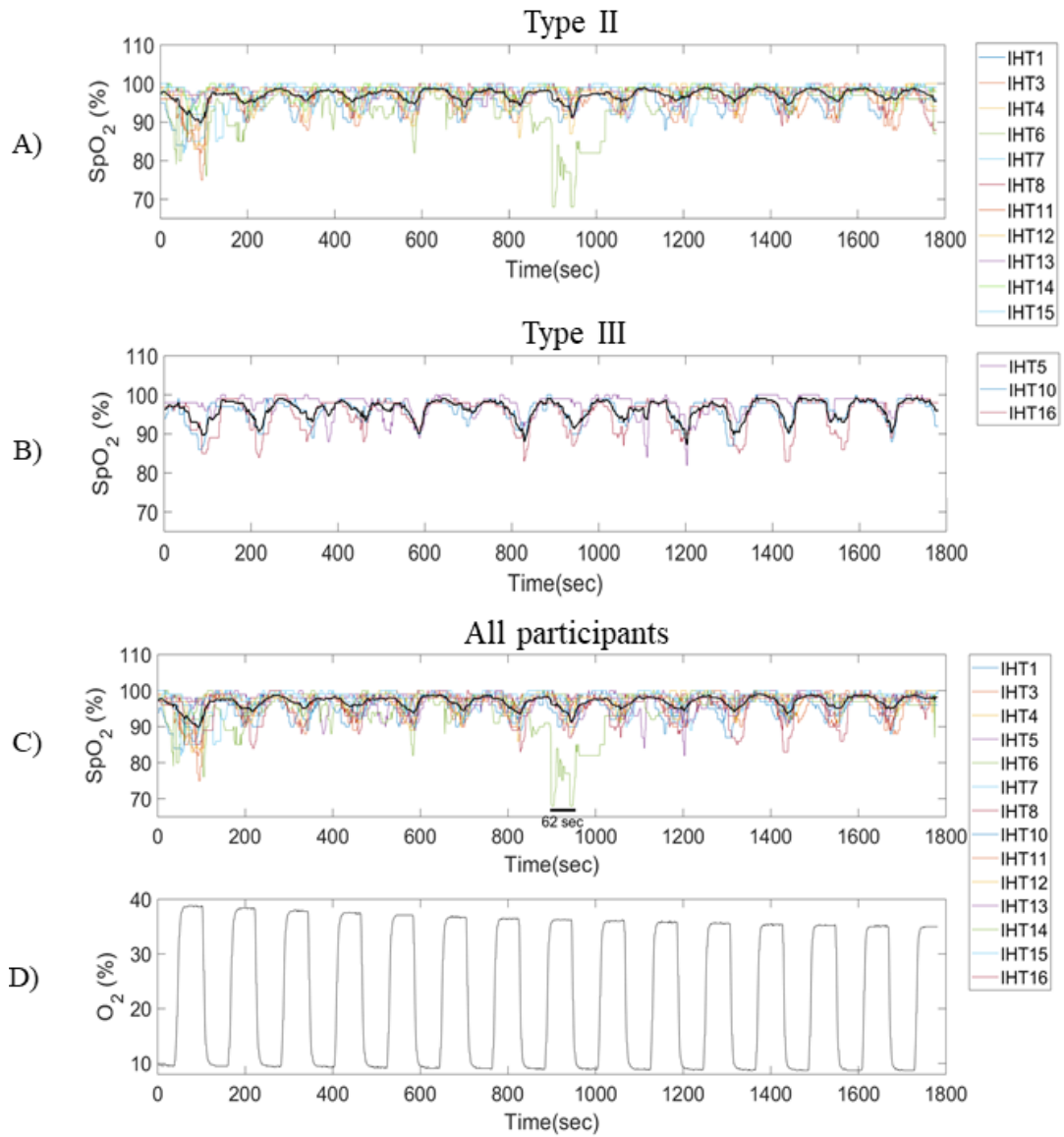


Figure.2.8. SpO₂ (%) recorded during the IHT intervention graphed over time (sec). SpO₂ of all the participants that were allocated to **A) Type II** (n=11) and **B) Type III** (n=3) during the hypoxia test and **C) all participants** graphed together (n=14). **D) Shows the IHT intervention with O₂ (%)**.

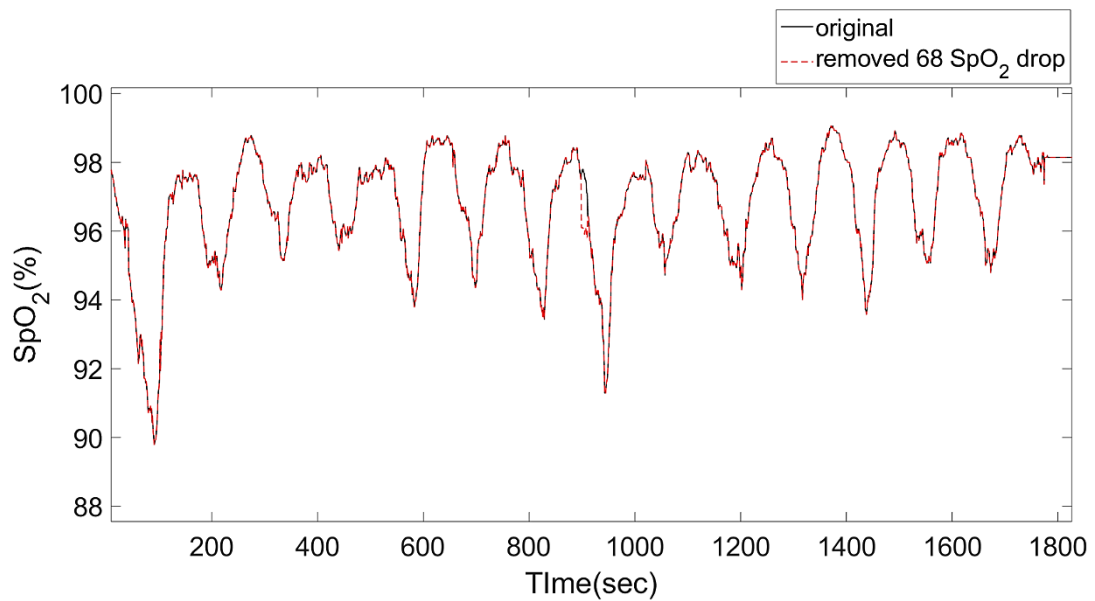


Figure.2.9. Original average of SpO_2 (%) in black and following the removal of the 68 SpO_2 drop by participant IHT6 is displayed with a dashed red line.

In Figure.2.10 the box plots show the spread of the data of the SpO_2 . The first box plot displays the SpO_2 response of participants allocated in Type II, the second box plot displays the SpO_2 response of participants allocated in Type III and the last box plot shows the data of all participants together.

In Figure.2.10.A (Type II) the median SpO_2 (%) is displayed in red at 98 % and the lower quartile (25th percentile) and upper quartile (75th percentile) are displayed in blue, 96 % and 99%, respectively. The minimum value is 68% and maximum is 100%. For Figure.2.10.B (Type III) the median is 98% and the quartiles are 95% and 98%. The maximum and minimum are 100% and 82%. For the entire dataset the median remained at 98% with lower (25th percentile) and upper quartiles (75th percentile), at 96% and 99%, respectively (Figure.2.10.C). The minimum SpO_2 (%) is 68% which corresponds to participant IHT6 and the maximum SpO_2 (%), 100%, which corresponds to the recovery period. Table.2.5 shows the lowest SpO_2 level reached by each participant which ranges between 75% and 92% (if 68% drop is not included). This is a big range and highlights that there are individual differences in the response to IHT.

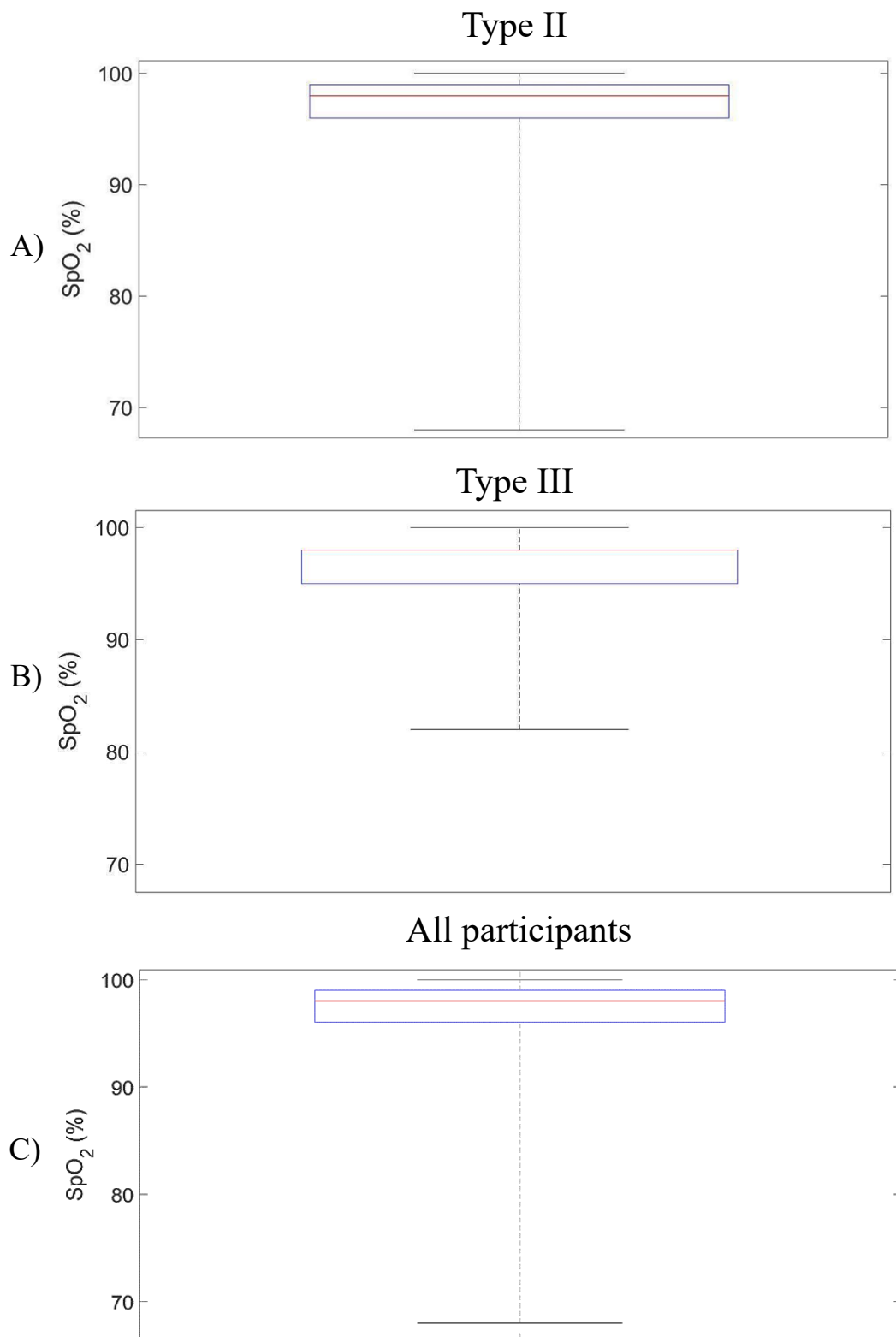


Figure.2.10. A box plot that displays the median in red and the 25th and 75th percentiles in blue. The whiskers show the minimum and maximum SpO₂ (%). Participants allocated to Type II are displayed in **A**) (n=11), those in Type III are displayed in **B**) (n=3) and **C**) displays the spread of the data for all of the participants (n=14).

Table.2.5. Lowest SpO₂ level reached by each participant during IHT

Participant	Hypoxia test result	Lowest SpO ₂ (%)
IHT1	Type II	83
IHT3	Type II	82
IHT4	Type II	88
IHT5	Type III	82
IHT6	Type II	68
IHT7	Type II	82
IHT8	Type II	88
IHT10	Type III	86
IHT11	Type II	75
IHT12	Type II	83
IHT13	Type II	91
IHT14	Type II	92
IHT15	Type II	89
IHT16	Type III	83

2.6.4.3. Time shift and rate of rise and drop analysis on the grand average SpO₂

Figure.2.11 shows the average SpO₂ response (shown in black in Figure.2.8) together with the O₂ intervention. It is clear that the concentration of oxygen the participants breathed, as part of the intervention, was not in synch with measurements of SpO₂. This made it challenging to predict the participants' response to hypoxia. In Figure.2.11 the original response of SpO₂ and O₂ (A) is illustrated and in (B) the SpO₂ response is shifted so is in synch with the first couple of cycles of O₂ intervention. From Figure.2.11.B it is clear that the SpO₂ changed over time and an increase in the time shift suggests adaptation (highlighted with a blue box in Figure.2.11.B).

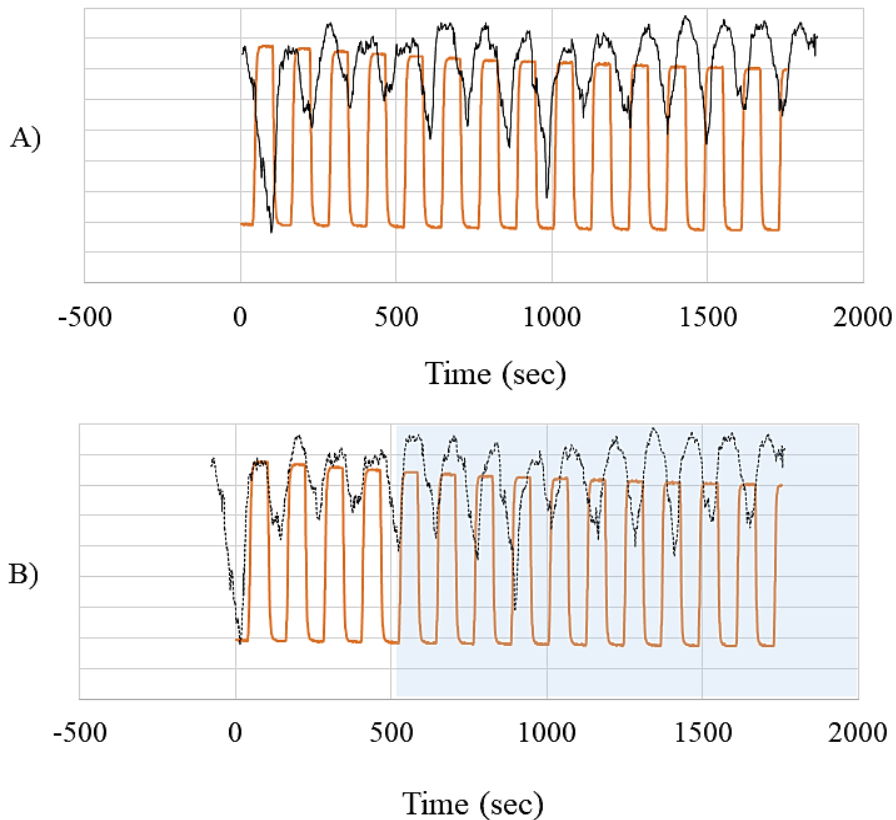


Figure.2.11. Demonstrating the SpO₂ (black line) and O₂ (orange line) measurements. A) Shows the original response and B) shows the response shifted so the first cycles are in sync with the O₂ delivered to the participants. The blue box highlights when the response was out of sync showing well how the SpO₂ changes over time. Please note that a y-axis is not added because the graphs have been overlaid and moved around.

Figure.2.12.A displays the average period of the grand average SpO₂ waveform and (B) displays the slope measurements to study the rate of drop in SpO₂ in each cycle and the rate of recovery in SpO₂ in each cycle. Measurements of slope are displayed in Figure.2.13.

The rate of recovery measured from the grand average waveform of SpO₂ was 0.13 ± 0.06 SpO₂%/sec and the mean rate of drop in SpO₂ was 0.09 ± 0.02 SpO₂%/sec (mean \pm standard deviation) (Figure.2.13.A). Moreover, there is a rapid recovery in the first interval with a slope of 0.27 SpO₂%/sec (Figure.2.13.A). In the subsequent intervals the rise in SpO₂ increase was shallow suggesting some stabilization in the physiological/homeostatic response (Figure.2.13.A). A shallow slope is also observed in the rate of drop in SpO₂. This suggests that the intervention was well tolerated.

Figure.2.12.C displays the time shift analysis and the results are shown in Figure.2.13.B. The period of the response was 123 ± 8 seconds (Figure.2.12.A) and on average there was a time shift of 85 ± 10 seconds (mean \pm standard deviation) (Figure.2.13.B). Moreover, there was an adaptation to the brief hypoxic episodes as the time shift started at around 80 seconds and later on increased to 100 seconds (Figure.2.13.B).

Overall, these measurements show that over time there was a consistency in the physiological response to IHT. The IHT intervention seemed safe and was well tolerated by the participants. Moreover, it appeared that over time there was an adaptation to the brief hypoxic intervals as it took longer for their saturation of oxygen to drop.

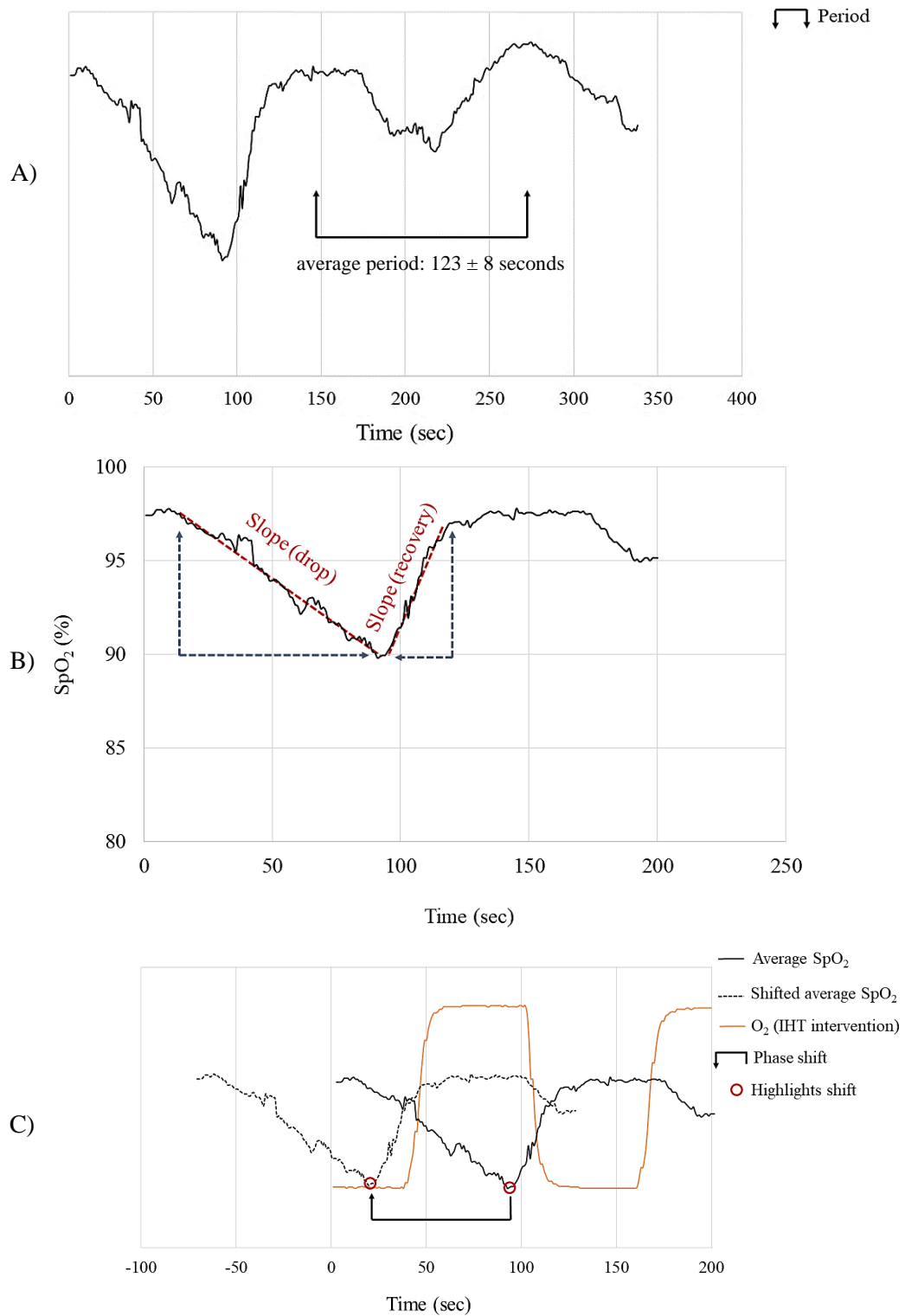


Figure.2.12. Demonstrating the analysis on the grand average SpO₂ response. A) Displays the period which is on average 123 ± 8 seconds, B) demonstrates the rate of drop and rate of recovery and lastly, C) shows the time shift of the SpO₂ response compared to the O₂ response. If the SpO₂ was in synchrony with O₂ delivery the location of SpO₂ would be similar to the staggered line response.

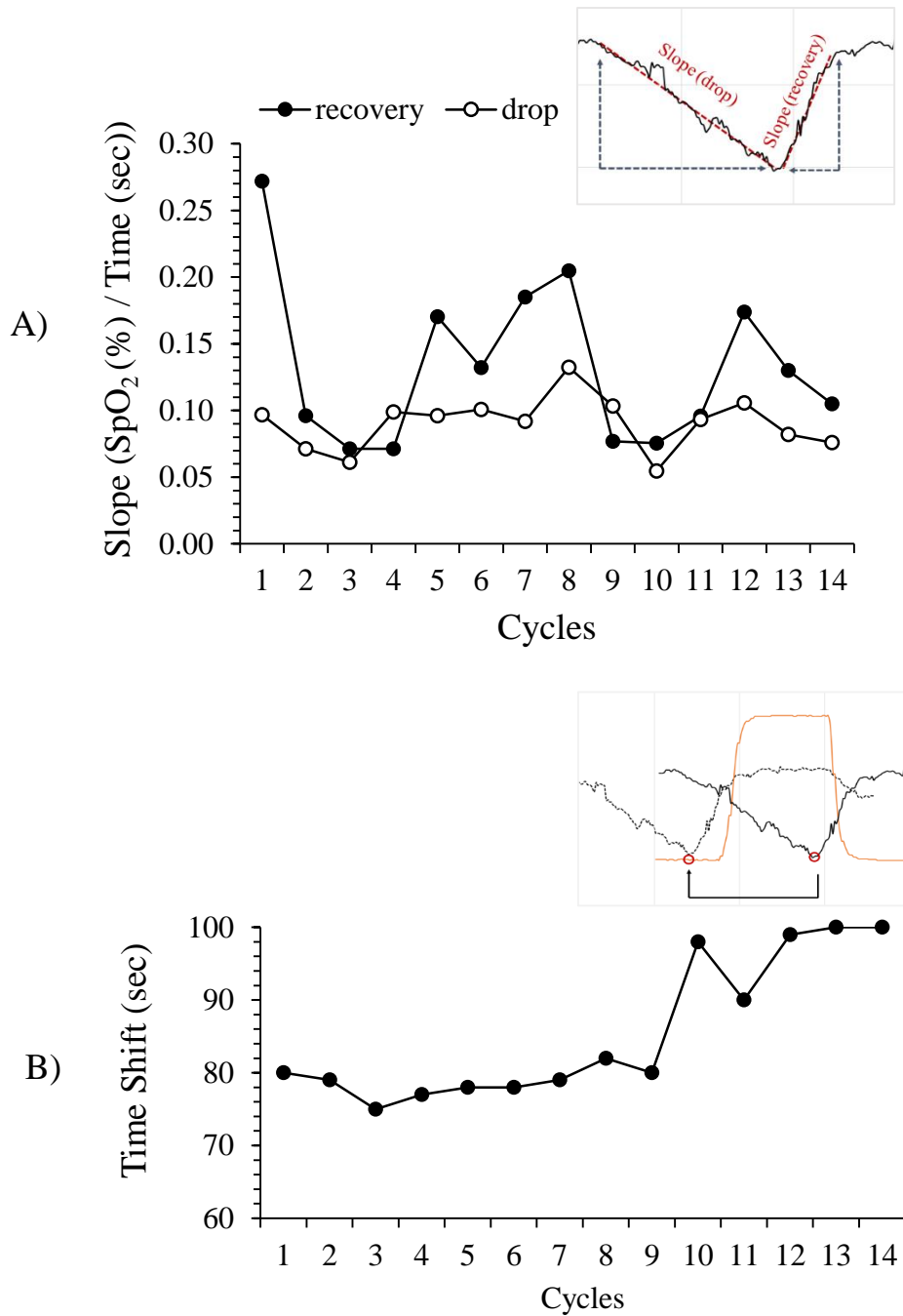


Figure.2.13. **A)** The rate of recovery and rate of drop in SpO₂(%)/Time (sec) calculated for each cycle of the grand average response. **B)** The time shift of the SpO₂ (seconds) response from the O₂ delivery response measured for each cycle of the grand average response.

2.6.4.4. Average rate of recovery and drop in SpO₂ across all participants and time shift

Figure 2.14, 2.15 and 2.16 display the rate of drop and rate of recovery in SpO₂ for all the participants (n=14), type II (n=11) and type III (n=3), respectively. These measurements provide information on how quickly the participants are using up

oxygen and how fast they recover when given hyperoxia. The slopes seem consistent throughout the intervention. However, it appears that in the first cycle of hypoxia Type II participants (Figure.2.15 B)) have a steeper rate of recovery compared to Type III participants (Figure.2.16 B)). Unfortunately, the comparison can not be statistically compared because of the lack of participants allocated in Type III (n=3). In Type III, as previously mentioned, there are only 3 participants.

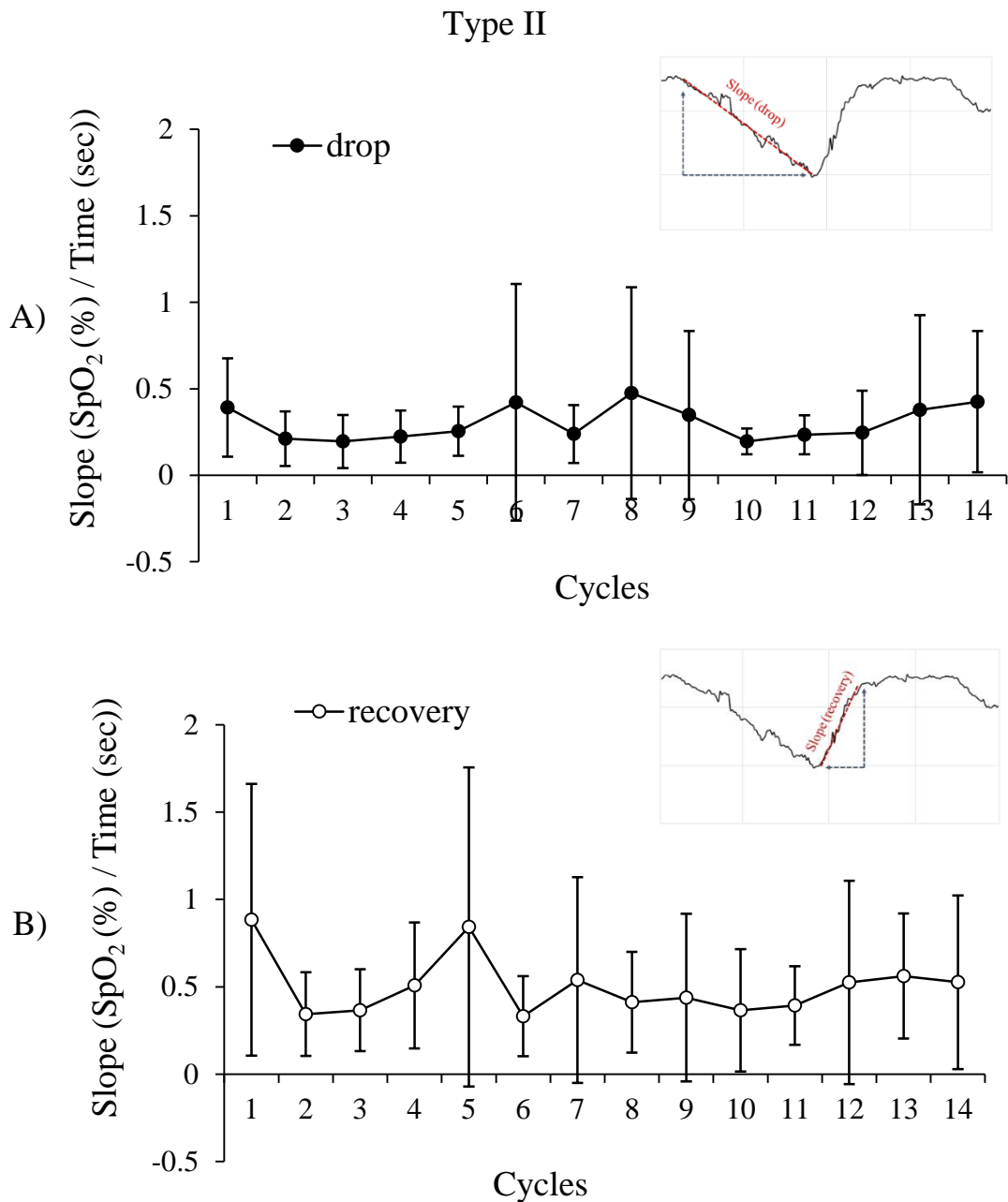


Figure.2.15. A) The rate of drop in SpO₂(%)/Time (sec) calculated for each cycle of the SpO₂ response and B) the rate of recovery in SpO₂. This is an average of all the participants that were allocated in Type II (n=11) and the standard deviation is displayed as error bars.

Type III

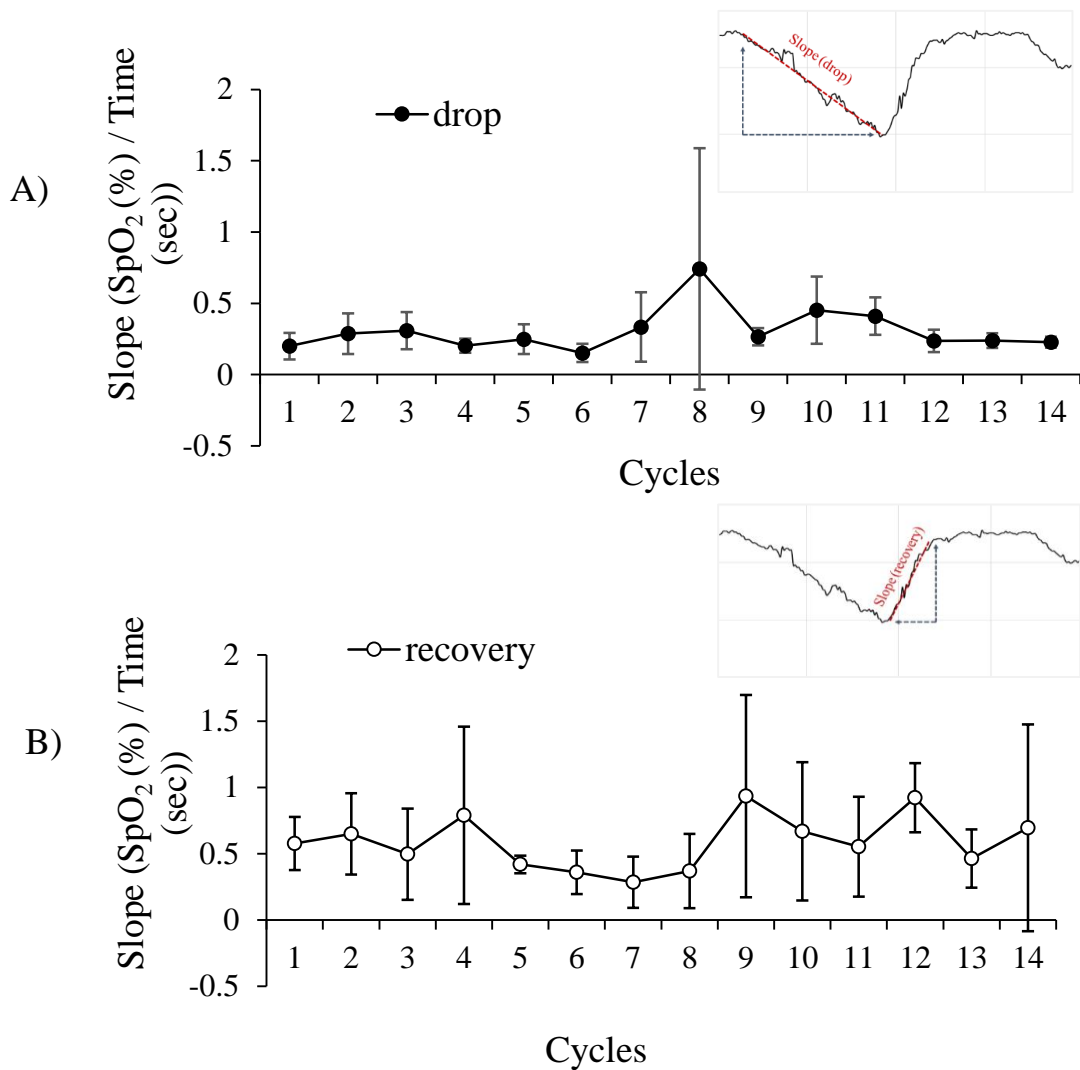


Figure.2.16. **A)** The rate of drop in SpO₂(%)/Time (sec) calculated for each cycle of the SpO₂ response and **B)** the rate of recovery in SpO₂. This is an average of all the participants allocated in Type III (n=3) that were allocated in Type II and the standard deviation is displayed as error bars.

Figure 2.17 provides information on the time shift (lag) of the SpO₂ signal compared to the timing of the change in inspired oxygen levels. If the responses were perfectly synchronised then the lag time would be zero and no time shift would be seen. The linear regression line fitted in the first few cycles showed a positive correlation of 0.94 when all the participants were included, 0.87 for Type II participants and 0.78 for Type III participants. A positive correlation in the time shift indicated that participants took longer to respond to low oxygen breathing. Moreover, it was evident that there is an increase in the standard deviation meaning that there was

a higher variability in the participants response. This suggests that participants may have been using a different methods to compensate for the low oxygen, such as an increase in tidal volume or an increase in breathing frequency.

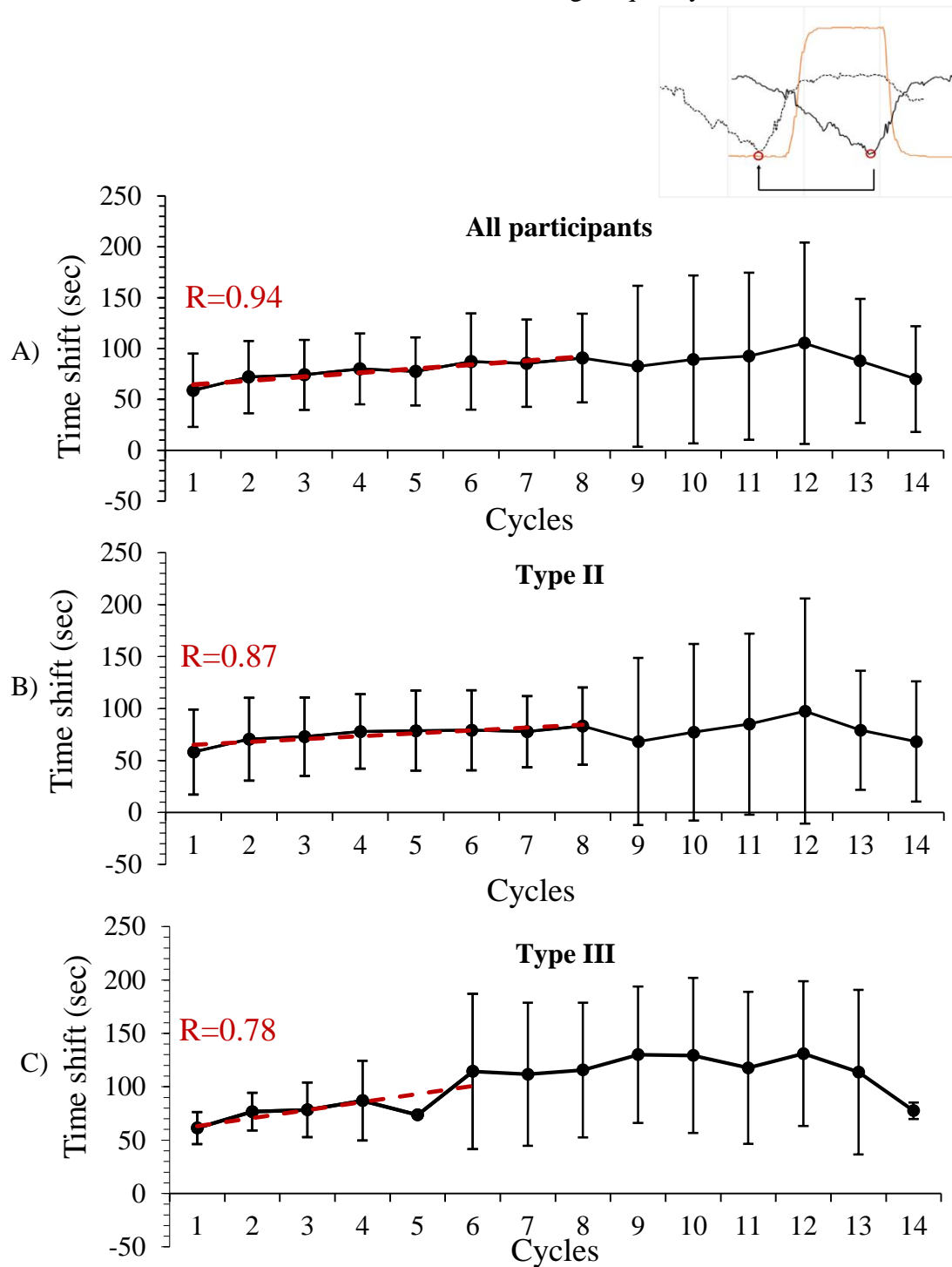


Figure.2.17. Time shift of the SpO₂ (seconds) response from the O₂ delivery response measured for each cycle. The measurements were averaged across all participants (A), across all Type II participants (B) and lastly, across all Type III participants (C). The data are displayed as mean \pm standard deviation. The red staggered line displays the positive correlation of the first few cycles and the R value is reported on each graph.

2.6.4.5. Heart rate

Figure.2.18 shows the heart rate measured from each participant which remained within 57 bpm to 81 bpm throughout the tests (Table.2.6) despite 9.00% FiO₂ hypoxia exposure. Accordingly, no adverse effect on heart rate was observed with IHT.

As you can see from Figure.2.18 graphs from each participant were separately produced and grouped in relation to whether the person was a Type II or Type III responder. No obvious differences between participants in Type II and Type III groups were apparent in heart rate measures. Again statistical analysis could not be performed as only 3 participants were allocated to Type III. Interestingly, the participant with the lowest heart rate, IHT3, was allocated as Type II in the hypoxia test (Table.2.6).

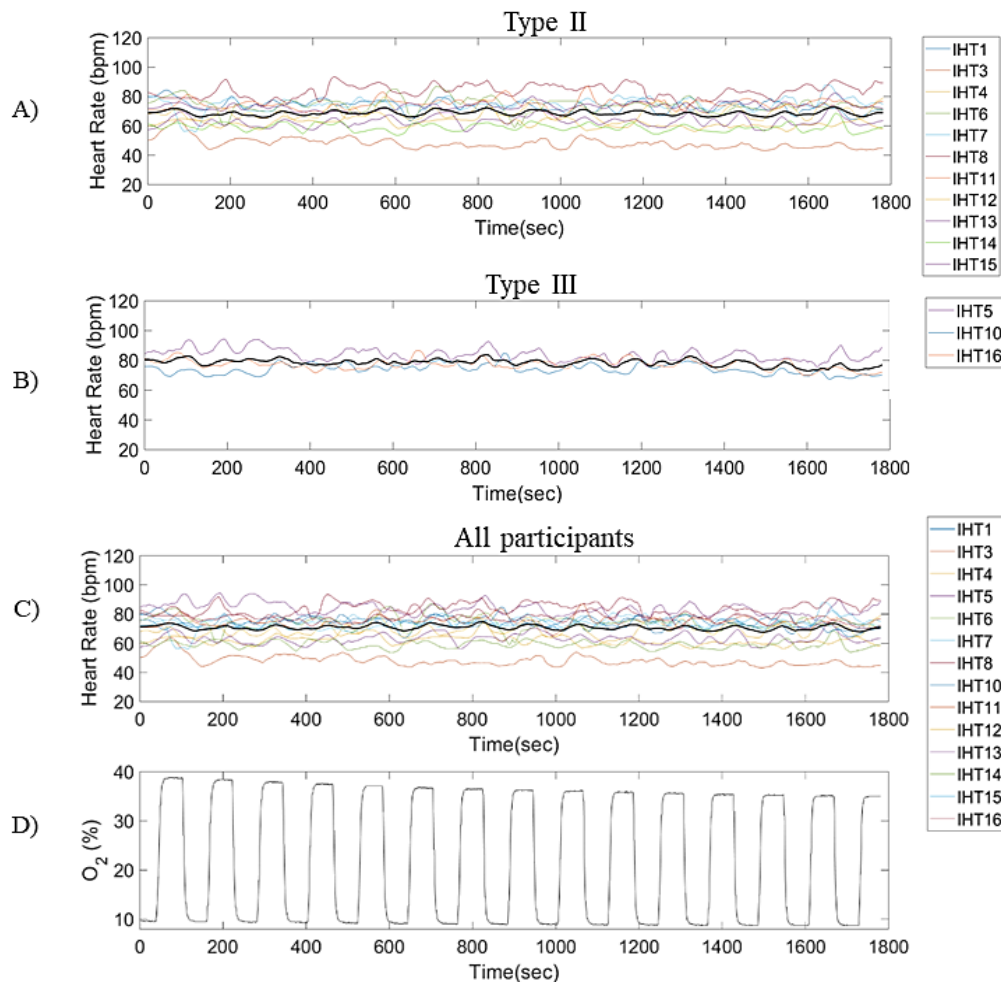


Figure.2.18. Heart rate recorded during the IHT intervention graphed over time (sec). Heart rate of all participants that were allocated **A)** Type II (n=11) and **B)** Type III (n=3) during the hypoxia test and **C)** all participants graphed together (n=14). **D)** Shows the IHT intervention with O₂ (%).

The box plots of Figure 2.19 show the spread of heart rate measurements for participants in Type II (Figure.2.19.A), Type III (Figure 2.19.B) and for all participants (Figure.2.19.C).

Figure.2.19.A the median heart rate is displayed in red which at 71 bpm and the lower quartile (25th percentile) and upper quartile (75th percentile) are displayed in blue (62 bpm and 76 bpm, respectively). The minimum heart rate was 43 bpm which corresponded to participant IHT3 and the maximum of 93 bpm was observed in participant IHT8, (see also Table.2.6). For Type III subjects (Figure.2.19.B) the median was 78 bpm and the quartiles 74 bpm and 82 bpm. The maximum and minimum heart rates recorded were 94 bpm and 67 bpm. When Type II and III data were pooled (Figure.2.19.C), the median heart rate (bpm) equalled to 73 bpm and the lower quartile (25th percentile) and upper quartile (75th percentile) were 64 bpm and 77 bpm, respectively. The maximum and minimum was 94 bpm and 43 bpm. Table.2.6 shows the range of heart rate for each participant.

These data collectively confirmed that there was no obvious change in heart rate measurements across Type II or III participants or between the Type classifications.

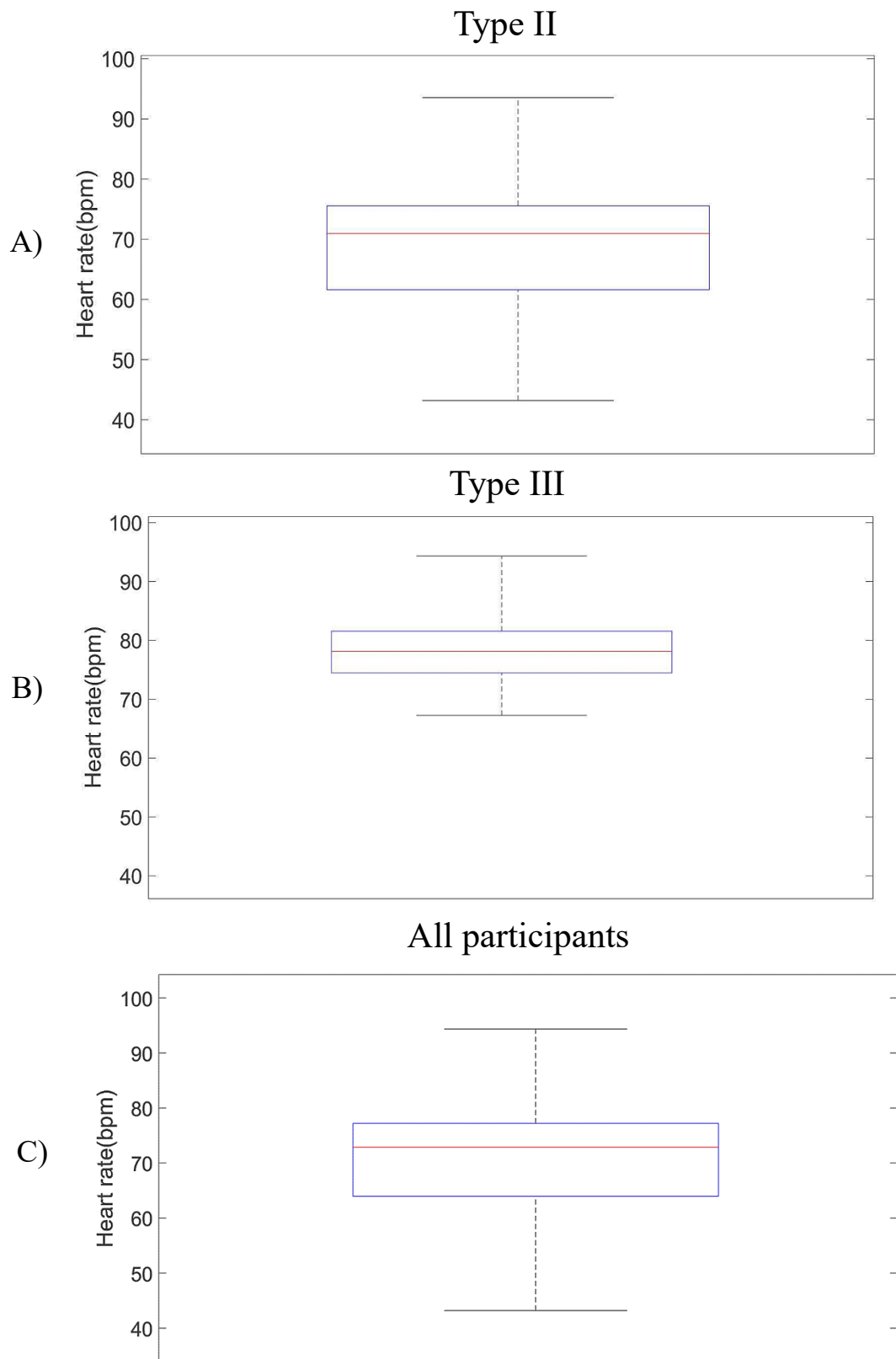


Figure.2.19. A box plot that displays the median in red and the 25th and 75th percentiles in blue. The whiskers show the minimum and maximum heart rate (bpm). Participants allocated to Type II are displayed in A) ($n=11$), those in Type III are displayed in B) ($n=3$) and C) displays the spread of the data for all of the participants ($n=14$).

Table.2.6. Range of heart rate for each participant during IHT

Participant	Hypoxia test result	Heart rate range (bpm)
IHT1	Type II	63 to 84
IHT3	Type II	43 to 64
IHT4	Type II	56 to 73
IHT5	Type III	76 to 94
IHT6	Type II	59 to 87
IHT7	Type II	56 to 88
IHT8	Type II	70 to 93
IHT10	Type III	67 to 85
IHT11	Type II	66 to 87
IHT12	Type II	59 to 80
IHT13	Type II	56 to 74
IHT14	Type II	54 to 69
IHT15	Type II	67 to 83
IHT16	Type III	70 to 87

2.6.4.6. Heart rate variability (HRV)

Figure.2.20, illustrates the ANS response during IHT, providing information on how challenging the intervention was for the participant. An increase in sympathetic nerve activity over the course of IHT indicated a challenging intervention that could perhaps have led to adverse effects, such as a sustained high blood pressure and heart rate.

The top panel Figure 2.20.A shows the average HRV measurements for participants that had a Type II response during the hypoxia test, Figure 2.20.B illustrates measures from Type III subjects and the Figure 2.20.C the average response of all participants.

From these results we can see that Type II average response has a higher RR interval ranging between 847 ms and 939 ms compared to Type III subjects where the RR response occurred between 722 ms and 826 ms. Statistical analysis was not deemed appropriate as the number of Type III subjects was 3.

As expected, fluctuations in the RR intervals were apparent in response to the IHT intervention but the values were consistently within the normal range (600 ms to 1000 ms) (Umetani et al., 1998).

In contrast, the results for rMSSD are much lower (2 ms to 12 ms) compared to the normal levels reported in the literature (19 ms to 75 ms) (Shaffer and Ginsberg et al., 2017; Umetani et al., 1998) (Figure.2.20). This perhaps indicates enhanced sympathetic activity.

Overall, in Figure.2.20 we can clearly see that the participants have been challenged by the IHT intervention but there was no increase in sympathetic activity over time. This means that the intervention is well tolerated and safe.

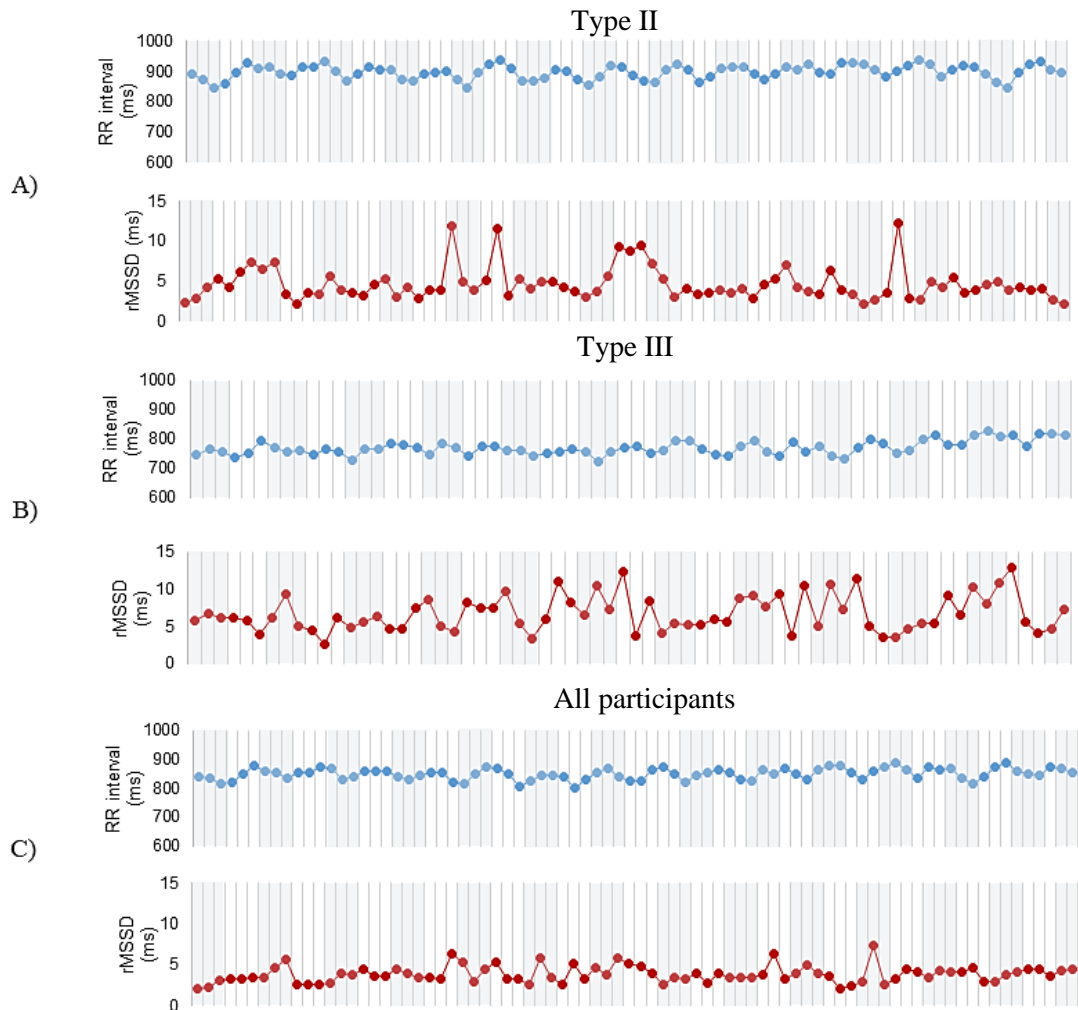


Figure.2.20. During IHT measurements of RR intervals (ms) and rMSSD (ms). Measurements during hypoxia are highlighted in grey. The measurements in between the grey ones are taken during the normoxia interval. **A)** Displays the average of all Type II participants, **B)** displays the average of all Type III participants and **C)** is an average of all participants together.

2.7. Discussion

Mild to moderate intermittent hypoxia exposure has been reported to induce widespread advantageous physiological effects throughout the body and researchers are beginning to look closely at its potential uses to treat certain conditions, improve fitness, and enhance athletic performance. As already mentioned, the dose, intervals, and duration of the IHT intervention is not standardised. However, the literature suggests that mild to moderate IHT protocols can deliver beneficial effects while avoiding the potential adverse effects associated with chronic severe IHT that occurs in cases of OSA.

This chapter explored the IHT intervention from a safety perspective by measuring a range of vital sign measures including blood pressure, heart rate, HRV and SpO₂ in healthy subjects exposed to an IHT protocol. The protocol that was adopted has been suggested by Trumbower et al. (2012) and used to dose iSCI patients as a therapy to aid motor function recovery. The literature has reported that this IHT protocol is capable in improving walking ability, muscle strength and standing balance (Trumbower et al., 2012; Hayes et al., 2014; Navarrete-Opazo et al., 2017).

Our preliminary measurements showed that the IHT intervention composed of 1 minute hypoxia (FiO₂= 9.00%) interspersed with 1 minute recovery (FiO₂= 21.00% to 40.00%) does not adversely stress the respiratory or cardiovascular systems whilst extending the hypoxia period to 2 minutes did result in participant discomfort and reports of fatigue and dizziness. These adverse signs occurred despite the GO2Altitude device cycling between hypoxia and hyperoxia. Collectively resulting in the view that to preserve a safe environment for the future experiments to be reported in the thesis, the IHT protocol of 1 minute hypoxia (FiO₂= 9.00%) interspersed with 1 minute recovery (FiO₂= 21.00% to 40.00%) should be adopted.

The results suggest that with this IHT intervention the response to low oxygen intervals vary among participants but is generally safe. Concerning changes in blood pressure, heart rate, HRV and SpO₂ were not observed, however, the results show that there is a variability in each participant's tolerance to IHT and perhaps a personalised intervention needs to be examined in the future when implementing IHT clinically and

in subjects with comorbidity. Moreover, it may be valuable to consider whether several exposures of the intervention cause an adaptation. This means that a different protocol needs to be administered to the patient following several exposures to IHT, to maintain an adequate homeostasis challenge over time. More details on this chapter's results and speculations are described in the sections below.

2.7.1. Results from pilot studies on the IHT intervention

Two pilot studies were completed before finalising the IHT intervention that will be used in the following chapters of the thesis. Primarily, the investigation begun with the logistics of removing the mask every hypoxia interval. The purpose was that the intervention given to iSCI patients involved hypoxia and normoxia intervals rather than hypoxia and hyperoxia intervals that were provided by the hypoxia machine used in this laboratory. Difficulties in controlling timing of mask on and off motions introduced variation in the hypoxia/normoxia intervals and reduced subject compliance during the experiment. Nevertheless, in the tests completed no observational difference could be detected in the vital sign measurements when normoxia ('mask off') periods were compared to hyperoxia ('mask on') recovery intervals. Accordingly, the hyperoxia cycling of the GO2Altitude device was not considered to be a hindrance to intermittent hypoxia stimulation.

It is important to mention here that the level of hyperoxia given to the participant by the hypoxia machine depends on how low their SpO₂ dropped during the hypoxia interval. In this way the machine delivers adequate oxygen concentration capable of recovering the SpO₂ levels back to normal within the 1 minute resting interval. It is believed that in healthy subjects, where oxygen uptake across the lungs is not compromised and when there is no underlying cardiovascular disease, that haemoglobin oxygen saturation occurs sufficiently rapidly that there would be minimal differences in end-capillary oxygen levels irrespective of normoxia or hyperoxia air breathing.

Following this study, the investigation progressed by examining a longer dose of hypoxia. The purpose was to find an intervention that challenged the homeostasis of healthy participants to a level reported in the literature. The dose duration of hypoxia was set to 2 minutes while the dose duration of normoxia was set to 1 minute. This

protocol was not well tolerated by healthy young participants as they experienced breathlessness and dizziness during the IHT intervention. Just a 30 second increase in the duration of hypoxia interval crossed the line from a safe intervention to one that exhibited adverse effects.

Trumbower et al. (2012) also studied a longer interval of hypoxia which was set to 1.5 minutes and reported good tolerance by the selected iSCI patients. The patients recruited for this experiment did not display underlying cardiovascular and respiratory complications. It would have been interesting to study this protocol in healthy subjects but the hypoxia machine in the experiments could not achieve 1.5 minutes of hypoxia.

As a longer duration of hypoxia was not well tolerated by our participants the investigation continued using the original protocol by Trumbower et al. (2012) which involved 1 minute intervals of hypoxia with 1 minute intervals of normoxia. The following sections provide results of blood pressure, heart rate, HRV and SpO₂ with this IHT dose.

2.7.2. Blood pressure and heart rate

Measurements of blood pressure before, during and following IHT showed that the intervention was safe. In fact, it seemed that IHT slightly decreased the blood pressure. In the average across all participants the systolic blood pressure decreased during IHT and further decreased in measurements right after IHT and slowly recovered in measurements at 15 minutes and 30 minutes following IHT. The range of systolic blood pressure in this study was 95 mmHg to 135 mmHg which was similar to the range reported by Hayes et al. (2014) of 85 mmHg to 160 mmHg.

Similar to blood pressure, heart rate measurements were within a normal range, considering that the participant was exposed to brief periods of hypoxia. The heart rate range reported by Hayes et al. (2014) was 40 bpm to 160 bpm and for our study it was 43 bpm to 94 bpm. Please keep in mind that Hayes et al. (2014) used a slightly longer duration of hypoxia, 1.5 minutes, which could account to a slightly higher systolic blood pressure and heart rate.

2.7.3. HRV

Studies investigating the benefits of IHT in iSCI patients have not considered HRV. This measure provides information on ANS activity. Measurements of HRV were derived from heart rate measurements that were taken during the IHT intervention. The focus was to examine whether the intervention was safe and well tolerated by the healthy participants. Measurements of RR and rMSSD show that the intervention challenged the participants without an increase in sympathetic activity over time that would indicate potential issues with the intervention.

2.7.4. SpO₂

Moreover, SpO₂ was measured and the majority of the participants in this study with the 1 minute hypoxia and 1 minute normoxia protocol dropped to an SpO₂ level of around 75% to 89 % which is similar to the levels reported in iSCI patients, 75% to 85% (Trumbower et al., 2012; Trumbower et al., 2017; Lynch et al., 2017; Navarrete-Opazo et al., 2016b; Hayes et al., 2014). Furthermore, Christiansen et al. (2018), who investigated the same IHT protocol in healthy subjects within the same age group as our subjects, reported an SpO₂ drop of $81.3 \pm 1.2\%$ (mean \pm standard deviation, n=21) and no adverse effects. Our study reports similar values: $83.7 \pm 6.4\%$ (mean \pm standard deviation, n=14).

Moreover, some important information that has not yet been reported in the literature is that 69% of the participants had their lowest drop in SpO₂ in their first exposure of hypoxia and looking at the grand average SpO₂ response it seems that following the first exposure to hypoxia, participants had the steepest rate of recovery. The steeper rate of recovery was also seen in the average response across all participants allocated in Type II but not observed in participants allocated in Type III. Apart from the first cycle in the rate of recovery the rest of the measurements are consistent. A consistency in the measurements were also observed in the rate of drop in SpO₂. This indicates that the intervention is well tolerated.

Lastly, the SpO₂ response cannot be easily predicted as it is out of synch from the O₂ percentage delivery, and it seems that the lag time measured in seconds increases as participants become more accustomed with the intervention. This is observed in the

measurements taken from the grand average SpO₂ waveform as well as in the average taken from measurements across all participants. A positive correlation of 0.94 was observed in the first few cycles of the intervention. Subsequently the response is variable because participants are more stimulated and are possibly using different mechanism to compensate for low oxygen breathing.

In the future clinicians may need to take into consideration that over time there is an adaptation to the IHT intervention dose and this may require to change the dose of IHT so the patient can still receive the benefits of the intervention. This is likely to occur with cumulative interventions and it is worth investigating this in the future. Moreover, even though measurements on the rate of drop and rate of recovery in SpO₂, as well as the time shift, did not provide additional insight from this study, they are valuable measures to monitor how the physiology is adapting to IHT (adaptations are likely to be related to an improvement of respiratory fitness following several IHT exposures).

2.7.8. Conclusion

To conclude, this chapter focussed on finding an appropriate IHT intervention that challenged the homeostasis of our healthy subjects by briefly reducing the SpO₂ levels. This chapter shows that the IHT intervention, which comprised of 1 minute hypoxia interspersed with 1 minute normoxia, was successful in dropping the SpO₂ level of our participants to levels reported in the literature. Moreover, the safety of this intervention was studied by monitoring blood pressure, heart rate, SpO₂ and HRV. There were no adverse effects reported as well as no concerning changes in heart rate and blood pressure. Similar outcomes were reported in healthy subjects and patients with iSCI (Trumbower et al., 2012; Trumbower et al., 2017; Christiansen et al., 2018). Following this chapter, the investigation will continue with examining the mechanism of action of IHT on spinal pathways in healthy subjects.

3.1. Introduction

3.1.1. Intermittent hypoxia and iSCI

Intermittent hypoxia is an attractive potential supplementary treatment to further enhance motor improvement observed following existing rehabilitation methods or as a standalone treatment for clinical populations that cannot sustain or engage in intensive physical rehabilitation approaches (Trumbower et al., 2012; McCaughey et al., 2016; Hayes et al., 2014; Welch et al., 2020). There are several studies that have been conducted on iSCI patients showing that even with few exposures to IHT there are functional benefits in walking speed, walking endurance, dynamic balance and muscle strength (Trumbower et al., 2012; Trumbower et al., 2017; Hayes et al., 2014; Navarrete-Opazo et al., 2016b; Navarrete-Opazo et al., 2017). However, there is limited information on the mechanism through which IHT exerts an influence or where its sites of action exist within cortical or spinal motor or sensory pathways.

Research on IHT as a potential therapy for iSCI rests on the foundation that it strengthens synaptic inputs to phrenic and other respiratory motor neurons leading to spinal respiratory plasticity and perhaps a similar cascade of events may also lead to plastic changes in somatic motor pathways (Kinhead et al., 2001; Baker-Herman and Mitchell, 2002; Bach and Mitchell, 1996; Ling et al., 2001; Hoffman et al., 2010; Golder and Mitchell, 2005; Hoffman and Mitchell 2013; Fields, Springborn and Mitchell, 2015; Agosto-Marlin and Mitchell, 2017; Hoffman et al., 2013; Hoffman et al., 2010).

3.1.2. Investigating the mechanism of action

The first step to understanding more about the neural mechanisms associated with the functional benefits observed following IHT in human subjects should include conducting neurophysiological tests to assess the functional integrity of ascending and descending pathways of the spinal cord and whether IHT alters excitability in these systems. Christiansen et al. (2018) was the first to provide evidence that IHT alters corticospinal function in humans by measuring MEPs. The study used an IHT protocol

that consisted of 15 cycles with alternating exposures of 1 min hypoxia ($FiO_2=0.09$) and 1 min normoxia ($FiO_2=0.21$) and assessed cortical, subcortical and intracortical excitability before, immediately after and at 15, 30, 45, 60 and 75 min post-IHT. Christiansen et al. (2018) observed an increase in MEPs measured from the first interosseous muscle (FDI) and in one participant the effect lasted up to 120 min following IHT. However, the increase in MEP amplitude was observed without seeing changes in motoneuronal excitability. Motoneuronal excitability was measured using F-wave following supramaximal stimulation of the ulnar nerve at the wrist suggesting a cortical effect mediates the effect of IHT on MEPs (Christiansen et al., 2018).

3.1.3. Somatosensory evoked potentials (SEPs)

As cortical excitability is influenced by sensory feedback it is also important to determine if increased excitability or conduction change in ascending spinal tracts is influenced by IHT. Furthermore, as traumatic SCI commonly leads to disruption of both sensory and motor pathways (Marino et al., 2003) and motor control is dependent on sensory feedback, it is important to examine whether IHT changes the transmission of sensory stimuli along those spinal tracts commonly damaged in SCI. Testing of dorsal column tracts using somatosensory evoked potentials (SEPs) provides an opportunity to do this in a standard and simple way.

SEPs largely activate the larger myelinated muscle and cutaneous afferents in peripheral nerve (Type A fibres) that transmit information via the DCML pathway (Markand, 2020, p.139). This is a three-order sensory neuron ascending pathway where the first-order neurons have their cell bodies at the dorsal root ganglia neurons and relay sensory information, such as touch, proprioception, vibration and pressure from skin, muscles, tendons, joints and viscera, to be processed within the primary somatosensory cortex and relayed via the thalamus (Weidner, Rupp and Tansey, 2017, p.34-39; Macerollo et al., 2018). Refer to Chapter 1 Section 1.3 Figure.1.1.

SEP recordings are commonly used as research and clinical assessments to pinpoint disruption and conduction problems in sensory pathways (i.e. trauma or cord compression) as well as demyelination (i.e. multiple sclerosis) (Nuwer, 1998; Cruccu

et al., 2008) and in the cortical or sub-cortical (thalamic) response to a sensory stimulus.

3.1.4. Recording SEPs

The SEP technique was first described by Dawson in 1947 and is used to investigate the integrity of ascending spinal pathways by recording postsynaptic evoked potentials using surface scalp electrodes following a transcutaneous brief electrical stimulation of a superficial peripheral mixed nerve (i.e. median nerve or posterior tibial nerve) (Macerollo et al., 2018; Caizhong et al, 2014; Maguiere et al, 1999; Cruccu et al., 2008). Potentials recorded following stimulation of a lower limb peripheral nerve (i.e. posterior tibial nerve) have a longer latency compared to upper extremity potentials (i.e. median nerve) (Giblin, 1964; Cruccu et al., 2008) due to the longer conduction distances within the respective peripheral nerves and ascending fibres lying within the dorsal columns. Individual evoked potentials recorded by scalp EEG are of very low in amplitude around 10 μ V (tens of μ V smaller than baseline EEG activity) and require amplification, pre-processing using standard filter settings and event averaging for adequate analysis of the waveform latency, size and shape (Markand, 2020, p.2; Maguiere et al., 1999).

SEPs, as mentioned, are usually recorded from the brain but they can also be recorded from the spinal cord. Spinal SEPs have a smaller amplitude and are generally more difficult to record. However, having the ability to record SEPs from the brain and spinal cord allows scientists and clinicians to assess of the functional integrity of the somatosensory pathway at different levels. In the clinic, spinal SEPs are frequently used to evaluate the possible presence of a spinal lesion in multiple sclerosis patients (Markland, 2020). In this study, measuring the first components of cortical SEPs was sufficient to evaluate the somatosensory pathway of healthy participants.

3.1.5. Monopolar and bipolar SEP recordings

SEPs can be recorded using monopolar or bipolar EEG electrode configurations (Macerollo et al., 2018). The bipolar configurations mainly record the near-field potentials generated following activation of the neural pool after far-field effects are minimised by the differential recording between closely spaced electrodes.

Monopolar recording measures both near-field and far-field potentials (King and Dumitru, 1994; Passmore, Murphy and Lee, 2014) across electrodes that are placed at a greater distance apart than for bipolar recordings. Far-field potentials are usually small in amplitude as they are generated by brain areas far away from the recording electrode (King and Dumitru, 1994; Passmore, Murphy and Lee, 2014). The configuration used or recommended for use depends on the need of the investigation but in all cases bipolar configurations can be derived from multichannel monopolar montages by simple arithmetic calculations between pairs of electrodes.

3.1.6. Nomenclature of SEPs

To reveal the underlying time-locked components of the SEP waveform, it is generally recommended to average between 500-1000 samples. The waveform consists of peaks and troughs, as seen in Figure.3.1, where each component is named based on the polarity of the waveform, (P for positive and N for negative), followed by the latency in ms. For example, the N20 is a negative peak with a latency close to 20ms (Markand, 2020, p.11; Cruccu et al., 2008) in the upper limb. However, note that the use of terms such as N20 can capture waveforms of latencies near to 20ms but considerable variance in the latency can exist between subjects due to height or limb length differences.

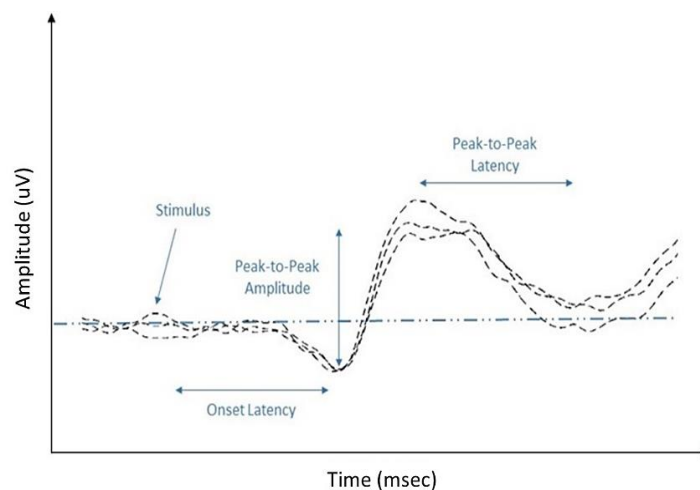


Figure.3.1. Diagram of the analysis performed for the SEP data. These are three baseline SEPs recorded in this experiment.

3.1.7. SEP: Frequency of stimulation

The frequency of stimulation is chosen carefully by considering the site that is being stimulated (Markand, 2020, p.2). It is important to appropriately select the frequency of stimulation as a high frequency can impact the waveform morphology whereas a low frequency increases the acquisition time (Markand, 2020, p.2). For median nerve and posterior tibial nerve around a 3-5 Hz stimulation pulse is usually advised (Markand, 2020).

3.1.8. SEP: Filters

For SEP recordings, filters may be used to improve signal-to-noise ratio. There are many different filter types: low-pass, high-pass, band-pass and band-stop and they should be used carefully as filters can introduce artificial components that affect latency and amplitude of the signal (Navid et al., 2019) and once a standard filter setting has been chosen it should not be changed otherwise comparison between repeated measures can be problematic. Furthermore, in clinical investigations where latency components are commonly measured for diagnostic purposes it is important to capture high frequency features and it is common to adopt one of the following common filter settings 0.5-1000 Hz, 3-1000 Hz and 30-1000 Hz (Navid et al. (2019) and a high sampling rate between 5 KHz to 20 KHz.

3.1.9. Difficulties recording evoked potentials

Difficulties when recording evoked potentials can include: high impedance of stimulating electrodes or recording EEG electrodes and high amplitude electromagnetic artefacts arising from the local environment, the electric stimulus waveform or subject movement causing motion of the electrode or its cable (Markand, 2020, p.143). Reducing electrode impedance requires good electrode placement technique involving cleansing the electrode site from oils and dead skin thereby allowing the electrode to make good contact with the skin and using an appropriate electrolyte gel as an interface between the electrode and skin. Use of non-polarising metal as the electrode (e.g. gold or silver/silver chloride) is recommended and a recording environment with low levels of electromagnetic interference is normally essential (Poornima et al., 2013). A frequent high amplitude background artefact is

muscle activity arising from the muscles of the face and neck (Markand, 2020, p.143) and to avoid this, subjects are instructed to stay still and relax as much as possible during periods of SEP data collection (Ozkul and Uckardes, 2002).

3.1.10. SEP analysis

Analysis of SEPs generally include: onset latencies, peak-to-peak latency, absolute peak amplitude and peak-to-peak amplitude. (Macerollo et al., 2018). These measurements are used to make inferences regarding changes in neural activity and conduction along the somatosensory pathway. Onset latency is the time it takes for the stimulus to generate an evoked potential within the input target neuronal networks of the somatosensory cortex (Poornima et al., 2012). It provides information on central and peripheral conduction time and is affected by limb length and height, nerve conduction velocity and the excitability of the thalamocortical relay neurones within the pathway. The earliest or first cortical SEP peak denotes arrival of activation to the cortex and this is the component greatly affected by height, limb length and overall conduction time (Poornima et al., 2012). Peak-to-peak latency, absolute peak amplitude and peak-to-peak amplitude provide information on excitability (Marcello et al., 2018).

An increase in amplitude of cortical SEPs is associated with hyperexcitability. For instance, Hamada et al. (2007) showed that in amyotrophic lateral sclerosis (ALS) there is an increase in N20 amplitude meaning that for the same strength of stimulation the somatosensory cortex response is greater than expected, a sign of hyperexcitability of the neurons activated in the cortex by the incoming sensory stimulation. As sensory inputs are capable in modulating motor cortical excitability it is thought that this may represent a form of plasticity where the response to sensory input is heightened to compensate for effects of the disease (Hamada et al., 2007). Accordingly, it is the objective of this chapter to explore if features of SEPs generated by peripheral nerve stimulation are sensitive to IHT.

In Figure.3.1 illustration of three baseline SEP measurements are shown and these form the basis of the measurements made in SEP analysis used here. In Table.3.1 a listing of the common parameters associated with median and posterior tibial SEP

recordings are given. In this study SEPs were recorded following the stimulation of the median nerve as it is a simpler task to keep the stimulation electrodes in place over this nerve for the entire 2 hour experiment when compared with sites for tibial nerve stimulation.

Table.3.1. Parameters for median and posterior tibial SEPs (table used with permission; Markand, 2020, p.142)

Technical factors	Recording parameters
1. Nerves to be stimulated	Median N. in the upper limbs Posterior tibial N. in the lower limbs
2. Site of stimulation	Wrist for the median and ankle for the posterior tibial nerves
3. Stimulating electrode	Surface electrode or needle electrodes Cathode placed proximal to anode
4. Stimulator	Constant current or constant voltage
5. Stimulus	Rectangular monophasic electrical pulses of 100–300 microsecond in duration
6. Stimulus rate	3–5/sec
7. Stimulus intensity	Consistent and visible muscle twitch
8. Analysis time	40–50 msec for median SSEPs 80–100 msec for posterior tibial SSEPs
9. Filters	30–3000 Hz (–6 db/octave)
10. Sweeps per replication	<500, usually 1000
11. Replications	At least two
12. Sedation	Often required for optimal recording

3.1.11. Median nerve SEP waveform meanings

For median nerve stimulation, the first identifiable event related wave occurs around 20ms. This component originates in Brodmann’s area 3b of the primary somatosensory cortex (Andrew et al., 2015; Passmore, Murphy and Lee, 2014). This is an important peak to study as it represents the response to the arrival of the afferent volley via the DCML to the somatosensory cortex. The second peak, N27 is associated with processing of information by the posterior parietal cortex and secondary somatosensory cortex (Poornima et al, 2013). The third wave at around 30 ms involves sensorimotor integration between sites including the thalamus, premotor areas, basal ganglia and primary motor cortex (Andrew et al., 2015; Passmore, Murphy and Lee, 2014; Mauguiere, 2005; Kamoda, 2001). This peak is affected by voluntary muscle contraction (Passmore, Murphy and Lee, 2014) and pathology. For instance, muscle tone in patients with Parkinson’s disease increases the amplitude of N30 peak (Passmore, Murphy and Lee, 2014).

3.1.12. SEPs and neuroplasticity

Of interest for this study is the interpretation that an increase in SEP peak amplitude is indicative of an increase in primary cortical neural activation that if persistent may be indicative of synaptic plasticity in the somatosensory cortex (Andrew et al., 2015). Plasticity in the sensorimotor brain regions have been observed following a motor training task (Haavik Taylor and Murphy, 2007; Andrew et al., 2015) and given that IHT is reported to influence motor cortical excitability it is important to establish if parallel changes may arise in the response of the somatosensory/sensorimotor activation to sensory stimuli.

3.1.13. Abnormal cortical SEPs

Abnormal cortical SEPs include the absence of a waveform which is associated with somatosensory brain damage or deafferentation and changes in peak-to-peak latencies (Markland, 2020, p.167-168; Passmore, Murphy and Lee, 2014). The table below, Table.3.2, summarises the common median nerve SEP abnormalities when pathology is present. In this study detrimental effects on SEPs in response to IHT will also be looked for as adverse events.

Table.3.2. Median nerve SEP abnormalities and interpretations (table used with permission; Markand, 2020, p.168)

	Median SSEP findings	Most probable interpretation
1	N9, N13, and P14 are normal, but N20 is delayed (prolonged IPL P14-N20)	Conduction defect between foramen magnum and sensory cortex, but not involving the cortex
2	N9, N13, and P14 are recordable at normal latencies, but cortical response is absent	A dysfunction either in the sensory cortex itself or the thalamocortical projections to the sensory cortex
3	N9 and N13 are recordable at normal latencies, but P14 and N20 are absent	Conduction block in the intracranial somatosensory pathways rostral to foramen magnum
4	Normal N9 but delayed N13 or P14 (N9-P14 or N9-N13 IPL prolongation)	A conduction defect in the sensory system central to the brachial plexus and below the foramen magnum (peripheral and/or central involvement)
5	Normal N9, prolongation of both N9-N13 (P14) and N13 (P14)-N20 IPLs	Conduction defect central to the brachial plexus below and above the foramen magnum
6	N9 has prolonged latency, but centrally generated components are proportionately delayed (i.e., IPLs are normal)	Conduction abnormality is peripheral as may occur with a neuropathy
7	N9 is absent but centrally generated components recordable at normal latencies	Test is interpreted as normal; absent N9 may be technical
8	N9 is absent and N20 recordable but at a prolonged latency with delayed or absent N13 and/or P14 components	Slowing of conduction most likely peripherally (e.g., neuropathy) with or without central conduction slowing

N9 measured from brachial plexus potentials; N13 measured from dorsal column potentials; P14 measured from sub-cortical potentials; interpeak latencies (IPLs)

3.1.14. Continuous hypoxia and SEPs

The effect of IHT on the somatosensory system, based on current publications has not yet been investigated. There are however, animal and human studies, that have examined the effect of continuous hypoxia on SEPs. However, it is important to mention that studies investigating IHT's ability to induce motoneuronal plasticity have highlighted that the intermittent aspect of the treatment is critical in eliciting plastic changes in motoneurons (Baker and Mitchell, 2000; Trumbower et al., 2012) and this form of hypoxia and its effects on SEPs remains untested in human or animal studies.

Haghighi et al. (1992) recorded cortical and spinal (measured from electrodes placed on the skin surface over the spine) SEPs during right posterior tibial nerve stimulation in rats following graded hypoxia (moderate $FiO_2=15.75\%$, severe $FiO_2=10.5\%$, extreme $FiO_2=5.25\%$) for 10 minutes and subsequent re-oxygenation for 15 minutes.

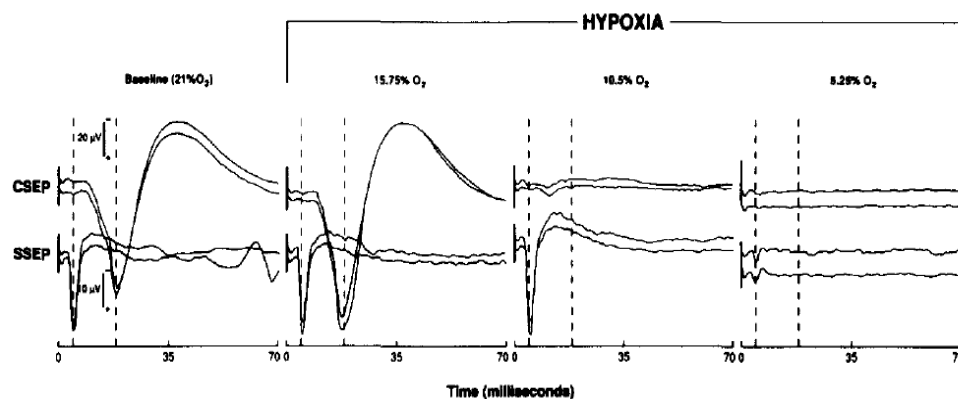


Figure.3.2. Cortical SEP (CSEP) and spinal SEP (SSEP) under normoxia (baseline) and hypoxia (figure used with permission from Haghighi et al., 1992)

Moderate hypoxia did not change cortical or spinal SEP latencies when compared to baseline but cortical SEP amplitude increased by 34 % compared to baseline ($p=0.02$) following re-oxygenation (Haghighi et al., 1992). The study concluded that spinal SEPs are less sensitive to cortical SEPs during hypoxia and that the transient increase in cortical SEP amplitude is probably associated with the disinhibition of intracortical inhibitory interneurons (Iwayama et al., 1986; Haghighi et al., 1992). A similar moderate prolonged hypoxic exposure ($FiO_2=11\%$) for 10 minutes in healthy subjects, however, showed no changes in latency and amplitude of

cortical SEPs measured during posterior tibial nerve stimulation (Ledsome et al., 1996).

In addition, Haghidhi et al. (1992) observed a slowing in frequency of the SEP waves in severe hypoxia (indicative of slowed conduction and reduced excitability) and complete silencing of SEPs in extreme hypoxia in adult rat studies. Similar results with severe hypoxia were also observed in dogs (Mcpherson, Zeger and Traystman, 1986). This is shown in Figure.3.2 from the Haghidhi et al. (1992) study which clearly demonstrates the cortical and spinal SEPs at baseline and its changes following 10 min of hypoxia (moderate, severe and extreme). Such results illustrate the effect of prolonged extreme hypoxia on brain tissue and may indicate a stress response as O₂ delivery to the brain declines.

3.1.15. Aims and objectives

This study investigated the effects of IHT on the somatosensory system by examining changes in latency (onset latency and peak-to-peak latency) of the SEP waveform recorded from the sensorimotor cortex during IHT and changes in amplitude of the SEP waveform before, during and following IHT up to 30 minutes. This is the first study to examine the central sensory effects of the IHT protocol used on iSCI subjects by Trumbower et al (2012).

SCI disrupts sensory and motor pathways in the spinal cord and motor rehabilitation requires both survival within motor output pathways and sensory feedback pathways. Accordingly, the hypothesis is that if IHT induces plasticity in cortical systems effects may be demonstrable in tests of both sensory and motor pathway function. Christiansen et al. (2018) who studied the effects of IHT on corticospinal function of healthy subjects reported an increase in MEP amplitude. Therefore, we expect that if IHT acts on the somatosensory pathways we will observe an increase in SEP amplitude following IHT even in healthy subjects. SEP amplitude has been reported to increase in rats following a 10 min continuous hypoxia exposure (Haghidhi et al., 1992). Therefore, perhaps continuous conditioning of short hypoxic exposures may lead to plastic changes in sensory pathways. The null hypothesis stated that no significant detectable difference in amplitude or latency of SEP signals

following IHT would occur and this result would isolate any effects of IHT to motor output pathways independent of sensory pathways. The effects of IHT on SEP amplitude and latency were examined using a One-way ANOVA. Therefore, a p-value of > 0.05 would indicate no significant detectable difference in the results. A One-way ANOVA was chosen because it statistically compares the variance in group means while considering only one independent factor which in this case is IHT.

3.2. Methodology

3.2.1. Subjects

Ethics approval was obtained from the ethics committee of the University of Strathclyde. Six healthy young volunteers (4 men and 2 women; 28.5 ± 3.8 years) were recruited from staff and students at the University of Strathclyde. All subjects were pseudo-anonymised by allocating a study ID-number that began with IHT followed by an integer (ex: IHT1). The purpose of this was to maintain confidentiality and protect the participant's identity. Exclusion criteria were the same as those reported in Chapter 2. Please refer to Appendix.I.1) to look at the Activity and Health Questionnaire.

3.2.2. Experimental design

The study consisted of two sessions. In the first session the volunteers were asked to read through the information sheet, provide a written consent and lastly, perform the hypoxia test. If the participant was happy to proceed with the IHT intervention, and also considered as Type II or III following a hypoxia test, they were scheduled for the second session a week later.

In the second session SEPs were measured. The testing conditions were controlled. The experiment took place in a quiet room with dimmed lights to aid relaxation of the participant (Ozkul and Uckardes, 2002). SEPs were recorded from surface scalp electrodes while stimulating pulses were applied to the median nerve at the index finger using ring electrodes (Ozkul and Uckardes, 2002; Kalogianni et al., 2018).

Prior to recording SEPs, cleaning of the skin where electrodes will be placed is required to reduce the impedance. SEP recordings were taken prior, during and following IHT. Three recordings were taken prior to the IHT intervention to look at

consistency, one recording towards the end of the IHT intervention and three recordings following IHT (immediately after, at 15 min and 30 min). During IHT heart rate and SpO₂ levels were monitored.

3.2.3. Peripheral stimulation: Median nerve

3.2.3.1. Skin impedance

Prior to placing the electrodes for stimulation the skin was cleaned using an abrasive gel (Nuprep, Weaver) and alcohol wipes.

3.2.3.2. Site of stimulation

Stimulating at the wrist area is the conventional way of recording upper limb SEPs. However, the preliminary measurements in pilot tests showed inconsistency in stimulation conditions. The problem was not just the placement of the electrode because that could be adjusted by marking the skin but the pressure of the electrode on the skin was the factor that created the main problem due to the prolonged duration of experiments. Experiment duration lasted around 2 hours and fixation of the stimulation electrode at the wrist could not be adequately controlled for in between measurements leading to unreliable control over stimulation intensity of the nerve. To control this problem, it was decided to stimulate the digital branch of the median nerve at the index finger using adhesive ring electrodes. The ring electrode was much easier to fix in a constant position throughout the experiment and was not displaced by arm/wrist/hand movement.

3.2.3.3. Ring electrode placement

The ring electrodes were placed on the index finger. The anode ring electrode was placed on the most distal phalange and the cathode on the middle phalange. (Ozkul and Uckardes, 2002; Kalogianni et al., 2018; Halonen et al., 1988).

3.2.3.4. Sensation threshold

The sensation threshold was detected by increasing the stimulation by 0.1 mA up to the point where the individual consistently reported feeling the stimulation. During the SEP recording the stimulation was set to 3 times the sensation threshold. The stimulator used was a Digitimer DS7A (Digitimer Ltd., Hertfordshire, Uk) (Ozkul and Uckrades, 2002). A monophasic square wave with a pulse width of 200 µs was used and a stimulation frequency of 4 Hz applied.

3.2.4. Electroencephalography (EEG)

3.2.4.1. Scalp preparation

An abrasive gel (Nuprep, Weaver) was used to clean the scalp at each electrode site and a blunted needle and syringe was used to inject the gel between the scalp and electrode. Electrode impedance was monitored and recording conditions were considered adequate when impedance was equal or below 5 k Ω (Samra et al., 1987). The earlobe reference electrode site was also cleaned using the Nuprep abrasive gel as low impedance here is also important to achieve good recording conditions in monopolar or bipolar configurations.

3.2.4.2. EEG recording of SEPs

SEPs were recorded using Ag/AgCl surface EEG electrodes which were placed and located on the scalp using an EasyCap (Brain Vision Uk) (Nakata et al., 2017). There were various EasyCap sizes available, and each participant was fitted with the appropriate cap. With the appropriately sized cap, the Cz electrode was positioned midway the nasion and inion and midway the preauricular points resulting in good location of the other electrode sites defined by the international 10:10 system (Acharya et al. *J Clin Neurophysiol* 2016;33: 308–311).

3.2.4.3. Montage of electrodes

Monopolar and bipolar SEP measurements were used for the study. The monopolar analysis centred on the following electrodes determined by handedness: Cc and FCc with bipolar records determined between Cc and FPz and CPc and FPz where FPz was set as the reference. Accordingly, for the bipolar analysis the EEG recording from FPz was subtracted from the records obtained from Cc and CPc electrodes. Bipolar analysis was stated as Cc-FPz and CPc-FPz.

As mentioned, bipolar recordings were measured by subtracting the reference (FPz) from the electrode of interest to accentuate near-field potentials. Near-field potentials are those generated near the cortex surface and thus anatomically close to the recording electrode (Passmore et al., 2014). Cortical near-field potentials are recorded better when using a bipolar analysis (Muzyka and Estephan, 2019). In the

electrode cap montage used in these experiments the ground electrode was placed on the contralateral ear of the nerve being stimulated (Ozkul and Uckardes, 2002).

The electrodes chosen were around the somatosensory area for recording SEPs following median nerve stimulation. Figure.3.3 has the electrodes that were recorded during the experiment highlighted. Please keep in mind that SEPs were recorded following the stimulation of the median nerve on the dominant hand. Therefore, if the left hand was stimulated then FC4, C4 and CP4 would be the electrodes to record from.

3.2.5. Components of SEP waveform

The early components, N20, P25 and N30, were studied (Kawaguchi et al.,2015). The reason for studying the early cortical components is that the waveform is reproducible, and the early components are less variable in latency among subjects with an intact nervous system (Mauguiere, 1999).

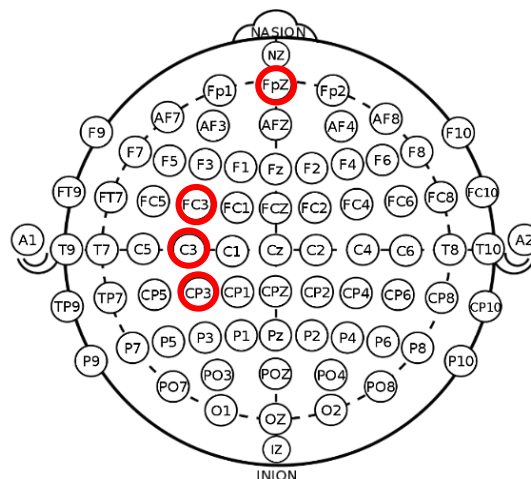


Figure.3.3. The highlighted electrodes show the montage used for participant that their right hand is dominant. If the participant's left hand was dominant then FC4, C4 and CP4 would be highlighted. Please keep in mind that the left hemisphere controls movement on the right side of the body and the right hemisphere controls movement on the left side of the body.

(image used with permission and modified from

https://commons.wikimedia.org/wiki/File:International_10-20_system_for_EEG-MCN.svg) [Accessed 3 April 2021])

3.2.6. Signal processing

SEPs were recorded using Curry 7 software from 4 channels and FPz was set as the reference electrode for bipolar analysis. EEG was sampled at 2500 Hz using the Synamps amplifier with a gain of 1000. The band pass filter was set to 30-1000 Hz.

Each recording (pre-, during and post- IHT) lasted 4 minutes with a break of at least 5 minutes in between recordings and the frequency of stimulation was set to 4Hz (Maguiere et al., 1999). Therefore, around 960 traces were averaged for each SEP recording.

The epoch length around each nerve stimulation event was set to 120 ms (-20 before the trigger onset to 100 ms after the trigger onset) to allow capture of the main components of the median nerve short latency SEP peaks (N20, P25 and N30). Using Curry 7 software the data were epoched and the epochs contaminated with artefacts were removed. The baseline was set to pre-trigger and saved as an eeg epoch file. This file was then transferred to Matlab where a code was customised to process and analyse the Cc, FCc and CPc electrode recordings (Cc: monopolar, FCc: monopolar, Cc-FPz: bipolar, CPc-FPz: bipolar).

Epochs were event averaged using the time of nerve stimulation as the trigger event. It is important to mention that the pre-IHT average (pre-IHT_{avg}) involved averaging all the epochs from the three pre-IHT recordings (pre-IHT₀, pre-IHT₅ and pre-IHT₁₀) after checking for stability/reproducibility. The peak-to-peak amplitude, onset latency and peak-to-peak latency were studied from the SEP waveform (Wall et al., 1991). The data were normalised to pre-IHT_{avg}.

3.2.7. Analysis: SEPs

Primarily, measurements of onset latency (from the trigger to peak N20, P25 and N30) and peak-to-peak latency (for N20-P25 and P25-N30) were measured from SEPs recorded 20 minutes into the IHT intervention for each participant. SEP recording lasted for 4 minutes and epochs for each 1 minute interval was averaged and the onset latency and peak-to-peak latency was calculated. A two-tailed paired t-test was performed for each participant to study if there was a significant difference between hyperoxia and hypoxia latency measurements. In the results section the absolute difference between hypoxia and hyperoxia intervals (in ms) is reported for each participant an asterisk displays if there was a significant difference between hypoxia and hyperoxia intervals.

The analysis then mainly consisted of studying peak-to-peak amplitudes for N20-P25 and P25-N30. However, the repeatability of pre-IHT peak-to-peak amplitude

measurements was first analysed as it was essential to have consistent baseline measurements before introducing an intervention. The analysis then proceeded with studying whether the excitability of SEPs changes following the intervention.

As mentioned, before completing a statistical analysis of the SEP measurements, comparing pre-IHT, during IHT and post-IHT measurements, the analysis was focussed on the reliability or the extent that pre-IHT SEP measurements of peak-to-peak amplitude can be replicated. Prior to any interventions, the reliability and replicability of the SEP measurements were checked using ICC. The score for ICC ranges from 0 to 1 where excellent reliability is > 0.75 ; moderate to good reliability is $0.74-0.40$; and poor reliability is < 0.40 (Cacchio et al., 2011). If the pre-IHT data showed a good reliability for peak-to-peak amplitude, we proceeded with the analysis.

Primarily, a normal distribution curve of each measurement was graphed to look at whether the data follows a normal distribution. This is important when deciding on the statistical analysis. Before plotting the distribution, the DC bias was removed. The bin width for the normal distribution graph was set to 1.5. Normal peak-to-peak amplitude was normalised to $\text{pre-IHT}_{\text{avg}}$. Additionally, on each normal distribution graph the mean, standard deviation and number of epochs recorded was reported above the graph.

Prior to completing a One-way ANOVA, the Levene's test was performed to examine whether the data had homogeneity of variances. The datasets had homogeneity of variances and thus the analysis proceeded with a One-way ANOVA. Subsequently, as the One-way ANOVA showed no significant differences among the groups (pre-IHT, during IHT and post-IHT) a post-hoc test was not required. The statistics, graphs and tables were created in Matlab, SPSS and Excel. This analysis was completed on each participant and on the grand average for measurements of SEPs taken before, during and following IHT.

The results section will first present the data from the first participant, IHT1, as a typical case study and then present the grand average. For the grand average measurements, the entire dataset of each participant was used to create an average SEP waveform for each electrode (Fc, Cc, Cc-FPz and CPc-FPz) and the peak-to-peak

amplitude were obtained for each recording (pre-IHT₀, pre-IHT₅, pre-IHT₁₀, during IHT, post-IHT₀, post-IHT₁₅, post-IHT₃₀). The data for both, individual responses and the grand averages, are normalised to the pre-IHT_{avg} by dividing the values by the mean value of the pre-IHT.

3.2.8. Analysis: SpO₂ and heart rate

SpO₂ and heart rate was monitored during the IHT session. The lowest SpO₂ value each participant reached and the range of heart rate are reported in a table created in Excel.

3.3. Results

The results section will first show a table with the participant details. Each participant prior to completing this experiment had to go through a hypoxia test. The results of the hypoxia test are reported in a table. Moreover, during IHT SpO₂ and heart rate was monitored using the GO2 altitude machine. This information will also be displayed in a table. Subsequently, latency results will be presented prior to showing the peak-to-peak amplitude.

3.3.1. Participant details

All participants recruited for this study showed good tolerance to hypoxia (Table.3.3). During and following the IHT session, they reported no adverse effects. During the intervention their SpO₂ levels dropped to around 82 % on average and their heart rate was between 58 to 82 bpm. These values are similar to what has been reported in the literature on iSCI patients that underwent the same IHT intervention (Trumbower et al., 2012; Hayes et al., 2014).

Table.3.3. Participant details, hypoxia test, lowest SpO₂ reached and heart rate range

Participant	Sex	Age	Hypoxia Test Response	Lowest SpO ₂ (%)	Heart rate range (bpm)
IHT1	Male	35	Type II	83	63 to 84
IHT3	Male	31	Type II	82	43 to 64
IHT4	Male	27	Type II	88	56 to 73
IHT6	Female	26	Type II	68	59 to 87
IHT7	Female	27	Type II	82	56 to 88
IHT8	Male	25	Type II	88	70 to 93

3.3.2. Onset latency analysis during IHT

3.3.2.1. Cc and Cc-FPz

SEPs were recorded 20 minutes into the IHT intervention for 4 minutes. SEP epochs were averaged for each 1 minute interval and measurements of onset latency were gathered. Next, the mean and standard deviation of the two hypoxia interval and the two hyperoxia intervals were calculated. The absolute difference in onset latency is reported in the table below (Table.3.4). Statistical analysis of onset latency between hypoxia and hyperoxia intervals showed no significant difference. This was observed for all participants and at all electrodes (Cc, Cc-FPz, FCc and CPc-FPz) where SEPs were analysed. The range of absolute onset latency difference for Cc was 0.04 to 1.29 ms and for Cc-FPz is 0.04 to 1.61 ms. The results suggested that the reduction of oxygen did not affect the conduction velocity of SEPs and knowing this there is no need to report latency measurements following IHT.

Table.3.4. Absolute difference between SEP onset latency measured during hypoxia and onset latency measured during hyperoxia for Cc and Cc-FPz

Absolute Onset Latency Difference (<i>Hypoxia – Hyperoxia</i>) (mean±standard deviation) (ms)			
Participant	N20	P25	N30
Cc Onset Latency			
IHT1	0.04 ±0.29	1.29 ±0.91	0.19 ±0.95
IHT3	0.04 ±0.86	0.28 ±0.06	0.08 ±0.11
IHT4	0.12 ±0.17	0.52 ±0.40	0.20 ±0.29
IHT6	0.81 ±0.23	0.20 ±0.06	0.04 ±0.29
IHT7	0.44 ±0.17	0.44 ±0.29	0.52 ±0.06
IHT8	0.65 ±0.11	0.28 ±0.40	0.36 ±0.63
Cc-FPz Onset Latency			
IHT1	1.05 ±1.60	0.24 ±0.23	0.48 ±0.65
IHT3	1.17 ±2.45	1.61 ±1.03	1.41 ±0.63
IHT4	0.04 ±0.06	0.85 ±0.40	1.04 ±0.48
IHT6	0.51 ±0.07	1.05 ±0.34	0.21 ±0.38
IHT7	0.04 ±0.74	0.89 ±0.34	0.56 ±1.03
IHT8	0.60 ±0.40	0.24 ±0.23	1.18 ±0.19

3.3.2.2. FCc

Comparable to the results above, the absolute onset latency difference ranged between 0.04 to 1.03 ms in SEP recordings taken from the FCc electrode (Table.3.5).

Table.3.5. Absolute difference between SEP onset latency measured during hypoxia and onset latency measured during hyperoxia for FCc

Absolute Onset Latency Difference (<i>Hypoxia – Hyperoxia</i>) (mean±standard deviation) (ms)			
Participant	N20	P25	N30
FCc Onset Latency			
IHT1	-	-	-
IHT3	0.16 ±0.00	1.01 ±0.29	0.26 ±0.13
IHT4	0.04 ±0.17	0.44 ±0.39	0.00 ±0.00
IHT6	0.93 ±1.20	0.77 ±1.08	1.03 ±0.44
IHT7	-	-	-
IHT8	0.36 ±0.51	0.16 ±0.80	0.52 ±0.29

3.3.2.3. CPc-FPz

A similar range was also observed in CPc-FPz among participants (0.04 to 2.01) (Table.3.6). It is important to note that for each participant, there was no statistical difference ($p>0.05$) between hypoxia and hyperoxia measurements.

Table.3.6. Absolute difference between SEP onset latency measured during hypoxia and onset latency measured during hyperoxia for CPc-FPz

Absolute Onset Latency Difference (<i>Hypoxia – Hyperoxia</i>) (mean±standard deviation) (ms)			
Participant	N20	P25	N30
CPc-FPz Onset Latency			
IHT1	0.40 ±0.23	0.65 ±0.46	2.01 ±1.60
IHT3	0.65 ±0.68	1.37 ±0.56	0.48 ±0.00
IHT4	0.04 ±0.06	0.04 ±0.63	0.96 ±1.16
IHT6	0.56 ±0.00	0.69 ±0.51	0.90 ±0.55
IHT7	-	-	-
IHT8	0.20 ±0.29	0.20 ±0.06	0.79 ±0.25

3.3.3. Peak-to-peak latency

3.3.3.1. Cc and Cc-FPz

Similar results were also observed with peak-to-peak amplitude (Table.3.7) Statistical analysis between hypoxia and hyperoxia measurements for each participant showed no significant difference ($p>0.05$).

Table.3.7. Absolute difference between SEP peak-to-peak latency measured during hypoxia and peak-to-peak latency measured during hyperoxia for Cc and Cc-FPz

Absolute Peak-to-peak Latency Difference (<i>Hypoxia – Hyperoxia</i>) (mean±standard deviation) (ms)		
Participant	N20-P25	P25-N30
Cc Onset Latency		
IHT1	1.33 ±1.20	0.97 ±2.05
IHT3	0.60 ±0.17	1.17 ±1.31
IHT4	0.40 ± 0.57	0.73 ±1.25
IHT6	1.01 ±0.29	0.24 ±0.80
IHT7	0.89 ±0.46	0.08 ±0.34
IHT8	0.93 ±0.51	0.08 ±0.23
Cc-FPz Onset Latency		
IHT1	0.81 ±1.37	0.08 ±1.03
IHT3	0.28 ±0.06	2.86 ±1.88
IHT4	0.89 ±0.34	2.02 ±0.68
IHT6	1.69 ±0.23	1.21 ±0.23
IHT7	0.85 ±0.17	0.40 ±0.11
IHT8	0.36 ±0.63	1.17 ±0.06

3.3.3.2. FCc

A significant difference between hypoxia and hyperoxia was observed in participant IHT6 in the P25-N30 peak-to-peak latency (1.90 ± 0.17 , $p=0.04$) (Table.3.8).

Table.3.8. Absolute difference between SEP peak-to-peak latency measured during hypoxia and peak-to-peak latency measured during hyperoxia for FCc

Absolute Peak-to-peak Latency Difference (<i>Hypoxia – Hyperoxia</i>) (mean±standard deviation) (ms)		
Participant	N20-P25	P25-N30
FCc Onset Latency		
IHT1	-	-
IHT3	1.17 ±0.51	0.89 ±2.05
IHT4	0.93 ±0.97	0.89 ±1.37
IHT6	0.60 ±0.86	1.90 ±0.17*
IHT7	-	-
IHT8	0.20 ±0.29	0.36 ±0.86

Asterisk (*) is used to display a significant difference between hypoxia and hyperoxia measurements during IHT.

3.3.3.3. CPc-FPz

Similar to the onset latency there was no significant difference between hypoxia and hyperoxia intervals during the IHT intervention. The table below (Table.3.9) reports the absolute onset latency difference (Hypoxia- Hyperoxia).

Table.3.9. Absolute difference between SEP peak-to-peak latency measured during hypoxia and peak-to-peak latency measured during hyperoxia for CPc- FPz.

Absolute Peak-to-peak Latency Difference (<i>Hypoxia – Hyperoxia</i>) (mean±standard deviation) (ms)		
Participant	N20-P25	P25-N30
CPc-FPz Onset Latency		
IHT1	-	-
IHT3	1.90 ±0.51	2.74 ±1.14
IHT4	0.08 ±0.34	0.69 ±2.11
IHT6	1.25 ±0.51	0.24 ±1.25
IHT7	-	-
IHT8	0.4 ±0.34	0.85 ±0.51

3.3.4. Peak-to-peak amplitude: IHT1

3.3.4.1. SEP amplitude histogram distributions

The following results illustrate a typical case (participant IHT1). The Figure.3.4 shows a monopolar and bipolar SEP recording made at the Cc electrode prior to IHT. The bipolar recording is obtained by arithmetic subtraction of the simultaneous monopolar recordings corresponding to electrode sites Cc and FPz. The SEP plots in (A) and (B) of Cc electrode, together with the feature amplitude distribution, illustrate the same data but with a different spatial filter associated with the conversion from monopolar to bipolar representation of the SEP waveforms. A feature of the bipolar derivation is a broadening of the distributions of amplitude measures associated with the removal of far-field contributions to the monopolar data. The pre-IHT measurements serve as the control data for comparisons of SEPs collected during IHT and recovery from IHT.

Figure.3.5, Figure.3.6, Figure.3.7 and Figure.3.8 shows the histogram distribution of measurements taken pre-, during and post-IHT at electrode sites Cc, FCc and CPc for subject IHT1, respectively. The data approximated to a normal

distribution facilitating the statistical analysis on whether there was a significant difference between pre-, during and post-IHT SEP measurements of peak-to-peak amplitude.

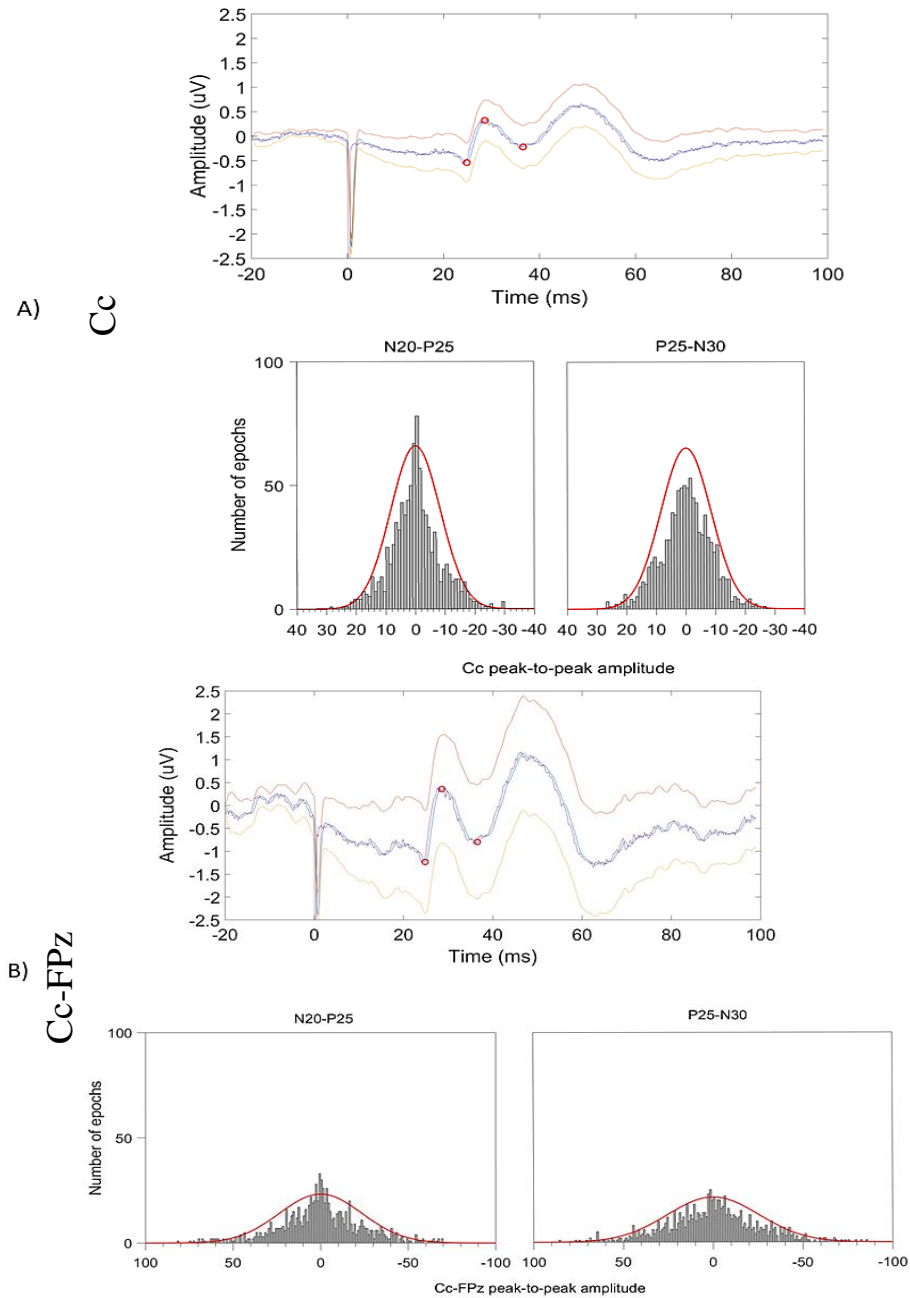


Figure.3.4. An example of a pre-IHT SEP recording and the normal distribution of the peak-to-peak amplitude. The SEP plot displays the average evoked potential waveform in purple and the confidence interval in shades of orange. The blue waveform is the average evoked potential waveform with a filter (400 Hz). The blue waveform is used for the identification of peaks and troughs. The red circles show the peaks identified by a custom written Matlab code. **A)** Cc monopolar recording with the normal distribution curve for N20-P25 and P25-N30. **B)** Cc-FPz recording with the normal distribution curve for N20-P25 and P25-N30. The histograms are corrected for the mean.

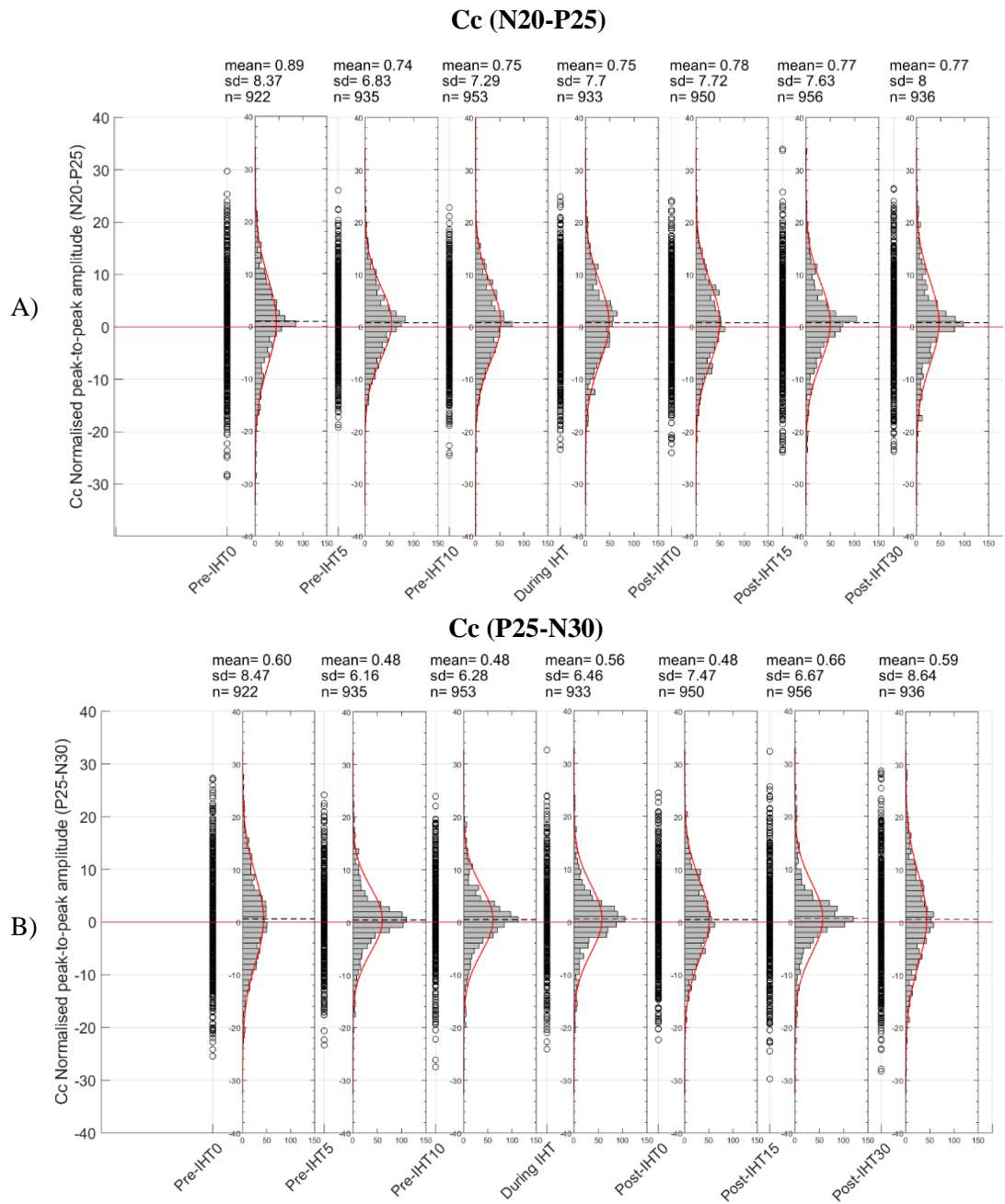


Figure.3.5. Participant IHT1 normalised peak-to-peak amplitude. The main graph displays the data plotted using hollow circles. For each time point (pre-, during and post-IHT) a histogram is also plotted (bin width is 0.1). The staggered line on the normal distribution curve highlights the mean. Please note that the data is normalized to pre-IHT_{avg}. **A**) Cc (N20-P25) and **B**) Cc (P25-N30). The mean, standard deviation (SD) and the number of epochs (n) are listed above each normal distribution graph.

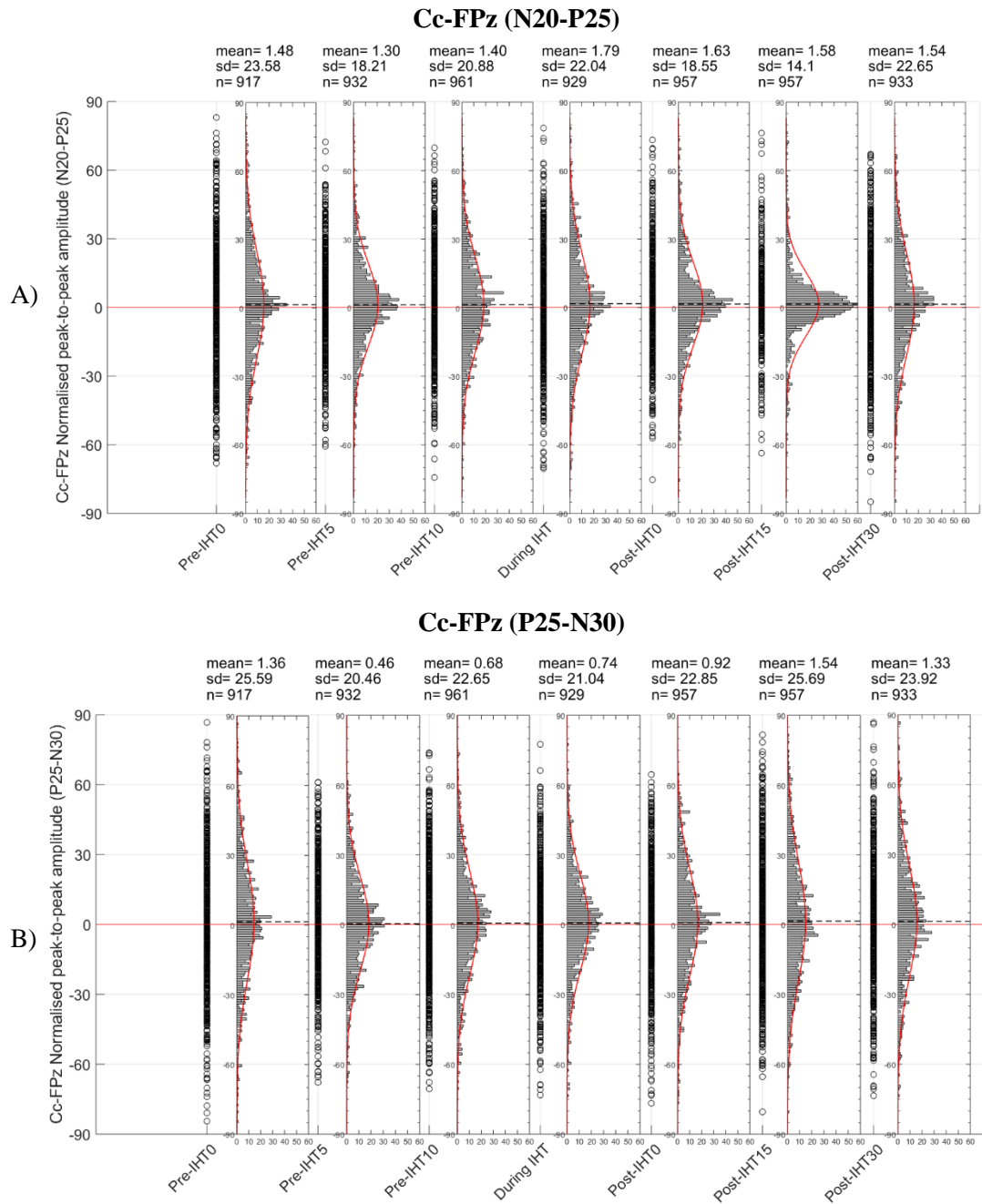


Figure.3.6. Participant IHT1 normalised peak-to-peak amplitude. The main graph displays the data plotted using hollow circles. For each time point (pre-, during and post-IHT) a histogram is also plotted (bin width is 0.1). The staggered line on the normal distribution curve highlights the mean. Please note that the data is normalized to pre-IHT_{avg}. **A)** Cc-FPz (N20-P25), **B)** Cc-FPz (P25-N30). The mean, standard deviation (SD) and the number of epochs (n) are listed above each normal distribution graph.

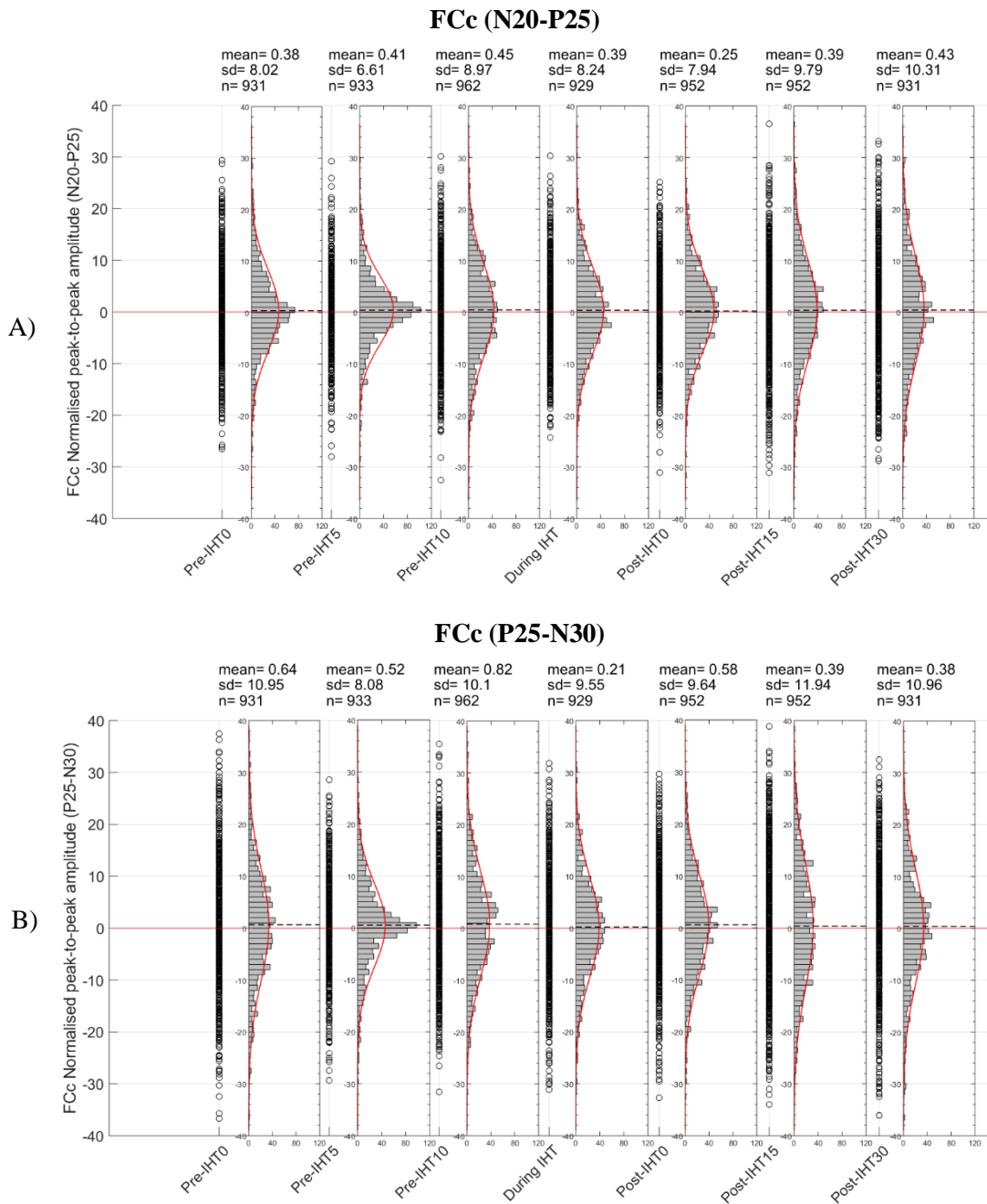


Figure.3.7. Participant IHT1 normalised peak-to-peak amplitude. The main graph displays the data plotted using hollow circles. For each time point (pre-, during and post-IHT) a histogram is also plotted (bin width is 0.1). The staggered line on the normal distribution curve highlights the mean. Please note that the data is normalized to pre-IHT_{avg}. **A)** FCc (N20-P25), **B)** FCc (P25-N30). The mean, standard deviation (SD) and the number of epochs (n) are listed above each normal distribution graph.

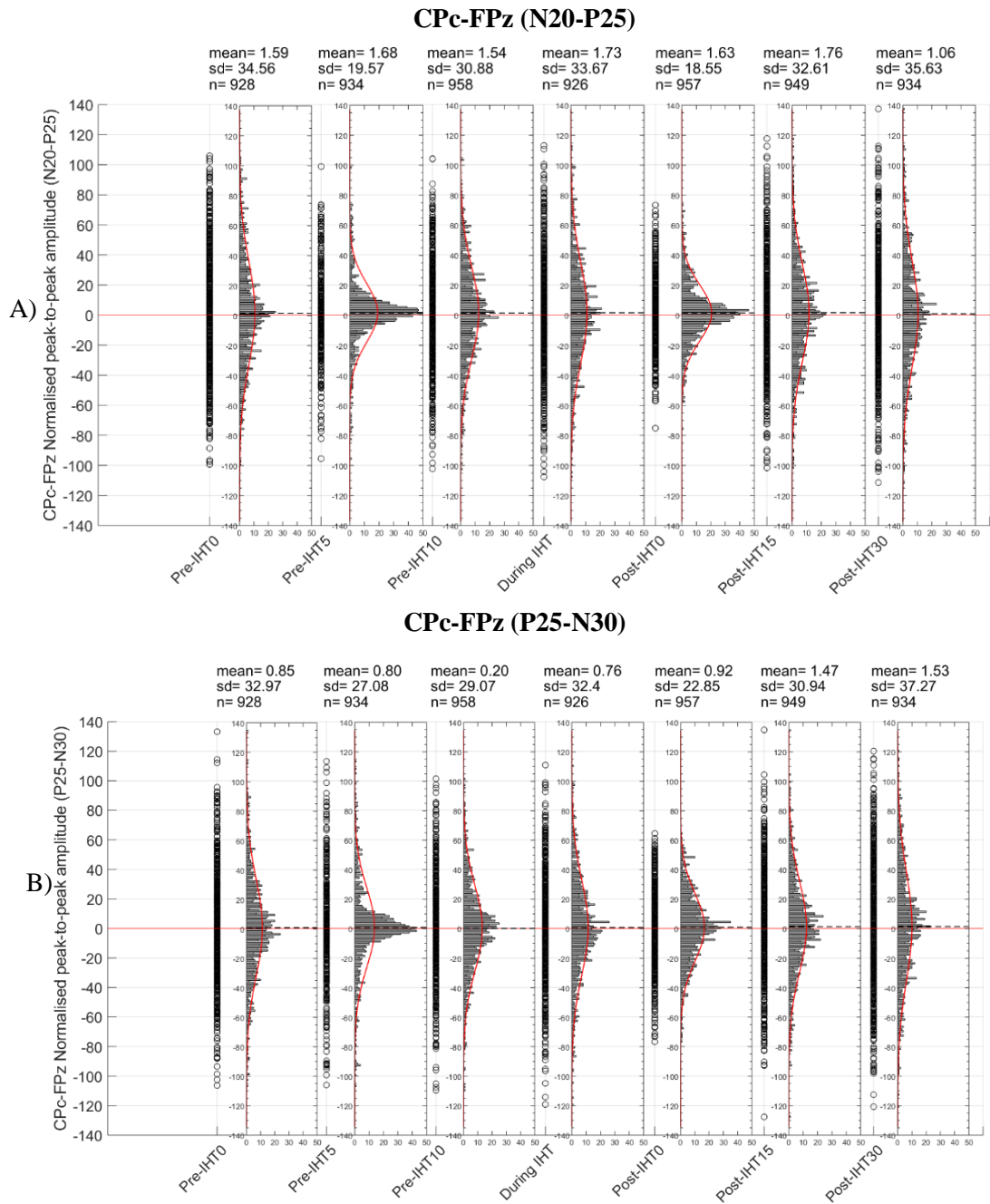


Figure 3.8. Participant IHT1 normalised peak-to-peak amplitude. The main graph displays the data plotted using hollow circles. For each time point (pre-, during and post-IHT) a histogram is also plotted (bin width is 0.1). The staggered line on the normal distribution curve highlights the mean. Please note that the data is normalized to pre-IHT_{avg}. **A)** CPc-FPz (N20-P25), **B)** CPc-FPz (P25-N30). The mean, standard deviation (SD) and the number of epochs (n) are listed above each normal distribution graph.

3.3.4.2. Peak-to-peak amplitude

3.3.4.2.1. Cc and Cc-FPz

Measurements of peak-to-peak amplitude (N20-P25 and P25-N30) for monopolar (Figure.3.9) and bipolar (Figure.3.10) recordings of the Cc electrodes show no significant differences across IHT intervention or recovery.

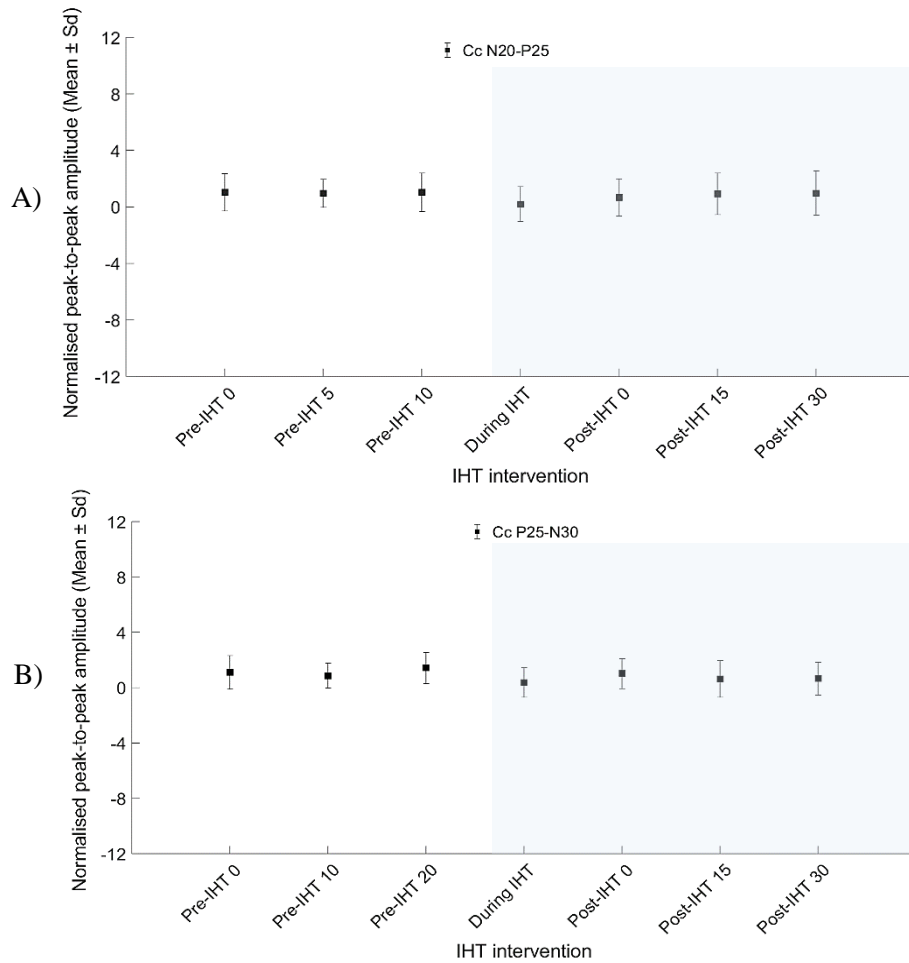


Figure.3.9. Cc monopolar analysis for IHT1: Normalised peak-to-peak amplitude for **A**) N20-P25 and **B**) P25-N30 (Mean±SD). The blue box highlights during and post-IHT measurements.

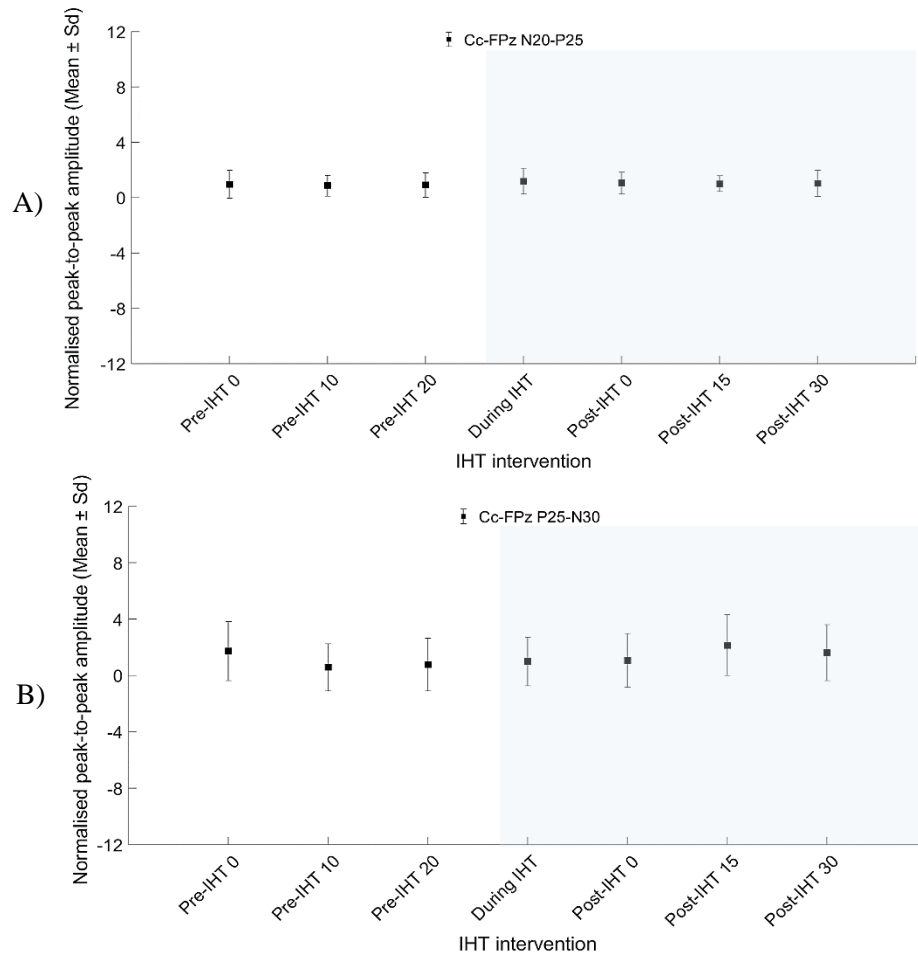


Figure.3.10. Cc-FPz analysis for IHT1: Normalised peak-to-peak amplitude for **A)** N20-P25 and **B)** P25-N30(Mean±SD). The blue box highlights during and post-IHT measurements.

3.3.4.3.2. FCc

The FCc electrode site showed no significant difference in the peak-to-peak amplitude when comparing pre-, during and post-IHT SEP measurements (Figure.3.11). This result was similar to that obtained at the Cc electrode site.

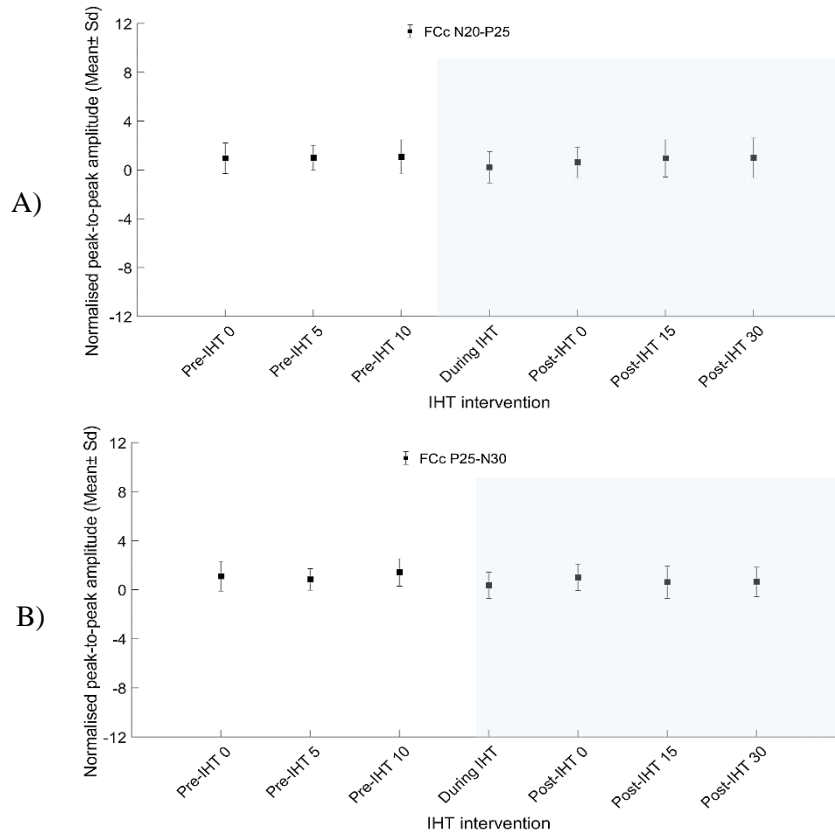


Figure.3.11. FCc analysis for IHT1: Normalised peak-to-peak amplitude for A) N20-P25 and B) P25-N30(Mean±SD). The blue box highlights during and post-IHT measurements.

3.3.4.3.3. CPc -FPz

Lastly, the CPc analysis of peak-to-peak amplitude also showed no significant difference when comparing pre-, during and post-IHT (Figure.3.12). However, despite the lack of significant statistical differences Figure.3.12.B illustrates larger standard deviation compared to the other graphs and may have represented a higher level of variance in the SEP generator dipoles that this montage was most sensitive to.

Nevertheless, despite the increased variance no patterns of change related to IHT were apparent.

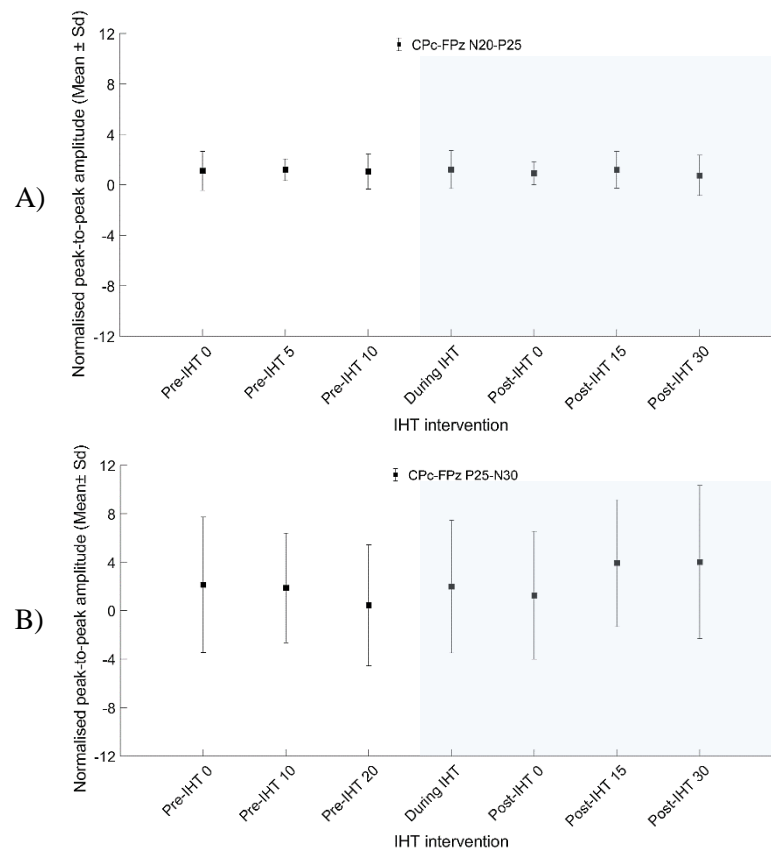


Figure.3.12. Cpc bipolar analysis for IHT1: Normalised peak-to-peak amplitude for A) N20-P25 and B) P25-N30 (Mean±SD). A blue box highlights during and post-IHT measurements.

3.3.5. Individual responses: Peak-to-peak amplitude

The same analysis as the one reported for participant IHT1 was conducted on all subjects. As demonstrated by participant IHT1, no significant change in SEP peak-to-peak amplitude was observed when comparing pre-, during and post-IHT measurements in any of the participants.

3.3.6. Peak-to-peak amplitude: Grand average

3.3.6.1. Reliability of pre-IHT data

Table.3.10 summarises the results from the intraclass reliability analysis between the three pre-IHT measurements (pre-IHT₀, pre-IHT₅ and pre-IHT₁₀). The ICC score ranges from 0 to 1 report excellent reliability (ICC > 0.75). For peak-to-peak

amplitude the data were also considered very reliable with an ICC value of between 0.95-0.99 for all recordings except for CPc-FPz where reliability was considered as good with an ICC value of 0.61 for N20-P25 and 0.68 for P25-N30 (Table.3.10) and mirrors the final observation on variance made in Section 3.3.4.3.3. with reference to subject IHT1.

Table.3.10. ICC analysis of the pre-IHT data (recorded at 0, 5 and 10 minutes) for Cc, Fc and CPc electrodes

Montage (peak-to-peak)	Mean± SD	ICC	Confidence Interval (95%)
Cc (N20-P25)	0.74± 0.29	0.99	0.98 to 0.99
Cc (P25-N30)	0.63± 0.32	0.95	0.82 to 0.99
Fc (N20-P25)	0.46± 0.11	0.99	0.97 to 1.00
Fc (P25-P230)	0.55± 0.20	0.99	0.95 to 1.00
Cc-FPz (N20-P25)	1.61± 0.51	0.99	0.95 to 1.00
Cc-FPz (P25-N30)	1.12± 0.66	0.98	0.92 to 1.00
CPc-FPz (N20-P25)	1.48± 0.55	0.61	-0.29 to 0.94
CPc-FPz (P25-N30)	1.01± 0.55	0.68	-0.22 to 0.95

3.3.6.2. Histogram distribution

Figure.3.13, Figure.3.14, Figure.3.15 and Figure.3.16 shows that all the datasets for Cc, Cc-FPz, FCc and CPc-FPz approximate normal distributions, respectively. Therefore, the investigation can proceed with the statistical analysis.

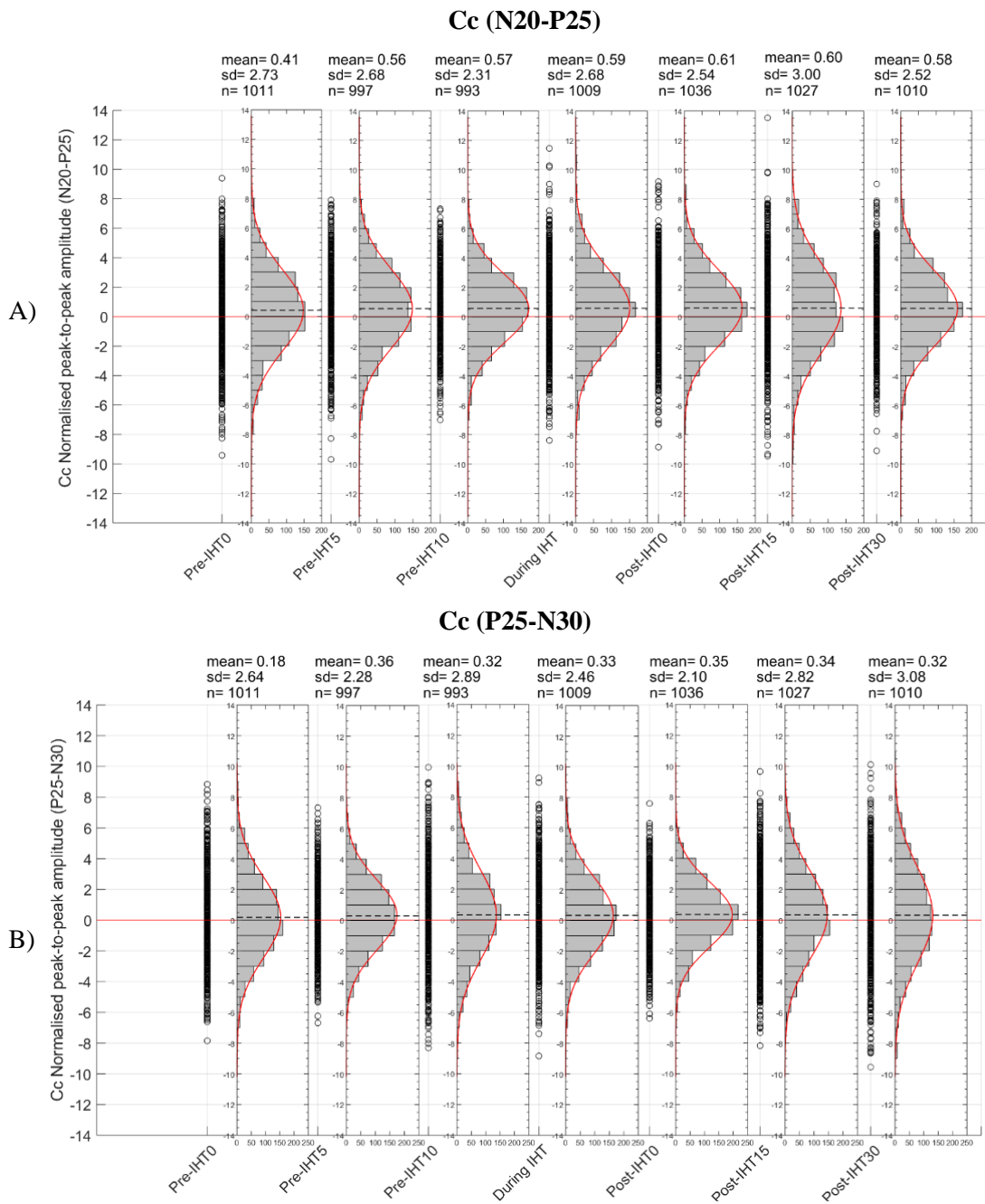


Figure.3.13. Grand average normalized peak-to-peak amplitude. The main graph displays the data plotted using hollow circles. For each time point (pre-, during and post-IHT) a histogram is also plotted (bin width is 0.1). The staggered line on the normal distribution curve highlights the mean. Please note that the data is normalized to pre-IHT_{avg}. **A)** Cc (N20-P25), **B)** Cc (P25-N30). The mean, standard deviation (SD) and the number of epochs (n) are listed above each normal distribution graph.

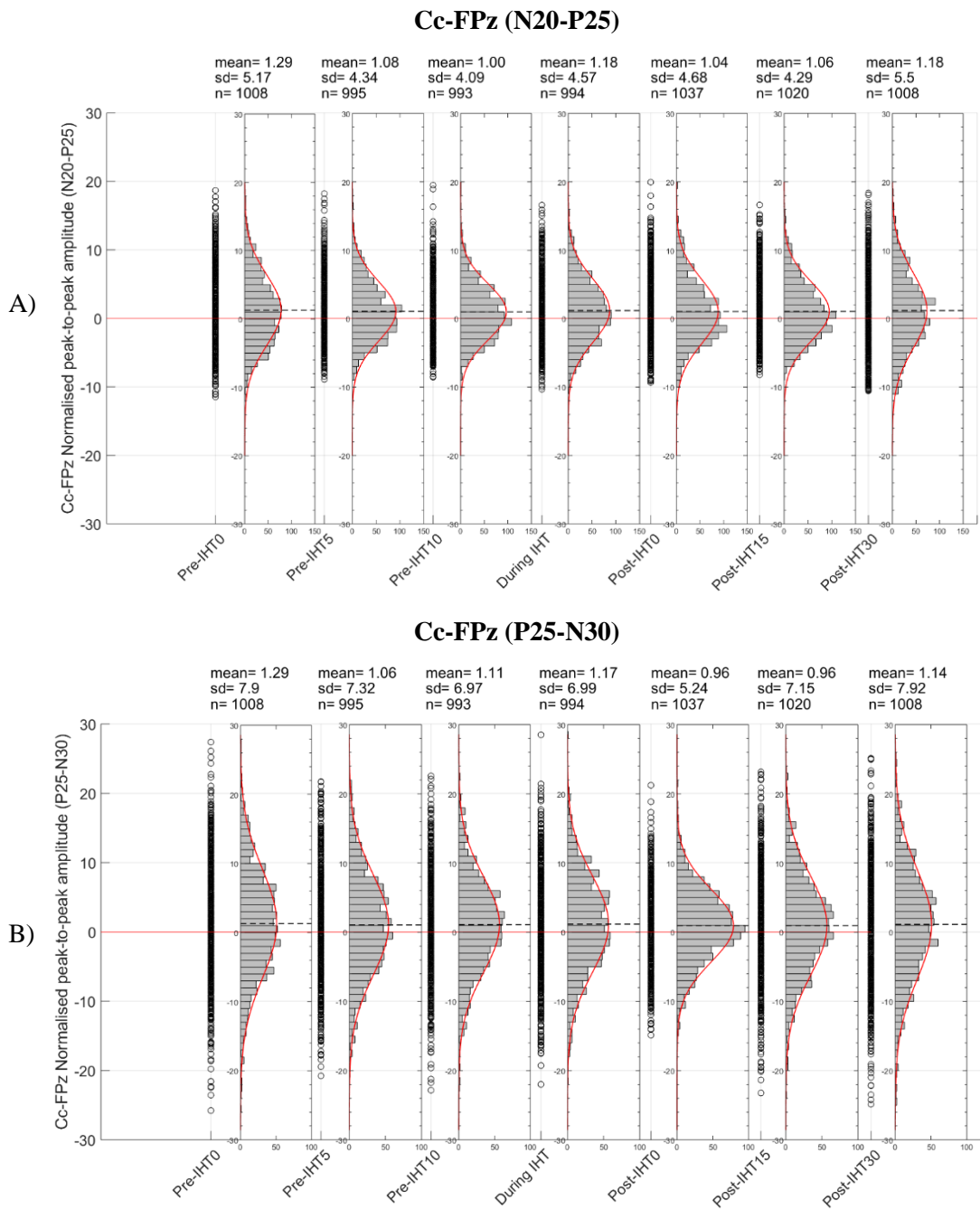


Figure.3.14. Grand average normalized peak-to-peak amplitude. The main graph displays the data plotted using hollow circles. For each time point (pre-, during and post-IHT) a histogram is also plotted (bin width is 0.1). The staggered line on the normal distribution curve highlights the mean. Please note that the data is normalized to pre-IHT_{avg}. **A**) Cc-FPz (N20-P25), **B**) Cc-FPz (P25-N30). The mean, standard deviation (SD) and the number of epochs (n) are listed above each normal distribution graph.

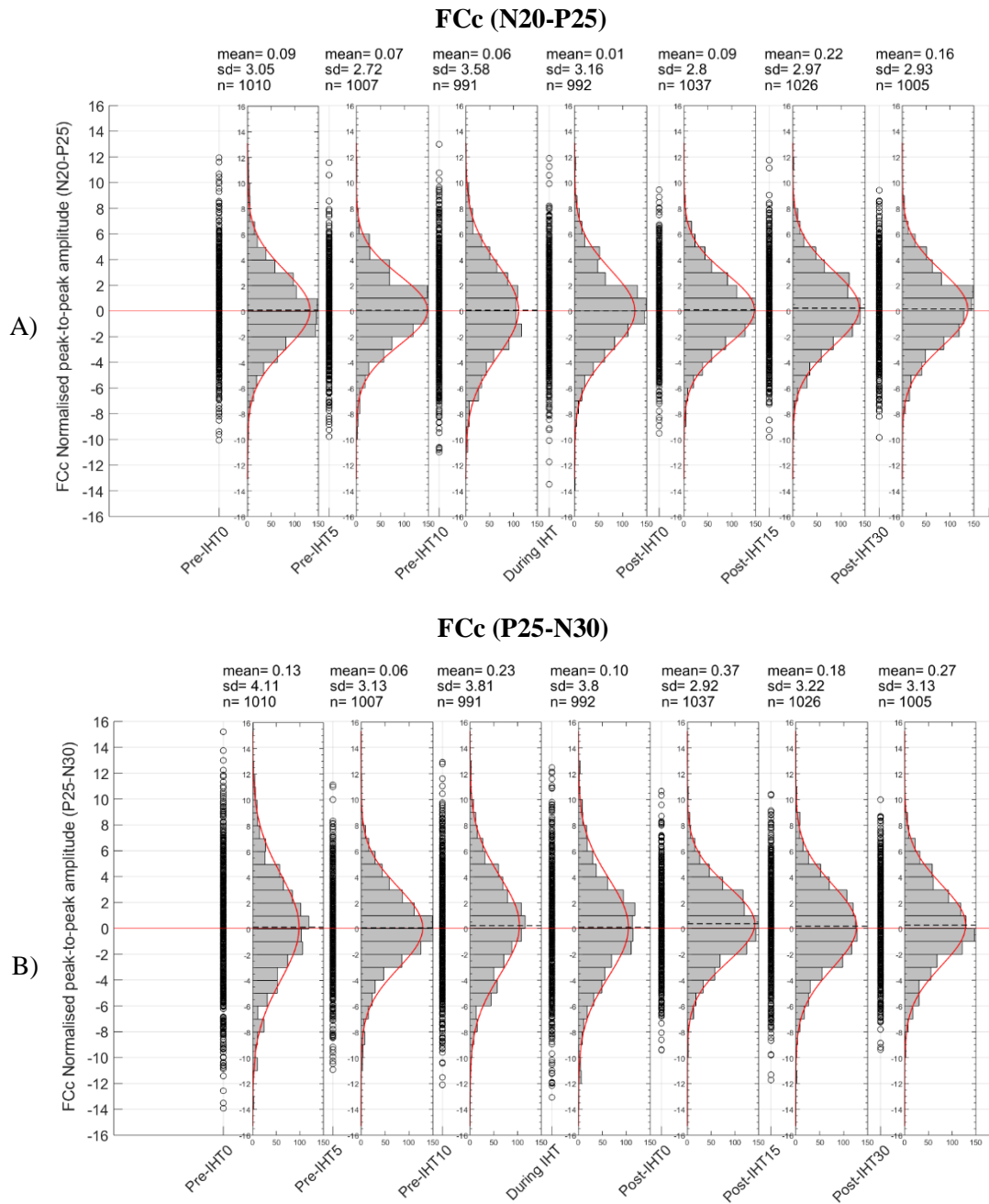


Figure.3.15. Grand average normalized peak-to-peak amplitude. The main graph displays the data plotted using hollow circles. For each time point (pre-, during and post-IHT) a histogram is also plotted (bin width is 0.1). The staggered line on the normal distribution curve highlights the mean. Please note that the data is normalized to pre-IHT_{avg}. **A)** FCc (N20-P25), **B)** FCc (P25-N30). The mean, standard deviation (SD) and the number of epochs (n) are listed above each normal distribution graph.

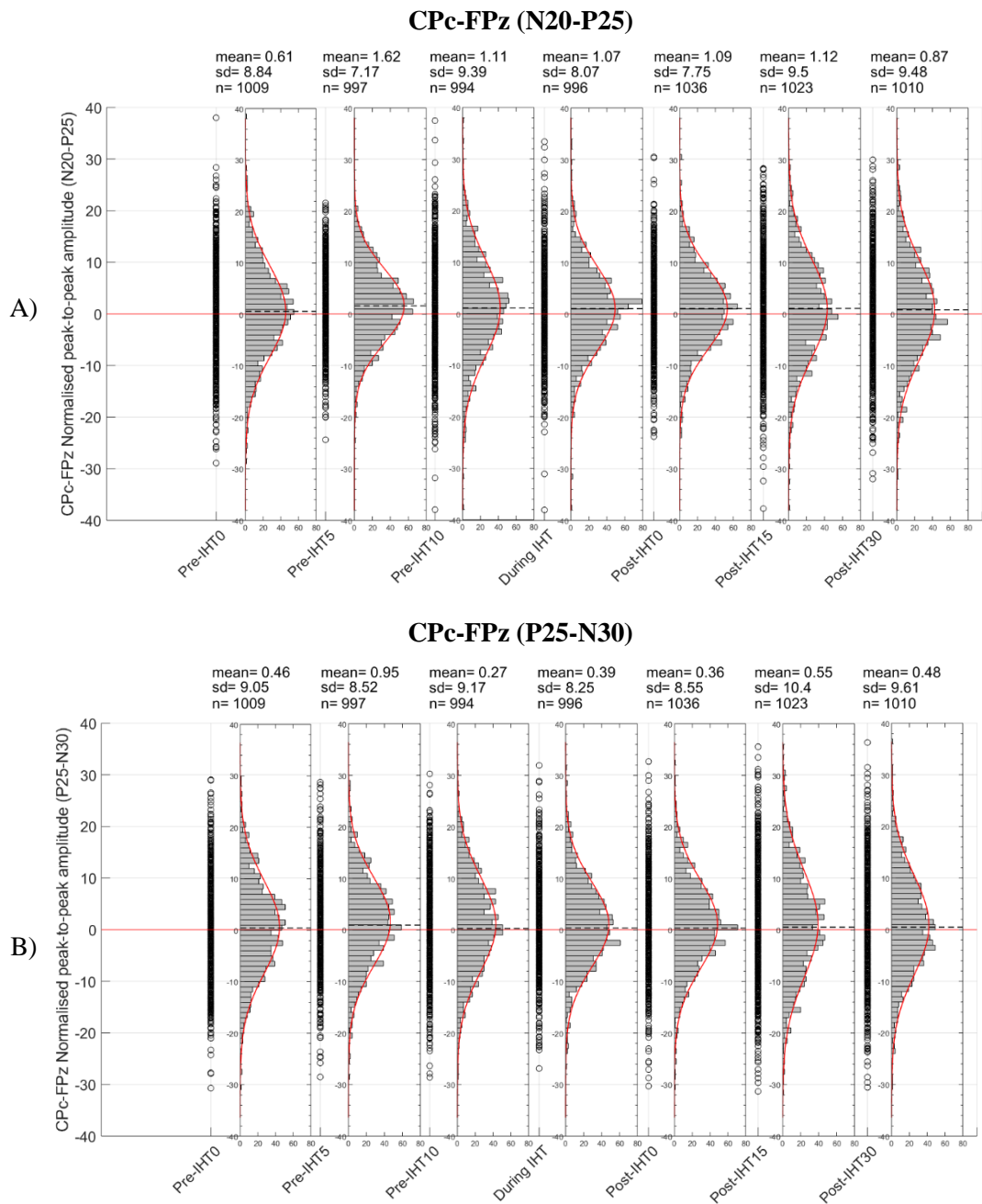


Figure.3.16. Grand average normalized peak-to-peak amplitude. The main graph displays the data plotted using hollow circles. For each time point (pre-, during and post-IHT) a histogram is also plotted (bin width is 0.1). The staggered line on the normal distribution curve highlights the mean. Please note that the data is normalized to pre-IHT_{avg}. **A)** CPc-FPz (N20-P25), **B)** CPc-FPz (P25-N30). The mean, standard deviation (SD) and the number of epochs (n) are listed above each normal distribution graph.

3.3.6.3. Peak-to-peak amplitude

3.3.6.3.1. Cc and Cc-FPz

Figure 3.17 shows the peak-to-peak amplitude for the following peaks: N20-P25 and P25-N30. All datasets had homogeneity of variances, and the One-way ANOVA test did not reveal significant differences in peak-to-peak amplitudes between pre-, during and post-IHT across all datasets (One-Way ANOVA, $p > 0.05$).

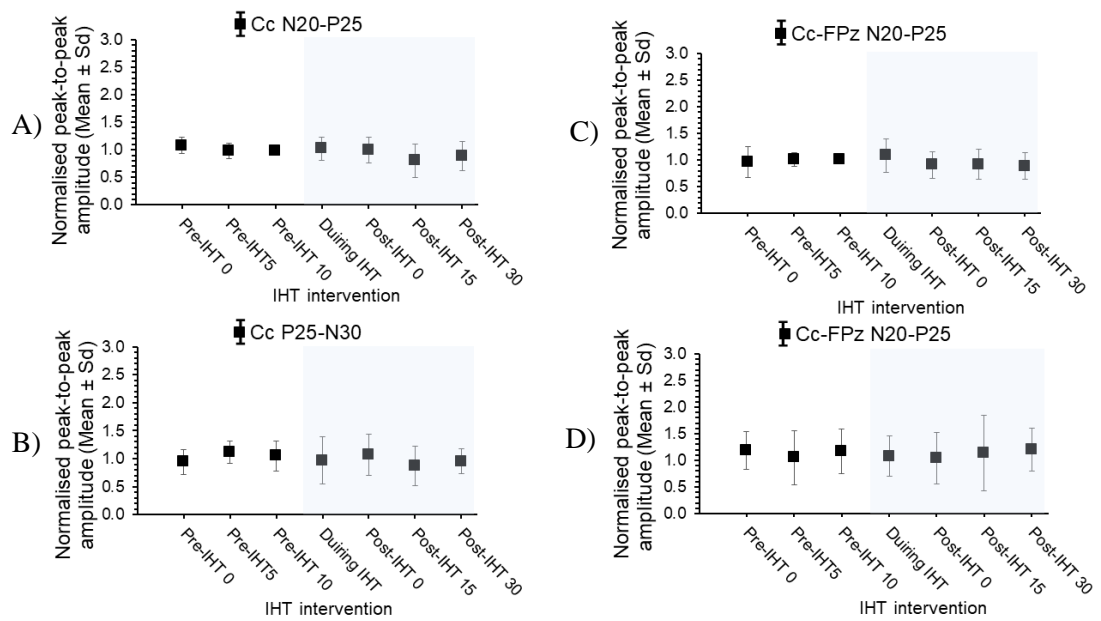


Figure 3.17. Normalised grand average peak-to-peak amplitude of N20-P25 and P25-N30 for Cc and Cc-FPz (Mean \pm SD). The graph highlights during and post-IHT measurements using a blue box. **A)** Cc (N20-P25), **B)** Cc (P25-N30), **C)** Cc-FPz (N20-P25), and **D)** Cc-FPz (P25-N30).

3.3.6.3.2. FCc

Similar results were observed in the monopolar analysis of FCc (Figure.3.18).

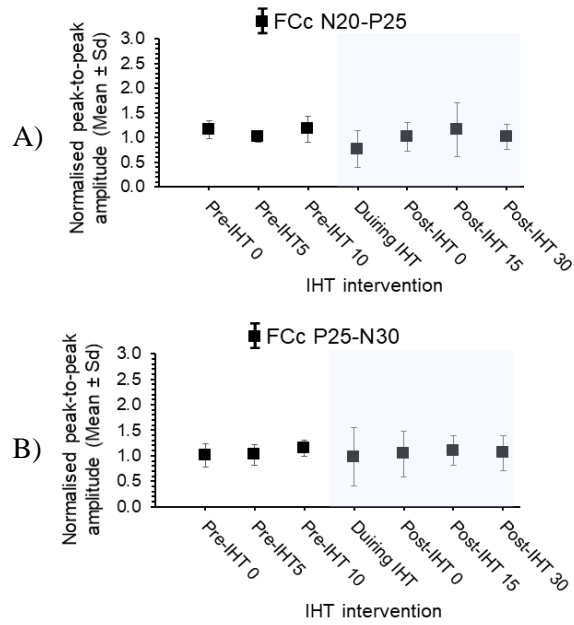


Figure.3.18. Normalised grand average peak-to-peak amplitude of A) N20-P25 and B) P25-N30 for FCc (Mean \pm SD). The graph highlights during and post-IHT measurements using a blue box.

3.3.6.3.3. CPc-FPz

Lastly, for CPc-FPz measure no significant differences were reported between pre-, during and post-IHT (One-Way ANOVA, $p > 0.05$) (Figure.3.19).

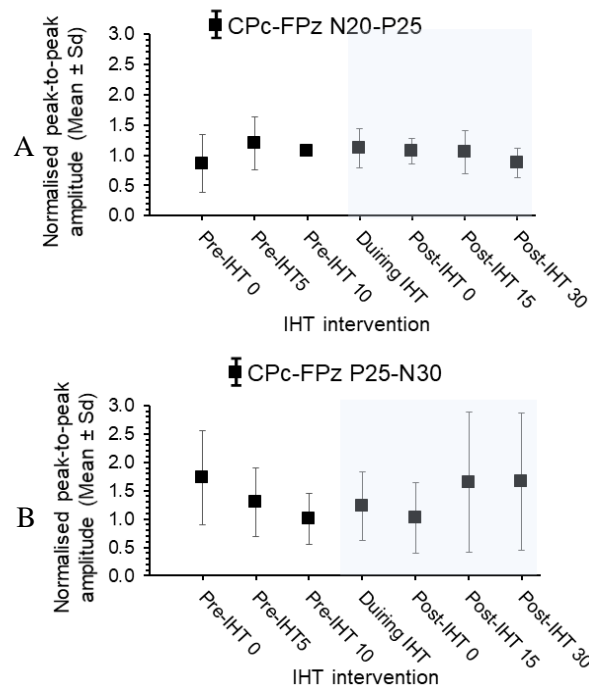


Figure.3.19. Normalised grand average peak-to-peak amplitude of **A)** N20-P25 and **B)** P25-N30 for CPc-FPz (Mean ±SD). The graph highlights during and post-IHT measurements using a blue box.

3.4. Discussion

It has been shown in the literature that IHT has the potential to improve motor performance in patients with iSCI and provides an additive effect when paired with task specific motor training (Trumbower et al., 2012; Trumbower et al, 2017; Hayes et al., 2014; Navarrete-Opazo et al., 2016b; Navarrete-Opazo et al., 2017). However, little information is available on the effects that IHT has on motor and sensory pathways of the spinal and supraspinal regions, which would be informative to understand IHT's mechanism of action and ultimately assist in optimising IHT as a therapy.

This study investigated the effect IHT had on ascending spinal tracts conduction and excitability in healthy volunteers. To assess this, SEP recordings were taken from the somatosensory cortex using EEG non-invasive scalp electrodes

following direct electrical stimulation of a peripheral nerve. Three SEP recordings were taken at baseline to assess consistency, one during and three measurements at 0, 15 and 30 minutes after the termination of a 30 min IHT exposure. The responses were quantified by mainly measuring the mean peak-to-peak amplitude. The statistical analysis involved the comparison of the datasets (pre-, during and post-IHT) using a One-way ANOVA.

3.4.1. SEPs and MEPs

The initial assumption was that the results from our SEP study would covary with the increase in MEP amplitude observed in the study by Christiansen et al. (2018). However, our results on healthy human participants showed a high ICC reliability in baseline SEP measurements of peak-to-peak amplitude and no detectable changes following a single exposure to IHT. Similar results were also observed in the analysis of individual responses. Additionally, this is a second repetition in our lab of SEP recordings following a single exposure of IHT in healthy subjects and both studies concluded no detectable changes in the transmission of sensory information via DCML pathway.

3.4.2. Conclusion

In conclusion, in animal models it has been shown that IHT increases BDNF expression in respiratory motoneurons and the spinal synaptic plasticity observed is serotonin dependent. Furthermore, it has been shown to enhance connectivity of midcervical spinal interneurons. However, the impact of IHT on spinal pathways has not been extensively investigated. In this study a single exposure of IHT in a group of healthy subjects has shown not to induce significant changes in the transmission or processing of somatosensory input to the sensorimotor cortex. This may indicate that the effects of IHT may be more localised to specific networks rather than exert a generalised effect across multiple neural pathways and systems.

Chapter.4. Creating a manual navigated coil placement system for TMS

4.1. Introduction

After studying the effects of IHT on SEPs, a major aim of this project was to investigate the effects of IHT on MEPs. To measure MEPs, a TMS coil is placed over the motor cortex and the stimulus targets the hotspot for the selected target muscle. Precise positioning of the coil is important for reliable MEP measurements. Studies generally use a navigated TMS system, however, our laboratory lacked such specialised equipment. Thus, a prerequisite requirement for the success of this project was to develop an in-house navigation system with equivalent or better accuracy than commercial alternatives and which would aid the experimenter to reposition the coil to the chosen orientation for every TMS stimulation. This chapter will discuss reliability of TMS coil placement, navigation systems available in the market and the navigation system created for this project to record reliable MEP measurements.

4.1.1. Reliability of TMS coil placement

Since 1985, when the first TMS system was demonstrated (Barker, Jalinous, and Freeston, 1985), the precise positioning of the TMS coil for stimulation has been a major challenge (Fang et al., 2019). In the past decades, optically tracked stereotactic systems have been developed that make TMS stimulation as precise as 0.1 mm to the target site and offering researchers more precision and reproducibility in TMS studies.

Julkunen et al. (2009) compared the accuracy of a navigated TMS system with a non-navigated TMS system and found that following 20 repeated stimulations the navigated TMS was < 1.8 mm away from the target stimulus site whereas non-navigated TMS could be 60.2 mm distant. However, commercial navigation systems are very expensive (around 50 to 100 k) and some require a magnetic resonance image (MRI) of the subject's brain making it difficult for laboratories without access to these systems to benefit from improved coil positioning (Kesar, Stinear and Wolf, 2018; Darling, Wolf and Butler, 2006; Kiers et al., 1993).

TMS researchers without prior anatomical imaging, that can be referenced to overlying skull locations, are constrained to position the coil based on generic reference to external landmarks of the head and by interactive stimulation that searches

for a ‘hotspots’ where stimulation is most effective in eliciting a response (Fang et al., 2019). The approximation of the ‘hotspot’ for stimulation, when searching for sites in the motor cortex controlling specific muscles, is verified by looking at the amplitude of the MEP waveforms in the target musculature. This makes the methodology relatively accurate but it can be difficult to reproduce and is a time consuming procedure. Specifically, scientists target the area of the brain that creates the largest MEP with the lowest TMS stimulus strength. Unfortunately, a millimeter change in the location, orientation and/or angling of the coil to the underlying cortex can lead to significant variations in the induced electric field produced in the brain and the change in current density at the target site (Danner et al., 2008; Knecht et al., 2005). Therefore, by controlling the position and orientation of the coil this limitation can be controlled and more consistent stimulating conditions can be achieved (Ambrosini et al., 2018).

According to the literature, to obtain scientifically reliable MEP measurements it is essential to consider the unique size and shape of the cranium and the location and orientation of anatomical structures in the brain of each participant (Ginhoux et al., 2013; Ruohonen and Karhu, 2010; Fang et al., 2019). The most advanced navigated TMS systems use MRI anatomical brain scans and digitizing pens or stylus to create a 3D head and cortex mapping model (Fang et al., 2019) allowing surface sites overlying areas of interest to be efficiently targeted by motion tracking of markers placed on the head and coil that cross-reference the coils position and orientation to the head model. This is particularly helpful when exploring the effects of TMS on non-motor areas where a clear evoked action following stimulation does not exist (Ruohonen and Karhu, 2010; Sandro, 2017, p. 4).

4.1.2. Navigated systems

Navigation systems that are currently available are found in Table.4.1. These systems were developed by Brainsight, Localite and Syneika. The Brainsight TMS navigation system allows scientists to position the TMS coil to the target location based on an MRI image and it can reconstruct the whole brain using Brainsight automated curvilinear reconstruction tools. Moreover, it provides the experimenter with feedback on the coil position and trajectory (Brainsight TMS Navigation by Brainbox, 2021). Similar systems are provided by Localite and Syneika. To further

improve the accuracy and repeatability of TMS stimulation, Axilium Robotics has developed a robotised positioning of the coil that is compatible with the Brainsight, Localite and Syneika systems. This robotic arm, which controls the placement of the coil, compensates for subject head movement (Axilium Robotics - Robot for transcranial magnetic stimulation, 2021). Please refer to Chapter 1 Section 1.10.3.2 Figure.1.17 for an image of the Axilium system.

The Axilium Robotics TMS-Robot is the first robotic arm developed to aid researches and health care professionals with coil positioning. Axilium has also produced a cheaper alternative to the TMS-Robot, the TMS-Cobot system. This system can be used with a neuronavigation tracking system or an optical tracking system (Axilium Robotics - Robot for transcranial magnetic stimulation, 2021). Furthermore, it is designed to be operated either autonomously or manually directed by the experimenter.

Table.4.1. Navigation systems available in the market

Navigation system	Precision
Brainsight TMS navigation system	~1mm
Localite	~ 1-2 mm
SyneikaONE	~ 2 mm

The precision values are taken from each company website. Links are found in the references.

Table.4.2. Robotic systems available in the market

Robotic Systems	Precision	Details
Axilium Robotics TMS-Cobot	< 2 mm	Robotised + manual pre-positioning of coil
Axilium Robotics TMS-Robot	0.1 mm	Robotised positioning of coil

The precision values are taken from each company website. Links are found in the references.

A less expensive option to the TMS-Cobot is to use an open-source software for manual TMS coil navigation known as StimTrack (Ambrosini et al., 2015). StimTrack uses an optical tracking system, Polaris Vicra (Northern Digital Inc.), with volumetric accuracy of 0.25 mm and makes use of reflective markers to monitor the position of the coil relative to the cortex. The software is written in C++ language and

requires manual TMS coil positioning. The accuracy of this navigation system for coil placement is 0.7 mm for translation and $< 1^\circ$ for rotation which is similar to manual navigation systems available in the market (Ambrosini et al., 2018).

4.1.3. StimTrack

To monitor coil position and orientation the StimTrack system requires the use of a pointer that selects specific landmarks to define the head and coil local reference frames (Ambrosini et al., 2018) (see Figure.4.1). Once a ‘hotspot’ is identified, the transformation matrix between the coil local reference frame and head local reference frame is stored (Ambrosini et al., 2018). The system is then setup and provides the user with continuous feedback on coil position. StimTrack source code is available and can be modified by researchers (Ambrosini et al., 2018).

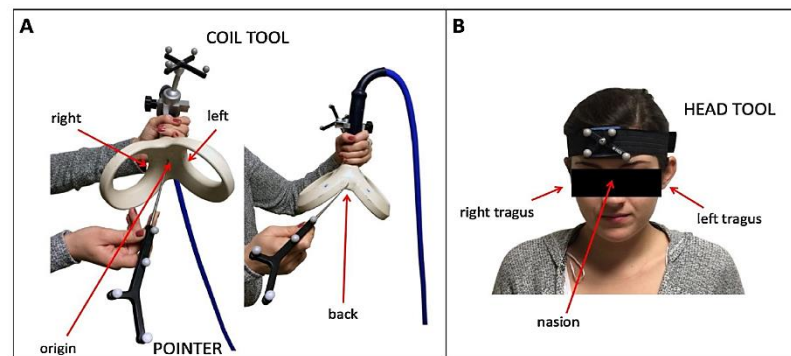


Figure.4.1. The points selected are highlighted with red arrows in A) and B) and the infrared markers used on the head and coil (A and B) (image used with permission from Ambrosini et al., 2018).

The system uses a graphical user interphase (GUI) allowing the experimenter to identify the local reference frames, save the ‘hotspot’ and visualise the position of the coil in reference to the head in real-time (Ambrosini et al., 2018). The system saves the local reference frames and ‘hotspot’ for future use. Moreover, it is compatible to use with any TMS coil (double-cone coil, figure-of-eight coil and circular coil).

StimTrack performance was evaluated by using three different experiments. Primarily, the experimenters studied the repeatability of locating the ‘hotspot’ within

and between different sessions (Ambrosini et al., 2018). Secondly, they compared the accuracy to the Brainsight commercial navigation system. The mean difference between StimTrack and Brainsight was 0.2 mm for distance to target and 0.9°, 0.7° and 0.4° for roll, pitch and yaw angles (Ambrosini et al., 2018). Lastly, the experimenters completed a test-retest protocol on human participants and studied intra- and inter- session reliability on motor threshold and area under the curve. The study reported a high reliability of 0.9 in both intra- and inter-session measurements of motor threshold and area under the curve (Ambrosini et al., 2018) demonstrating that technical solutions for coil positioning can be implemented at relatively low cost.

4.1.4. Coil tracking using two webcams

Moreover, Washabaugh and Krishnan (2016) created a coil tracking system for TMS utilising two webcams, reflective markers and computer stereovision. They showed that the system was able to track coil position with an accuracy of around 5 mm in translation and 1° in rotation (Wahabaugh and Krishnan, 2016). The study reported that with this coil navigation system the MEPs were two times larger compared to the non-navigated condition (Wahabaugh and Krishnan, 2016). But this may reflect on the competence of the user and level of training in TMS techniques.

4.1.5. Aims and objectives

A major aim of this study was to investigate the effects of IHT on MEPs but in order to do this, it was necessary to have reliable baseline MEP measurements. Thus, a prerequisite project aim was to develop a system which would aid the experimenter to reposition the coil to the chosen orientation for every TMS stimulation based on existing motion capture/visualization equipment. To achieve this, the work described in this chapter followed the concept proposed from Washabaugh and Krishnan (2016) and Ambrosini et al. (2018) to create a positioning system based on the use of the type of reflective markers used in motion capture systems and to employ Vicon motion capture cameras under the control of a customised Matlab code to guide the experimenter with coil placement. The choice of camera was simply based on availability within the Biomedical Engineering department and software can be adapted to other IR-sensing cameras such as OptiTrack. A feature of the developed

system was that co-registration of the coil with a selected ‘hotspot’ site was necessary for stimulation to be triggered thereby providing a high targeting hit rate.

4.2. Methodology

4.2.1. Manual coil placement for TMS

The manual navigation system involved the use of five reflective markers placed on the participant’s forehead and four placed on the stimulating TMS coil (see Figure.4.2) allowing their position to be tracked by six motion capture Vicon cameras (Vicon Bonita) (see Figure.4.3) These cameras were positioned around the workspace so that each could see at least 8 out of the 9 markers. Tracker motion capture software by Vicon was then used to create two objects from the cluster of markers, one on the participant’s forehead and one on the stimulating coil.



Figure.4.2. Positioning of the markers on the forehead and double- cone coil.

The best position of the coil on the participant’s head for stimulation was chosen using trial and error search informed by monitoring MEPs in target muscles using Spike2 software (CED). Information on the position of the two objects in 3D space was then portrayed on a GUI. This allowed the experimenter to view the ‘hotspot’ template as well as the position of the coil with respect to the participant’s head in real-time (Figure.4.4). Since the position of the coil was viewed with respect to the participant’s head placement, any movement from the participant’s head was compensated (Washabaugh and Krishnan, 2016; Ambrosini et al., 2018).

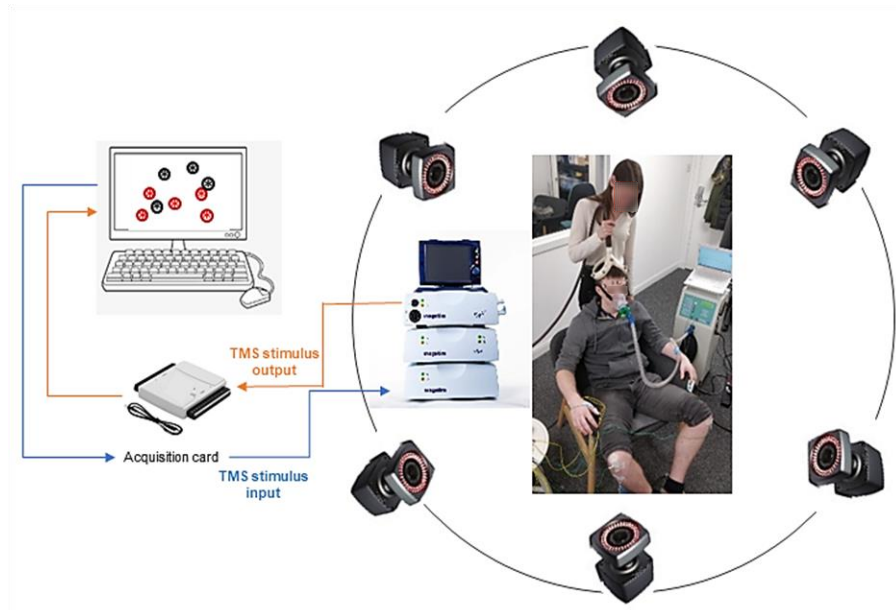


Figure.4.3. Diagram of the manual navigation system for TMS coil positioning. When finding the target site for stimulation every TMS stimulus was sent as an output to the acquisition card. This information was used in the customised Matlab code to save the data of the coil position with respect to the head. The acquisition card also allowed for TMS to receive stimulation triggers from the customised Matlab code once the placement of the coil was within the level of precision set prior to the experiment. (Magstim stimulator image was used with permission from <https://www.magstim.com/us-en/>) [Accessed on 10 December 2020]

Once the experimenter matched the coil to the template a stimulus is triggered simultaneously. This was accomplished by using a data acquisition card by National Instruments connected to the input trigger of the TMS system (see Figure.4.3). A customised code written in Matlab signaled the TMS to trigger automatically once the experimenter matched the coil to the template. The code also allowed the experimenter to choose the level of accuracy for each axis of motion: alpha, beta, gamma (pitch, yaw and roll) and distance. The higher the accuracy, the more demanding it would be for the experimenter to match the coil position to the ‘hotspot’ template. For the simplicity of the system, all the axes of movement were incorporated as one using the cost function. Please refer to Figure.4.2 and Figure.4.3 for a basic understanding of the setup and Figure.4.4 which shows the GUI and the muscle response following a TMS stimulus.

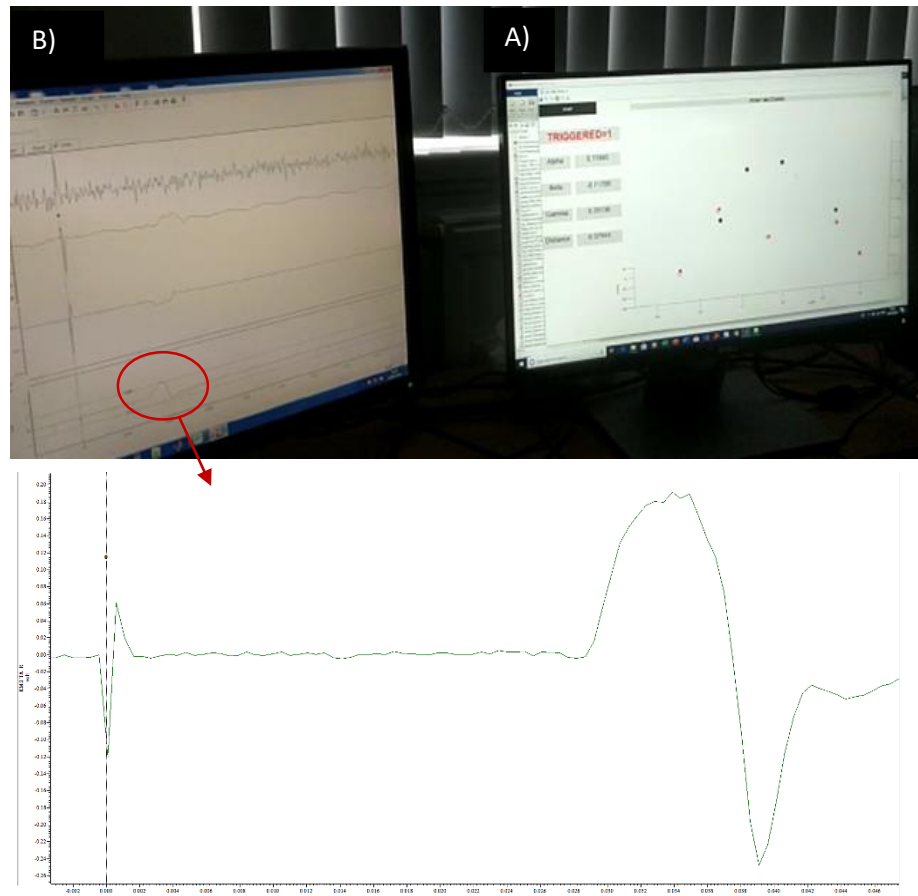


Figure.4.4. A) GUI which provides a visual representation of the markers on a 3D graph, the number of triggers and the difference in rotation (alpha, beta ad gamma) and distance between 'hotspot' and real-time position of the coil. B) Shows the MEP waveform following the trigger in Spike2 software. The red circle highlights the target muscle MEP.

4.2.2. Calibration of cameras

Manual calibration of the six cameras took place prior to each experiment. Calibration was completed in Tracker software and required the use of a calibration wand.

4.2.3. Matlab code

In Matlab, a customised code was written which allowed the experimenter to find the 'hotspot' for TMS stimulation and utilized a data acquisition card for communication between the TMS card and the PC controlling the experiment. In this study the target site of interest was the 'hotspot' for the tibialis anterior muscle. Finding the 'hotspot' involved placing the coil in an approximate position for tibialis

anterior muscle MEP generation and subsequently searching for the coil placement where the stimulus created the largest MEP output with the lowest stimulation strength.

Once the TMS was triggered the signal was sent to the PC and a custom written Matlab programme was used to process the information. The Matlab programme saved the position of the head and coil markers, the direction of the coil and head objects (alpha, beta and gamma), the distance between the center of the coil and head objects, the rotation matrix of the coil and the head objects, the head and coil transformation matrix and the head center matrix that were calculated in Tracker software.

Information on several stimulations were recorded until the ‘hotspot’ was located. The best coil position was then chosen by looking at the amplitude of the MEP waveform of the target muscle in Spike2. Once the ‘hotspot’ template was chosen, the data saved for this stimulation were uploaded to the Matlab customised programme.

The Matlab GUI programme provided a visual guide to aid the experimenter place the coil with great precision at the ‘hotspot’. The programme provided the template (or otherwise referred to here as the ‘hotspot’) arrangement as well as the real-time coil and head arrangement (Figure.4.4; Figure.4.5). In the GUI programme, the coil position was displayed for the experimenter in color red and the head position in color black (Figure.4.4, Figure.4.5). The real-time data are displayed as a circle

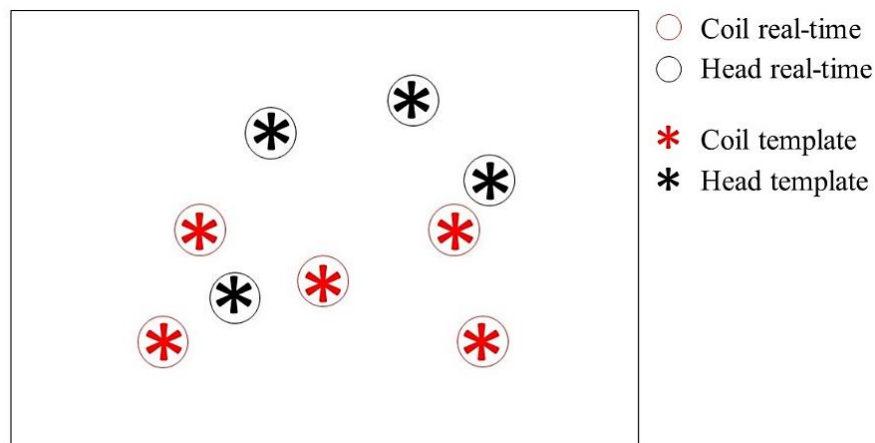


Figure.4.5. Coil position in color red and head position in color black. The asterisk () represents the ‘hotspot’ template and the circle represents the real-time placement of the objects. This is an example of the coil position matching the ‘hotspot’ template.*

while the template as an asterisk (Figure.4.4, Figure.4.5). For the experimenter, the goal was to match the coil to the template ('hotspot') or the circle around the asterisk.

Apart from a visual representation of the reflective markers, the difference between the template and real-time data for alpha, beta, gamma (pitch, yaw and roll) and distance was also given (Figure.4.6). Pitch, yaw and roll, as described by Ambrosini et al. (2018) and Souza et al. (2018), are given in degrees while distance is given in mm. The purpose of providing these measurements is to help the experimenter with the direction of movement required to match the coil to the template. Moreover, we also used these measurements to calculate the cost function in order to provide a measure of performance.

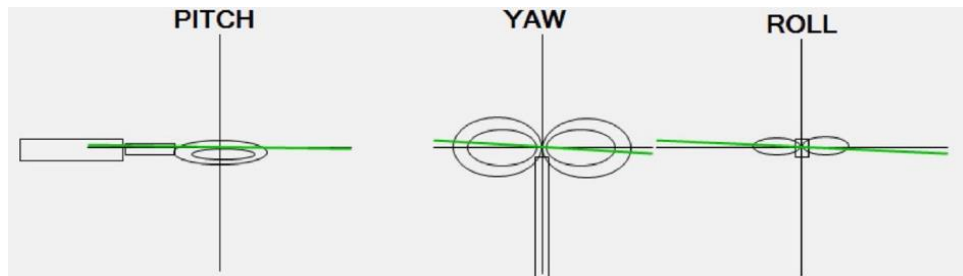


Figure.4.6. Figure-of-eight TMS coil pitch, yaw and roll angle variations (image used with permission from Ambrosini et al,2018).

For the coil to match to the 'hotspot' template and trigger the TMS machine automatically the rotation of the coil needs to be less than 0.8° and the translation less than 0.8 mm. The accuracy level can be set by the experimenter. The value 0.8 is used here as this is the level of accuracy considered as an acceptable compromise between accuracy and the time necessary to achieve alignments during our TMS experiments. The key calculations used to calculate pitch, yaw, roll and distance as well as calculations to compensate for head movement are described below.

4.2.4. Key calculations

1) Calculations for the axes of movement (alpha, beta and gamma) and distance (Washabaugh and Krishnan, 2016).

A three-dimensional object can be rotated about three orthogonal axes: a rotation of β about the x-axis, a rotation of γ about the y-axis and a rotation of α about the z-

axis. The rotations are a simple extension of the two-dimensional matrix. Please refer to Section 4.2.3 Figure.4.6 for an image of the rotations.

These rotations were calculated to help with positioning of the coil to match the template in real-time and for calculating the coil mismatch using the cost function.

Shown below are the rotations about each axis.

$$\begin{array}{l}
 \begin{array}{ccc}
 1 & 0 & 0 \\
 \mathbf{R}_x(\beta) = \begin{array}{ccc}
 0 & \cos(\beta) & -\sin(\beta) \\
 0 & \sin(\beta) & \cos(\beta)
 \end{array} & \text{for a rotation through } \beta \text{ about the } \mathbf{x}\text{-axis.}
 \end{array} \\
 \\
 \begin{array}{ccc}
 \cos(\gamma) & 0 & \sin(\gamma) \\
 \mathbf{R}_y(\gamma) = \begin{array}{ccc}
 0 & 1 & 0 \\
 -\sin(\gamma) & 0 & \cos(\gamma)
 \end{array} & \text{for a rotation through } \gamma \text{ about the } \mathbf{y}\text{-axis.}
 \end{array} \\
 \\
 \begin{array}{ccc}
 \cos(\alpha) & -\sin(\alpha) & 0 \\
 \mathbf{R}_z(\alpha) = \begin{array}{ccc}
 \sin(\alpha) & \cos(\alpha) & 0 \\
 0 & 0 & 1
 \end{array} & \text{for a rotation through } \alpha \text{ about the } \mathbf{z}\text{-axis.}
 \end{array}
 \end{array}$$

By multiplying these rotations together, a single rotation matrix was created.

$$\begin{array}{l}
 \text{Rotation matrix:} \\
 \\
 \begin{array}{ccc}
 r_{11} & r_{12} & r_{13} \\
 \mathbf{R} = \begin{array}{ccc}
 r_{21} & r_{22} & r_{23} \\
 r_{31} & r_{32} & r_{33}
 \end{array}
 \end{array} \\
 \\
 \mathbf{R}_z(\alpha)\mathbf{R}_y(\gamma)\mathbf{R}_x(\beta) \\
 \begin{array}{ccc}
 \cos(\gamma)\cos(\alpha) & \sin(\beta)\sin(\gamma)\cos(\alpha) - \cos(\beta)\sin(\alpha) & \cos(\beta)\sin(\gamma)\cos(\alpha) + \sin(\beta)\sin(\alpha) \\
 = \begin{array}{ccc}
 \cos(\gamma)\sin(\alpha) & \sin(\beta)\sin(\gamma)\sin(\alpha) + \cos(\beta)\cos(\alpha) & \cos(\beta)\sin(\gamma)\sin(\alpha) - \sin(\beta)\cos(\alpha) \\
 -\sin(\gamma) & \sin(\beta)\cos(\gamma) & \cos(\beta)\cos(\gamma)
 \end{array}
 \end{array}
 \end{array}$$

Using the rotation matrix above, the angles for α , β and γ were calculated. These were used to aid with the precise placement of the coil to the ‘hotspot’ as well as for the cost function calculation.

$$\begin{array}{l}
 \gamma = \sin^{-1}(r_{31}) \\
 \beta = \sin^{-1}\left(\frac{r_{32}}{\cos(\gamma)}\right) \\
 \alpha = \sin^{-1}\left(\frac{r_{21}}{\cos(\gamma)}\right)
 \end{array}$$

Moreover, the distance between the coil object centroid and the head object centroid was also calculated. The centroid of the objects was provided in real-time by the Vicon motion capture system.

$$Distance = pdist2(\text{coil object centroid}, \text{head object centroid})$$

pdist2 is Matlab function that returns the distance between each pair of observations in the coil and head objects.

2) Calculations to compensate for head movement during coil placement in real-time.

Prior to incorporating the calculations described below the experimenter has a visual representation of the coil and head on the GUI where movement of the head is not controlled making it very difficult to match the coil to the template unless we immobilised the participants head. The calculations described below compensate for head movement. Essentially the calculations move the real-time coil and head position to the template and any movement of the head is viewed as a coil movement in the GUI. Please refer to Figure.4.8.

From the Vicon motion capture system the software captures the head points, coil points, head center, coil center and head rotation matrix. This information was used for the calculations that will follow. While going through each step please refer to Figure.4.7 provides a visual aid for each step undertaken. Also, please note that in the calculations RT is short for real-time and Rh is short for head rotation.

- a) Translation of real-time head to the origin (Figure.4.7.B)

$$Head\ points_{RT} transformation = Head\ points_{RT} - Head\ centre_{RT}$$

- b) Rotation of new real-time head to match the orientation of the template head (Figure.4.7.C).

$$Head\ points_{RT} transformation = Hotspot\ template_{Rh}^{-1} \times (RT_{Rh}) \times Head\ points_{RT} transformation$$

- c) Now that the rotation was the same, the new real-time head moved back to the location where the template head was (Figure.4.7.D)

$$\begin{aligned} \text{Head points}_{RT} \text{ transformation} \\ = \text{Head points}_{RT} \text{ transformation} + \text{Hotspot template}_{\text{Head center}} \end{aligned}$$

- d) The same transformation was then applied to the coil object (Figure.4.7). By applying these transformations to the coil object we were compensating for head movement.

$$\begin{aligned} \text{Coil points}_{RT} &= \text{Coil points}_{RT} - \text{Head centre}_{RT} \\ \text{Coil points}_{RT} \text{ transformatio} \\ &= \text{Hotspot template}_{Rh}^{-1} \times (RT_{Rh}) \times \text{Coil points}_{RT} \text{ transformation} \\ \text{Coil points}_{RT} &= \text{Coil points}_{RT} + \text{Hotspot template}_{\text{Head center}} \end{aligned}$$

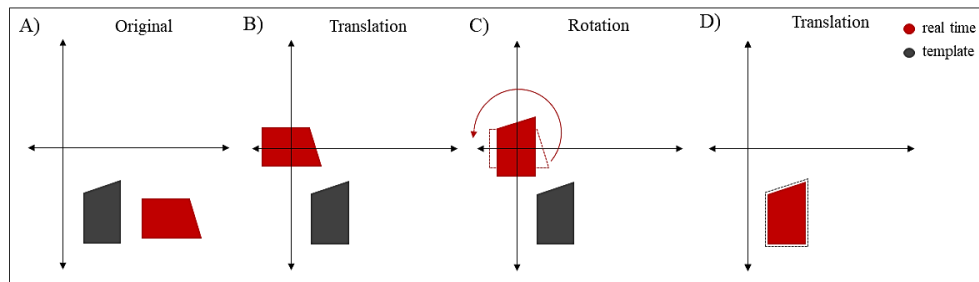


Figure.4.7. Diagram showing the steps of the calculations. **A)** the location of the real time and template objects. **B)** translation of the real time object to the origin. **C)** rotating the real time object at the origin to match the template orientation. **D)** place the real time object at the template location.

The diagram below provides an additional visual aid of the head movement compensation. In Figure.4.8.A) the original diagram shows a scenario of coil and head placement. When the participant rotated the head the experimenter was required to rotate the coil to find again the optimum location for stimulation. In Figure.4.8.B) the diagram provides an illustration of the GUI. In the first panel it shows the head movement and in the second panel it shows the compensation for head movement. In the GUI the investigator during the experiment sees only the compensation panel of Figure.4.8.B). Essentially these calculations made it easier for the experimenter to match the coil to the template. Otherwise it would have required the matching both the head and coil to the template.

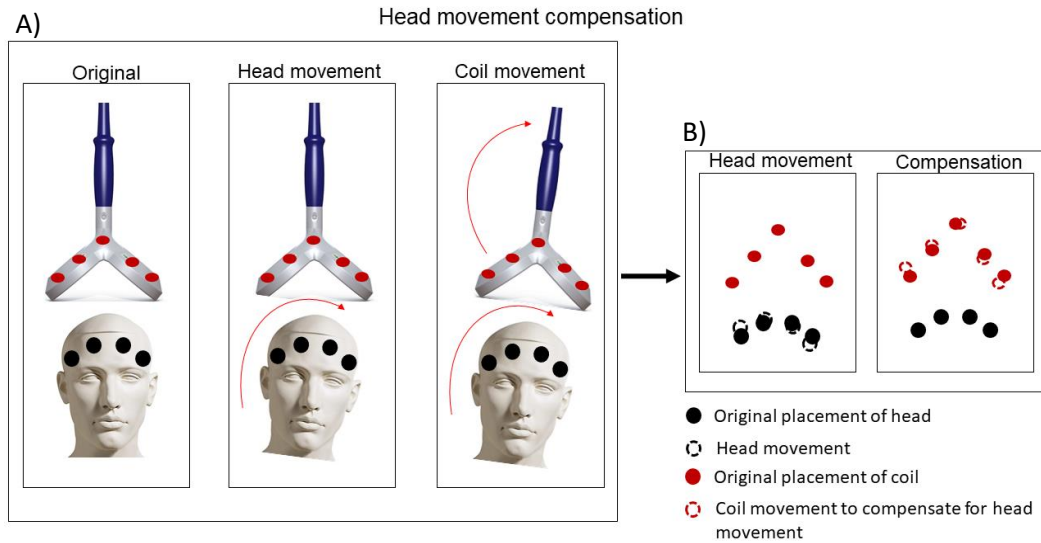


Figure.4.8. Head movement compensation. **A)** shows a scenario of the head and coil placement (original), head movement and the coil movement to find again the position for stimulation. **B)** has two panels the first one shows the head movement and the second panel shows how the coil moves and compensates for the head movement. This makes matching of the coil to the template easier for the experimenter and it does not require to immobilize the participants head during the experiment. This principle is used by commercial TMS systems. (image of the mannequin was used with permission from <https://www.shopequip.co.uk/mannequins/male+mannequin+head+823-C284-12725.html>) [Accessed on 13 April 2021] (image of the Magstim double-cone coil was used with permission from <https://www.magstim.com/>) [Accessed on 13 April 2021]

3) Cost function

For the purpose of this experiment, the navigation error was expressed with a single value so we could measure the placement mismatch between the template and real-time data. To do this we defined the cost function, which measures how well the output of the navigation TMS system performed while taking into account the threshold that was set during the experiment. The function returns the error between the predicted value, which in our case is the ‘hotspot’ template, and actual outcomes, which were the stimulations in real-time (Ferrer and Sanfeliu, 2015; Yin, Paiva and Billard, 2014). In the cost function shown below this is defined as $(a_{Actual} - a_{Temp})$ and the squared error $((a_{Actual} - a_{Temp})^2)$ relates to Gaussian noise. The errors for pitch, yaw, roll and distance were added and divided by $2N$ which ensured that the cost function is not dependent on the number of elements in the sample. This part of the equation is important when you compare models. In this study the cost was expressed

as a percentage and was normalised to the maximum error which in our case it was set to 0.8.

The cost function is defined as:

$$Cost = \frac{(\alpha_{Actual} - \alpha_{Temp})^2 + (\beta_{Actual} - \beta_{Temp})^2 + (\gamma_{Actual} - \gamma_{Temp})^2 + (\delta_{Actual} - \delta_{Temp})^2}{2N}$$

where 'Actual' is the coil arrangement in real-time and 'Temp' is the 'hotspot' template coil arrangement

where 'α' is pitch, 'β' is yaw, 'γ' is roll and 'δ' is distance

where 'N' is the number of samples

4.3. Discussion

This chapter describes the development of a manual navigation system for coil placement that was built to enhance the reproducibility of our MEP experiments. This system was built on the common principles of other manual navigation systems for TMS coil placement using motion capture video analysis. The system was configured to operate with an accuracy of 0.8 mm for translation and 0.8° for rotation, similar to other manual TMS coil navigation systems (Washabaugh and Krishnan, 2016; Ambosini et al., 2018). As previous studies have reported, these manual visualisation systems are low-cost and enhance the reproducibility of coil placement. However, compared to commercial navigated TMS systems, they do not take into account the geometry of the head or provide integration with brain imaging (Washabaugh and Krishnan, 2016; Ambosini et al., 2018). Therefore, for these systems an MRI image is not required. Laboratories that do not have access to the commercially available navigated TMS systems but have access to motion capture IR-cameras can readily create a low-cost TMS coil navigation system.

Compared to previous manual navigation systems for coil placement, the customised Matlab code allowed the experimenter to choose the level of accuracy. However, with higher accuracy demands came the extra difficulty for the experimenter to match the coil to the template. Despite this, it is also possible to use the system for training purposes as with experience the experimenter's technique improves thereby

allowing higher accuracy targeting to be achieved. The other benefit of this system is that stimulus delivery is automated and does not require attention from the experimenter to trigger the TMS. From our observations, with some experience using this system, the experimenter can achieve very high accuracy.

Moreover, compared to previous manual navigation systems we used the cost function to describe the mismatch of the real-time coil to the template. The cost function is used in robotics to test how badly the robot is behaving. Subsequently, the robot uses this information to enhance its performance. The cost function measures the performance of the system using the predicted result which in this case was the accuracy level set prior the experiment and the actual result the experimenter achieved during the study. Subsequently, the cost value was given as a percentage and normalised to the highest possible error. In this way we were able to report in general the performance of our system. With this analysis, however, information of the error individually for pitch, roll, yaw and distance cannot be provided. However, it can be stated that in all these parameters the error was below 0.8. At this level of accuracy, we were confident of our coil placement and importantly could rule out poor coil positioning as a confounding variable in our MEP measurements.

In the future, the system created may be further improved by having better visual representations of the objects in multiple view angles. The GUI provided a 3D view of the object but it required the experimenter to change the view manually. Furthermore, it would be beneficial to compare the system we created with Ambrosini et al. (2018) by conducting the experimental tests he used to test the repeatability and accuracy of his system. However, one aspect of the approach adopted here and by Ambrosini was that the positioning was dependent on either being able to identify a motor 'hotspot' via MEP or that a scalp location above a target area can be predicted without MEP generation being necessary. For example, when targeting non-motor areas effects of TMS targeting would still require to be referenced to prior anatomical brain image with a scalp surface location as target.

Chapter.5. Studying the effects of IHT on the corticospinal pathway in healthy subjects

5.1. Introduction

5.1.1. Intermittent hypoxia

IHT has the potential to be implemented alone or in combination with a task specific training as a form of rehabilitation in iSCI patients (McCaughey et al., 2016; Trumbower et al., 2012; Hayes et al., 2014; Navarrete-Opazo et al., 2017) and potentially other neurophysiological conditions affecting motor function. Its action depends on the presence of serotonergic innervations and BDNF expression (Mitchell, 2001).

Animal models show significant recovery in grasping and locomotion in response to IHT and in patients with iSCI a significant recovery has been observed in ankle plantar flexion, walking speed, dynamic balance and walking endurance (Trumbower et al., 2012; Hayes et al., 2014; Navarrete-Opazo et al., 2017; Trumbower et al., 2017). The actions on walking endurance are most likely associated with general respiratory plasticity adaptation and an increased exercise tolerance induced following IHT (Hayes et al., 2014). Moreover, some iSCI patients report that following a month of daily IHT exposure, they were able to walk without walking aids suggesting a more diverse plasticity occurring in motor function capability involving power and muscle coordination (Navarrete-Opazo et al., 2016b). Furthermore, patients with moderate sleep apnoea that underwent IHT exhibit an enhanced motor improvement compared to those without sleep apnoea (Vivodtzev et al, 2020). Despite these acknowledged improvements in motor function, it is recognised that there is insufficient information on how IHT's impacts on the physiology of ascending and descending spinal pathways. Christiansen et al (2018) was the first study to investigate corticospinal function following a single exposure to IHT and this study will be referred further below.

5.1.2. Assessing sensory and motor pathways

Following SCI, the conduction of sensory and motor information is disrupted. In Chapter 3 the effects of IHT on cortical SEPs were investigated. The components that

were studied involved the initial arrival and processing of evoked sensory activation of the sensory cortex of the brain. This complementary chapter of the thesis focuses on the neurophysiological assessment of the CST, an important descending pathway involved in the execution of voluntary motor control.

The neurophysiological technique to study the integrity and excitability of the CST on different muscles in this thesis is referred to as TMS and involves single pulse non-invasive magnetic stimulation of the motor cortex and the recording of a muscle EMG potential otherwise known as motor evoked potential (MEP).

5.1.3. TMS and MEPs

As mentioned in the literature review, the early pioneers of brain stimulation in humans are Penfield and Boldrey (1937) who localised regional motor function within the cortex by stimulating the surgically exposed brain of conscious patients. Following from this, Merton and Morton (1980) used transcranial electrical stimulation (TES) as a non-invasive method to evoke MEPs for the study of the CST in humans. However, electrical stimulation of the cortex is extremely uncomfortable, due to scalp afferent stimulation, and is only rarely adopted in modern research studies.

TMS introduced by Baker in 1985 overcomes this problem by using a magnetic coil to induce stimulation. During stimulation the device discharges a large capacitor through the coil and the resulting brief, but large magnetic field, induces a corresponding electrical field in the brain (Rothwell et al., 1992; Hallett, 2000). This rapidly changing electrical field has the potential to activate neurons and cause propagation of action potentials through brain pathways. When targeting the motor cortex with TMS the corticospinal tract is stimulated leading to the activation of the muscles innervated by the stimulated brain region (Groppa et al., 2012). Specifically, a single TMS pulse over the primary motor cortex activates layer 2/3 excitatory and inhibitory neurons that project to layer 5 excitatory corticospinal neurons. Layer 5 corticospinal neurons are also activated by low intensity stimulation due to the activation of pre-synaptic inputs to the targeted neurons. Thus, at low intensities MEPs are a consequence of indirect synaptic activation whereas with higher intensities the

cells themselves are directly excited by the current induced by TMS leading to direct an action potential production (Hallett 2007; Wilson, Moezzi and Rogasch, 2021).

5.1.4. TMS coils

There are a wide range of coil shapes used in TMS with some coils giving focality and limited depth penetration while others have a greater penetration but lack focality (Knecht et al., 2005; Groppa et al., 2012). Coil choice is directed by the need of the study and the intended area targeted for stimulation. For instance, to generate MEPs in lower limb muscles, a coil with greater penetration is required due to the deep central location of the cortical areas controlling the leg, while for arm, hand or face areas which are more superficial to the skull can be more easily stimulated by a coil with greater focality (Groppa et al., 2012). More information regarding the different TMS coils, is available in Chapter 1 Section 1.10.3.

5.1.5. Accuracy of TMS stimulation

Since TMS is used to non-invasively activate neurons in the motor cortex, it can be a challenge to locate the area of interest and it usually requires operator training and significant experience. Something to consider before using TMS to activate the CST, is the basic somatotopic mapping of the cortex (Figure.5.1), the cortical homunculus. As seen in Figure.5.1, the contralateral leg area lies more central and deeper in the brain compared to the equivalent arm area which is located on the surface and lateral to the midline. As mentioned above this organisation is very important in determining coil choice as well as determining the placement and angling of the coil on the scalp. However, the experimenter can only partially rely on this illustration as there are individual differences and extensive overlap in cortical muscle representation.

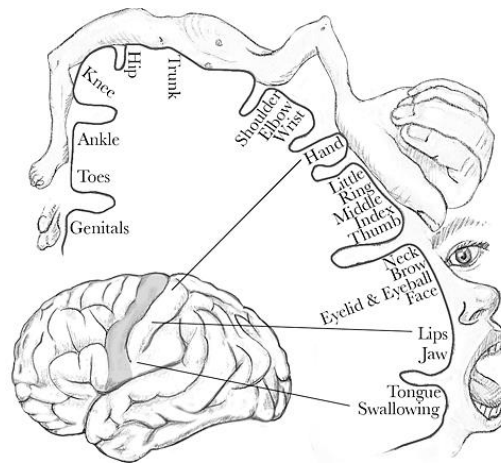


Figure.5.1. A map of the areas of the motor cortex that are dedicated to motor function. (image used with permission from <https://www.ebmconsult.com/articles/homunculus-sensory-motor-cortex>) [Accessed on 12 March 2020]

Along with this illustration, positioning of the TMS coil is based on external landmarks on the head and trial and error searching (Fang et al., 2019). Scientists also can use the EEG caps for guidance as certain electrode positions roughly correspond to areas of the arm (C₃ and C₄) or leg (C_z) areas. However, even a millimetre change in the location and orientation of the coil can impact greatly the amplitude of the resulting MEPs (Danner et al., 2008).

One way to test the reliability of MEPs is the intra-class correlation coefficient (ICC) (Bastani and Jaberzadeh, 2012). Bastani and Jaberzadeh (2012) concluded that 10 to 15 MEPs are required to obtain a good ICC reliability value. In this study the ICC analysis will be used to assess the reliability of the baseline measurements taken prior to IHT exposure.

In clinical and research applications it is important to ensure that TMS stimulation is accurate and reproducible. In this case specialised nTMS systems are available which track coil position related to head coordinates. However, these systems are very expensive and not all sites in the United Kingdom have access to such equipment resulting in some level of uncertainty when interpreting results. The nTMS system can also incorporate MRI brain scans allowing more precise targeting of areas of interest (Fang et al., 2019). More information is available in Chapter 4.

5.1.6. MEP waveform analysis

Following a TMS stimulus directed to the motor cortex recording of MEPs can be measured from the muscle belly of the target muscle by standard EMG equipment. After recording MEPs, the features of the waveform are analysed. Commonly studied features are: latency, peak-to-peak amplitude, absolute amplitude and the area under the rectified MEP. Changes in these measures can provide information about the integrity, conduction and excitability of the CST.

The latency measures the time it takes for the signal transduced to appear at the periphery and consists of the central and peripheral conduction time (Rotenberg, Horvath and Pascual-Leone, 2014). It is measured in milliseconds and is affected by nerve conduction velocities, height, muscle length and the conduction distance of the muscle from the cortex (Rotenberg, Horvath and Pascual-Leone, 2014). The peak-to-peak amplitude is calculated from the initial EMG peak to the next and measured in micro- or millivolts (Rotenberg, Horvath and Pascual-Leone, 2014). It provides information on the maximum voltage difference whereas the absolute amplitude of the MEP is quantified from the stimulus to the first positive or negative peak (Rotenberg, Horvath and Pascual-Leone, 2014). Lastly, the magnitude of an MEP can be also measured using the area under the curve (AUC) which takes into consideration the duration of the waveform (Rotenberg, Horvath and Pascual-Leone, 2014).

5.1.7. Corticospinal function in healthy subjects

Through analysis of features of the MEP waveforms, scientists can determine the integrity of the corticospinal descending tracts and the effects of an intervention such as IHT. Christiansen et al. (2018) were the first to present evidence on the effects of IHT on corticospinal function in healthy human subjects. The study used an IHT protocol that consisted of 15 cycles with alternating exposures of 1 min hypoxia ($FiO_2=0.09$) and 1 min normoxia ($FiO_2=0.21$) and studied the corticospinal function by measuring cortical and subcortical (cervicomedullary) MEPs and intracortical activity (ICF and SICI) in the FDI finger muscle. Cortical and subcortical MEPs were measured following a stimulus to the motor cortex and by electrically stimulating the

CST at the cervicomedullary level, respectively. MEP measurements were taken before IHT, immediately after and at 15, 30, 45, 60 and 75 min post-IHT.

The study reported an increase in MEP magnitude following IHT and the effects of IHT were considered to be subcortical because no change was observed in the magnitude of short-interval intracortical inhibition (SICI) and intracortical facilitation (ICF) circuits following IHT. Christiansen et al (2018) also noted that IHT has long lasting effects on CST excitability, reporting that in one subject it took 120 minutes for the MEP amplitude to return to baseline following IHT (Christiansen et al., 2018).

As the results suggested that the effects were likely a response to a spinal cord mechanism, the study proceeded with investigating the subcortical effects of IHT. They examined whether IHT influenced spike-timing dependent plasticity (STDP). STDP involves the combination of a TMS stimulus and a peripheral somatosensory stimulus that are delivered at different interstimulus intervals (Taylor and Martin, 2009; Müller-Dahlhaus, Ziemann and Classen, 2010). The simultaneous arrival of these evoked signals is capable in changing the excitability of the motor cortex. The results show that the MEP amplitude was significantly larger by 40% in STDP coupled with IHT between 30 and 45 min following the intervention, when compared with STDP coupled with sham intervention and IHT alone. Similar results were observed between 60 min and 75 min following the intervention. (Christiansen et al., 2018)

Based on the data by Christiansen et al. (2018), it seems likely that IHT's actions modulate corticospinal-motoneuronal synaptic plasticity with an effect that is at a subcortical level. Subcortical effects were studied using STDP and established that motor cortex excitability following IHT increased in a manner similarly to STDP and when combined produced a significantly higher increase in MEP amplitude. However, this change did not affect motoneuronal excitability directly (measured using F-wave amplitude and F-wave persistence) (Christiansen et al., 2018), leaving the precise mechanism of action unresolved.

5.1.8. Aims and objectives

This study's investigation will be focussed on examining the effect of IHT on lower limb MEP measures. This was achieved in healthy participants by examining the MEP peak-to-peak amplitude and area under the rectified MEP before, during and up to 30 minutes following IHT on healthy subjects. To ensure that the coil placement was accurate for each stimulation, a bespoke TMS navigation system was developed for the purpose of this experiment (see Chapter 4).

This is the first study to date investigating the effect of IHT on MEPs on the lower limb. The target muscle was the right tibialis anterior (TA R). Concurrently, several other muscles were stimulated too and these were: the right soleus (SOL R), left tibialis anterior (TA L) and right first dorsal interosseous (FDI) muscles. Studying the effects of IHT on lower limb muscles would provide information directly related to results on the effects of IHT on gait and postural control. In contrast, Christiansen et al (2018) studied the upper limb (FDI muscle) which is important for hand function and fine motor skills. Moreover, by simultaneously taking measurements from multiple muscles the study may provide information on general excitability changes affecting the cortex following IHT.

Christiansen et al.'s (2018) study on upper limb MEP measurements reported a significant and lasting increase in FDI MEP magnitude in healthy subjects following IHT. Consequently, the hypothesis is that if IHT induces plasticity in corticospinal pathways, it can be expected to produce a significant increase in the magnitude of lower limb MEP and thereby potentiate locomotor function in the leg. The null hypothesis being tested states that there will be no significant difference in peak-to-peak amplitude or AUC of the MEP waveform following IHT.

Compared to Christiansen et al. (2018) this study examined both the peak-to-peak amplitude of MEPs and AUC. AUC is believed to be a more effective measure of MEP magnitude because it captures the entire evoked potential waveform shape and duration.

The effects of IHT on MEP waveform analysis were examined statistically using a Welch ANOVA. A p-value of > 0.05 would denote no significant difference

in the results. The alternative hypothesis was that there would be a significant difference in the peak-to-peak amplitude and AUC of the MEP waveform following IHT with a p-value of <0.05 . The purpose of studying these muscles together was to investigate whether IHT caused a general change in MEP peak-to-peak amplitude and AUC. The three lower limb muscles (TA R, TA L and SOL R) studied have both contralateral and ipsilateral CST pathways and that the CST neurons for the lower limb lie more central and deeper in the brain compared to the FDI R muscle that has its contralateral and ipsilateral areas closer to the skull surface and lateral to the midline. This suggests that even though the double-cone coil used to activate the TA R muscle is less focal, than using another type of TMS coil, it is likely that it will have poor capability in activating the FDI R muscle based on the designated target TA R muscle.

In addition to direct measures of MEP amplitude, the success rate, described as a percentage of the total TMS stimulations that produced a MEP with a minimum amplitude of 0.05 millivolts (Groppa et al., 2012), will be quantified. The purpose of this was to observe whether following IHT there was a change in the overall excitability of the brain leading to an increase in the presence of MEPs not only in the target muscle, TA R, but also of the other muscles that were monitored (TA L, SOL R and FDI R). A change in stimulus success rate in these muscles would indicate a general mechanism operating across the entire motor system of the CNS.

5.1.9. Summary of findings

In this chapter the results show some interesting outcomes:

- 1) Despite the use of a navigated coil placement system (where the error in coil placement distance is < 0.8 mm and the error in the angling of the coil is below 0.8°) the MEP peak and trough of baseline measurements varied on average by 15% and 11%, respectively. With this peak and trough variability the MEP amplitude coefficient of variation ($(\text{standard deviation} / \text{mean}) * 100$) was reported to be 38% and MEP AUC coefficient of variation 35% in baseline measurements. These values were similar to what has been reported in the literature (Darling et al., 2006) and means that small changes in excitability are difficult to statistically identify within TMS studies of this type that look for time dependent changes in MEPs.

2) A significant increase in peak-to-peak amplitude and AUC was observed mainly following IHT when compared to baseline measurements in the target muscle (TA R) as well as in the SOL R and TA L muscles and this significant increase was apparent in individual responses and in grand averages.

3) For the target TA R muscle, 4 (IHT6, IHT11, IHT12 and IHT13) out of the 8 participants showed a significant increase in MEP amplitude with a percentage change of +121 % during and following IHT when compared with pre-IHT_{all}. Moreover, 3 of those participants (IHT6, IHT12 and IHT13) showed a significant increase in MEP AUC when comparing during IHT and post-IHT measurements with pre-IHT_{all} with a percentage change of +148%.

4) For TA L, 4 (IHT10, IHT11, IHT12 and IHT13) out of 7 participants that responded showed a significant increase in AUC with an average percentage change of +127% when comparing during and post-IHT measurements with pre-IHT_{all}. Out of these participants, 3 (IHT10, IHT12 and IHT13) also displayed a significant increase in peak-to-peak amplitude with an average percentage change of +103% when comparing during IHT and post-IHT with pre-IHT_{all}.5) For SOL R, a significant increase in peak-to-peak amplitude was observed between pre-IHT_{all} with post-IHT measurements and during IHT with post-IHT measurements in 1 participant (IHT10) (average percentage change of +36%). In contrast, in MEP AUC measurements, IHT12 showed a significant increase when comparing during IHT and post-IHT₂₀ with pre-IHT_{all} and the average percentage change was +83%. Moreover, participant IHT11 showed a significant increase in AUC when comparing post-IHT₂₀ and post-IHT₃₀ with during IHT and the percentage change was 362% and 179%, respectively.

6) IHT2 was the only participant that displayed a significant decrease in all three muscles (TA R, TA L and SOL R) for both MEP amplitude and MEP AUC when comparing baseline with post-IHT measurements. On average the percentage change was around -50% for both MEP measurements.

7) The grand average MEP measurements for TA R, TA L and SOL R muscles showed a significant increase between pre-IHT_{all} and post-IHT measurements in

both the MEP amplitude and MEP AUC. The percentage change in MEP AUC was +44% for TA R, +44% for TA L and +42% for SOL R. Compared to MEP AUC, a lower percentage change was observed in grand average MEP amplitude for TA R (+24%) whereas a higher percentage change was observed in the grand average MEP amplitude for TA L (+81%) and SOL R (+91%) the percentage.

8) Lastly, the results suggested that the effects of IHT were long lasting, as there was an increase in MEP amplitude and AUC up to the 30-minute MEP measurement post-IHT. However, results also suggest that perhaps in TA L and SOL R muscles, where the stimulation was not specifically targeting these muscles, the CST excitability returned back to baseline at post-IHT₃₀ suggesting some combination of effects.

Overall, these observations on the effects of IHT on MEPs measured from lower limb muscles, illustrated that potential benefits could be brought about in lower limb function within rehabilitation programmes incorporating IHT protocols.

5.2.Methodology

5.2.1. Subjects

Ethics approval was obtained from the departmental ethics committee of the University of Strathclyde. Eight healthy adults (5 men and 3 women; mean age, 27; range, 25 to 30 years) were recruited from staff and students of the University of Strathclyde. Exclusion criteria were described in Chapter 2 Section 2.2.1. Moreover, volunteers who had undergone orthopaedic surgery, had ferrous metal or implanted medical devices and/or tendon or ligament injury to the knee or ankle were excluded from the study. Please refer to Appendix.I.1) Activity and Health Questionnaire.

5.2.2. Experimental design

The study consists of participants attending two sessions. In the first session the volunteers were asked to read through the information sheet, provide written consent and lastly, perform a hypoxia test. If the participant consented and performed well in the hypoxia test they were booked for the second session (the TMS experiment with IHT), a week later. The aim was to record MEPs in the target muscle (TA R)

before, during and following IHT. EMG electrodes were also placed on SOL R, TA L and FDI R to enable monitoring of any general trends in MEPs in muscles simultaneously with those evoked on the target TA R muscle.

In the second session, measurements of MEPs were taken twice prior IHT at 0 and 10 minutes (pre-IHT₀ and pre-IHT₁₀), once during IHT (around 20 minutes into the intervention) and thereafter every 10 minutes up to 30 minutes following IHT (post-IHT₁₀, post-IHT₂₀ and post-IHT₃₀) (please refer to Figure.5.2). For the IHT protocol please refer to Chapter 2 Section 2.2.2. During IHT measurements of heart rate and saturation of oxygen were taken to monitor the safety of the intervention.

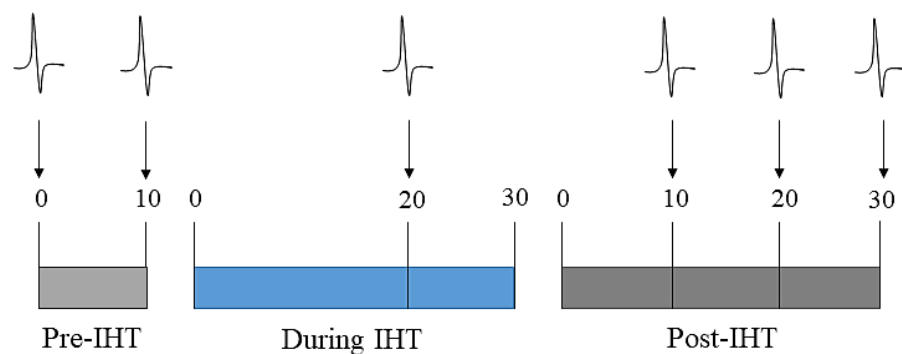


Figure.5.2. This diagram provides the timeline of the second experimental session. The experiment is divided into 3 blocks: pre-IHT, during IHT and post-IHT. MEP measurements were taken pre-IHT (at 0 and 10 minutes), during IHT (20 minutes into the intervention) and post-IHT (at 10, 20 and 30 minutes).

TMS was used to stimulate the CST. This is a non-invasive and painless stimulation protocol that measures the excitability of this motor pathway based on MEP recordings in related muscles. Single pulses of TMS were delivered using a copper double-cone coil insulated with plastic (Magstim double cone coil). The TMS coil was placed over the motor cortex area and following a stimulus the resulting EMG waveform (MEP) recorded using Spike2 software.

In this study the right tibialis anterior (TA R) muscle was targeted by TMS. The activity of the muscle following the stimulus was recorded using a standard EMG protocol (the high pass filter was set at 30 Hz and a low pass filter at 1000 Hz and the data were sampled at 2 kHz) (Christiansen et al., 2018). In Figure.5.3 the experimenter has centred the double-cone coil over the motor cortex to activate the TA R muscle. Markers on the coil and on the participant's forehead are placed for the nTMS system, described in the previous chapter (Chapter 4), and used to ensure reproducible coil placement once the stimulation site ('hotspot') has been identified.



Figure.5.3. Experimental set-up where the participant is given IHT. Please note the grey reflective markers on the participant's forehead and on the double-cone coil. These clusters of markers are detected by motion capture cameras as objects and are used to aid the experimenter with coil placement.

5.2.3. Transcranial magnetic stimulation (TMS)

5.2.3.1. Double-cone coil

The cortical areas projecting to and innervating the spinal segments that supply the lower limb are located around 3 cm in depth from the scalp and with the fields generated by this coil there are multiple muscles co-activated by the stimulus (Deng, Lisanby and Peterchev, 2013; Terao and Ugawa, 2002).

5.2.3.2. Stimulation ‘hotspot’

Prior to the IHT intervention, the ‘hotspot’ was located for the activation of the TA R muscle. The ‘hotspot’ was determined as the site where the TMS coil produces the highest amplitude of MEPs at the lowest stimulation intensity (Klomjai et al., 2015; Rossini et al., 1994). Subsequently, a sequence of pulses is generated in order to determine the sites stimulation threshold. The lowest intensity stimulus capable of generating at least 10 MEPs > 50 μ V out of the sequence of 20 stimuli was defined as threshold for the target muscle. The coil placement and orientation, where the ‘hotspot’ was identified, was saved as a template using the navigation system and during stimulation the experimenter manually matched the coil to the template in real time. Please refer to Chapter 4 Section 4.2 for the methodology of the manual navigated placement of the TMS coil.

5.2.3.3. Stimulation intensity

The intensity of the stimulus used in the experiment was at 120% of the resting MEP threshold, and a series 20 single TMS pulses to the target area were given using a 10 second interstimulus interval (Rotenberg, Horvath and Pascual-Leone, 2014; Bastani and Jaberzadeh, 2012). TMS stimulations were given at the same intensities pre-IHT (at 0 and 10 minutes), during IHT (20 minutes into the intervention) and post-IHT (at 10, 20 and 30 minutes).

5.2.4. Electromyography (EMG)

5.2.4.1. Skin preparation

Prior to fixing EMG electrodes, the skin needs to be prepared. A hypoallergic abrasive gel (Nuprep, Weaver) and alcohol wipes were used to remove surface dead skin cells and any oils on the skin at the recording site. This is an important step to ensure good electrode-skin contact and to lessen artefacts during recording. Skin preparation is a standard procedure that has already been mentioned in previous chapters of this report.

5.2.4.2. EMG setup

Following skin preparation, pre-gelled passive disposable silver/silver chloride electrodes were placed on the skin with respect to the direction of the muscle fibres and with an inter-electrode distance of 20 mm from the centre of one electrode to the other (Tang et al., 2018). Careful placement of the electrodes helps to minimise nearby muscle crosstalk (Merletti, 1999) and palpation of the different muscles helped achieve site selection.

For the TA muscle, the bipolar electrodes were placed 1/3 between the head of the fibula and head of the medial malleolus, at the muscle belly (Kujirai et al., 1992). For the SOL muscle, the electrode was placed 2/3 between the medial condyle of the femur and the medial malleolus (SENIAM, 2021). The ground electrode for the lower limb recordings was placed over electrical inactive tissue, the patella (SENIAM, 2021) and conductive gel was used for better electrode-skin contact. For the FDI muscle the EMG electrodes were placed between the thumb and index finger and the ground electrode was placed on an inactive bony prominence, the interphalangeal joint of the thumb (Tang et al., 2018).

5.2.4.3. Maximum voluntary contraction

Following the placement of the electrodes the maximum voluntary contraction was recorded for each muscle to ensure that there was no clipping of the EMG data during recording. Clipping occurs when the signal saturates the limits of the amplitude used for capturing the EMG waveforms and care is needed in experiments like this where MEPs are recorded repeatedly over time so not to compromise data accuracy.

5.2.4.4. Motor evoked potentials (MEPs)

MEPs were recorded in a relaxed state following single TMS pulses. EMG electrodes pick-up the summation of action potentials from the multiple motor units recruited to generate an MEP (Rotenberg, Horvath and Pascual-Leone, 2014). The resulting MEP waveform and the time of the stimulus trigger are recorded in the Spike2 software.

5.2.5. Signal processing: MEPs

The results relating to the data for the TA R muscle were used as the basis for not only the analysis of the muscle behaviour but also that of the other muscles where MEPs were recorded from. Accordingly, any TMS stimulations that did not create an MEP in TA R muscle were disregarded from data statistics even if a response or not was present in other muscles. In addition, as the first stimulations usually create abnormally large MEP waveforms (Hashemirad et al., 2017), these MEPs were excluded, as were MEPs with prior EMG activity levels showing that the subject was not relaxed. The purpose of excluding some measurements was to decrease variability (Hashemirad et al., 2017). Moreover, of course, increasing the number of TMS stimulations will in turn increase reliability (Hashemirad et al., 2017; Bastani and Jaberzadeh, 2012), however, this must be balanced with respect to the continuing comfort of the subject, the duration of the experiment and the potential for TMS itself to evoke lasting excitability changes if high repetition rates are presented.

The analysis of the MEP waveform included: peak-to-peak amplitude and AUC. The peak-to-peak amplitude of the MEP was measured from the first max peak to the next minimum trough within the MEP. To measure the AUC, a full-wave rectification was used and the area was measured by taking the integral of the curve, determining the MEP duration, and was expressed as mV x ms (Rotenberg, Horvath and Pascual-Leone, 2014). The analysis was carried out by a script operated in Spike2. The data were then transferred to Matlab where it was normalised to the pre-IHT average (pre-IHT_{avg}) of the pre-IHT₀ and pre-IHT₁₀ measurements.

5.2.6. Analysis: MEPs

1) Variability of baseline MEP peaks and troughs (investigated only in the target muscle (TA R))

To evaluate the consistency of baseline MEPs following navigated TMS, the mean waveform of 10 to 20 MEPs were averaged and graphed along with the standard error of the mean (SEM). SEM provides the accuracy of a sample mean by measuring the variability from one sample to another. SEM is calculated by dividing the standard deviation with the square root of the sample size. Above each graph the percentage of

variability of the peak and trough is provided along with the navigation error. Please keep in mind that the navigation error is below 0.8 mm in distance and 0.8 degrees in rotation (the threshold of error was set prior the experiment). More about the navigation error calculation and the value displayed is provided in the previous chapter (Chapter 4).

In addition to the measurements of variability in the MEP waveform components, the analysis of coefficient of variability (CV) of MEP amplitude and MEP AUC was also performed. CV is measured by dividing the mean from the standard deviation. In this report CV is provided as a percentage. Measurements of CV for MEP amplitude and MEP AUC were provided to compare the results with others in the literature.

2) ICC analysis of baseline MEPs measurements (MEP amplitude and AUC)

Subsequently, the study investigated the peak-to-peak amplitude and the area under the rectified MEP which here is referred to as area under the curve (AUC). Primarily, the study design focussed on completing an ICC analysis of the baseline measurements of peak-to-peak amplitude and AUC for individuals.

There are different types of ICC analysis. To choose the appropriate ICC analysis the guidelines by Koo and Li (2016) were used. The ICC analysis chosen is the absolute agreement (or within subject reliability) as the baseline measurements were taken using the test-retest method (Koo and Li, 2016).

The ICC score ranges from 0 to 1 where excellent reliability is > 0.75 ; moderate to good reliability is $0.74-0.40$; and poor reliability is < 0.40 (Cacchio et al., 2011). Along with ICC, a two tailed t-test was also performed to investigate whether there is a significant difference between pre-IHT₀ and pre-IHT₁₀ baseline measurements and to validate pooling the pre-IHT measurements into one control dataset (referred to as pre-IHT_{all}). A p-value < 0.05 indicated a significant difference between the baseline measurements. It is important to mention that the small sample size can affect the results from ICC (Shoukri, Asyali and Donner, 2004) and two-tailed t-test.

3) Normal Distribution and statistics

TMS studies where changes over time are being investigated are limited to the amount of data that can be collected at set time points and by the inter-stimulus (max frequency 0.1 Hz). MEPs are inherently highly variable but to enhance the reliability, a navigated TMS system was used. Tests to examine the homogeneity of variance (Levene test) and the distribution of the dataset (Shapiro-Wilk test) were performed and showed that the datasets collected lacked homogeneity of variance due to sample size limitations. This problem is well known within the scientific community who accept that between 10 to 20 good MEPs per TMS stimulation block is considered adequate for statistical analysis (Groppa et al., 2012).

In the results section, normal distribution plots and measurements of mean, standard deviation and number of MEPs are provided. In terms of statistics, a Welch ANOVA was completed because the datasets lacked homogeneity of variances and had unequal sample sizes. If the p-value of the Welch ANOVA is < 0.05 , then the analysis proceeded with the Games-Howell post-hoc test which does not assume equal variance and sample sizes.

4) Data presentation

The data (mean MEP amplitude and mean AUC) are displayed using a boxplot to show the distribution together with the navigation error to highlight the accuracy of the coil placement. These graphs were completed for each individual (example (IHT13) given in the results section) and pooled for the grand average. Additionally, along with boxplots, a graph showing the mean \pm SD is provided for the grand average results.

Subsequently, significant comparisons (based on the Welch ANOVA along with the Games-Howell post-hoc test) between IHT stages (pre-, during and post-IHT), for each individual, are displayed on a grid. The grid illustrates, using upwards and downwards arrows, whether the comparisons, in peak-to-peak amplitude and AUC, between the IHT stages are significantly higher or lower than baseline.

Data processing and graphing was carried out in Matlab. The test on homogeneity of variance and the ANOVA statistical analysis was completed in SPSS.

The results from SPSS were then transferred to Matlab and added to the graphs to show a significant difference between MEP measurement comparisons. Please keep in mind that this analysis was completed on the entire dataset and on each individual participant. An example of an individual participant analysis will be shown in the results section (specifically participant with the code IHT13).

5) Success rate

The number of successful activations of the TA R, TA L, SOL R and FDI R muscles, that achieved an MEP amplitude (Groppa et al., 2012) were counted in each stimulation block. The success rate was thereafter calculated as the percentage of MEPs from the total number of TMS stimulations per block (Sihle-Wissel, Scholz and Cunitz, 2000). Graphs of success rate for each participant are provided. On this graph measurements of mean AUC and mean peak-to-peak amplitude were also provided in order to see if there is a pattern in the data gathered. The purpose of completing this analysis was to see whether IHT affected the excitability of the brain regions by increasing or decreasing the success rate of the target muscle together with other muscles that were recorded (Sihle-Wissel, Scholz and Cunitz, 2000). The graphs were completed in Excel.

5.2.9. Analysis: SpO₂ and heart rate

During the IHT session measurements of SpO₂ and heart rate were routinely monitored. The lowest SpO₂ value each participant reached, and the range of heart rate are reported in a table created in Excel.

5.3. Results

Before presenting the results on MEPs, the section will begin with the participant details, hypoxia test response, SpO₂ response and heart rate. The analysis will then proceed by presentation using results from a single participant (IHT13). Primarily, the analysis on baseline MEP peak and trough variability will be displayed only on the target muscle (TA R). After demonstrating the variability of baseline MEPs, the peak-to-peak amplitude analysis will be shown and successively, results on AUC. Please keep in mind that in the sections discussing the results for participant IHT13, results of other participants will be also be referenced. After introducing the

analysis on individual participants, the remaining results section will focus on the grand average measurements of peak-to-peak amplitude, primarily, and subsequently, AUC.

5.3.1. Participant details

The participants recruited for this study had a good tolerance to hypoxia (Table.5.1). During IHT, their SpO₂ levels reduced to around 83 % on average and their heart rate ranged between 52 to 81 bpm. These values are similar to the values reported in the SEP experiments presented in the previous chapter and what has been reported in the literature on iSCI patients (Trumbower et al., 2012).

Table.5.1. Participant details, hypoxia test, lowest SpO₂ and heart rate range

Participant	Sex	Age	Hypoxia Test Response	Lowest SpO ₂ (%)	Heart rate range (bpm)
IHT2	Male	30	Type II	Not available	Not available
IHT6	Female	27	Type II	68	59 to 87
IHT10	Male	25	Type III	86	67 to 85
IHT11	Male	26	Type II	75	66 to 87
IHT12	Female	26	Type II	83	59 to 80
IHT13	Male	26	Type II	91	56 to 74
IHT14	Male	26	Type II	92	54 to 69
IHT15	Female	26	Type II	89	67 to 83

5.3.2. Participant IHT13

To provide an illustration example of the results, the data for subject IHT13 are presented as a single case prior to the collection results from all participants for each of the measured MEP parameters (AUC and peak-to-peak amplitude).

5.3.2.1. Peak and trough variability in baseline measurements of the target muscle (TA R) in subject IHT13

Primarily, the study investigated the peak and trough variability of baseline MEP measurements (pre-IHT₀ and pre-IHT₁₀) for the target muscle (TA R) (Figure.5.4). With a navigation error of 10.5% for pre-IHT₀ and 14.5 % for pre-IHT₁₀ (this is a misalignment of the coil below the threshold which was set to 0.8), participant IHT13 has a peak MEP variability of 23.01 % and trough variability of 12.38% during

the pre-IHT₀ MEP measurement and a peak variability of 20.6 % and a trough variability of 16.12 % for the pre-IHT₁₀ MEP measurements (Figure.5.4). Moreover, measurements of peak variability across all the participants ranged from 7.86% to 23.01 % and trough variability from 4.41% to 16.30 % (please refer to Appendix.II.1)).

Table.5.2 states the average peak variability and trough variability between pre-IHT₀ and pre-IHT₁₀ and states the CV for MEP AUC and MEP amplitude. On average, using a navigated TMS system, and with the above percentages in peak and trough variability for the TA R target muscle, the CV for AUC was 35% and for MEP amplitude was 38%. Similar values have been reported in the literature (Darling et al, 2006).

This section highlights that with a coil position error below 0.8 mm in distance and 0.8 °in rotation there remains considerable variability in MEP responses exceeding 20% in some cases, that cannot be reduced further by improving stimulation conditions.

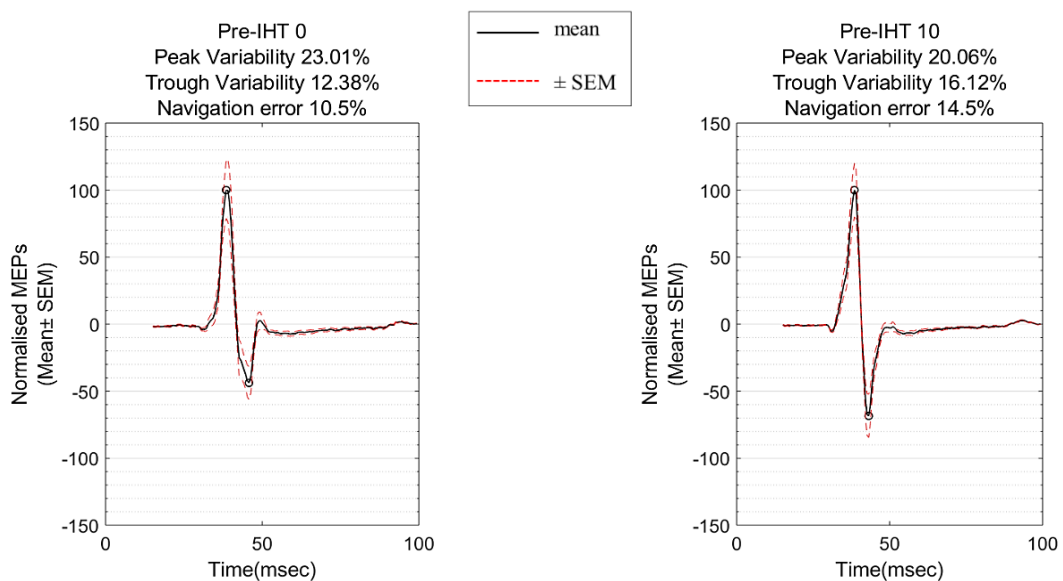


Figure.5.4. Participant IHT13 peak and trough variability of the MEP waveform (mean ± SEM) for pre-IHT₀ and pre-IHT₁₀. The measurements displayed are for TA R muscle. The red dotted lines represent the SEM and the black line represents the mean. The black circles highlight the peak maximum and minimum.

Table.5.2. Peak and trough variability along with MEP AUC and MEP amplitude CV

Participant	Peak variability (mean \pm SD) (%)	Trough variability (mean \pm SD) (%)	MEP AUC CV (%)	MEP amplitude CV (%)
IHT2	8.09 \pm 0.33	5.30 \pm 0.30	23	24
IHT6	20.97 \pm 3.69	10.79 \pm 2.86	45	42
IHT10	9.47 \pm 0.13	8.00 \pm 0.88	25	25
IHT11	17.27 \pm 6.55	14.21 \pm 1.82	23	41
IHT12	13.13 \pm 3.79	8.52 \pm 5.11	34	34
IHT13	21.54 \pm 2.09	14.25 \pm 2.64	63	62
IHT14	12.51 \pm 1.66	10.89 \pm 0.26	25	31
IHT15	15.93 \pm 1.47	16.16 \pm 0.21	43	40

Please note that the mean and standard deviation of the variability is for pre-IHT₀ and pre-IHT₁₀.

5.3.2.2. Reliability of pre-IHT peak-to-peak amplitude

Subsequently, the study investigated the peak-to-peak amplitude of the MEP waveform. This section demonstrates the reliability of the peak-to-peak amplitude baseline measurements for participant IHT13 (Figure.5.5). For pre-IHT peak-to-peak amplitude reliability analysis, participant IHT13 displayed an ICC value of 0.216 (confidence interval: -0.323 to 0.664). For IHT13 the reliability of the baseline measurements was poor since the ICC value was <0.40 , which again highlights the inherently high variability in sequential MEP measurements even at rest. ICC analysis of other participants ranged from either good (between 0.74 to 0.40) to poor (for results on other participants please refer to Appedix.II.2)).

However, accepting the reality of the intrinsic variability of the MEP responses and to increase the confidence in the baseline measures (pre-IHT₀ and pre-IHT₁₀), a two-tailed paired t-test between pre-IHT blocks was performed. As no significant difference was detected between the datasets the pre-IHT blocks were combined. Thus, for IHT13 post-IHT MEP data are statistically tested against the pooled pre-IHT data which is referred to as pre-IHT_{all}. This data pooling was also done for all subjects.

This analysis concludes that the variability while high is acceptable and comparable to studies in the literature (Malcolm et al., 2006) and by showing that there is no significant difference between pre-IHT₀ and pre-IHT₁₀ data blocks the baseline pooling helps to increase baseline data reliability, and the analysis can proceed with a statistical comparison of MEP peak-to-peak measurements prior, during and post-IHT.

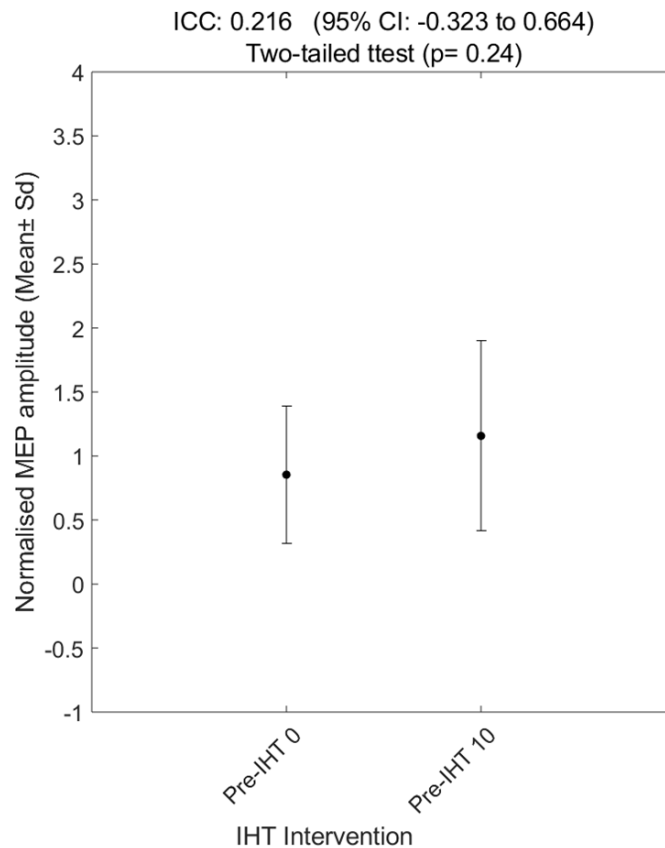


Figure.5.5. Normalised mean \pm SD of pre-IHT₀ and pre-IHT₁₀ peak-to-peak amplitude for participant IHT13. On top of the graph the ICC value and the 95% confidence interval is stated as well as the p-value from the two-tailed paired t-test. The ICC score ranges from 0 to 1 where excellent reliability is > 0.75 , moderate to good reliability is 0.74 to 0.40 and poor reliability is < 0.40 (Cacchio et al., 2011). If the p-value is < 0.05 then there is a significant difference in the two baseline datasets.

5.3.2.3. Peak-to-peak amplitude

The normal distribution graphs for TA R (Figure.5.6), TA L (Figure.5.7) and FDI R (Figure.5.8) show the amplitude distribution of each dataset block (pre-IHT₀, pre-IHT₁₀, during IHT, post-IHT₁₀, post-IHT₂₀ and post-IHT₃₀). The datasets shown here are from participant IHT13.

Looking at TA R the mean and standard deviation increases over the study time (Figure.5.6). The increase in the mean following IHT is clearly displayed in Figure.5.6 with a shift of the normal distribution curve moving towards the left and the staggered lines displaying the mean moving above the baseline (graphed using a red continuous line). This effect is present in measurements 10 minutes after IHT and up to the last

measurement taken 30 minutes following IHT (Figure.5.6). This suggests long lasting effects in excitability following the intervention. Similar results have been reported in studies using the IHT intervention on healthy subjects (Christiansen et al., 2018) and patients with iSCI (Trumbower et al., 2012). The same response as in the target muscle (TA R) is also observed in TA L (Figure.5.7).

In both TA R and TA L the number of stimulations analysed were ≥ 10 MEPs in each dataset distribution. FDI R was also activated following a stimulus directed to the TA R muscle but for this muscle the number of samples gathered were much lower than for TA R or TA L.

This was detected in many participants. Out of the 8 participants only 4 (IHT6, IHT10, IHT14 and IHT15) displayed a response in the FDI R muscle. However, the number of stimulations that created a response were few. The location in the motor cortex to activate the FDI R muscle difference in MEP success most likely reflects the difference in anatomical location of the individual muscle 'hotspot' but also may reflect on upper limb movement during the test periods.

Measurements for SOL R were not observed following TMS stimulation in this participant. Most likely this occurred because the threshold for the soleus muscle is much higher compared to the target muscle (TA R). Overall, activation of the SOL R, TA L and FDI R muscles that were recorded along with the target muscle (TA R) is likely and is dependent on individual differences. Out of 8 participants only participant IHT13 did not display a response in the SOL R muscle. Moreover, for the TA L muscle, out of 8 participants, only IHT15 did not show a response. (refer to Appendix.II.3)).

TAR

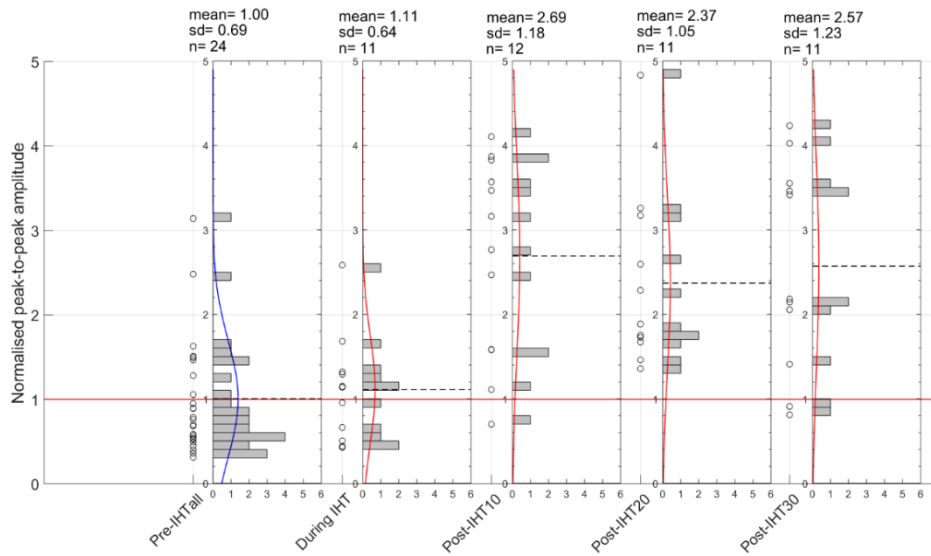


Figure.5.6. Normal distribution curve of MEPs peak-to-peak amplitude for TA R at pre, during and post-IHT. The main graph displays the data plotted using hollow circles. For each time point (pre-, during and post-IHT) a histogram is also plotted (bin width is 0.1). The dotted black line on the histogram highlights the mean. Above each histogram it lists the mean, standard deviation (SD) and the number of data gathered (n). Pre-IHT_{all} is the result of pooling together the pre-IHT₀ and pre-IHT₁₀ data. The normal distribution curve for this dataset is shown in blue so it is distinct from the other datasets. Lastly, the red line across all graphs shows the baseline. Datasets are normalised to pre-IHT_{avg}.

TAL

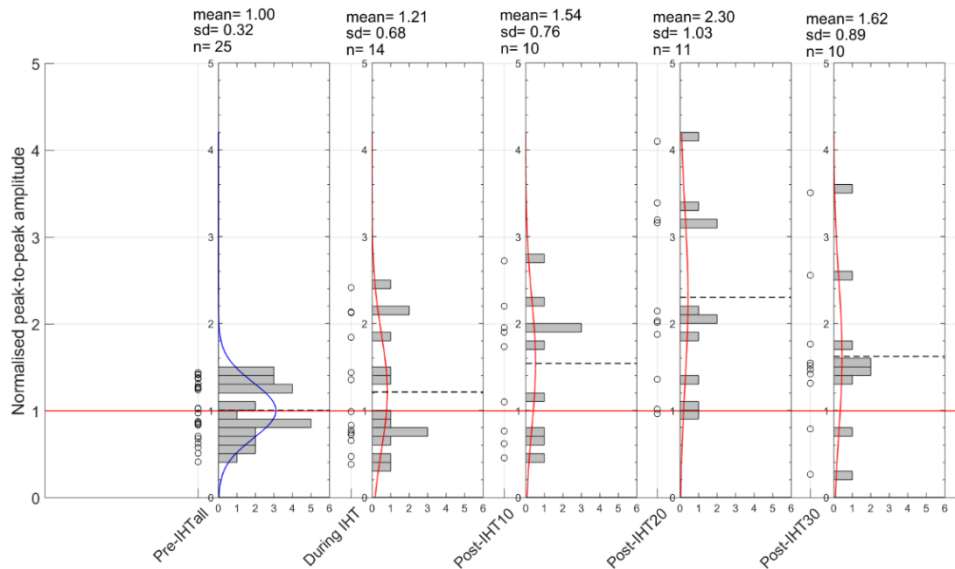


Figure.5.7. Normal distribution curve of MEPs peak-to-peak amplitude for TA L at pre, during and post-IHT. The main graph displays the data plotted using hollow circles. For each time point (pre-, during and post-IHT) a histogram is also plotted (bin width is 0.1). The dotted black line on the histogram highlights the mean. Above each histogram it lists the mean, standard deviation (SD) and the number of data gathered (n). Pre-IHT_{all} is the result of pooling together the pre-IHT₀ and pre-IHT₁₀ data. The normal distribution curve for this dataset is shown in blue so it is distinct from the other datasets. Lastly, the red line across all graphs shows the baseline. Datasets are normalised to pre-IHT_{avg}.

FDI R

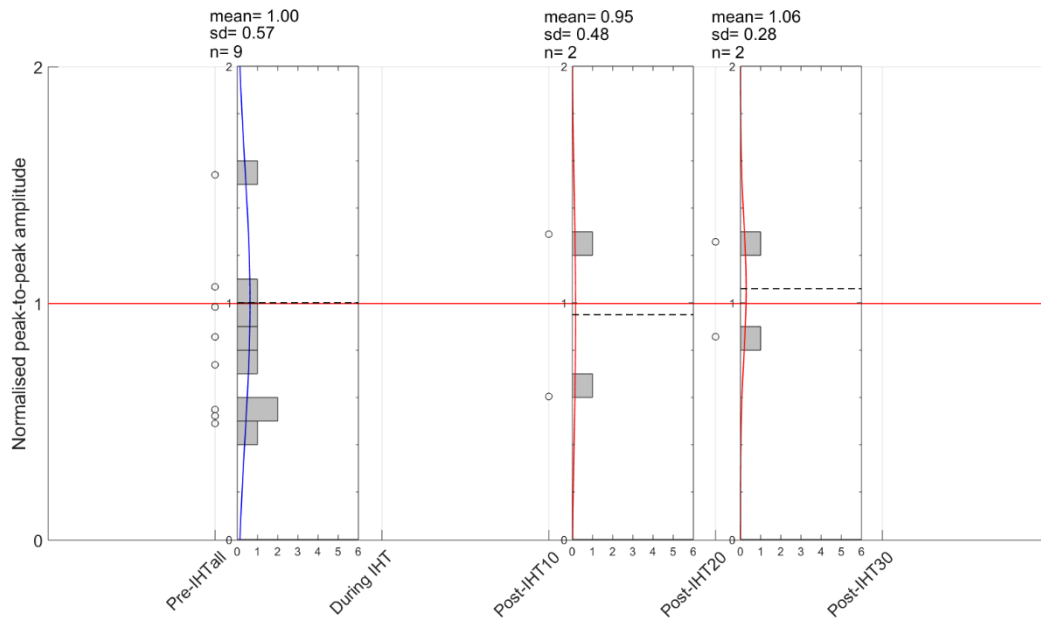


Figure.5.8. Normal distribution curve of MEPs peak-to-peak amplitude for FDI R at pre, during and post-IHT. The main graph displays the data plotted using hollow circles. For each time point (pre-, during and post-IHT) a histogram is also plotted (bin width is 0.1). The dotted black line on the histogram highlights the mean. Above each histogram it lists the mean, standard deviation (SD) and the number of data gathered (n). Pre-IHT_{all} is the result of pooling together the pre-IHT₀ and pre-IHT₁₀ data. The normal distribution curve for this dataset is shown in blue so it is distinct from the other datasets. Lastly, the red line across all graphs shows the baseline. Datasets are normalised to pre-IHT_{avg}.

As the dataset for IHT13, and for all the participants recruited in this study, lacked homogeneity of variance and the datasets have unequal sample sizes, a Welch ANOVA was chosen and this analysis was completed in all three muscles, (TA R, TA L, and FDI R). Please keep in mind that for this participant no MEPs were recorded on the SOL R muscle and most likely this occurred because the threshold for SOL is higher compared to the target muscle (TA R). For participant IHT13, a significant difference was present for TA R and TA L.

Figure.5.9 displays the MEP responses for pre- IHT, during and post-IHT in the TA R, TA L, SOL R and FDI R muscles. A significant increase post-IHT, for participant IHT13 is observed in TA R and TA L muscles. For the TA R muscle there is a significant increase in the mean peak-to-peak amplitude MEP measurement at post-IHT₁₀, post-IHT₂₀ and post-IHT₃₀ when compared to the pre-IHT_{all} data and the

percentage change is around + 169%, + 137% and + 157%, respectively (Figure.5.9). A significant increase in the MEP amplitude was also present when comparing during-IHT with post-IHT₁₀ (percentage change: + 142 %), post-IHT₂₀ (percentage change: + 114%) and post-IHT₃₀ (percentage change: + 132%) measurements (Figure.5.9). Furthermore, with an increase in the mean peak-to-peak amplitude there is also an apparent increase in the median following IHT (please refer to the TA R boxplot in Figure.5.9.A). This observation strongly suggests that the intervention was capable in enhancing the excitability of the CST.

Moreover, a similar increase in peak-to-peak MEP amplitude was observed in TA L muscle (Figure.5.9). A significant increase was observed between pre-IHT_{all} with post-IHT₂₀ (percentage change: +130%). Again, similar to TA R, the median also increases along with the mean following IHT, making the results more robust from a distribution perspective.

For participant IHT13, overall, the increase in MEP peak-to-peak amplitude following IHT is statistically present in both the TA R and TA L muscles. Moreover, looking at other individual responses in MEP amplitude, out of the 8 participants 3 (IHT2, IHT12 and IHT13) show a significant difference in both TA R and TA L muscles (Table.5.4; Table.5.5). From these participants, one (IHT2) shows a significant decrease. More on individual responses will be discussed in the next section.

Overall, IHT is capable in enhancing the excitability of the CST and from the results of IHT13 it seems that the effects last beyond the IHT intervention time and this prolonged enhanced excitability is also present in other participants (IHT6, IHT10 and IHT12). Moreover, as clearly observed in participant IHT13, and in other participants, this enhanced excitability is not restricted to single muscle pools thereby extend the observation made previously on the FDI muscle and reported by Christiansen et al (2018).

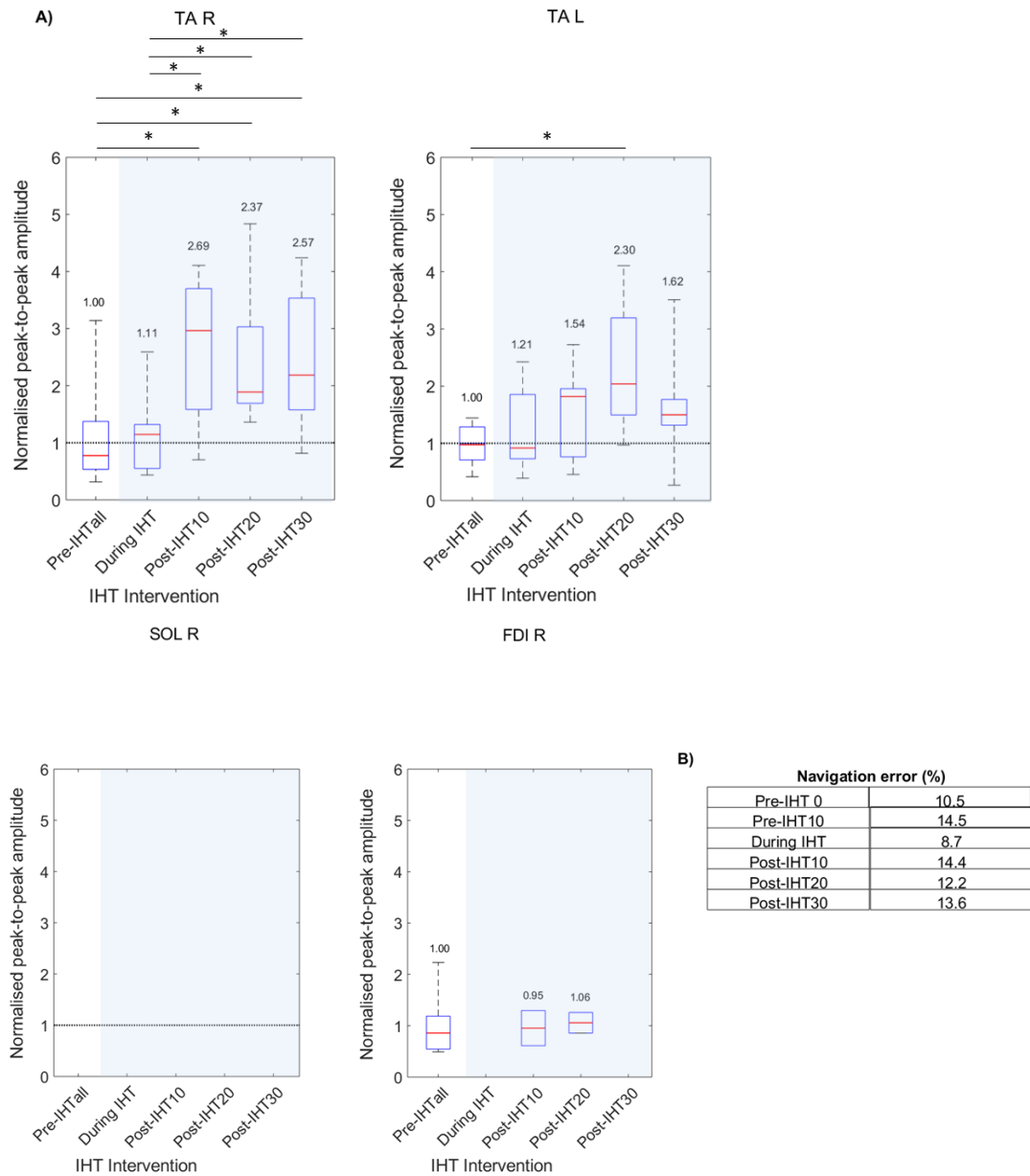


Figure.5.9. A) demonstrates the TA R, TA L, SOL and FDI normalised peak-to-peak amplitude distribution where the red line displays the median, the blue lines display the 25th and 75th percentiles and the whiskers show the minimum and maximum normalised peak-to-peak amplitude. Mean value is added on top of each boxplot. Welch ANOVA was used to examine if there is a significant difference in peak-to-peak amplitude over time ($p < 0.05$). The Games-Howell Post-hoc test was used to determine where the significant difference lies. Significant difference is displayed with an *. A blue shade on the plots highlights the time during and after IHT. B) table shows the navigation error during pre-, during and post-IHT.

5.3.2.4. Group responses: Peak-to-peak amplitude

Looking at group responses, for the target TA R muscle, 4 (IHT6, IHT11, IHT12 and IHT13) out of the 8 participants showed a significant increase in MEP amplitude with an average percentage change of +121% (Table.5.4) during and following IHT when compared with the pre-IHT_{all} measurement (Table.5.4).

A significant increase was also observed in TA L and SOL R muscles when comparing pre-IHT_{all} peak-to-peak amplitude with during IHT and post-IHT. For TA L a significant increase between pre-IHT with post-IHT measurements was observed in two (IHT12 and IHT13) out of 7 participants that showed a response in this muscle with an average percentage change of +140% (Table.5.5) and for SOL R a significant increase was observed in one participant (IHT10) out of 7 participants that showed a response in this muscle with a percentage change of +40% (Table.5.6).

It is interesting to mention that in one participant, IHT12, the TA R amplitude results show a significant decrease during IHT when compared to baseline measurements with an average percentage change of around -42% (Table.5.4). Moreover, a decrease at during IHT was also present in IHT10 in the TA L muscle when compared to pre-IHT_{all} (-38%).

Lastly, compared to other participants, IHT2, displayed a significant decrease in all three muscles (TA R, TA L and SOL R) when comparing pre-IHT_{all} and during measurements with post-IHT₂₀ and post-IHT₃₀ measurements. In this participant the MEP magnitude decreased following IHT and there was no apparent period of excitability change prior to this significant reduction (see boxplots in Appendix.II.3)). For participant IHT2 the pattern is the same in all muscles where there were enough responses (TA R, TA L and SOL R) to complete statistics. On average the percentage change when comparing pre-IHT_{all} measurements with post-IHT in IHT2 is -36% for the TA R muscle (Table.5.4), -57% for TA L (Table.5.5) and -58 % for SOL R (Table.5.6).

Apart from IHT2, all other responders show a significant increase in MEP peak-to-peak amplitude following IHT. This is not only apparent in the target muscle but in the other muscles where MEPs were monitored. Moreover, IHT seems to have a long lasting effect. In this study the effects are evident up to the post-IHT₃₀ measurement whereas Christiansen et al (2018), who investigated the duration of effect in one healthy subject reported it took 120 minutes before MEP magnitude returned to control values.

Table.5.3. Peak-to-peak amplitude Games-Howell post hoc results

TA R					
	pre-IHT _{all}	during IHT	post-IHT ₁₀	post-IHT ₂₀	post-IHT ₃₀
pre-IHT _{all}		↕↘	↗	↘↗	↘↗↗
during IHT			↗↗	↗↗	↗↗
post-IHT ₁₀					
post-IHT ₂₀					
post-IHT ₃₀					

TA L					
	pre-IHT _{all}	during IHT	post-IHT ₁₀	post-IHT ₂₀	post-IHT ₃₀
pre-IHT _{all}		↘		↘↗↗	
during IHT				↘↗	↘↗
post-IHT ₁₀				↘	↘
post-IHT ₂₀					↗
post-IHT ₃₀					

SOL R					
	pre-IHT _{all}	during IHT	post-IHT ₁₀	post-IHT ₂₀	post-IHT ₃₀
pre-IHT _{all}				↘	↘↗
during IHT				↘	↗
post-IHT ₁₀				↘	
post-IHT ₂₀					↗
post-IHT ₃₀					

Legend	
	IHT2
	IHT6
	IHT10
	IHT11
	IHT12
	IHT13
	IHT14
	IHT15

Please note that the results provided are comparisons of the left column with the horizontal column only. A significant increase is shown with an arrow up (↗) and a significant decrease with an arrow down (↘). A legend on the right allocates a color to each participant.

Table.5.4. TA R muscle significant individual responses (p-value and % change reported)

TA R				
Participant	Comparisons	Change (increase or decrease)	% Change	p-value
IHT2	pre-IHT _{all} with post-IHT ₂₀	↓	-38%	0.009
	pre-IHT _{all} with post-IHT ₃₀	↓	-34%	0.001
IHT6	pre-IHT _{all} with during IHT	↑	+99%	0.033
IHT11	pre-IHT _{all} with post-IHT ₃₀	↑	+75%	0.018
IHT12	pre-IHT _{all} with during IHT	↓	-42%	0.000
	during IHT with post-IHT ₁₀	↑	+79%	0.035
	during IHT with post-IHT ₂₀	↑	+107%	0.000
	during IHT with post-IHT ₃₀	↑	+128%	0.002
IHT13	pre-IHT _{all} with post-IHT ₁₀	↑	+169%	0.005
	pre-IHT _{all} with post-IHT ₂₀	↑	+130%	0.018
	pre-IHT _{all} with post-IHT ₃₀	↑	+157%	0.021
	during IHT with post-IHT ₁₀	↑	+142%	0.012
	during IHT with post-IHT ₂₀	↑	+114%	0.045
	during IHT with post-IHT ₃₀	↑	+132%	0.041

Please note that the comparisons with a significant decrease are highlighted in grey.

Table.5.5. TA L muscle significant individual responses (p-value and % change reported)

TA L				
Participant	Comparisons	Change (increase or decrease)	% Change	P- value
IHT2	pre-IHT _{all} with post-IHT ₂₀	↓	-58%	0.009
	during IHT with post-IHT ₂₀	↓	-68%	0.000
	during IHT with post-IHT ₃₀	↓	-45%	0.000
	post-IHT ₁₀ with post-IHT ₂₀	↓	-61%	0.012
	post-IHT ₂₀ with post-IHT ₃₀	↑	+71%	0.015
IHT10	pre-IHT _{all} with during IHT	↓	-38%	0.018
	during IHT with post-IHT ₃₀	↑	+73%	0.006
IHT12	pre-IHT _{all} with post-IHT ₂₀	↑	+150%	0.000
	during IHT with post-IHT ₂₀	↑	+160%	0.000
IHT13	pre-IHT _{all} with post-IHT ₂₀	↑	+130%	0.022
IHT14	post-IHT ₁₀ with post-IHT ₃₀	↓	-48%	0.011

Please note that the comparisons with a significant decrease are highlighted in grey.

Table.5.6. SOL R muscle significant individual responses (p-value and % change reported)

SOL R				
Participant	Comparisons	Change (increase or decrease)	% Change	p-value
IHT2	pre-IHTall with post-IHT20	↓	-64%	0.000
	pre-IHTall with post-IHT30	↓	-47%	0.000
	during IHT with post-IHT20	↓	-62%	0.016
	post-IHT10 with post-IHT20	↓	-56%	0.043
IHT10	pre-IHTall with post-IHT30	↑	+40%	0.019
	during IHT with post-IHT30	↑	+32%	0.023
	post-IHT20 with post-IHT30	↑	+67%	0.013

Please note that the comparisons with a significant decrease are highlighted in grey.

5.3.2.5. Reliability of pre-IHT AUC

Following the analysis of peak-to-peak amplitudes the study also examined measurements of the area under the rectified MEP. As with peak-to-peak amplitude, the study first looked at the reliability of baseline measurements using ICC (Figure.5.10).

For pre-IHT AUC reliability analysis, participant IHT13 violated the reliability model since the reliability statistics displayed a negative Cronbach's alpha. Cronbach's alpha measures the internal consistency (Figure.5.10). As already mentioned MEPs are variable and because AUC measurements take into account the duration of the MEP waveform and accordingly shows greater variability compared to peak-to-peak amplitude.

Subsequently, a two-tailed paired t-test was conducted to examine whether there is a significant difference in AUC between pre-IHT₀ and pre-IHT₁₀ (Figure.5.10). In participant IHT13 the results showed no significant difference between these pre-IHT control measurements and, as already mentioned in the MEP amplitude results section, the datasets were pooled.

The other participants displayed a range of ICCs with one showing good reliability (IHT15) but the majority showing poor reliability (IHT6, IHT10, IHT11, IHT12 and IHT14). Moreover, a significant difference between pre-IHT measurements

was seen in IHT6 (0.75 ± 0.39 ; 1.18 ± 0.45), IHT10 (1.10 ± 0.34 ; 0.85 ± 0.17) and IHT11 (0.84 ± 0.21 ; 1.16 ± 0.24) (pre-IHT₀; pre-IHT₁₀) (please refer to Appendix.II.2).

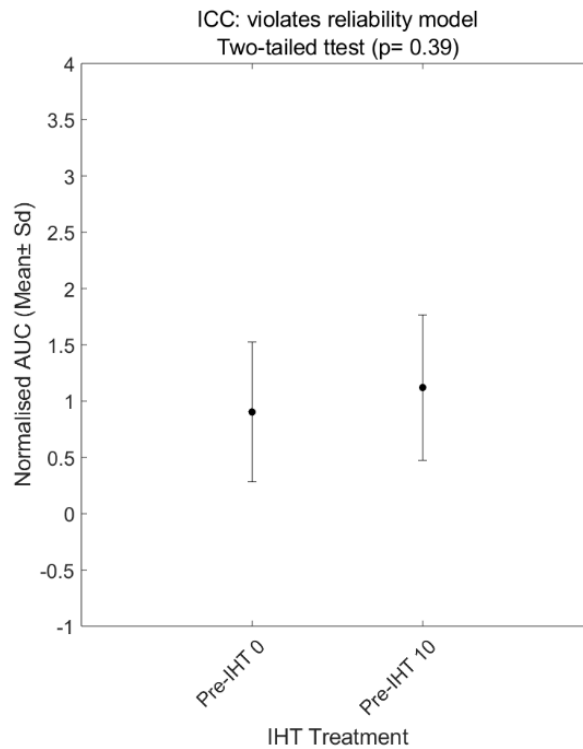


Figure.5.10. Normalised mean \pm SD of pre-IHT₀ and pre-IHT₁₀ AUC for participant IHT13. On top of the graph the ICC value and the 95% confidence interval is stated as well as the p-value from the two-tailed paired t-test. The ICC score ranges from 0 to 1 where excellent reliability is > 0.75 , moderate to good reliability is 0.74 to 0.40 and poor reliability is < 0.40 (Cacchio et al., 2011). If the p-value is < 0.05 then there is a significant difference in the two baseline datasets.

5.3.2.6. AUC

A histogram of the AUC measurements for participant IHT13 were graphed to show the distribution of the datasets for TA R (Figure.5.11.), TA L (Figure.5.12), and FDI R (Figure.5.13). As with MEP peak-to-peak amplitude, in the MEP rectified AUC there is a shift of the normal distribution curve towards the left in both TA R and TA L muscles. However, compared to TA R, in TA L muscle it appears that the MEP magnitude at pre-IHT₃₀ decreases and this may suggest that the MEP magnitude in this muscle slowly goes back to baseline levels.

TAR

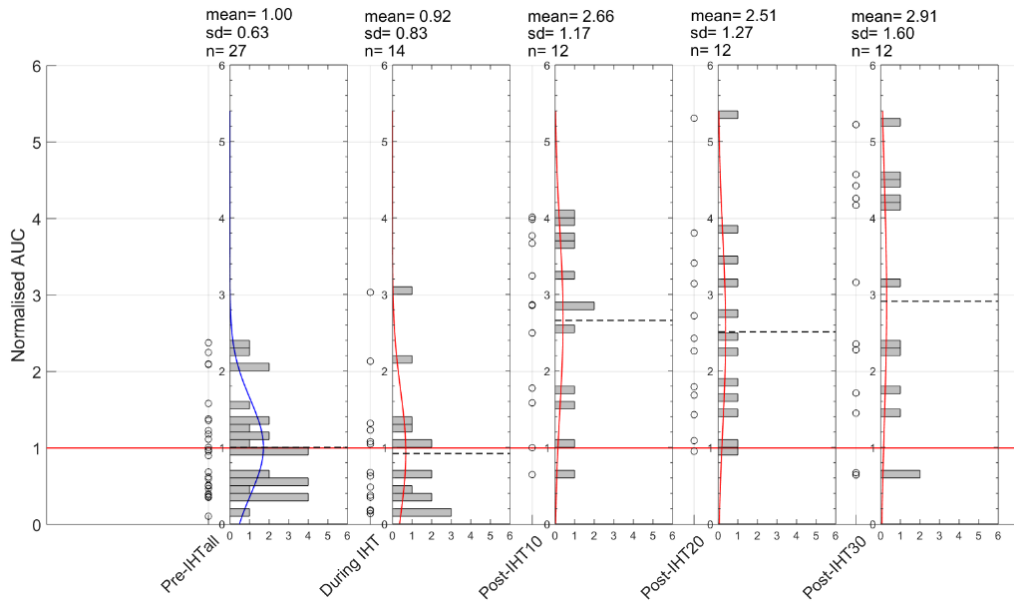


Figure.5.11. Normal distribution curve of MEPs AUC for TAR at pre, during and post-IHT. The main graph displays the data plotted using hollow circles. For each time point (pre-, during and post-IHT) a histogram is also plotted. The dotted black line on the histogram highlights the mean. Above each histogram it lists the mean, standard deviation (SD) and the number of data gathered (n). Pre-IHT_{all} is the result of pooling together the pre-IHT₀ and pre-IHT₁₀ data. The normal distribution curve for this dataset is shown in blue so it is distinct from the other datasets. Lastly, the red line across all graphs shows the baseline. Datasets are normalised to pre-IHT_{avg}.

TAL

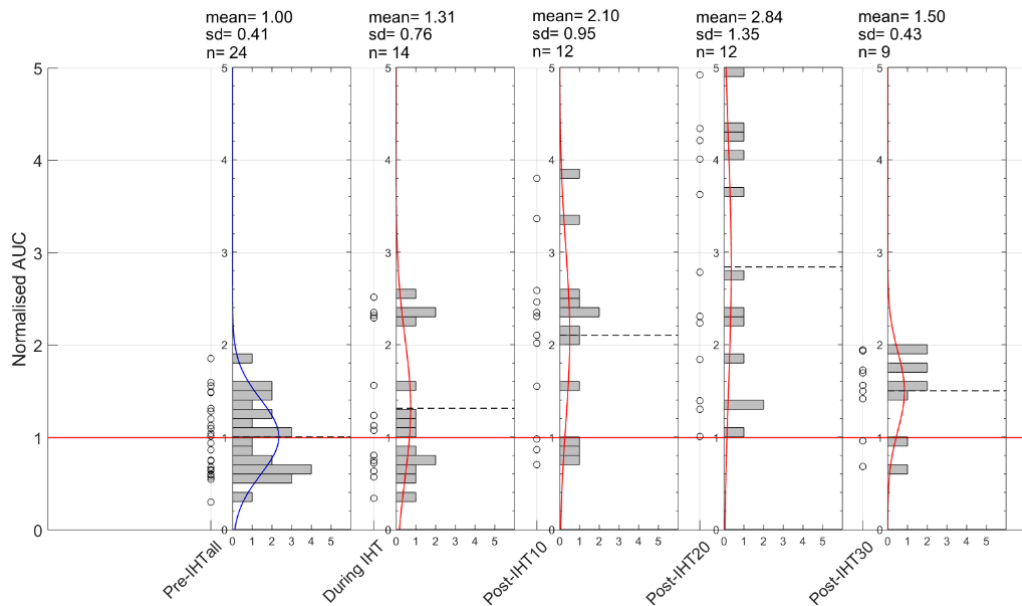


Figure.5.12. Normal distribution curve of MEPs AUC for TAL at pre, during and post-IHT. The main graph displays the data plotted using hollow circles. For each time point (pre-, during and post-IHT) a histogram is also plotted. The dotted black line on the histogram highlights the mean. Above each histogram it lists the mean, standard deviation (SD) and the number of data gathered (n). Pre-IHT_{all} is the result of pooling together the pre-IHT₀ and pre-IHT₁₀ data. The normal distribution curve for this dataset is shown in blue so it is distinct from the other datasets. Lastly, the red line across all graphs shows the baseline. Datasets are normalised to pre-IHT_{avg}.

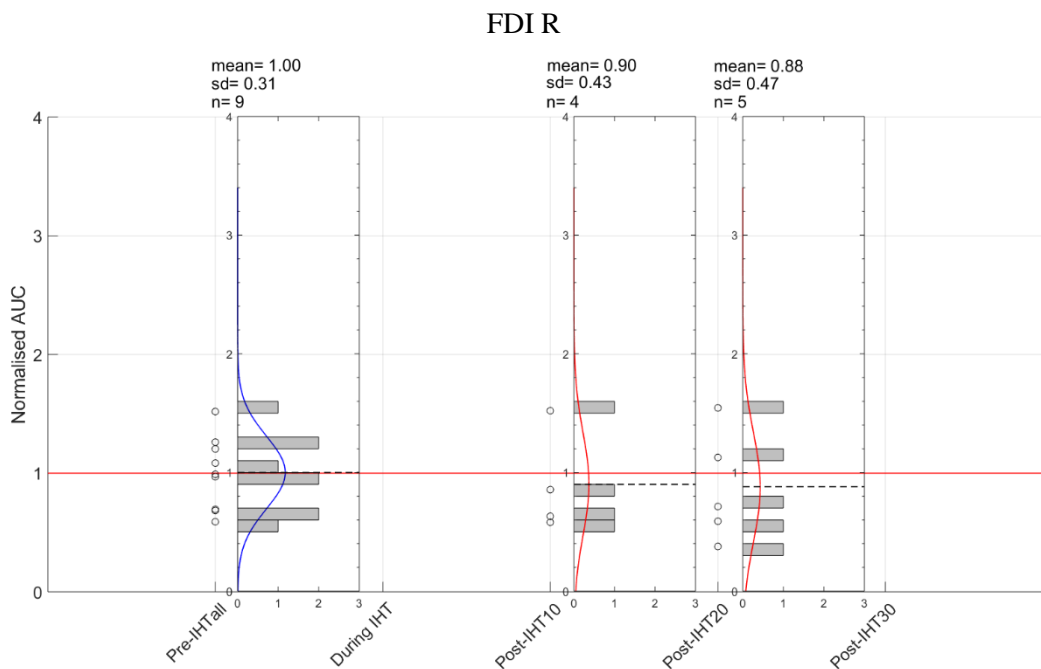
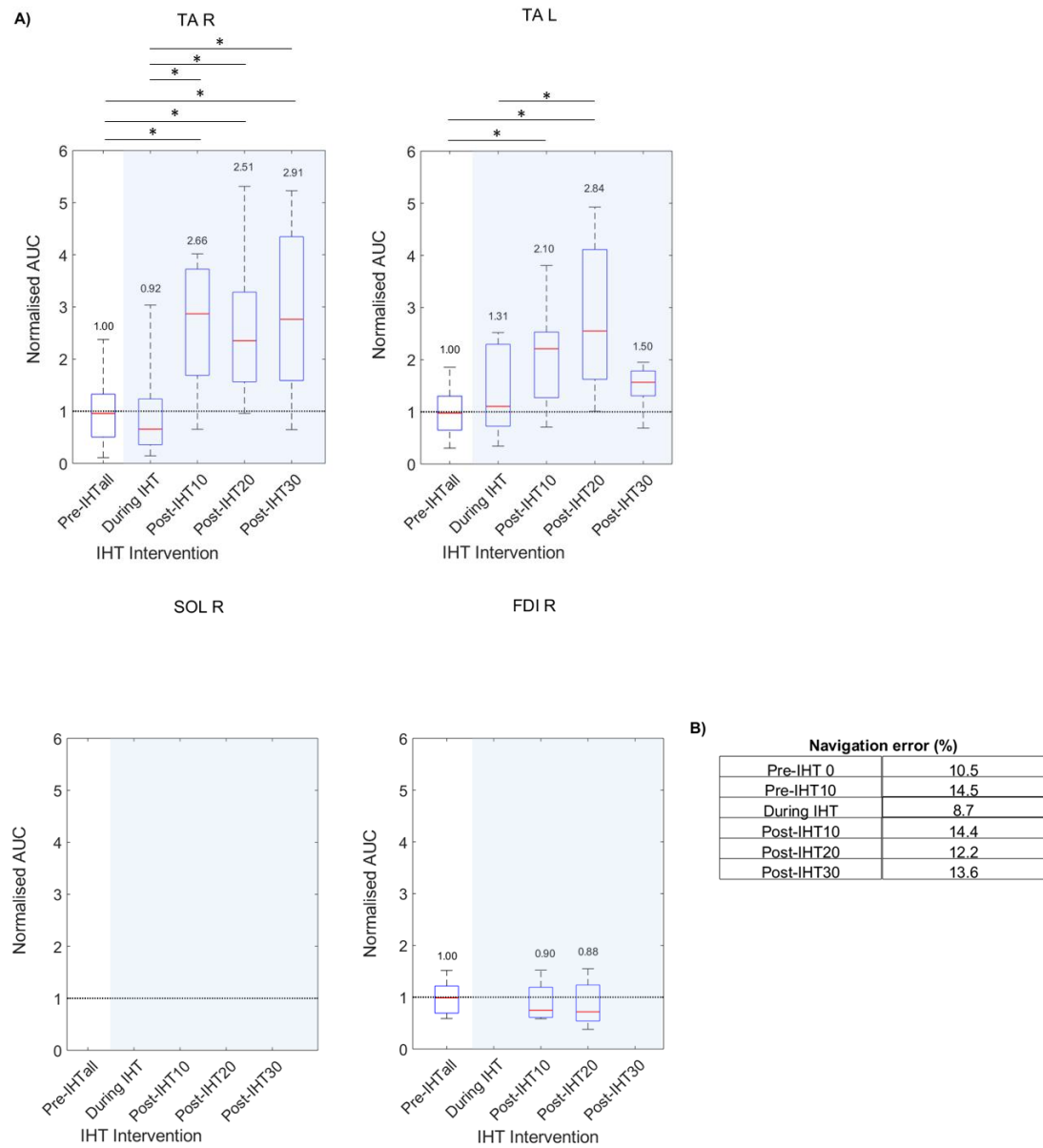


Figure.5.13. Normal distribution curve of MEPs AUC for FDI R at pre-, during and post-IHT. The main graph displays the data plotted using hollow circles. For each time point (pre-, during and post-IHT) a histogram is also plotted. The dotted black line on the histogram highlights the mean. Above each histogram it lists the mean, standard deviation (SD) and the number of data gathered (n). Pre-IHT_{all} is the result of pooling together the pre-IHT₀ and pre-IHT₁₀ data. The normal distribution curve for this dataset is shown in blue so it is distinct from the other datasets. Lastly, the red line across all graphs shows the baseline. Datasets are normalised to pre-IHT_{v_g}.

Figure.5.14 displays the AUC of the MEP waveform at pre-, during and post-IHT for the TA R, TA L, SOL R and FDI R muscles and the table (B) displays the percentage of the navigation error. Significant increase in AUC is observed in TA R muscle and TA L (please refer to Figure.5.14). Generally, a significant increase in MEP AUC is present in post-IHT measurements when compared to pre-IHT and during IHT measurements. As an average, the percentage change between pre-IHT MEP AUC measurements compared to post-IHT in TA R muscle is +169% (Figure.5.14; Table.8) and in the TA L muscle is +147% (Figure.5.14; Table.5.9). Also, as in the MEP amplitude measurements, the MEP AUC show an increase in both the mean and median following IHT.

In participant IHT13 there is a consistency in the results as a significant increase in MEP magnitude following IHT is present in both AUC and peak-to-peak amplitude measurements. Moreover, since this increase in MEP magnitude is present

in multiple muscles this suggests a strong indication that IHT changes the excitability of the CST.



*Figure.5.14. A) demonstrates the TA R, TA L, SOL and FDI normalised AUC distribution where the red line displays the median, the blue lines display the 25th and 75th percentiles and the whiskers show the minimum and maximum normalised AUC (n=9). Mean value is added on top of each box plot. Welch ANOVA was used to examine if there is a significant difference in AUC over time ($p < 0.05$). The Games-Howell Post-hoc test was used to determine where the significant difference lies. Significant difference is displayed with an *. A blue shade on the plots highlights the time during and after IHT. B) table shows the navigation error during pre-, during and post-IHT.*

5.3.2.7. Group responses: AUC

The tables below highlight the significant individual responses for TA R (Table.5.8), TA L (Table.5.9), SOL R (Table.5.10) and FDI R (Table.5.11). The same three participants (IHT6, IHT12 and IHT13) that showed a significant increase in peak-to-peak amplitude also show a significant increase in AUC at the target muscle (TA R), as expected. On average the percentage change between pre-IHT_{all} with post-IHT was +140% (Table.5.8) for MEP AUC whereas for MEP amplitude it was +121% (Table.5.4). Both measurements of MEP magnitude have a high percentage change and the effects last beyond the 30-minute intervention (Table.5.3; Table.5.4; Table.5.7; Table.5.8).

Similar to peak-to-peak amplitude measurements, AUC shows a significant increase in TA L and SOL R muscles. The significant increase in TA L AUC was seen between pre-IHT_{all} and post-IHT measurements and between during IHT and post-IHT measurements in 4 (IHT10, IHT11, IHT12 and IHT13) out of 7 participants that displayed a response in this muscle (Table.5.7, Table.5.9). Please keep in mind that out of these 4 participants, 2 (IHT12 and IHT13) also displayed a significant increase in peak-to-peak amplitude. The average percentage change in TA L muscle in MEP peak-to-peak measurements when comparing baseline with post-IHT was +140% (Table.5.5) and in MEP AUC is +128% (Table.5.9). Overall consistency in MEP amplitude and MEP AUC results of individual participants provide a strong indication that IHT is capable in enhancing the excitability of the CST.

For the SOL R muscle a significant increase in peak-to-peak amplitude between pre-IHT_{all} with post-IHT measurements and during IHT with post-IHT measurements was observed 1 participant (IHT10) with an average percentage change of +40% (Table.5.6). However, in this section where AUC was studied, only participant IHT12 showed a significant increase in MEP AUC between pre-IHT_{all} and post-IHT measurements, with an average percentage change of +87% (Table.5.10). Moreover, participant IHT11 showed a significant increase in AUC when comparing post-IHT₂₀ and post-IHT₃₀ with during IHT and the percentage change was 362% and 179%, respectively.

Lastly, when investigating peak-to-peak amplitudes in the previous section, a significant decrease was observed between pre-IHT_{all} and post-IHT measurements in one participant (IHT2). MEP AUC measurements also show a significant decrease when comparing pre-IHT_{all} with post-IHT measurements (Table.5.7) and this effect is present in all three lower limb muscles (TA R, TA L and SOL R). This decrease in MEP AUC occurs after the intervention and becomes significant after 30 minutes following the intervention. The percentage change in TA R following IHT is -32% (Table.5.8), in TA L is -64% (Table.5.9) and SOL R is -44% (Table.5.10). This is the only participant that showed this response and the results do not suggest that this significant decrease is rebound to an initial excitability rise at any stage post-IHT. Rather, it showed a reduction in MEP amplitude over time (to see the boxplot please refer to Appendix.II.4)).

Overall, in both MEP amplitude and MEP AUC it seems that there is a rise in excitability that lasts for at least 30 minutes in most subjects but there are exceptions (IHT11 and IHT14 in the TA L muscle). In these participants, the reduction in MEP magnitude followed soon after a period of excitability in the TA L muscle. In participant IHT11 a significant decrease in the TA L is present between post-IHT₁₀ and post-IHT₂₀ with a percentage change of -53% and in participant IHT14 between post-IHT₁₀ and post-IHT₃₀ with a percentage change of -47% (see Appendix.II.4); Table.5.7; Table.5.9). Please keep in mind that in IHT11 this significant decrease was not present in MEP amplitude while a significant decrease in IHT14 between post-IHT₁₀ and post-IHT₃₀ was also present in MEP amplitude with a percentage change of -48% (Table.5.3).

Table.5.7. AUC Games-Howell post hoc results

T A R					
	pre-IHT _{all}	during IHT	post-IHT ₁₀	post-IHT ₂₀	post-IHT ₃₀
pre-IHT _{all}			↑	↑↑	↓↑
during IHT			↑	↓↑↑	↑↑
post-IHT ₁₀					
post-IHT ₂₀					
post-IHT ₃₀					

T A L					
	pre-IHT _{all}	during IHT	post-IHT ₁₀	post-IHT ₂₀	post-IHT ₃₀
pre-IHT _{all}			↑↑↑	↑↑	↓↑
during IHT			↑		↑
post-IHT ₁₀				↓	↓
post-IHT ₂₀					
post-IHT ₃₀					

S O L R					
	pre-IHT _{all}	during IHT	post-IHT ₁₀	post-IHT ₂₀	post-IHT ₃₀
pre-IHT _{all}				↑	↓
during IHT				↑↑	↑
post-IHT ₁₀				↑	↓
post-IHT ₂₀					↑
post-IHT ₃₀					

F D I R					
	pre-IHT _{all}	during IHT	post-IHT ₁₀	post-IHT ₂₀	post-IHT ₃₀
pre-IHT _{all}					
during IHT					↓
post-IHT ₁₀					
post-IHT ₂₀					
post-IHT ₃₀					

Legend	
↑	IHT2
↑	IHT6
↑	IHT10
↑	IHT11
↑	IHT12
↑	IHT13
↑	IHT14
↑	IHT15

Please note that the results provided are comparisons of the left column with the horizontal column only. A significant increase is shown with an arrow up (↑) and a significant decrease with an arrow down (↓). A legend on the right allocates a color to each participant.

Table.5.8. TA R muscle significant individual responses (p-value and % change reported)

TA R				
Participant	Comparisons	Change (increase or decrease)	% Change	p-value
IHT2	pre-IHTall with post-IHT30	↓	-32%	0.004
IHT6	during IHT with post-IHT20	↓	-58%	0.031
IHT12	pre-IHTall with post-IHT20	↑	+53%	0.008
	during IHT with post-IHT20	↑	+94%	0.000
	during IHT with post-IHT30	↑	+101%	0.017
IHT13	pre-IHTall with post-IHT10	↑	+166%	0.005
	pre-IHTall with post-IHT20	↑	+151%	0.021
	pre-IHTall with post-IHT30	↑	+191%	0.020
	during IHT with post-IHT10	↑	+189%	0.005
	during IHT with post-IHT20	↑	+173%	0.021
	during IHT with post-IHT30	↑	+216%	0.018

Please note that the comparisons with a significant decrease are highlighted in grey.

Table.5.9. TA L muscle significant individual responses (p-value and % change reported)

TA L				
Participant	Comparisons	Change (increase or decrease)	% Change	p-value
IHT2	pre-IHTall with post-IHT30	↓	-64%	0.032
IHT10	pre-IHTall with post-IHT30	↑	+79%	0.029
	during IHT with post-IHT30	↑	+118%	0.003
IHT11	pre-IHTall with post-IHT10	↑	+69%	0.026
	during IHT with post-IHT10	↑	+141%	0.003
	post-IHT10 with post-IHT20	↓	-53%	0.003
IHT12	pre-IHTall with post-IHT20	↑	+198%	0.000
IHT13	pre-IHTall with post-IHT10	↑	+110%	0.027
	pre-IHTall with post-IHT20	↑	+184%	0.008
	during IHT with post-IHT20	↑	+117%	0.037
IHT14	post-IHT10 with post-IHT30	↓	-47%	0.013

Table.5.10. SOL R muscle significant individual responses (p-value and % change reported)

SOL R				
Participant	Comparisons	Change (increase or decrease)	% Change	p-value
IHT2	pre-IHTall with post-IHT30	↓	-44%	0.003
	post-IHT10 with post-IHT30	↓	-60%	0.002
IHT10	post-IHT10 with post-IHT30	↑	+44%	0.000
IHT11	during IHT with post-IHT20	↑	+362%	0.002
	during IHT with post-IHT30	↑	+179%	0.004
IHT12	pre-IHTall with post-IHT20	↑	+87%	0.003
	during IHT with post-IHT20	↑	+93%	0.003
	post-IHT10 with post-IHT20	↑	+65%	0.014

Table.5.11. FDI R muscle significant individual responses (p-value and % change reported)

FDI R				
Participant	Comparisons	Change (increase or decrease)	% Change	p-value
IHT11	during IHT with post-IHT30	↓	-55%	0.005

5.3.3. Grand average of all subjects

This section will focus on the combined grand average analysis of the peak-to-peak amplitude and AUC measurements from the sample group studied.

5.3.3.1. Peak-to-peak amplitude

Following individual analysis, the study proceeded to consider the data as a whole, by calculating the grand average MEP peak-to-peak responses to IHT. The peak-to-peak amplitude measurements from the MEP waveform were graphed and a histogram displays the amplitude frequency distribution for the TA R (Figure.5.15), TA L (Figure.5.16), SOL R (Figure.5.17) and FDI R (Figure.5.18). Following these graphs, Figure.5.19 and Figure.5.20 further summarise the change in population averages presenting the grand average in MEP amplitude at different time points following the IHT intervention for each of the muscles (TA R, SOL R, TA L and FDI

R) and incorporated the results of the Games-Howell post-hoc test showing where the significant differences exist.

With a navigation error below 0.8 mm in distance and 0.8 ° in rotation the results from TA R, TA L and SOL R display a significant increase in peak-to-peak amplitude between pre-IHT and post-IHT measurements. This is clear when looking at the staggered line (displaying the mean) in the normal distribution graphs (Figure.5.15; Figure.5.16; Figure.5.17). The mean increases above the baseline following IHT in TA R, TA L and SOL R. These results follow the pattern of the IHT intervention responders, which are around half of the participants recruited (Table.5.3). It is worth mentioning here that a hypothetical BDNF pathway is involved with the IHT intervention and, as already discussed in the literature review, there is a mutation in 25% of the population in the BDNF gene that reduces the potential for regeneration of neuronal pathways (Duman et al., 2016).

Looking back at individual participant measurements, this increase in MEP magnitude was apparent (with a significant difference) in 4 (IHT6, IHT11, IHT12 and IHT13) out of the 8 participants in the TA R muscle (Table.5.3). In the grand average MEP amplitude measurements for the TA R muscle the percentage change between pre-IHT_{all} with post-IHT measurements is +27 % and the percentage change (as an average) among participants (reported in the section above) was +121 % (Table.5.12; Figure.5.19; Figure.5.20). Moreover, in both the grand average and individual results the effects of the IHT intervention in the TA R muscle seem to be long lasting. This is also reported by other studies looking at this IHT intervention protocol (Christiansen et al., 2018; Trumbower et al, 2012). Similarly, to TA R, a significant increase was observed between pre-IHT_{all} and post-IHT₂₀ in TA L and SOL R muscles with a percentage change of +81 % and +93%, respectively. Moreover, in individual responses two (IHT12 and IHT13) out of 7 participants that showed a response in the TA L muscle with an average percentage change of +140% (Table.5.5) and one participant (IHT10) out of 7 participants that showed a response in the SOL R muscle with a percentage change of +40% (Table.5.6).

In contrast to TA R, the MEP magnitude of TA L and SOL R muscles drop at post-IHT₃₀ and this drop is significant between post-IHT₂₀ and post-IHT₃₀ for both muscles with a percentage change of -38% for TA L and -40% in SOL R (Figure.5.20; Figure.5.21; Table.5.12). Additionally, the pattern in the mean MEP amplitude observed in TA L and SOL R muscle is also present when looking at the median (Figure.5.19). The results strongly suggest that the MEP magnitude has returned back or close to baseline measurements. Also, looking back to individual responses this decrease in excitation was significant only in participant IHT14 in the TA L muscle between post-IHT₁₀ and post-IHT₃₀ (Table.5.5). This decrease in MEP amplitude in the SOL R and TA L muscles could be as a result of a combination of factors. It could be related from TA R's Ia inhibitory interneurons projecting to SOL R or crosstalk reflexes to TA L. Moreover, it could also result from TMS stimulation as it has the ability to modulate intercortical neuronal activity.

Overall, it seemed that in the targeted muscle there was an increase in the MEP amplitude up to the last measurement taken at post-IHT₃₀ but this was not the case in the other muscles recorded (TA L and SOL R). However, there is a distinct increase in MEP amplitude following IHT in individual results and the grand averages in the TA R, TA L and SOL R muscles and these results strongly indicate that IHT has the capacity to change the excitability of the CST. The percentage change as an average in peak-to-peak amplitude MEP response is around +56% (Table.5.12). Nevertheless, a sham experiment is important to confirm these results. Unfortunately, as a result of COVID this set of experiments could not be completed.

TAR

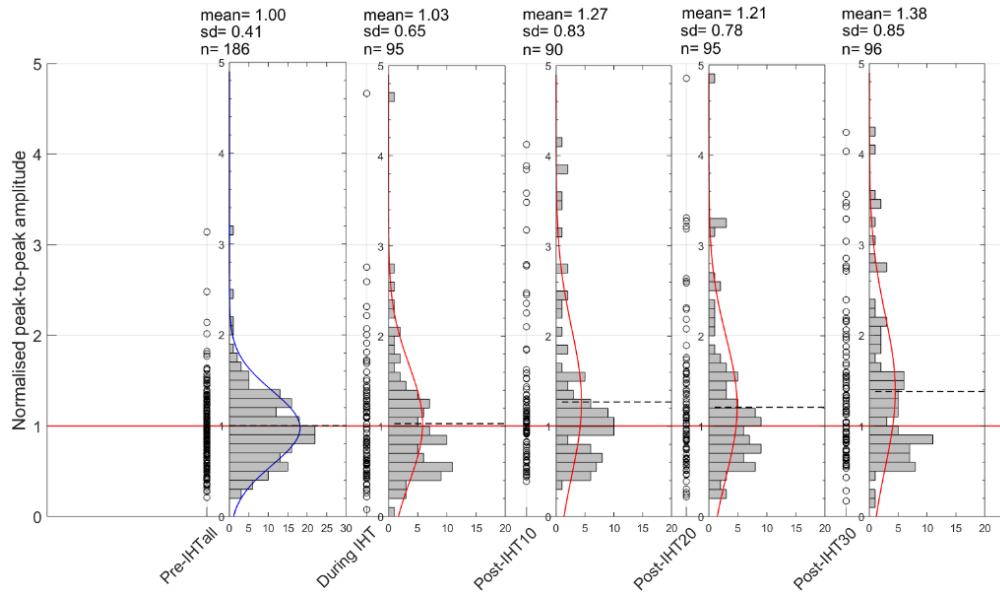


Figure.5.15. Normal distribution curve of the grand average MEPs peak-to-peak amplitude for TAR at pre, during and post-IHT. The main graph displays the data plotted using hollow circles. For each time point (pre-, during and post-IHT) a histogram is also plotted. The dotted black line on the histogram highlights the mean. Above each histogram it lists the mean, standard deviation (SD) and the number of data gathered (n). Pre-IHT_{all} is the result of pooling together the pre-IHT₀ and pre-IHT₁₀ data. The normal distribution curve for this dataset is shown in blue so it is distinct from the other datasets. Lastly, the red line across all graphs shows the baseline. Datasets are normalised to pre-IHT_{avg}.

TAL

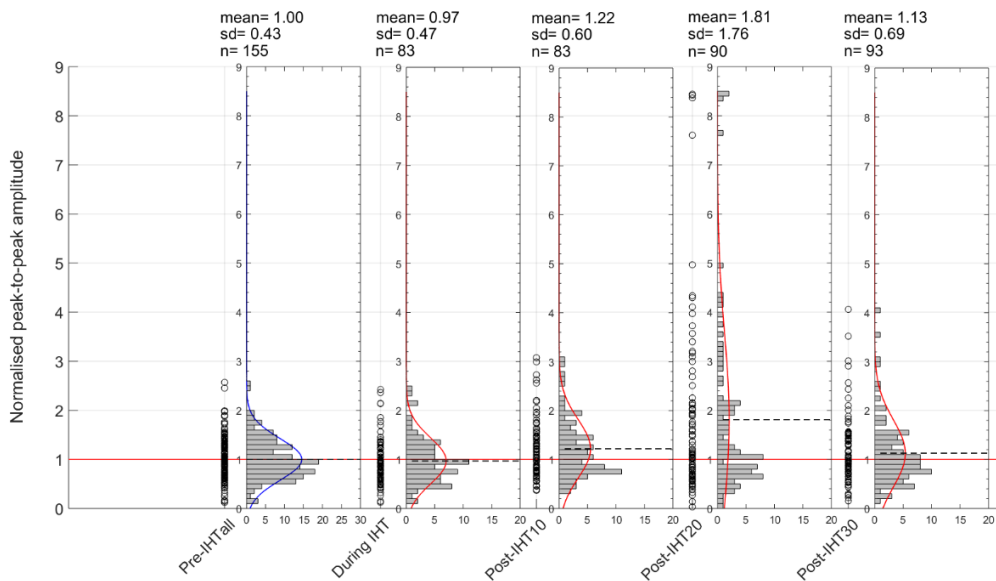


Figure.5.16. Normal distribution curve of the grand average MEPs peak-to-peak amplitude for TAL at pre, during and post-IHT. The main graph displays the data plotted using hollow circles. For each time point (pre-, during and post-IHT) a histogram is also plotted. The dotted black line on the histogram highlights the mean. Above each histogram it lists the mean, standard deviation (SD) and the number of data gathered (n). Pre-IHT_{all} is the result of pooling together the pre-IHT₀ and pre-IHT₁₀ data. The normal distribution curve for this dataset is shown in blue so it is distinct from the other datasets. Lastly, the red line across all graphs shows the baseline. Datasets are normalised to pre-IHT_{avg}.

SOL R

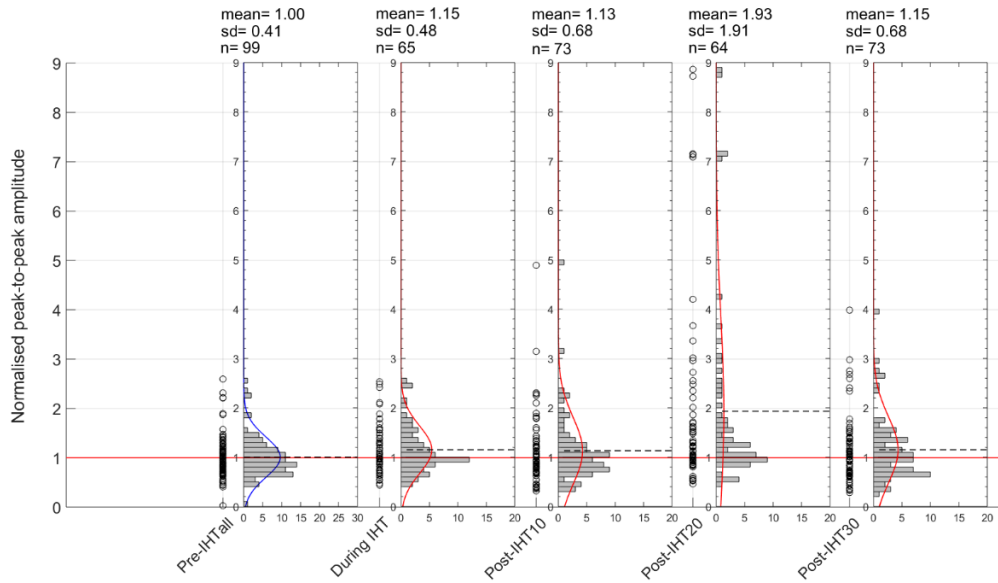


Figure.5.17. Normal distribution curve of the grand average MEPs peak-to-peak amplitude for SOL R at pre, during and post-IHT. The main graph displays the data plotted using hollow circles. For each time point (pre-, during and post-IHT) a histogram is also plotted. The dotted black line on the histogram highlights the mean. Above each histogram it lists the mean, standard deviation (SD) and the number of data gathered (n). Pre-IHT_{all} is the result of pooling together the pre-IHT₀ and pre-IHT₁₀ data. The normal distribution curve for this dataset is shown in blue so it is distinct from the other datasets. Lastly, the red line across all graphs shows the baseline. Datasets are normalised to pre-IHT_{avg}.

FDI R

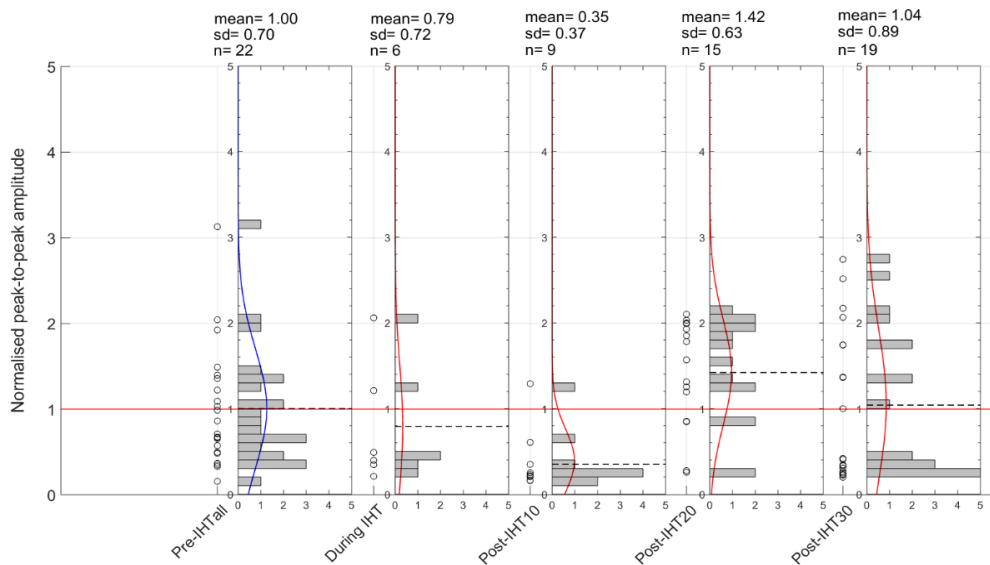


Figure.5.18. Normal distribution curve of the grand average MEPs peak-to-peak amplitude for FDI R at pre, during and post-IHT. The main graph displays the data plotted using hollow circles. For each time point (pre-, during and post-IHT) a histogram is also plotted. The dotted black line on the histogram highlights the mean. Above each histogram it lists the mean, standard deviation (SD) and the number of data gathered (n). Pre-IHT_{all} is the result of pooling together the pre-IHT₀ and pre-IHT₁₀ data. The normal distribution curve for this dataset is shown in blue so it is distinct from the other datasets. Lastly, the red line across all graphs shows the baseline. Datasets are normalised to pre-IHT_{avg}.

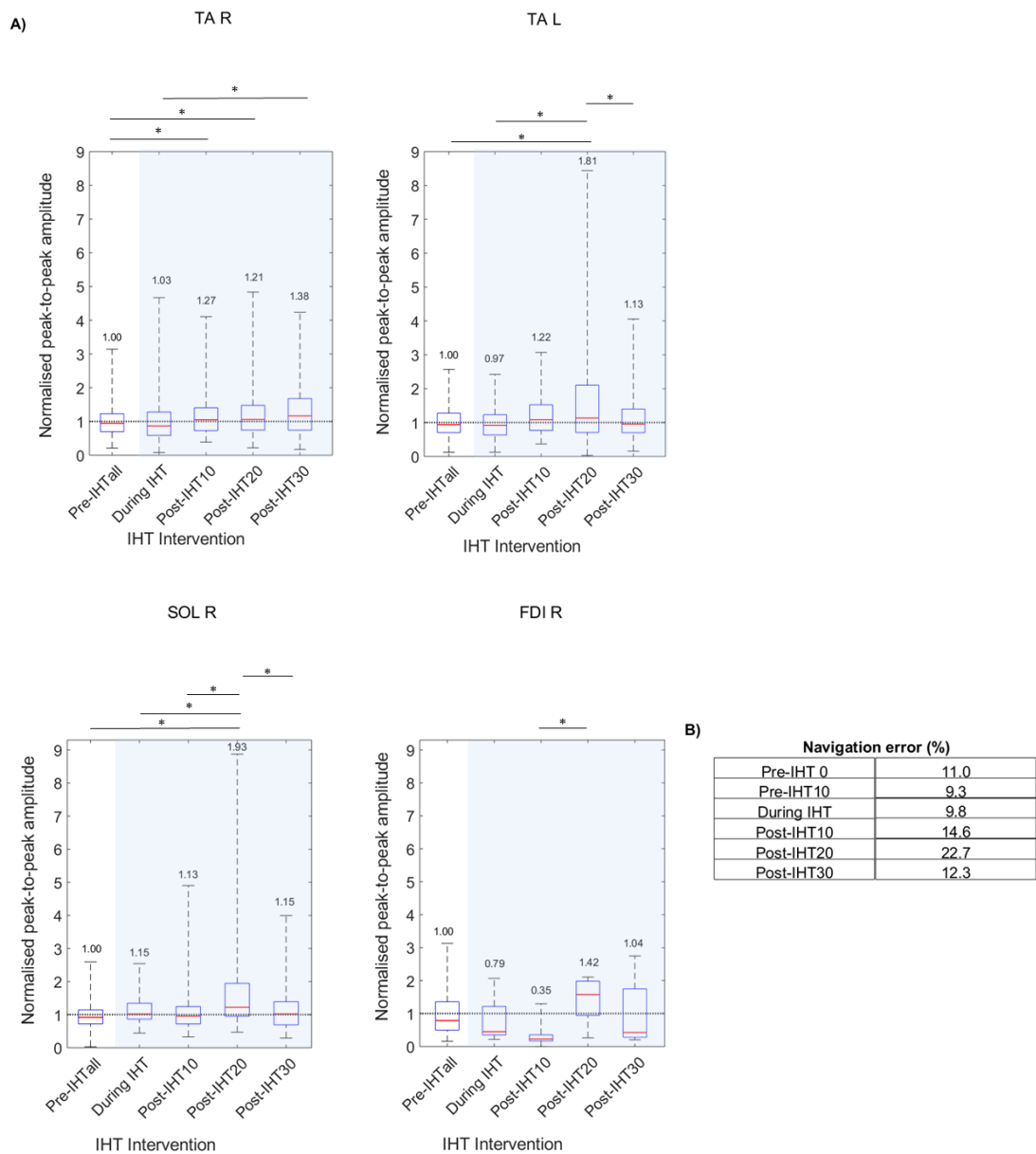
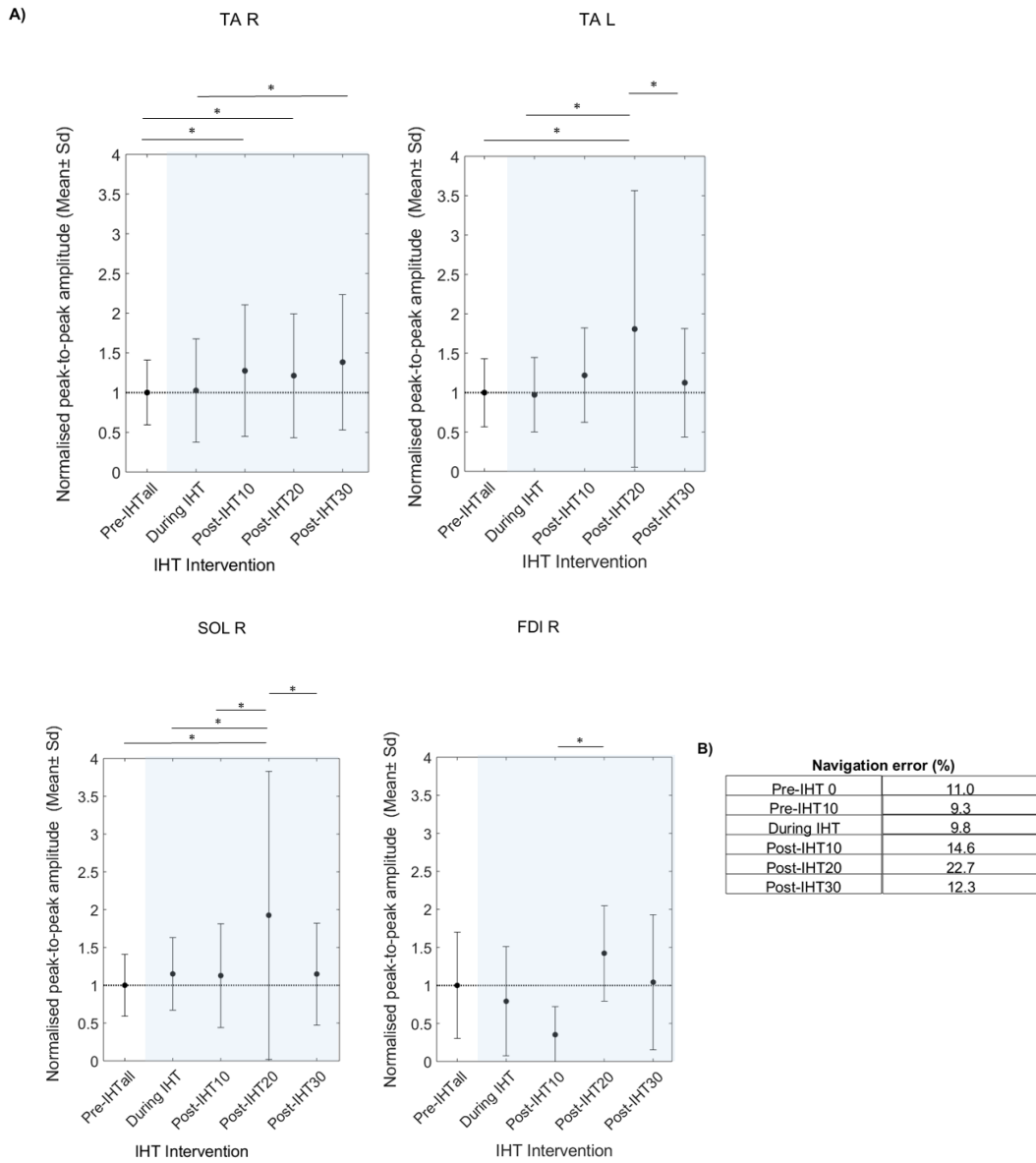


Figure.5.19. **A)** demonstrates the **TAR**, **TAL**, **SOL** and **FDI** normalised peak-to-peak amplitude distribution where the red line displays the median, the blue lines display the 25th and 75th percentiles and the whiskers show the minimum and maximum normalised AUC ($n=9$). Mean value is added on top of each box plot. Welch ANOVA was used to examine if there is a significant difference in AUC over time ($p<0.05$). The Games-Howell Post-hoc test was used to determine where the significant difference lies. Significant difference is displayed with an *. A blue shade on the plots highlights the time during and after IHT. **B)** table shows the navigation error during pre-, during and post-IHT.



*Figure.5.20. A) demonstrates the TA R, TA L, SOL and FDI normalised peak-to-peak amplitude mean \pm SD (n=9). Welch ANOVA was used to examine if there is a significant difference in peak-to-peak amplitude over time ($p < 0.05$). The Games-Howell post-hoc test was used to determine where the significant difference lies. Significant difference is displayed with an *. A blue shade on the plots highlights the time during and after IHT. B) table shows the navigation error during pre-, during and post-IHT.*

Table.5.12. Significant responses (p-value and % change reported) for each muscle (TA R, TA L, SOL R and FDI R)

Muscle	Comparisons	Change (increase or decrease)	% Change	p-value
TA R	pre-IHTall with post-IHT10	↑	+27%	0.031
	pre-IHTall with post-IHT20	↑	+21%	0.000
	during IHT with post-IHT 30	↑	+34%	0.023
TA L	pre-IHTall with post-IHT20	↑	+81%	0.001
	during IHT with post-IHT20	↑	+87%	0.001
	post-IHT20 with post-IHT30	↓	-38%	0.014
SOL R	pre-IHTall with post-IHT20	↑	+93%	0.005
	during IHT with post-IHT20	↑	+68%	0.036
	post-IHT10 with post-IHT20	↑	+71%	0.033
	post-IHT20 with post-IHT30	↓	-40%	0.041
FDI R	post-IHT10 with post-IHT20	↑	+306%	0.001

5.3.3.2. AUC

This section presents the grand average AUC. The results from the grand average AUC MEP analysis are similar to what was observed in peak-to-peak MEP amplitude following the IHT intervention. Below the normal distribution graphs display the spread of the AUC MEP data recorded at TA R (Figure.5.21), TA L (Figure.5.22), SOL R (Figure.5.23) and FDI R (Figure.5.24). As in all the previous normal distribution graphs there is a shift of the distribution towards the left following the IHT intervention.

In general, the grand average MEP AUC measurements, for TA R, TA L and SOL R muscles, show a significant increase between baseline and post-IHT. The average percentage change for TA R is +44%, TA L is +44% and SOL R is +42% (Table.5.13). A lower percentage change was observed in the grand average MEP amplitude for TA R (+27%) compared to MEP AUC (Table.5.12; Table.5.13). However, in TA L and SOL R the peak-to-peak percentage change is much higher compared to MEP AUC (TA L: +81% and SOL R: +93%) (Table.5.12; Table.5.13). Moreover, compared to the grand average peak-to-peak amplitude measurements, TA

L and SOL R do not display a significant decrease in MEP magnitude at post-IHT₃₀ (Table.5.13).

Looking at individual responses a significant increase in MEP AUC following IHT was observed in the same participants as seen in peak-to-peak amplitude (IHT6, IHT11, IHT12, IHT13) for TA R with an average percentage change of +140 % (Table.5.8) on average calculated for individuals, compared to +44% calculated in the grand average (Table.5.13). (Please keep in mind that the average percentage change of individuals only includes the responders where the grand average responses displayed here also include the non-responders.) Moreover, the increase in MEP magnitude is long lasting in both the individuals and the grand average and this is also apparent in both MEP measurements (peak-to-peak amplitude and AUC).

In TA L 4 (IHT10, IHT11, IHT12 and IHT13) out of 7 participants displayed a significant response with a percentage change of +128% (Table.5.9) on average calculated for the individual responses, compared to +44% calculated in the grand average AUC and in SOL R only IHT12 had a significant increase in AUC between pre-IHT and post-IHT measurements with a percentage change of +87% (Table.5.10), compared to +42% in the grand average (Table.5.13).

Lastly, as also seen in the grand average peak-to-peak amplitude FDI R did not follow the same trend as other muscles but overall the small number of MEP measurements gathered from participants limits any firm conclusion on the action of IHT on the recruitment of this muscle to MEPs in the study (Figure.5.19; Figure.5.24).

To conclude, the results of TA R, TA L and SOL R further highlight the findings that IHT enhances the excitability of CST to lower limb muscles and this is apparent in individual responses and the average responses of peak-to-peak amplitude and AUC.

TAR

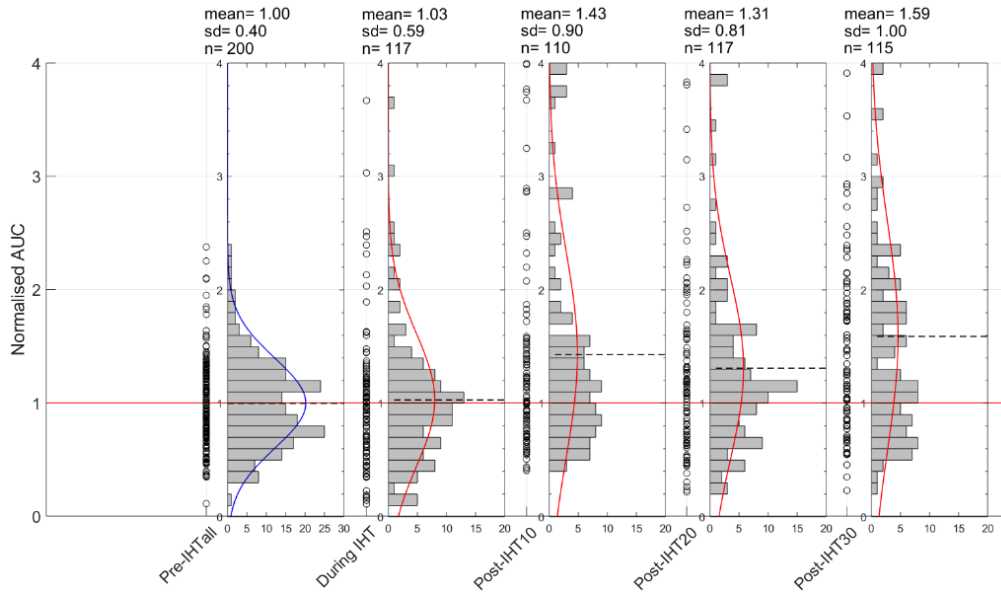


Figure.5.21. Normal distribution curve of the grand average MEPs AUC for TAR at pre, during and post-IHT. The main graph displays the data plotted using hollow circles. For each time point (pre-, during and post-IHT) a histogram is also plotted. The dotted black line on the histogram highlights the mean. Above each histogram it lists the mean, standard deviation (SD) and the number of data gathered (n). Pre-IHT_{all} is the result of pooling together the pre-IHT₀ and pre-IHT₁₀ data. The normal distribution curve for this dataset is shown in blue so it is distinct from the other datasets. Lastly, the red line across all graphs shows the baseline. Datasets are normalised to pre-IHT_{avg}.

TAL

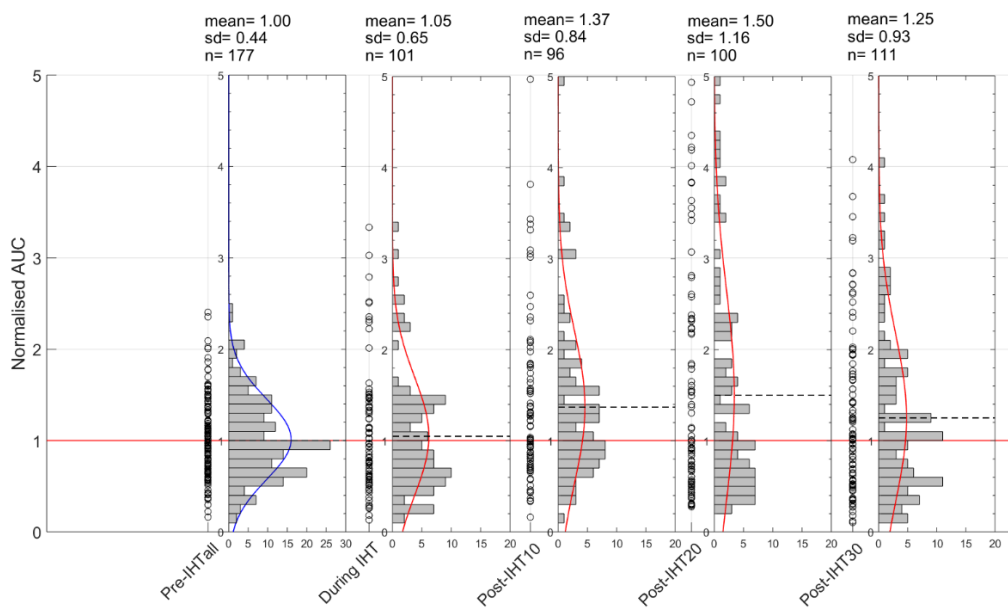


Figure.5.22. Normal distribution curve of the grand average MEPs AUC for TAL at pre, during and post-IHT. The main graph displays the data plotted using hollow circles. For each time point (pre-, during and post-IHT) a histogram is also plotted. The dotted black line on the histogram highlights the mean. Above each histogram it lists the mean, standard deviation (SD) and the number of data gathered (n). Pre-IHT_{all} is the result of pooling together the pre-IHT₀ and pre-IHT₁₀ data. The normal distribution curve for this dataset is shown in blue so it is distinct from the other datasets. Lastly, the red line across all graphs shows the baseline. Datasets are normalised to pre-IHT_{avg}.

SOL R

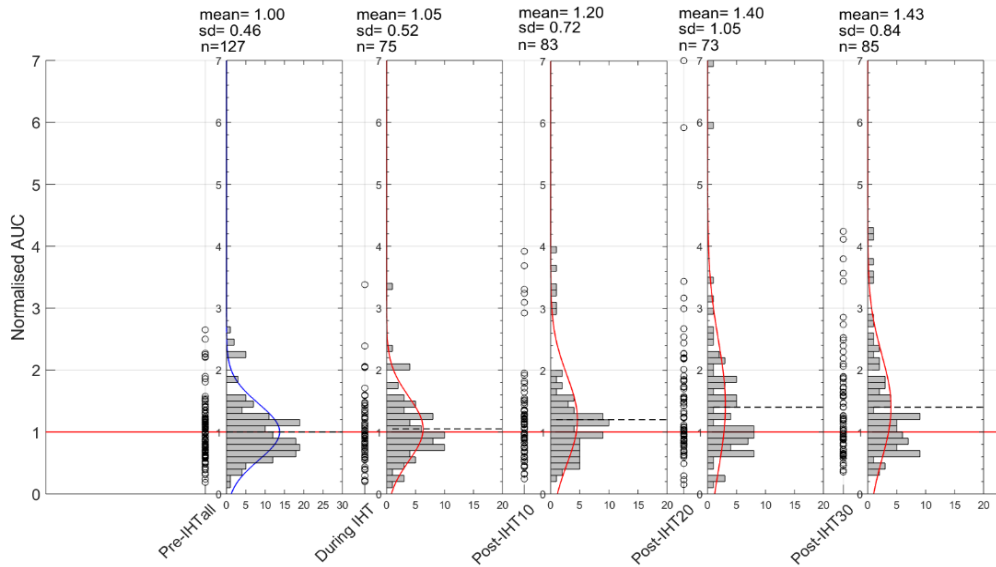


Figure.5.23. Normal distribution curve of the grand average MEPs AUC for SOL R at pre, during and post-IHT. The main graph displays the data plotted using hollow circles. For each time point (pre-, during and post-IHT) a histogram is also plotted. The dotted black line on the histogram highlights the mean. Above each histogram it lists the mean, standard deviation (SD) and the number of data gathered (n). Pre-IHT_{all} is the result of pooling together the pre-IHT₀ and pre-IHT₁₀ data. The normal distribution curve for this dataset is shown in blue so it is distinct from the other datasets. Lastly, the red line across all graphs shows the baseline. Datasets are normalised to pre-IHT_{avg}.

FDI R

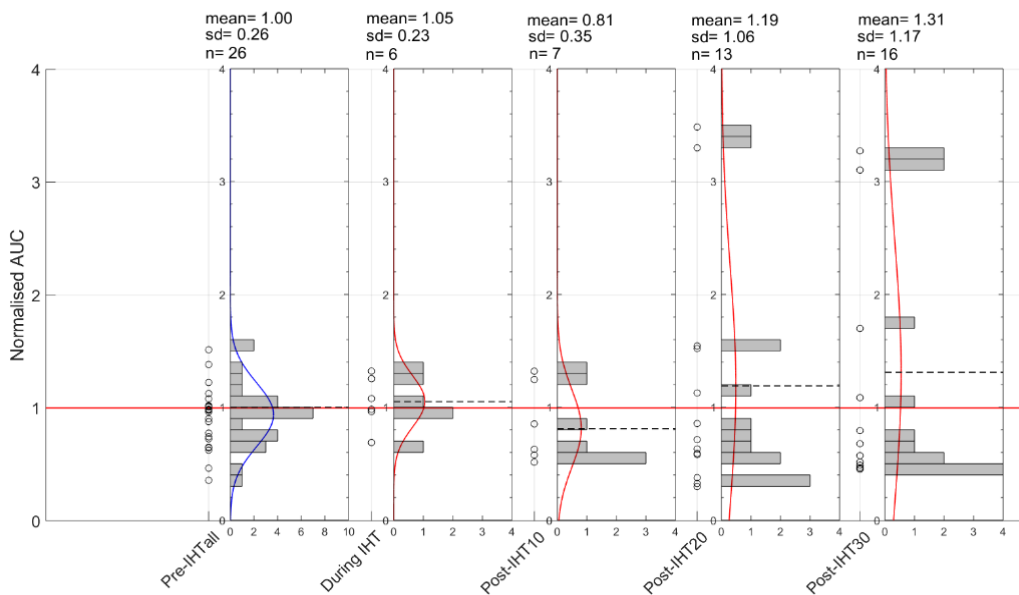


Figure.5.24. Normal distribution curve of the grand average MEPs AUC for FDI R at pre, during and post-IHT. The main graph displays the data plotted using hollow circles. For each time point (pre-, during and post-IHT) a histogram is also plotted. The dotted black line on the histogram highlights the mean. Above each histogram it lists the mean, standard deviation (SD) and the number of data gathered (n). Pre-IHT_{all} is the result of pooling together the pre-IHT₀ and pre-IHT₁₀ data. The normal distribution curve for this dataset is shown in blue so it is distinct from the other datasets. Lastly, the red line across all graphs shows the baseline. Datasets are normalised to pre-IHT_{avg}.

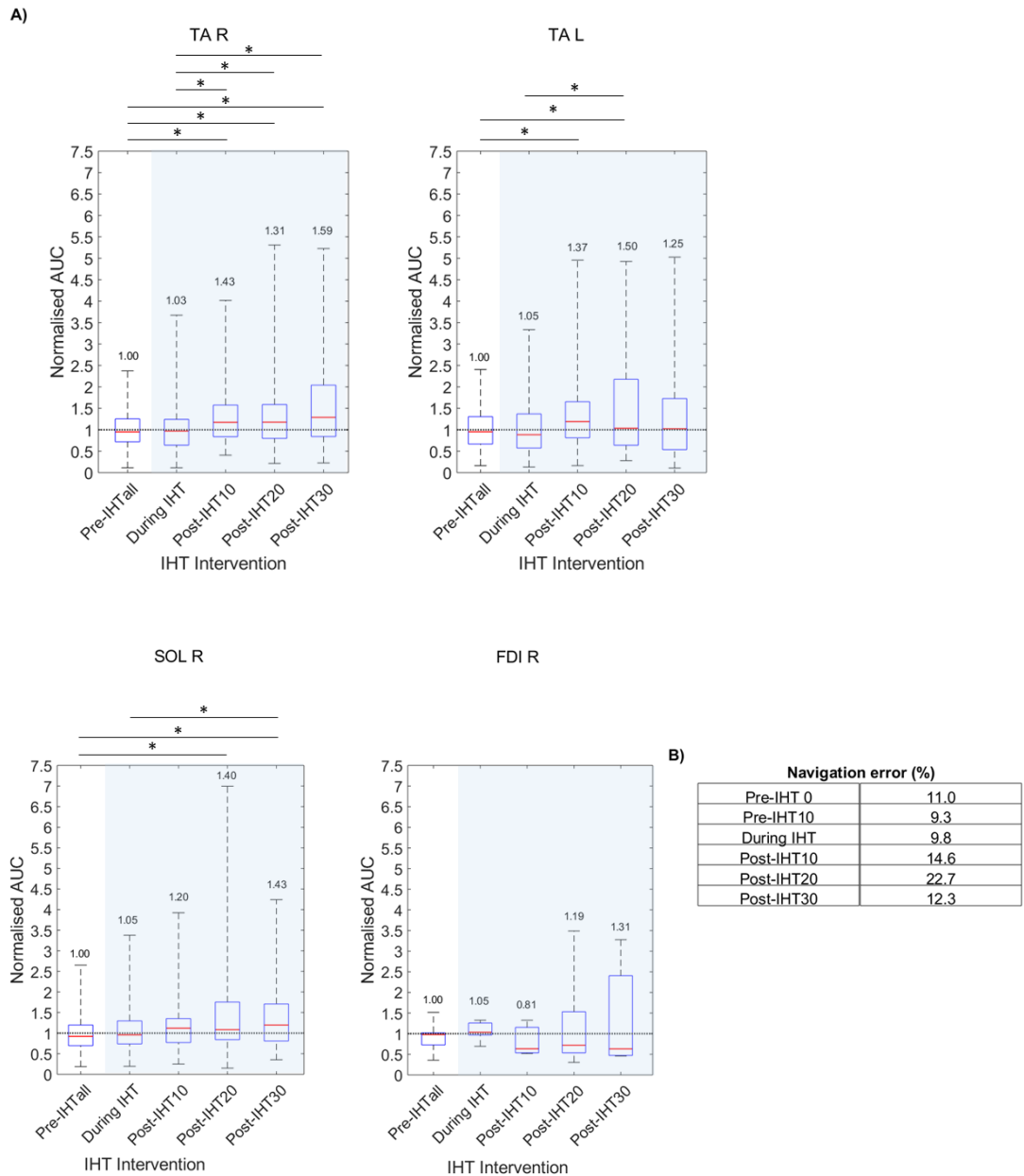


Figure.5.25. **A)** demonstrates the TA R, TA L, SOL and FDI normalised AUC distribution where the red line displays the median, the blue lines display the 25th and 75th the percentiles and the whiskers show the minimum and maximum normalised peak-to-peak amplitude ($n=9$). Mean value is added on top of each box plot. Welch ANOVA was used to examine if there is a significant difference in peak-to-peak amplitude over time ($p<0.05$). The Games-Howell post-hoc test was used to determine where the significant difference lies. Significant difference is displayed with an *. A blue shade on the plots highlights the time during and after IHT. **B)** table shows the navigation error during pre-, during and post-IHT.

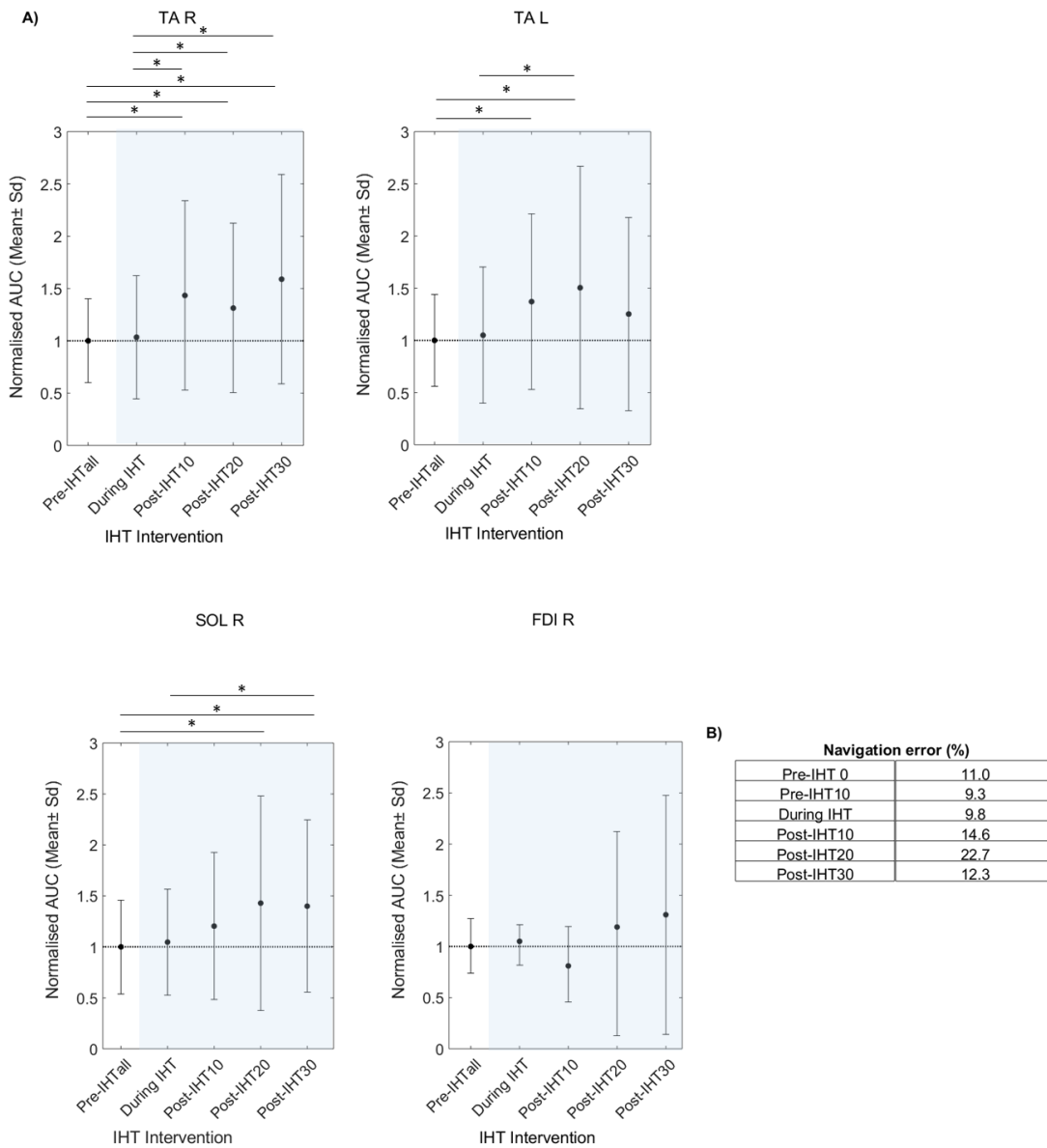


Figure.5.26. **A)** demonstrates the TA R, TA L, SOL and FDI R normalised AUC mean \pm SD ($n=9$). Welch ANOVA was used to examine if there is a significant difference in AUC over time. $p<0.05$. The Games-Howell Post-hoc test was used to determine where the significant difference lies. Significant difference is displayed with an *. A blue shade on the plots highlights the time during and after IHT. **B)** table shows the navigation error during pre-, during and post-IHT.

Table.5.13. Significant responses (p-value and % change reported) for each muscle (TA R, TA L, SOL R and FDI R)

Muscle	Comparisons	Change (increase or decrease)	% Change	p-value
TA R	pre-IHTall with post-IHT10	↑	+43%	0.000
	pre-IHTall with post-IHT20	↑	+31%	0.003
	pre-IHTall with post-IHT30	↑	+59%	0.000
	during IHT with post-IHT10	↑	+36%	0.043
	during IHT with post-IHT20	↑	+27%	0.000
	during IHT with post-IHT30	↑	+54%	0.000
TA L	pre-IHTall with post-IHT10	↑	+37%	0.003
	pre-IHTall with post-IHT20	↑	+50%	0.002
	during IHT with post-IHT20	↑	+43%	0.016
SOL R	pre-IHTall with post-IHT20	↑	+40%	0.012
	pre-IHTall with post-IHT30	↑	+43%	0.002
	during IHT with post-IHT30	↑	+36%	0.025

5.3.4. MEPs success rate for each muscle following TMS

In this series of experiments TMS was used to target the TA R ‘hotspot’. However, by recording from both nearby, distant and ipsilaterally generated MEPs, a broader understanding of the generalised nature of IHT effect can be investigated by reporting on the success rates for MEP generation in TA R, TA L, SOL R and FDI R. If the success rate changes it would suggest an action on general brain excitability following IHT across multiple cortical structures and regions independent of the TMS targeted region.

The figures below (Figure.5.27, Figure.5.28, Figure.5.29 and Figure.5.30) display the percentage of activation following several TMS stimulations for TA R (Figure.5.27), SOL R (Figure.5.28), TA L (Figure.5.29) and FDI R (Figure.5.30) as well as the mean AUC and mean peak-to-peak amplitude. The results are shown for each individual and the data are normalised to pre-IHT_{avg}.

Looking at the responses of all the muscles recorded, there is consistency between mean AUC and mean peak-to-peak amplitude within individuals but not with success rate (Figure.5.27; Figure.5.28; Figure.5.29; Figure.5.30). Also, the results show no clear pattern across individuals in success rate but do reveal individual

variances in MEP responsiveness. This in itself may be important when considering using IHT within a rehabilitation programmes. Moreover, it is important to mention that the results obtained by Christiansen et al (2018) studied intracortical facilitation and short-interval intracortical inhibition in healthy subjects and saw no significant change in cortical excitability through these pathways.

Lastly, it is also worth mentioning that for this study, an improved experimental design for the study of cortical excitability would have been through targeting upper limb muscles such as FDI R and using the figure-of-eight coil which is more focal compared to the double-cone coil used in this study. Using two figure-of-eight coils we could then activate both the contralateral and ipsilateral pathways of the FDI muscle before and after the intervention. Please keep in mind that the CST is composed of two pathways, the lateral corticospinal pathway and the anterior corticospinal pathway. Most motor fibres decussate at the pyramids and travel contralaterally (known as the lateral corticospinal pathway) whereas 10% to 20% travel ipsilaterally (known as the anterior corticospinal pathway). Following the stimulation of these pathways, an increase in success rate will suggest an enhanced cortical activity. Unfortunately, with this current experimental design it is hard to know whether the experimenter was activating ipsilateral and/or contralateral pathways of the lower limb muscles since the coil used probably excited both left and right cortices.

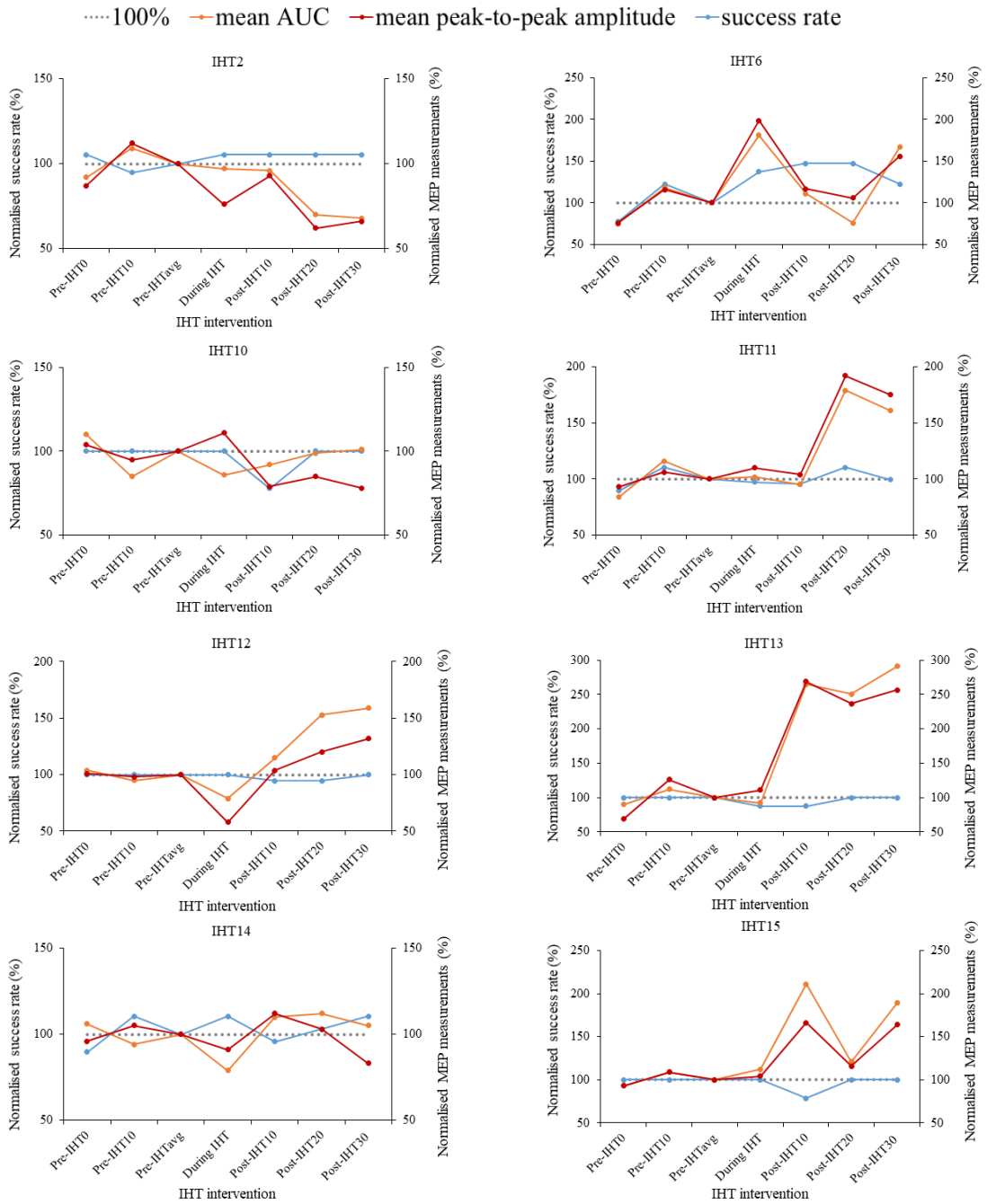


Figure.5.27. Left y-axis displays the normalised success rate (in blue), expressed as a percentage, for TA R muscle. The data is normalised to pre-average. The dotted line shows the 100% level. Right y-axis shows the mean AUC (in orange) and mean peak-to-peak amplitude (in red) as a percentage. Each graph shows the responses of participants: IHT2, IHT6, IHT10, IHT11, IHT12, IHT13, IHT14 and IHT15.

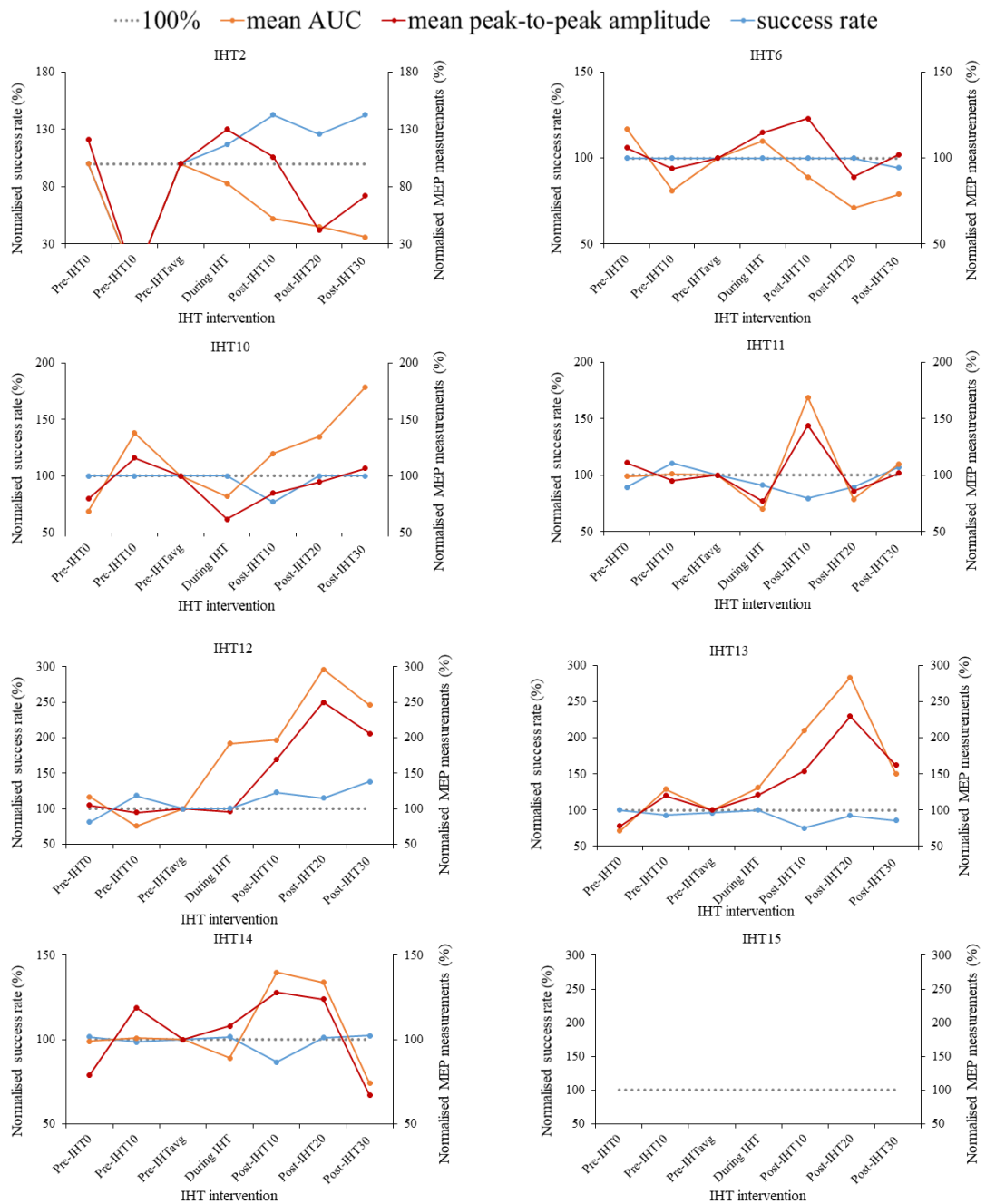


Figure.5.28. Left y-axis displays the normalised success rate (in blue), expressed as a percentage, for SOL R muscle. The data is normalised to pre-average. The dotted line shows the 100% level. Right y-axis shows the mean AUC (in orange) and mean peak-to-peak amplitude (in red) as a percentage. Each graph shows the responses of participants: IHT2, IHT6, IHT10, IHT11, IHT12, IHT13, IHT14 and IHT15.

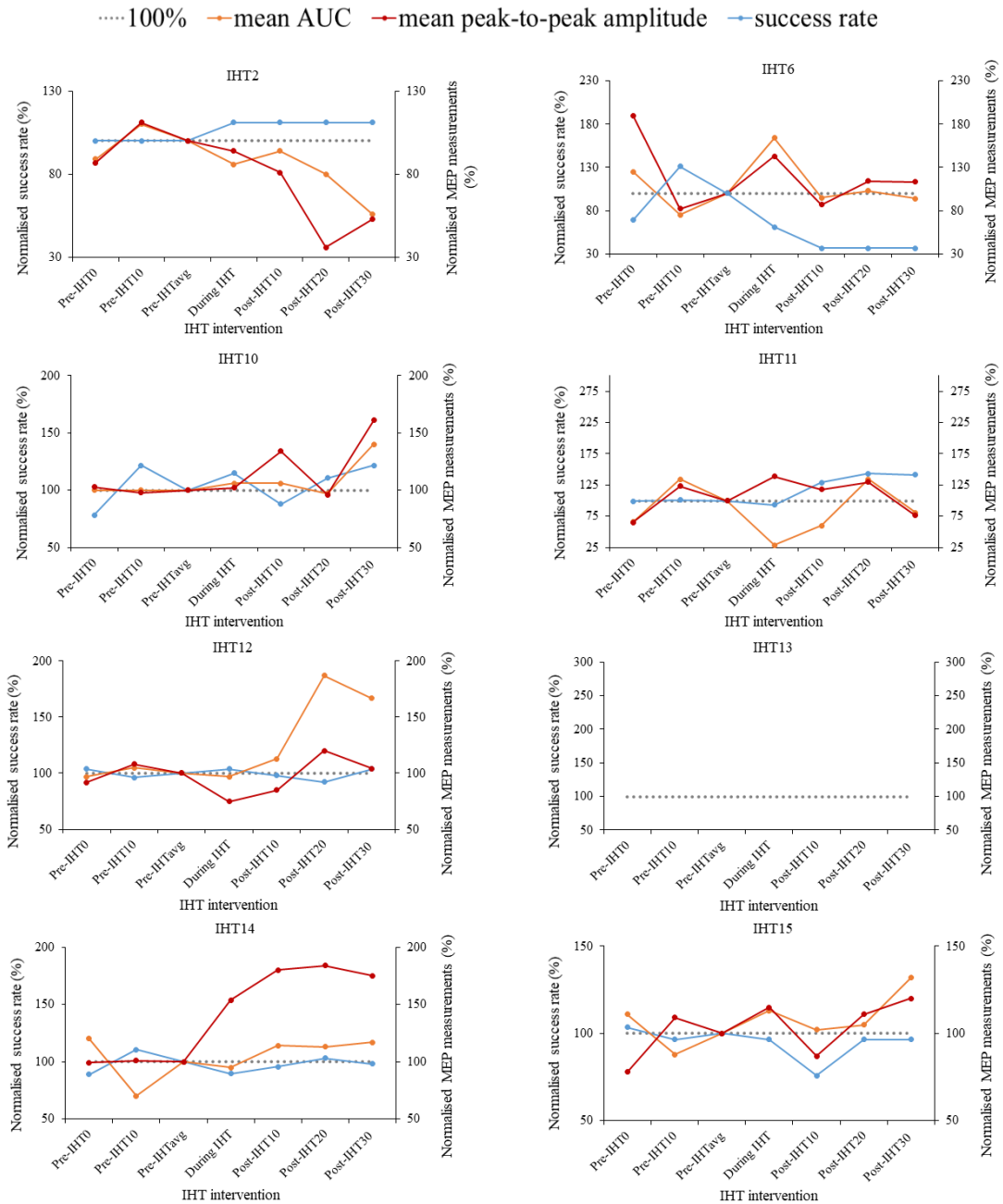


Figure 5.29. Left y-axis displays the normalised success rate (in blue), expressed as a percentage, for TA L muscle. The data is normalised to pre-average. The dotted line shows the 100% level. Right y-axis shows the mean AUC (in orange) and mean peak-to-peak amplitude (in red) as a percentage. Each graph shows the responses of participants: IHT2, IHT6, IHT10, IHT11, IHT12, IHT13, IHT14 and IHT15.

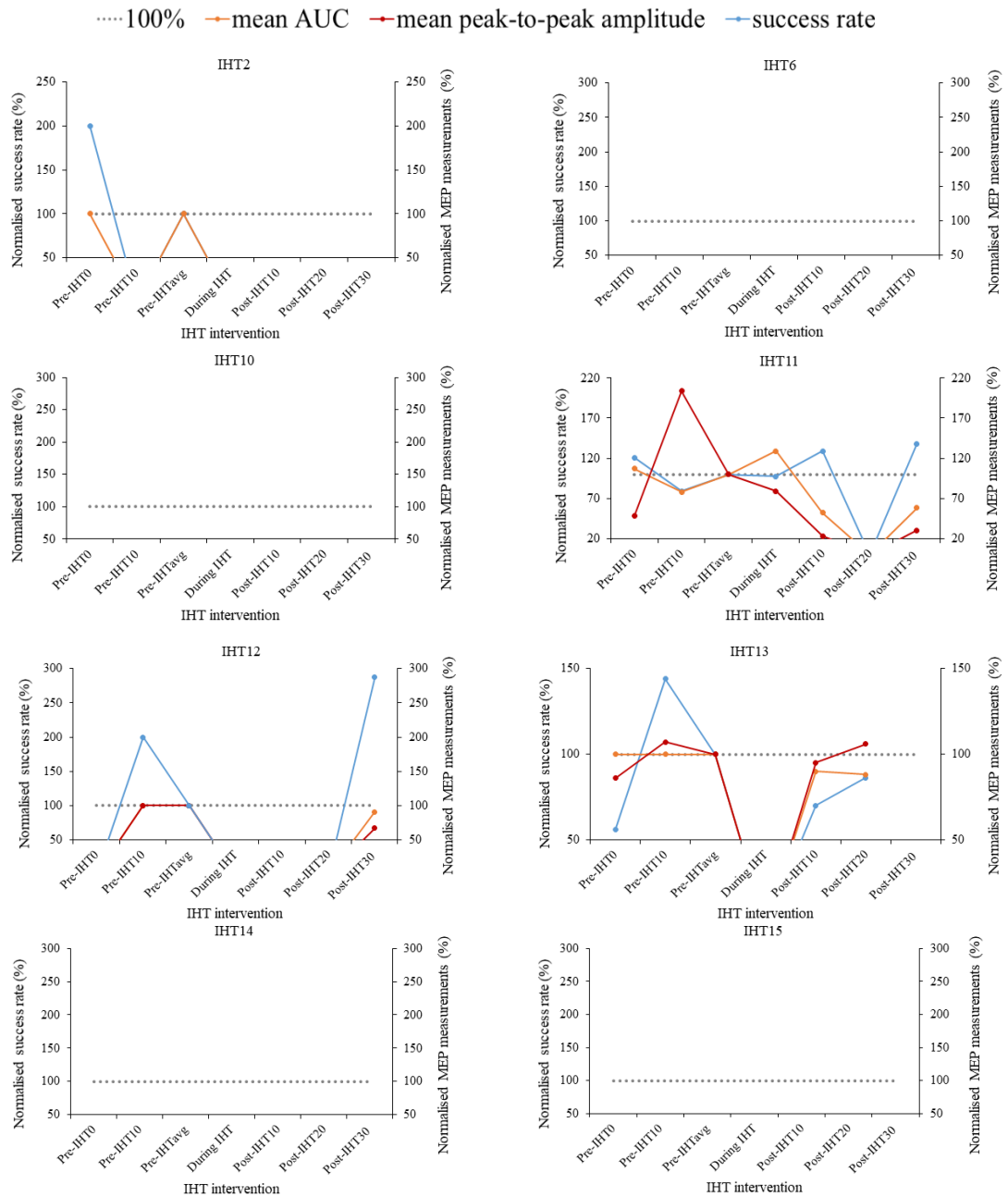


Figure.5.30. Left y-axis displays the normalised success rate (in blue), expressed as a percentage, for FDI R muscle. The data is normalised to pre-average. The dotted line shows the 100% level. Right y-axis shows the mean AUC (in orange) and mean peak-to-peak amplitude (in red) as a percentage. Each graph shows the responses of participants: IHT2, IHT6, IHT10, IHT11, IHT12, IHT13, IHT14 and IHT15.

5.4. Discussion

IHT has shown to improve motor performance in iSCI participants, however, there is little information on how IHT influences spinal pathways. In a previous chapter, the effect of a single IHT exposure on the neurophysiology of the dorsal columns of ascending tracts was examined by analysing components of the cortical SEP waveform. The study concluded that there was no significant difference in the cortical SEP waveform following IHT. In this chapter the effects on excitability of the descending CST was studied by analysing MEPs to a group of muscles before, during and after IHT in healthy subjects.

MEPs were recorded from muscles simultaneously following a stimulus on the motor cortex. The stimulus targeted the TA R muscle, however, because the double cone coil lacks focality, the EMG activity of other recruited muscles were also recorded and included an antagonistic lower limb muscle (SOL R), the TA of the opposite limb (TA L) and the hand muscle from the right side of the body (FDI R).

5.4.1. Reliability of pre-IHT MEP measurements

The investigation begun by studying the reliability of baseline MEP measurements. To determine the consistency of the MEPs the maximum and minimum peak variability of the MEP waveform was studied. On average 15% variability was observed in the maximum peak and 11% variability in the minimum peak. With this variability in MEP components measured from of the TA R muscle, the average CV in baseline AUC measurements for TA R across all participants in this study was 35% and the baseline peak-to-peak amplitude CV for the TA R was 38%. These values are similar to the 45% MEP amplitude CV reported by Darling et al. (2006) on a finger muscle that was activated by stimulating at 120% of the resting motor threshold using the figure-of-eight coil. Please keep in mind that the higher the CV the higher the level of variability and generally MEP measurements using the figure-of-eight coil are more reliable (Fleming et al., 2012).

What is important here is that with a coil placement that is as accurate as 0.8 mm in distance and 0.8° in coil rotation to the ‘hotspot’ the MEP components vary a lot and the CV for MEP amplitude and MEP AUC are high. However, as already

mentioned this variability in MEPs is accepted by the scientific community as a feature of TMS studies.

5.4.2. Improving the variability in MEP measurements

MEPs show a high degree of variability with respect to changes in background activation of muscles and small errors in coil placement and also the subject's anxiety or stress (Kesar, Stinear and Wolf, 2018). To minimise these effects, the study required the subjects to be relaxed (measured by absence of EMG activity preceding TMS), and excluded any data where the MEP was preceded by EMG or where a navigation error arose.

5.4.3. Corticospinal excitability following IHT

After completing an analysis on the baseline measurements to determine the reliability of the MEP waveform, peak-to-peak amplitude and AUC, the investigation continued by statistically comparing baseline, during and post-IHT measurements.

Looking at the grand average and the participants that responded to the intervention, a significant increase in MEP peak-to-peak amplitude and AUC was observed in all the lower limb muscles, where MEPs were recorded (TA R, TA L and SOL R), when comparing pre-IHT with post-IHT and sometimes between during IHT and post-IHT measurements. Similar results were observed by Christiansen et al. (2018) who studied MEPs on the upper limb of healthy young adults.

Christiansen et al (2018) reported a significant increase in MEP peak-to-peak amplitude measured from an upper limb muscle after 15 min (+29%; $p < 0.001$) and 30 min (+37%; $p < 0.001$) when compared to baseline. The target muscle in this study was TA R (a lower limb muscle) and similarly to Christiansen et al (2018) a significant increase in MEP peak-to-peak amplitude was detected after 10 min (+27%; $p = 0.031$) and 20 min (+21%; $p < 0.000$) when compared to the pooled baseline measurement (pre-IHT_{all}). However, a significant difference was not present in the grand average peak-to-peak amplitude between pre-IHT_{all} and post-IHT₃₀ as observed by Christiansen et al (2018) but it was a significant increase in MEP AUC measurements. Similar significant results were also present in the other lower limb muscles where MEPs were monitored but were not the target for stimulation (TA L and SOL R).

Additionally, a significant increase in post-IHT was observed when compared to baseline measurements of MEP AUC.

Unlike Christiansen et al's (2018) study, MEPs were also recorded 20 minutes into the IHT intervention and a significant increase was observed when comparing during IHT measurements with post-IHT for all 3 muscles (TA R, TA L and SOL R) and in both MEP measurements (amplitude and AUC). Moreover, there was a possibility that MEP magnitude of TA L and SOL R muscles at post-IHT₃₀ began to decrease and return back to baseline. However, this was significant in the MEP amplitude measurements and not in the MEP AUC.

Collectively, the study concludes that a single IHT session produces a significant increase in MEP peak-to-peak amplitude and AUC that persists for up to 30 minutes post-IHT in the majority of the subjects. This suggests a long lasting effect of IHT following the intervention and extends the observations reported by Christiansen et al. (2018) on the upper limb, and linking to the long lasting effects of IHT on motor function in patients with iSCI by showing the effects are not isolated to specific functional muscle groups. Moreover, Christiansen et al (2018) suggests that an enhanced excitability may last up to 120 minutes following the intervention, however, this value comes from one participant where MEP magnitude was monitored until it returned to baseline.

This time frame is clinically important since during this time of enhanced corticospinal excitability there is an opportunity for clinicians to perform rehabilitation training. Combining IHT with rehabilitation training could perhaps improve the functional outcome of the patient and even speed up recovery. As reported in the literature review, studies combining IHT with rehabilitation have been completed and suggest an enhanced functional outcome compared to IHT alone (Hayes et al., 2014; Navarrete-Opazo et al., 2016b; Navarrete-Opazo et al., 2017; Trumbower et al., 2017; Hayes et al., 2014), but knowing this time window for effectiveness, can optimise treatment outcomes.

5.4.4. Individual differences

It is important to mention that 2 (IHT14 and IHT15) out of 8 participants did not respond to the intervention. As already mentioned, BDNF neurotrophic factor is

involved with the IHT intervention and 25% of the population carry a mutation that influences their responsiveness. DNA samples would have provided further information on being unresponsive to the intervention. Clinically this is an important factor that scientists need to further investigate.

Furthermore, in one participant (IHT2), IHT had the opposite effect than expected (a significant decrease in MEP amplitude and MEP AUC rather than a significant increase when comparing baseline measurements with post-IHT). It is important to mention that this significant decrease did not follow a period of excitability and it was present (with a significant difference) in all three muscles (TA R, TA L and SOL R) for both MEP amplitude and MEP AUC.

Moreover, in two participants (IHT10 and IHT12) a significant decrease was observed during IHT when compared to baseline measurements of peak-to-peak amplitude but not in AUC. The reasoning for this effect is the reduced oxygen availability during the intervention. This causes intermittent drops in peripheral oxygen levels (as shown in Chapter 2) and possibly similar drops in oxygen concentrations are present in the brain. To date, there are no studies using this IHT protocol and showing fluctuations of oxygen concentration in the brain.

Overall, these results highlight that there are individual differences and this intervention may not be beneficial for every patient.

5.4.5. Success rate of MEPs following IHT

Lastly, success rate of MEPs was studied for the TA R, TA L, SOL R and FDI R muscles. Success rate has been used in the past to investigate MEPs in participants under anaesthesia during spinal surgery (Sihle-Wissel, Scholz and Cuniz, 2000; Kawaguchi et al., 1998). The measurements did not show any distinct pattern among participants. Therefore, no clear sign as to whether IHT enhanced cortical excitability making it more likely to elicit an MEP. However, Christiansen et al (2018) that looked at intracortical facilitation and short-interval intracortical inhibition reported no change following IHT when comparing it with baseline.

An important limitation of studying success rate in lower limb muscles was that the ipsilateral and contralateral fibres run centrally and it was hard to tell which

fibres were activated. To have a better control of the stimulation, it is suggested to use the figure-of-eight coil and activate upper limb muscles that their pathways do not run centrally.

5.4.6. Limitations of the study

A limitation of this study was that MEPs were measured only 30 minutes following the intervention. It may have been advantageous to measure MEPs for an extended period to observe how long it takes for the MEP to return to baseline. However, this has already been investigated by Christiansen et al (2018) for one participant and the study reported that the effects of IHT can last up to around 120 minutes. But repetition of this in a larger group is recommended.

An additional limiting factor in this experiment is a lack of a sham intervention. A sham single-blind experiment would have reinforced the results. It would have controlled for participant bias and possible changes in excitability as a result of sending multiple TMS stimulations over a two-hour session. This was planned but not executed due to covid-19 restrictions.

5.4.7. Conclusion

To conclude, the study demonstrates that IHT affects the magnitude of the MEP waveform in the TA R, TA L and SOL R muscles following the administration of 30 min IHT. The results show a general rise in peak-to-peak amplitude and AUC in all the lower limb muscles that MEPs were recorded from. The findings agree with Christiansen et al. (2018) that studied an upper limb muscle following the same IHT intervention in healthy subjects and also agrees with improvement in motor function observed in iSCI patients by showing that the effects of IHT are not isolated to specific functional muscle groups.

Chapter.6. Investigating the effects of IHT on muscle metabolic/contractile properties.

6.1. Introduction

Brief mild exposures of hypoxia are capable in initiating functional adaptations across multiple systems with no or little adverse outcomes. Accordingly, IHT has the potential to be used as a treatment to improve motor function in patients with iSCI (Trumbower et al., 2012; Hayes et al., 2014; Navarrete-Opazo et al., 2017). Currently, little information is available on the functional adaptations of ascending and descending pathways of the spinal cord (Christiansen et al., 2018). In the previous chapters, investigations were completed on these pathways by studying SEPs and MEPs. Results revealed that the effects of IHT appear to favour output pathways rather than having an influence on the general excitability of the entire CNS. However, to evaluate the true potential of IHT's ability to change neural pathways it is also important to study its peripheral effects and specifically it's actions on skeletal muscle.

6.1.1. Skeletal muscle and hypoxia

Skeletal muscle size and metabolic or contractile activity is altered following hypoxia as a consequence of the demand of O₂ exceeding O₂ availability (Chaillou, 2018; Lundby, Calbet and Robach, 2009). An important factor that senses a decrease in oxygen concentration and likely to cause most cellular adaptations in skeletal muscle as a result of hypoxia is the hypoxia inducible factor (HIF-1a) (Semenza et al., 2009). Moreover, it is likely that the adaptations to hypoxia differ if the exposure is continuous in comparison to intermittent, if it is severe, moderate or mild and if the exposure is acute or chronic.

Chronic exposure to high-altitude leads to loss in skeletal muscle mass and increase in capillary network and when training at high altitude an increase in mitochondria density and myoglobin is observed (Chaillou, 2018; Lundby, Calbet and Robach, 2009). Chronic severe intermittent hypoxia, usually observed in pathology, leads to a decrease in type I fibre and an increase in type II fibres when compared to age matched controls and thus leading to a reduction in muscle mass and strength and an increase in fatigability (Mador and Bozkanat, 2001; Chaillou, 2018). In contrast, localised intermittent hypoxia in muscle in the context of resistance training combined with

blood flow restriction leads to improved muscle strength, speed and muscle hypertrophy (likely to occur from recruitment of type II glycolytic fibres following fatigability of type I oxidative fibres) (Manimmanakorn et al., 2013b; Scott et al., 2015). Overall, the literature highlights that continuous or brief exposures of chronic or acute hypoxia cause metabolic changes in the muscle and leads to structural adaptations and in turn changes muscle contractile activity.

The IHT intervention studied in this thesis is likely to cause effects in skeletal muscle. We speculate the enhanced functional output observed in iSCI is a combination of effects, both in the CNS and in skeletal muscle. To date, there is insufficient information in the literature on mild to moderate systemic exposure of IHT, such as the treatment given to iSCI patients, and its effects on skeletal muscle metabolism.

6.1.2. Aims and objectives

In order to evaluate the true potential of IHT's ability to change neural pathways, the investigation proceeded with studying the effects of IHT on muscle strength, initially in the upper limb, at the FDI muscle, and later in the lower limb, at the TA muscle. The main requirement was to design an experiment where the baseline muscle force measurements were repeatable. In order to give confidence that an observed change in the magnitude of muscle force is as a result of changes in skeletal muscle metabolism following a single exposure to IHT.

Initially an experiment to investigate the effects of IHT on grip strength was conducted using a grip force transducer. However, the control measurements were too variable and thus, the experiment was discontinued. Subsequently, an experiment to study changes in muscle force of index finger abduction was designed which required transcutaneous magnetic stimulation (TcMS) was applied to the FDI muscle of the dominant hand which resulted in the abduction of the index finger (Kremenec et al., 2004). The reason for avoiding the use of electrical stimulation in this experiment was related to the inability to selectively stimulate the FDI muscle nerve non-invasively and the high levels of currents and voltages that activate pain receptors on the skin. FDI evoked via electrical stimulation is painful and uncomfortable for the participant

(Laufer et al., 2001). Force measurements were recorded using a sensor placed on the lateral side of the index finger. However, this experimental design failed because of having high variability in baseline measurements.

Following a review of the experimental plan, primarily due to overheating of the TMS coil resulting in a variable stimulation strength and thus unreliable data, a new plan was to direct the investigation towards studying the lower limb where it is easier to use electrical stimulation to activate the peroneal nerve and in turn acquiring more reliable measurements. This nerve is superficial and can be stimulated using electrical stimulation without the need for high currents. More information on the experimental design can be found in the section which explains a future study. This study was planned to be completed within 2020, however, as a result of the obstacles (closure of workshops and close down of all respiratory based work prior to official lockdown and therefore, no face to face work) that came along with the COVID-19 pandemic, the experiment was unable to be executed.

To conclude, following the investigation on spinal pathways it was believed essential to study whether the protocol of IHT given to iSCI patients also affected skeletal muscle metabolism and consequently force. The hypothesis states that IHT may not only change the excitability of remaining connections following injury but also affect skeletal muscle metabolism and as a result contractile force.

6.1.3. Summary of studies

The following sections will report observations from two different preliminary studies: 1) Grip strength study and 2) FDI force study.

6.2. Methodology: Grip strength

6.2.1. Subjects

Ethics approval was obtained from the ethics committee of the University of Strathclyde and 6 healthy adults were recruited (4 men and 2 women; mean age 28, range, 26 to 32 years).

6.2.2. Protocol and analysis

The participants were asked to come for two sessions where they were either given IHT or a sham intervention with a washout period of a week. The participants were unaware which intervention they were given. In the sham intervention the participants were given normoxia for 30 minutes whereas in the IHT intervention they were given intervals of hypoxia for 30 minutes. Please refer to Chapter 2 Section 2.2 for more details on the IHT intervention.

Five measurements of grip strength were taken at each time point (pre-, during and post- IHT). During IHT measurements of grip strength were taken 4 min before the end of IHT. Post-IHT measurements of grip strength were taken right after the intervention (post-IHT₀), 15 minutes after the intervention (post-IHT₁₅) and 30 minutes after the intervention (post-IHT₃₀). In the individual analysis, for each time point the grip strength measurements were averaged, normalised to pre-IHT₀ and graphed in Excel. A two-tailed paired t-test was used to compare pre-IHT₀ with during and post-IHT for each individual. Furthermore, a grand average of the grip strengths across all participants was also taken and again a two-tailed paired t-test was completed comparing pre-IHT₀ with during and post-IHT. A p-value of < 0.05 was accepted as a significant difference.

6.3. Results: Grip strength

Figure.6.1 shows the percentage grip force of the average and the individual responses. The asterisk in the figures indicate the significant comparisons of the average data from the two-tailed paired t-test, where the baseline measurements were compared with during and post-IHT measurements.

In the average grip force measurements following IHT there is a significant difference between pre-IHT₀ (100) and post-IHT₀ (94.19 ±14.43) (Figure.6.1). The values are reported here as (mean ± standard deviation). Average grip force measurements following a sham intervention displayed a significant difference between pre-IHT₀ (100) with during IHT (91.85 ±8.42), post-IHT₀ (86.25 ±9.34), post-IHT₁₅ (92.89 ±8.05) and post-IHT₃₀ (95.67 ±7.87) (Figure.6.1).

Moreover, a two-tailed paired t-test was also completed in individual measurements and the significant results for the IHT experiment are listed in Table.6.1 and the significant results for the sham experiment are listed in Table.6.2. The absolute average percentage change in grip force following IHT is $12 \pm 4.8\%$ (Table.6.1) and following the sham intervention is $12 \pm 4.4\%$.

Overall, given the results are highly variable in the sham intervention and no defined trend was observed following IHT. This study was abandoned as an unreliable protocol for investigating effects of IHT on muscle strength influence the participants to perform maximum effort throughout the experiment. To minimise the input of subject effort in the experiment the decision was taken to study muscle evoked reactions to external stimulation.

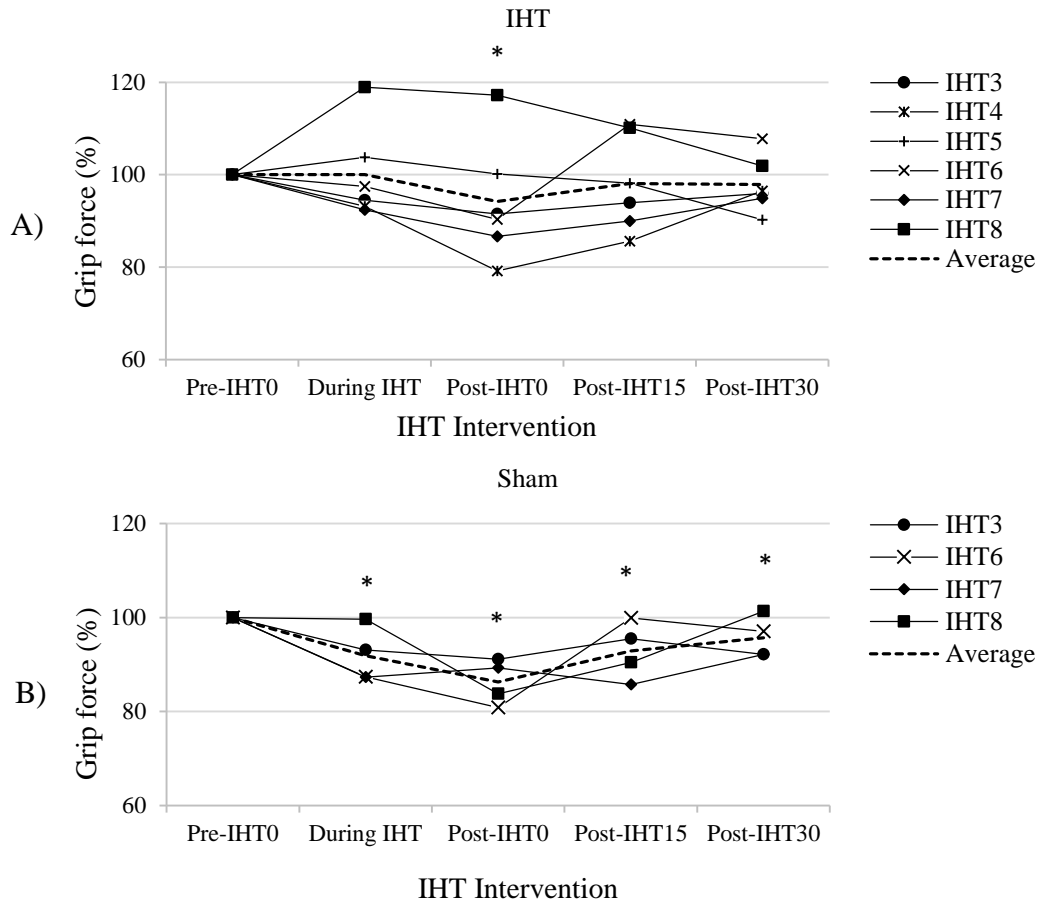


Figure.6.1. **A)** Normalised grip force measurements following IHT (n=6). **B)** Normalised grip force measurements following sham intervention (n=4). In each graph it also displays the average as a dashed line. Statistical analysis: two-tailed paired t-test comparing pre-IHT with during and post-IHT in average data. An * was used to show a significant difference where the p-value was < 0.05.

Table.6.1. Significant percentage change following IHT in individual comparisons

Participant	Comparisons	Change (increase or decrease)	% Change
IHT1	pre-IHT0 (100) with post-IHT0 (94.40 ± 3.83)	↓	-6 %
IHT4	pre-IHT0 (100) with post-IHT0 (79.21 ± 4.23)	↓	-21 %
IHT5	pre-IHT0 (100) with post-IHT15 (85.62 ± 9.23)	↓	-14 %
IHT6	pre-IHT0 (100) with post-IHT30 (90.27 ± 6.00)	↓	-10 %
IHT6	pre-IHT0 (100) with post-IHT15 (110.89 ± 2.18)	↑	+11 %
IHT6	pre-IHT0 (100) with post-IHT30 (107.76 ± 2.64)	↑	+8 %
IHT7	pre-IHT0 (100) with during IHT (92.42 ± 2.98)	↓	-8 %
IHT7	pre-IHT0 (100) with post-IHT0 (86.65 ± 3.05)	↓	-13 %
IHT7	pre-IHT0 (100) with post-IHT15 (89.98 ± 4.23)	↓	-10 %
IHT8	pre-IHT0 (100) with during IHT (118.95 ± 4.53)	↑	+19 %
IHT8	pre-IHT0 (100) with post-IHT0 (117.24 ± 4.64)	↑	+17 %

Please note that comparisons that lead to a significant decrease were highlight in grey.

Table.6.2. Significant percentage change following sham intervention in individual comparisons

Participant	Comparisons	Change (increase or decrease)	% Change
IHT3	pre-IHT0 (100) with post-IHT15 (95.49 ± 2.29)	↓	-5 %
	pre-IHT0 (100) with post-IHT30 (92.15 ± 3.51)	↓	-8 %
IHT6	pre-IHT0 (100) with during IHT (87.40 ± 4.14)	↓	-13 %
	pre-IHT0 (100) with post-IHT0 (80.86 ± 5.00)	↓	-19 %
IHT7	pre-IHT0 (100) with during IHT (87.33 ± 2.44)	↓	-13 %
	pre-IHT0 (100) with post-IHT0 (89.30 ± 2.63)	↓	-11 %
IHT8	pre-IHT0 (100) with post-IHT15 (85.71 ± 2.48)	↓	-14 %
	pre-IHT0 (100) with post-IHT30 (92.12 ± 2.47)	↓	-8 %
	pre-IHT0 (100) with post-IHT0 (83.78 ± 11.78)	↓	-16 %

Please note that comparisons that lead to a significant decrease were highlight in grey.

6.4. Methodology: FDI force measurements

6.4.1. Subjects

Ethics approval was obtained from the ethics committee of the University of Strathclyde and 5 healthy adults were recruited (3 men and 2 women; mean age 29, range, 26 to 36 years).

6.4.2. Protocol and analysis

This experimental design involved a magnetic stimulus directly activating the FDI muscle by evoking a contraction. This muscle is located in the web between the thumb and the index finger. The contraction of the FDI muscle initiated the abduction of the index finger. A strain gauge force sensor was placed alongside on the lateral side of the index finger and aligned with the interphalangeal joint (Erim et al., 1999). Hand constrains were used so that only index finger movement acted on the transducer following stimulation of the FDI muscle (Figure.6.2). The arrangement of the hand was kept the same for each participant and ensured that each stimulation by the TMS coil was at the same position. The thumb was strapped into place as well as the middle, ring and pinkie finger. Please refer to Figure.6.2 for more information on hand placement. This experimental rig was constructed by Stephen Murray, a technician in the department of Biomedical Engineering. Moreover, Stephen Murray constructed an

experimental rig to support the weight of the TMS coil above the stimulation site (Figure.6.3).

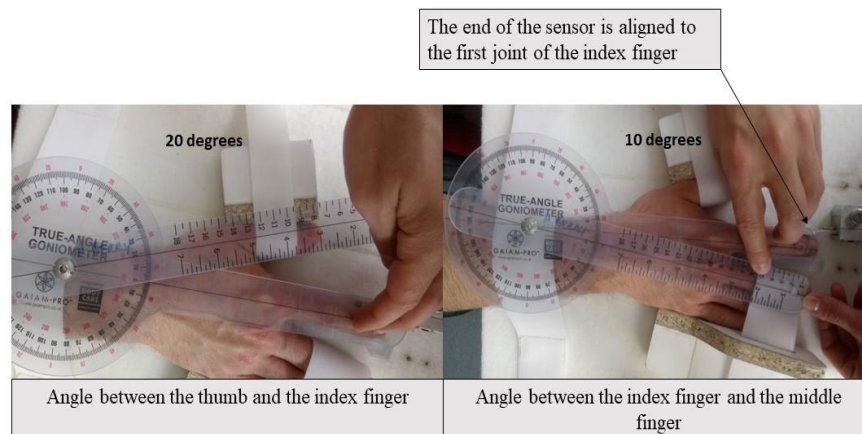


Figure.6.2. This figure shows the placement of the hand on the testing rig. The thumb was strapped and the angle between the thumb and index finger was kept 20 degrees. The middle, ring and pinkie finger were also strapped and the angle between the index finger and the middle finger was set to 10 degrees. Furthermore, the end of the sensor was aligned to the first joint of the index finger. This is the hand placement used for each participant.



Figure.6.3. This figure shows the placement of the hand on the testing rig where the hand is trapped in place and the experimental rig that holds the weight of the cooling coil.

To generate an evoked contraction a series of rapid TMS pulses were sent to the FDI muscle. Different coils were tested to examine which provided the best stimulation conditions for this experiment. The coils that were tested were: AirFilm coil (70mm) and the Alpha flat coil (40mm) by the Magstim Company Ltd in Whitland, UK. The smaller Alpha flat coil allowed a more targeted stimulation of the muscle, however, this coil heats up much faster than the larger diameter coil with a build-in cooling mechanism. When a TMS coil heats up its efficiency decreases and

this directly affects the stimulation output meaning that the TMS pulse weakens. Despite the advantage of its small size, this tendency for overheating meant that it was not suitable for the purpose of this study. Thus, the experiment proceeded with using the AirFilm cooling coil (70 mm).

6.4.3. AirFilm cooling coil (70 mm) experimental protocol and analysis

To examine repeatability and evoked force recordings were taken at 0, 15, 30, 40 and 50 minutes. The coil was positioned over the FDI muscle at a site generating an adequate contraction and fixed at this location throughout the experiment. Prior to starting the experiment, five maximum voluntary contractions (MVCs) were recorded and the power of the TMS stimulation was set to 20% of the MVC (Erim et al., 1999). At each stimulation point there were 3 repeat stimulations delivered 15 seconds apart. The stimulation frequency was set to 30 Hz and the pulses delivered during each repeat were 10. For the cooling coil there were 5 participants and in one subject, IHT1, the test was repeated on a different day. The mean and standard error of the mean (SEM) for each time point is displayed in a graph using Excel. The force was recorded using Spike2 software.

6.5. Results: FDI force measurements

Evoked force measurements were normalised to the measurements taken at time 0 min. As this was a control experiment the expectation was that the force would be stable at each time point (0, 15, 30, 40 and 50 min). In Figure.6.4 this was not observed, rather, the results show high variability. The variability was considered too high to form the basis for a controlled experiment without excessive repetition of the stimulus and needlessly prolonging the experiment's duration.

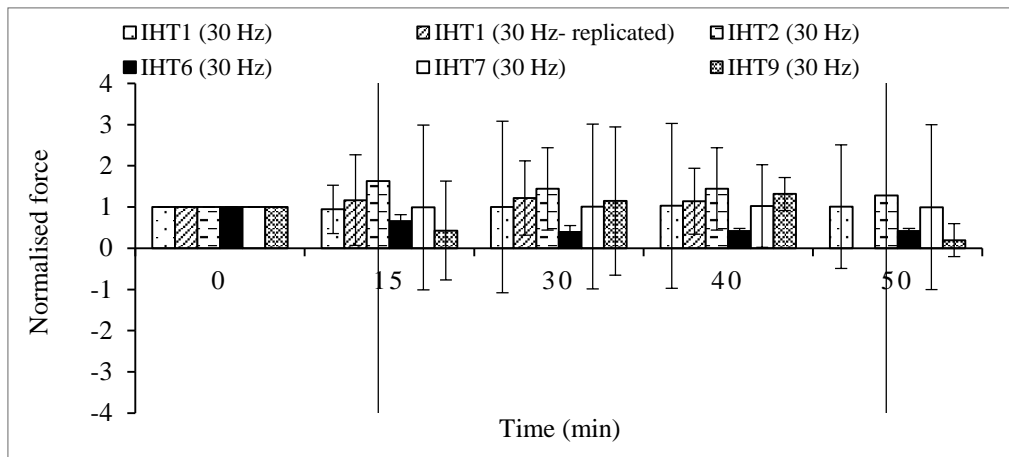


Figure.6.4. Normalised force measurements displayed in a bar graph with error bars (Mean± SEM, n=5). Each bar represents a different participant. Please note that participant with id IHT1 the experiment was replicated on a different day. Furthermore, at time 40 min for the IHT1 (30 Hz- replication) there is no data set.

6.6. Discussion

Research on IHT shows that it improves motor function in patients with SCI. However, there is inadequate information in the literature on the effects of IHT on spinal pathways. Previous results produced in this thesis have shown that IHT increases the magnitude of MEPs measured following the stimulation of the CST using TMS. To fully understand IHT's ability to enhance the excitability of this pathway it was considered important to also study the direct effect of IHT on skeletal muscle output force. As summarised in the introduction section of this report, there is limited understanding on the contractile and endurance characteristics of skeletal muscle following brief periods of hypoxia.

Accordingly, additional experiments were planned to look at electromagnetically stimulating the FDI muscle and measuring force using a strain gauge. However, as described above the pilot experimental set-ups have failed to produce repeatable results that allow effective comparison of data prior to and after IHT. The two essential methodological limitations contributed to high variability, these are: heating of the coil and imprecise control over the site of stimulation. Despite using a cooled coil to reduce coil heating the high frequency and inter-stimulus rate needed for these experiments contributed to unacceptable coil performance and this approach to activate muscle has been abandoned. The alternative approach was to revert to electrical stimulation of the ulnar nerve that innervates the FDI muscle but this method does not allow FDI

activation in isolation and is a painful procedure when evoking a tetanic contraction in hand muscles and so it was not attempted.

Moreover, to investigate the effect of IHT on muscle force output, an alternative experiment was being planned, which involved electrically stimulating a lower limb superficial nerve and recording muscle force using a force sensor that would have been placed on a foot rest (Leslie et al., 1999). Moving to a protocol for activation of a lower limb muscle was favourable because of ease of peripheral nerve stimulation and of force measurement. More information on this experimental design is described in the section below (6.7. Future study).

As mentioned above, the hypothesis to be tested was that brief periods of low oxygen levels are affecting skeletal muscle and could impact its metabolism and consequently force. Furthermore, the benefits observed in iSCI patients following a single exposure to IHT may partly be linked to changes in muscle performance. The following section will describe the future study which was planned to be complete but could not be done due to the COVID lockdown in 2020.

6.7. Future study

The planned experiment was to use functional electrical stimulation (FES) on the common peroneal nerve. The purpose of stimulating the common peroneal nerve is to generate dorsiflexion of the ankle that could be measured using a force sensing foot rest. This nerve innervates the tibialis anterior muscle of the lower leg that is responsible for the dorsiflexion of the ankle (Leslie et al., 1999).

FES of this nerve is well tolerated and can be easily accessed by transcutaneous stimulation. The best location for stimulating the common peroneal nerve can be determined by exploring the skin surface with a bar electrode placed on the side of the popliteal fossa where the nerve passes, along the medial edge of the biceps femoris and around the neck of the fibula within the peroneus longus and divides into the deep and superficial branches (Frigon et al., 2007; Bobet et al., 2005). Moreover, EMG can be used to record muscle activity over the belly of the tibialis anterior muscle simultaneously to the force measurements (Frigon et al., 2007). The location of stimulation will be the one that consistently produces an M-wave in the tibialis anterior

muscle at the lowest stimulation strength. The M-wave is the early EMG evoked response that occurs milliseconds after the stimulation. At the location where the optimal stimulation site is, two self-adhesive disposable silver/silver chloride electrodes will be located for the duration of the experiment. Primarily, the experiment will require measuring the M-wave threshold and the maximum M-wave. To generate a contraction, the level of stimulation will be set to 10% or 20 % of the maximum M-wave intensity. M- wave will be quantified using peak-to-peak amplitude and area under the rectified curve (Bobet et al., 2005).

The isometric force will be measured from the foot using a force sensor attached to the foot rest (an experimental rig similar to the one we aimed to use is shown in Figure.6.5). The position of the foot, ankle and knee joint angles will be

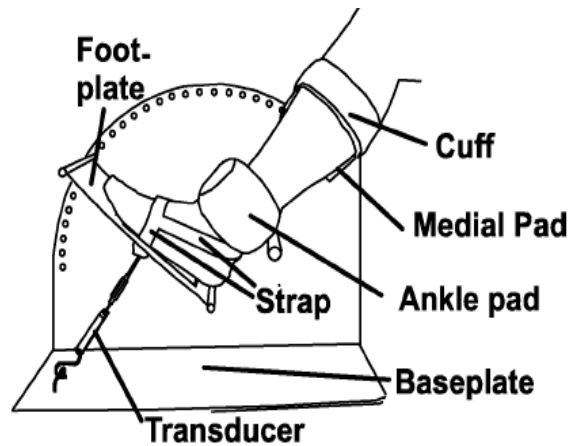


Figure.6.5. Experimental set up (diagram used with permission from Bobet, Gossen and Stein, 2005)

consistent across all participants (Bobet et al., 2005). Force measurements will be taken twice before IHT, once during and thereafter every 10 minutes up to 30 minutes post-IHT. Moreover, to ensure that the nerve excitability remains constant the maximum M-wave will be measured before and after IHT. For this study an ethics approval was granted but no recruitment occurred.

Chapter.7. IHT's mechanism of action and thoughts on implementing IHT in rehabilitation training

7.1. The impact of SCI to the individual and current needs in rehabilitation

SCI results in serious physical disability with secondary medical complications. Accordingly, SCI is a major life event where the individual needs to make many lifelong adaptations to a new way of living. In addition to the huge impact on the quality of life for the individual, living with SCI is also a financial burden with long term significant health care costs and living expenses with the level of injury impacting on prospects of gainful employment (Reeve Foundation, 2020; Savic et al., 2000).

Current intensive rehabilitation methods require very costly specialised equipment and are labour intensive. New treatment methods for SCI that improve recovery are needed and even more so in the recent past with a growing population of elderly patients becoming spinal cord injured (McCaughey et al., 2016). This of course has resulted from an ageing global population that are more socially and economically active coupled with a reduction of younger SCI patients due to better safety standards and initial trauma care for back and neck injuries (McCaughey et al., 2016; Jackson et al., 2004). As there are now more elderly patients with SCI than they were in the past, it is important to consider their physical capabilities and acknowledge that current rigorous rehabilitation methods designed to work for younger age groups are very challenging for elderly SCI patients to accomplish and sustain (Carpino et al., 2018).

7.2. What may be required in incorporating IHT during rehabilitation training

Consequently, this is a pressing issue and researchers are trying to find alternative interventions, that primarily will reduce the level of physical demands on the patient and staff and if possible, reduce the cost and time spent in rehabilitation. Moderate IHT recently became a very attractive intervention because it is inexpensive to purchase with limited additional maintenance costs above individual face masks. Most importantly IHT can reduce the physical demand for the patient as they will not be required to complete an intensive physical training session following IHT to obtain

significant functional benefits. This in turn also reduces labour time within the rehabilitation clinic.

The IHT intervention can be easily incorporated in a rehabilitation regime as it requires minimal training for staff to use a hypoxicator and during the session IHT requires minimal supervision. Moreover, safety monitoring (heart rate and SpO₂ levels) is integrated in most hypoxicators, thus, additional equipment to monitor safety of the patient is not required. Also, the hypoxicator used in this research project has a safety baseline that can be adjusted by the clinician and warns the clinician when the patient's atrial SpO₂ has dropped below a safety level. Lastly, an effective session can be quick, as it is meant for IHT protocol to last 30 minutes (Trumbower et al., 2012), and no physical effort is required from the patient.

However, it may require a hypoxia test, similar to the one used in this thesis, prior to exposing the patient to IHT to see if the patient can tolerate the lower inspirational oxygen. In this study all young healthy participants that volunteered to take part had a good tolerance to hypoxia, however, this may not be the case with SCI patients especially those with compromised respiration (Chapter 2). Furthermore, it may be beneficial to also record MEPs before and following the first session to see if the patient shows responsiveness to this treatment protocol. This is suggested to be implemented in the clinic since in this study some participants did not respond to the IHT intervention (Chapter 5). Moreover, as adaptation to hypoxia were observed in this study (Chapter 2), the IHT protocol may need to be adjusted after several sessions of IHT. One more thing to consider is that individuals respond differently to low oxygen levels (as seen in Chapter 2 some participants had a Type III response while others a Type II response in the hypoxia test) and a personalised IHT protocol needs to be considered. Therefore, the hypoxia test can be used as a test to see if the patient can tolerate low oxygen levels and then it can be used to monitor changes in tolerance to hypoxia over time as the patient is exposed to numerous sessions. The hypoxia test could also be used to monitor changes in tolerance to hypoxia over numerous sessions. Furthermore, rate of drop and recovery in SpO₂ as well as time shift of SpO₂ when compared to O₂ delivery (measurements reported in Chapter 2) are valuable measures

to include while monitoring patient's physiology during the IHT intervention as it will offer information on adaptation.

Lastly, IHT is likely to be advantageous only to incomplete SCI patients with spared serotonergic innervations in the brainstem and spinal cord as serotonin has been established to play an important role as to whether IHT causes an enhanced excitability or not (Baker-Herman and Mitchell, 2002; Bach and Mitchell, 1996; Lynch et al., 2001; Hoffman et al., 2010; Golder and Mitchell, 2005). Moreover, it is essential to consider how IHT will be implemented at early and chronic stages of iSCI. In all cases IHT can be easily implemented prior to rehabilitation and likely could benefit chronic patients that are at a stagnation point in their functional recovery. This reasoning comes from IHT's ability to enhance the baseline levels of BDNF (Welch et al., 2020). In terms of using IHT in acute iSCI patients it is likely to have benefits in enhancing the extent of functional recovery but the patient should be medically stable before IHT could be introduced to their treatment plan.

7.3. Key findings from this project

Above the need of a novel treatment for iSCI has been highlighted as well as the associated benefits of using IHT in the clinic and suggestions on integrating IHT in rehabilitation. Even though IHT is an attractive intervention to implement in rehabilitation there is insufficient information in the literature regarding the safety of the IHT protocol used by Trumbower et al. (2012) and the mechanisms associated with the functional benefits observed in iSCI patients.

The key findings from this project are as follows:

- 1) The IHT intervention by Trumbower et al (2012) is generally safe and with no increase in sympathetic activity over time but there is a variability in each participant's tolerance to IHT (Chapter 2)
- 2) There was no change in sensory evoked excitability following IHT compared to baseline (Chapter 3)
- 3) Considerable changes in MEP related activity were observed on the target muscle, as well as secondary effects on non-targeted muscles following IHT (Chapter 5) and

4) MEP recordings can be used in the clinic to study if the participant responds to IHT and whether following an IHT session the CST connection is stronger or weaker when compared to baseline

What follows below is a discussion on:

- 1) Current knowledge on the safety of the IHT protocol by Trumbower et al (2012), contributions from this thesis and some suggested considerations on using IHT in rehabilitation
- 2) The functional benefits associated with IHT in iSCI patients, current knowledge on IHT's mechanism of action and contributions from this thesis (specifically on the IHT's mechanism of action)
- 3) Discussing possible uses of TMS in clinical settings
- 4) A future study to understand the effects of IHT on skeletal muscle metabolism which was discussed in Chapter 6 and
- 5) Lastly, possible uses of IHT to treat other neurological diseases

7.4. Current knowledge on the safety of the IHT protocol by Trumbower et al. (2012) and thoughts on iSCI patient tolerance

To date there has been no study focusing on the cardiovascular and respiratory effects of this IHT protocol. Researchers tend to report that they monitored heart rate, blood pressure and SpO₂ and state that the intervention is safe (Trumbower et al., 2012; Trumbower et al., 2017; Navarrete-Opazo et al., 2016b; Navarrete-Opazo et al., 2017; Lynch et al., 2016; Hayes et al., 2014).

In terms of clinical application, it is important to mention that SCI can itself induce cardiovascular and/or respiratory complications in patients. Moreover, as already mentioned, the majority of patients that are now admitted to the clinic are elderly, meaning that it is likely they will exhibit some sort of cardiovascular and/or respiratory underlining condition (North and Sinclair et al., 2012; Rojas et al., 2014). Therefore, the IHT protocol may require adjusting for some patients and could perhaps be unsafe for others. Studies to date that have been investigating the effects of IHT on iSCI patients excluding those with cardiopulmonary complications (Trumbower et al.,

2012; Trumbower et al., 2017; Navarrete-Opazo et al., 2016b; Navarrete-Opazo et al., 2017; Lynch et al., 2016; Hayes et al., 2014). Without further study the exclusion of patients with underlying conditions affecting cardiovascular and respiratory function remains appropriate for studies on motor recovery in neurological cases.

Interestingly, moderate IHT could be a possible treatment for a variety of cardiovascular diseases as reported in the review by Serebrovskaya and Xi in 2016. Furthermore, Vogtel and Michels (2010) in their review mention that moderate IHT can be beneficial in patients with COPD as it improved lung diffusion capacity of carbon monoxide and increased exercise tolerance. Additionally, a recently published preliminary study reported that moderate IHT is beneficial in respiratory function in ALS patients by eliciting spinal respiratory motor plasticity, increasing intercostal muscle activity and enhancing tidal volume (Sajjadi et al., 2021). This ability to induce improved respiratory function is in keeping with the view that plasticity associated with hypoxia training is primarily a homeostatic mechanism to ensure oxygenation of the blood is adequate.

7.5. Results from the thesis on the safety and tolerance of the IHT intervention by Trumbower et al. (2012) and considerations for patients

The results in this research show that this IHT intervention is generally safe in healthy young volunteers (Chapter 2) and the findings agree with studies on iSCI patients undergoing IHT as a treatment (Trumbower et al., 2012; Trumbower et al., 2017; Navarrete-Opazo et al., 2016b; Navarrete-Opazo et al., 2017; Lynch et al., 2016; Hayes et al., 2014). However, the research also showed that extending the hypoxia period to 2 minutes resulted in adverse effects such as fatigue, dizziness and breathlessness suggesting a fine line between a beneficial treatment and one that creates adverse effects (Chapter 2).

In this study a hypoxia test was used to screen participants as to whether they can tolerate low oxygen breathing (Chapter 2). The response to the hypoxia test varied among healthy young participants and a variability in response was also observed during the IHT session. As reported in Chapter 2, following the hypoxia test, healthy young participants were allocated either to a basic level of tolerance to hypoxia or an

advanced level of tolerance. It would be interesting to compare statistically cardiorespiratory measurements between the two groups. Unfortunately, this could not be completed in this study as the number of participants in the advance level of tolerance group was limited. However, a difference in response suggests a possible need for personalised intervention. Also, from studying the characteristics of the SpO₂ response over time in each participant it was apparent that the lag time measured in seconds increased as the participants became accustomed with this IHT protocol (Chapter 2). There is an apparent change in the tolerance to low oxygen over time, suggesting the possible need to alter the dose of the IHT protocol after several exposures in order to adequately challenge the homeostasis of the patient (Chapter 2). However, these are just speculations as there is no current data displaying that those that have a better tolerance to IHT have less or more benefits in functional output. Moreover, the results displayed that the SpO₂ response cannot be easily predicted as it is out of synch from the O₂ percentage delivery (Chapter 2) and this can be dangerous when dealing with patients in the clinic that could have other underlining health conditions.

The use of a hypoxia test may be beneficial in clinical settings prior to exposing patients to the IHT intervention to classify the response of the individual to low oxygen breathing and adjust the IHT intervention dose and duration accordingly as well as monitoring changes in patient's tolerance to hypoxia over time. By monitoring changes in patient's tolerance to hypoxia the clinician can make an informed decision to alter the intervention so the patient's homeostasis is adequately challenged. With several IHT sessions it is also important to examine the safe frequency of delivering IHT. As previously mentioned, there is a fine line between a safe and beneficial intervention and one that is unsafe which may lead to adverse effects. Studies have reported that 5 consecutive days of IHT followed by 3 sessions a week for 3 weeks is safe for iSCI patients (Navarrete-Opazo et al., 2017; Trumbower et al., 2017). However, more research is required.

Overall, there is now knowledge based on the work that Christiansen et al. (2017) and this study that a single session of IHT causes corticospinal excitability healthy subjects (Chapter 5) and a functional improvement in patients (Navarrete-

Opazo et al., 2016b; Navarrete-Opazo et al., 2017; Lynch et al., 2016; Hayes et al., 2014; Trumbower et al., 2017). Moreover, several sessions of IHT over four weeks have been studied and show an increasing benefit of IHT on functional improvement over time (Navarrete-Opazo et al., 2016b). Studies looking at the effects of IHT over a longer period are required to investigate if there is a ceiling effect of IHT in patients. Furthermore, when a ceiling is reached, it may be beneficial to examine whether it is related to tolerance. If related to tolerance, changing the dose, duration and frequency of the intervention may surpass this effect and allow the patient to acquire the benefits of the treatment over a longer time period.

Lastly, without proper understanding of the systematic effects of IHT throughout the body, exposing patients over several sessions of IHT can be dangerous. Currently there is lack of knowledge on the effects of this intervention on cerebral oxygen concentration or the level of oxygenation that triggers adaptive reaction within the CNS as opposed to adverse outcomes. Cerebral oxygenation can be studied using near-infrared spectroscopy. It may be of interest to see the effects of IHT on brain oxygenation in a single IHT session and also after several sessions. Having an understanding of cerebral oxygen concentration during and following IHT will provide information on safety.

7.6. Functional benefits in iSCI following IHT

In patients with iSCI, it is believed that IHT enhances the excitability of spared motor neuron pathways which in this study lasted through to the last measurements taken at 30 minutes following IHT while Christiansen et al (2018) has reported from one participant that the effects last up to 120 minutes. This time window allows for many rehabilitation approaches currently being used to be performed following IHT. Combining IHT with conventional rehabilitation methods in this way has shown to have a greater significant effect on motor function, even following a single treatment in iSCI patients, when compared to rehabilitation training without prior exposure to IHT (Trumbower et al., 2012; Trumbower et al, 2017; Hayes et al., 2014; Navarrete-Opazo et al., 2016b; Navarrete-Opazo et al., 2017). Several studies have now been conducted using this intervention on iSCI patients and report improvements in walking speed, walking endurance, dynamic balance and muscle strength (Trumbower et al.,

2012; Trumbower et al, 2017; Hayes et al., 2014; Navarrete-Opazo et al., 2016b; Navarrete-Opazo et al., 2017). One study even reported that a few sessions of IHT coupled with rehabilitation training lead to functional improvement in some iSCI patients to the extent where they were able to walk without walking aids suggesting that IHT had an impact on both power and muscle coordination (Navarrete-Opazo et al., 2016b).

Also, it is important to consider that IHT has been shown to induce functional improvement in iSCI alone without the use of conventional rehabilitation methods (Trumbower et al., 2012) and this may be important when considering how to rehabilitate elderly patients. However, it is likely that some rehabilitation training will be required for long term changes in motor function to take place. Furthermore, it has been highlighted in the literature that a task-specific training needs to be paired with IHT in order to see functional benefits (Welch et al., 2020). Navarrete-Opazo et al (2017) mentioned that walking speed was significantly improved in patients participating in BWSTT but not in standing balance. Given that BWSTT is not specifically designed to improve standing balance, this may not be a surprise and suggests IHT should be paired with TST.

Regarding pairing IHT with TST, Welch et al (2020) proposed a hypothetical theory for this synergistic effect. The neural network model by Welch et al (2020) suggested that IHT activates the nucleus tractus solitarius which projects to the central pattern generator and both of these are likely to directly activate raphe nuclei in the brainstem. These raphe nuclei then project to phrenic and limb motor neurons. TST also directly activates task-specific circuits in phrenic and limb motor neurons (Welch et al., 2020). Moreover, Welch et al (2020) proposed that the factor heavily associated with an enhanced activity-induced plasticity is BDNF. In summary, the theory suggests that IHT creates a higher baseline BDNF level in the CNS that lasts for hours and when TST is introduced after IHT it triggers additional BDNF synthesis in task-specific motor circuits (Welch et al., 2020). Essentially, higher levels of BDNF seem to significantly enhance the activity-induced plasticity of TST (Welch et al., 2020).

7.7. Current knowledge on IHT's mechanism of action

IHT could be a great addition in rehabilitation, however, it is important to understand the neural and chemical mechanisms involved with IHT which causes these beneficial effects in iSCI patients. Primarily, information on the mechanism of action of IHT on somatic neuroplasticity originated from studies investigating the effects of this intervention on respiratory plasticity. It has been established that spared serotonergic innervation (in the brainstem and spinal cord) and BDNF are important factors to elicit LTF in phrenic motor neurons (Dale, Mabrouk and Mitchell, 2014; Baker-Herman et al, 2004; Kinkead et al., 2001). The main pathway (Q pathway) involves the activation 5-HT₂ receptor (serotonin type 2 receptor) on the surface of the phrenic motor neuron, activation of the G_q intracellular receptor, the synthesis of BDNF, activation of TrkB receptor and ultimately a strengthening of synapses between the brainstem and the spinal cord in animal models (Dale, Mabrouk and Mitchell, 2014).

There is also another pathway known as the S pathway that interacts with the Q pathway via cross-talk inhibition and the dose of IHT seems to play an important role in which pathway dominates. A moderate dose favours the Q pathway resulting in LTF, an intermediate dose cancels the two pathways out, and no plastic changes occur, and a severe dose favours the S pathway leading to adverse effects (Hoffman and Mitchell 2013; Fields, Springborn and Mitchell, 2015; Wu et al., 2020). This suggests that finding the correct dose of IHT is very important when treating patients.

Subsequently, Christiansen et al (2017) demonstrated an increase in MEPs on hand muscles following IHT and this increase in MEP amplitude lasted long after the end of the treatment. Moreover, Christiansen et al (2017) reported that IHT's actions likely result from corticospinal-motoneuronal synaptic plasticity. Moreover, they also showed that the effects of IHT intervention actions reside within the spinal cord since no change was observed in the magnitude of SICI and ICF circuits following IHT (Christiansen et al.,2017). In this thesis by looking at success rate of activating the target and non-target muscles pre-, during and post-IHT we indirectly measured cortical excitability (Chapter 5). The results did not show a clear pattern as to whether following IHT there was a change in success rate. Please keep in mind that a navigation

system was used, allowing at every stimulus a high precision in coil placement over the 'hotspot' (Chapter 6). Lastly, Christiansen et al (2017) found that IHT did not affect motoneuronal excitability directly, leaving the mechanism of action unresolved.

In this study the question of whether IHT creates a general excitability in the CNS in both sensory and motor spinal pathways as well as changes in muscle metabolism were of interest. The sensory ascending spinal pathway was studied by measuring SEP recordings from the somatosensory cortex using EEG following a peripheral stimulus and the motor descending spinal pathway was examined by recording MEPs from lower limb muscles following a stimulus to the motor cortex (Chapter 3; Chapter 5). To study the effects of IHT on these pathways, recordings were taken prior, during and up to 30 minutes after IHT.

The results in this project established that IHT favours the descending motor pathways rather than creating a general excitability change in the CNS (Chapter 3; Chapter 5). Furthermore, since the research reports a significant increase in MEP amplitude recorded from lower limb muscles it suggests that IHT could be used to improve gait, postural control and voluntary function in iSCI patients (Chapter 5). These findings add to the research by Christiansen et al. (2017) where it displayed that IHT creates enhanced excitability in the upper limb. The results also showed that the enhanced corticospinal excitability is not restricted to single muscle pools as MEP measurements were recorded from the target lower limb muscle (TA R) and other lower limb muscles (TA L and SOL R). Furthermore, as suggested by Christiansen et al (2017) the effects of IHT outlasted the intervention in the TMS targeted muscle. However, in the other lower limb muscles where MEPs were measured a significant decrease was observed 30 minutes following the IHT intervention and may be a consequence of secondary effects within spinal circuits (e.g. from Ia inhibitory interneurons from the TA R muscle projected to motor neurons of the antagonistic SOL R muscle or by crossed reflexes to the TA L muscle). To understand this better local changes in the spinal cord could be studied using H-reflex experiments. However, the effects could also be cortical as TMS modulates intracortical neural activity. These are speculations and further studies need to be conducted and on a larger sample size. Generally, the findings in Chapter 5 are in agreement and also add to the conclusions

made by Christiansen et al. (2017) on the upper limb. Furthermore, the results agree that functional benefits are likely to be observed in patients following IHT where some corticospinal pathways remain intact.

It is important to mention that MEPs, compared to SEPs, are more variable and the variability in MEPs in the study was acceptable and comparable to studies in the literature. Please keep in mind that with the experimental design used in Chapter 5 it was not feasible to increase the number of MEPs recorded, in order to enhance reliability, mainly because of safety as well as influence of TMS on intracortical neural activity. However, to enhance reliability a navigation system described in Chapter 4 was used and with a very high precision of coil placement over the ‘hotspot’ the peak and trough variability of the two baseline measurements was around 13% and with this peak and trough variability the coefficient of variability was calculated to be 35% for AUC and 38% for peak-to-peak amplitude for the target muscle. These values are similar to what is reported in the literature (Darling et al., 2006). Moreover, to enhance reliability, the two baseline measurements were pooled (Chapter 5).

Overall, the results in this study agree with the functional improvement reported in studies examining IHT on patients with iSCI and that these improvements reflect neuroplasticity (Chapter 5). However, a major limitation was not including tests with a sham condition. Having a sham treatment group would provide a robust means of controlling participant bias as well as possible changes in excitability as a result of repetitive TMS stimulation. While it was planned to complete this experiment, the rules imposed during the Covid-19 outbreak made such testing impossible to do due moratorium on experimental work in the laboratory. Nevertheless, it is important to highlight that the increase in MEP amplitude observed remains unlikely to be consequence of prior TMS stimulations associated with locating the hotspot site for the target muscle. In this study universally accepted methods developed in the late 1980s for locating the hotspot were employed which minimise the number of stimulations and the intensity of stimulation used for hotspot mapping. A key aspect of hotspot testing is not to stimulate at rates which lead to temporal summation of evoked synaptic effects or MEPs. Thus in hotspot detection the use of low TMS intensity, the use of appropriate interstimulus intervals (10 seconds) and prior

knowledge on the general anatomical search area (reducing the number of TMS events used) leads to robust mapping without concern of inducing lasting excitability changes interfering with experimental findings. This is further evidenced by the recent study by Hashemirad et al. (2017) who demonstrated that three time separated blocks of 20 TMS events at 120% of the RMT had no effect on MEP amplitude across each of the blocks (graph included in Appendix V). Such stability in TMS, MEPs over time in subjects receiving no interventions strengthen the validity of the results presented here which show a rise in MEP amplitude in the lower limb following IHT. As these results also extend upon the similar findings published on effects measured in the upper limb (Christiansen et al. 2018), the lack of a sham group within this study does not detract from the primary effect reported that a single IHT session promotes a long lasting facilitation of MEPs in the lower limb.

Moreover, it is important to highlight that in this study healthy young participants were recruited in preference to elderly participants. The choice for recruiting healthy young participants was primarily based on the desire to generate data comparable to the study by Christiansen et al. (2018) and secondly to gain experience of the technique, its tolerance and safety. This study was also the first use of IHT within the University of Strathclyde and was planned as the precursor to additional studies in elderly and patient cohorts. In this regard recruitment of elderly subjects potentially increases the risk of recruiting individuals with undiagnosed cardiovascular or respiratory conditions, thereby increasing the likelihood of an adverse event and therefore the need for more medical pre-test health assessments. Accordingly, (for ethical and safety reasons) the initial IHT research at Strathclyde was designed to acquire data in healthy young controls before moving into translational clinical studies with an experienced staff familiar with the IHT technique and its use in experimental design. An underlying principle of all the work produced by the Neurophysiology Laboratory at the University of Strathclyde is to only proceed to clinical studies when a technique has been evaluated as safe to use and is judged to have potential to benefit elderly subjects or patients. Studies on healthy adults are therefore a standard way to explore the potential of innovative techniques for use in rehabilitation.

7.8. Possible uses of TMS in clinical setting

After studying the effects of IHT on the corticospinal tract it was apparent that MEPs can be used in the clinic to screen non-responders to the intervention. To clarify, non-responders displayed no change in MEP amplitude following IHT when compared to baseline. There are two reasons identified that could possibly make a patient not respond to IHT: 1) the intervention is not challenging enough or 2) they carry a BDNF mutation. Chapter 2 clearly showed that individuals have different responses to the hypoxia test and the ‘moderate’ IHT intervention used here. This may also explain why some participants in this research responded to the intervention while others did not (Chapter 5).

Another possible reason why some participants did not respond to the intervention is the BDNF mutation that affects 25% of the population (Duman et al., 2016; Lamy and Boakye, 2013). It has been highlighted in the literature review that BDNF plays a major role in the mechanism of IHT’s action and this mutation discourages neuroplasticity (Duman et al., 2016; Lamy and Boakye, 2013; Welch et al., 2020). Lamy and Boakye (2013) reported that humans who carried the mutation had significantly lower spinal plasticity compared to those without the mutation following direct current stimulation. Thus, some patients may not respond to the IHT intervention because they carry this mutation. Testing for BDNF mutation in studies using IHT as a treatment for iSCI might be beneficial in understanding why some patients may not benefit from this intervention in the clinic.

Moreover, it is important to mention that intense training is capable in overcoming the effects of BDNF Val66Met mutation allowing plastic changes to take place (McHughen et al., 2011). Hence, we speculate that combining IHT with moderate rehabilitation training could have the same effect since IHT, as Welch et al. (2020) proposed, is believed to increase the baseline BDNF levels in the CNS. Further investigations are required to test this theory, however, if correct, IHT could help patients that are unresponsive to current rehabilitation methods as a result of the BDNF mutation. It is important to mention that BDNF levels can be decreased by aging and hormones, meaning that there are other factors that could lead to unresponsiveness (Lommatzsch et al., 2005; Numakawa et al., 2010).

It is hard to say what led to some participants responding to the intervention and others not. Moreover, the experiments were completed in healthy young subjects, meaning that in patients there could be more factors that can make them non-responsive to IHT, for instance, elevated inflammatory factors at the site of injury are known to affect plasticity (Tan, Barth and Trumbower, 2020). Overall, further investigations are required with larger sampling. However, what could be of benefit in the clinic is to test whether the patient is a responder to the IHT intervention by recording MEPs before and following IHT where an increase in the MEP amplitude would indicate that the patient is likely to respond to this treatment as part of this rehabilitation.

In this study it was also apparent that some participants can demonstrate a long term depression and thus will not benefit from the treatment. TMS can be used to screen for patients that show a depression in the MEP amplitude following IHT when compared to baseline. For instance, participant IHT2 in this study displayed a long term depression following IHT. This could be a frequent occurrence and more studies with a larger sample size are required. Long term depression could have been caused from repetitive TMS stimulation or it could be related to IHT's actions in the individual. If it is related to the IHT intervention, this highlights that the intervention may not be beneficial for every patient and screening will probably be required.

7.9. Future study: Studying skeletal muscle contractile activity following IHT

After studying the safety of the IHT intervention, the effects on sensory pathways and its effects on motor pathway the plan was to study skeletal muscle metabolism which in turn affects its muscle contractile activity. The hypothesis states that to understand further the true potential of IHT's ability to change the excitability of spinal pathways it is essential to examine possible changes in skeletal muscle metabolism that will in turn affect its contractile behaviour and power output. This would have been a major study for this thesis, however, because of Covid-19 this experiment was not able to be completed.

There is speculation that the functional benefits observed in iSCI, where scientists report a 20% to 82% increase in plantar flexion torque following a single intervention with IHT (Trumbower et al., 2012; Lynch et al., 2017; Sadhu et al., 2019),

are a combination of effects and perhaps IHT induced changes include potentiation of muscle contractile activity (Chapter 6). If IHT affects muscle metabolism it is likely to contribute to the increase in MEPs, muscle force and walking speed reported in the literature (Christiansen et al., 2017; Trumbower et al., 2012; Sadhu et al., 2019; Navarrete-Opazo et al., 2017).

7.10. Thoughts on the use of IHT to treat other neurological conditions

Lastly, it is important to consider how IHT can be used to help patients with other neurological conditions. IHT prior to rehabilitation can help stroke patient's connections between the damaged cortex, brainstem and spinal cord and compensate for the reduced level of corticospinal function resulting from stroke. Depending on the tissue damage and the needs of the patients, the clinician will be likely required to pair IHT with TST. A potential beneficial combination treatment method is pairing TMS stimulation (which can induce neuroplasticity in the brain), IHT and rehabilitation training. Currently there is no studies on the effects of IHT on stroke patients. Moreover, IHT may help with cerebral palsy and traumatic brain injury. In young children and babies, IHT seems to be an attractive intervention as it does not necessarily require a rehabilitation session to provide functional benefits. Also in children where the CNS is immature and the corticospinal tract has not yet fully developed, studying the effects of IHT will be advantageous for providing information on the mechanism of action. Furthermore, IHT can aid recovery after orthopaedic surgery, especially patients that spend a lot of time in bedrest where issues such as muscle weakness and atrophy accompany bedrest. Lastly, it is important to mention that there are speculations that IHT may be able to reduce spasticity and allodynia (Tan, Barth and Trumbower, 2010; Tashiro et al., 2015; Schulze et al., 2018). These speculations are associated with the ability of BDNF to upregulate KCC2 receptor in motoneurons. Reducing spasticity and neuropathic pain will be beneficial for SCI and other neurological conditions. Overall, there are many unexplored potential uses of IHT, above are some possible applications.

7.11. Conclusion

In terms of the mechanism of action, this research reports no effects of IHT on the sensory pathways while a significant increase in the excitability of the corticospinal tract innervating lower limb muscles was formed. The effects of IHT are thought to be subcortical (Christiansen et al., 2017). However, no studies have looked at changes of muscle metabolism following IHT and as a result possible change in muscle force remaining to be done. IHT could have effects both in the brainstem and spinal cord but also in muscle. Therefore, to date there remains a need for further understanding on IHT's mechanism of action.

In terms of incorporating IHT in the rehabilitation system that is currently in place, it is clear that a hypoxicator: 1) requires minimal training, 2) it does not require patients to do any activity whilst getting the IHT treatment, 3) it can be given whilst a patient sits or may be in bed and 4) is an inexpensive addition to the clinic and without any major maintenance expenses. Moreover, as reported in Chapter 2 the intervention is generally safe but there was apparent variability in tolerance and further research is required as to whether adjustments in the treatment is required. Lastly, it may be worth considering using a hypoxia test to study tolerance to hypoxia in patients and possibly screening patients by measuring MEPs.

However, whether IHT can be advantageous in treating the growing population of elderly iSCI patients is questionable because with an increase in age there is an increase in the likelihood of the individual having cardiopulmonary underlying conditions and IHT may not be a safe treatment of these patients (North and Sinclair et al., 2012; Rojas et al., 2014). However, the literature reports potential benefits of mild to moderate IHT on cardiopulmonary health suggesting to be acceptable to use in some cases. Further investigations are required but overall, it seems that IHT could be a promising treatment for iSCI and may also be of benefit patients with other neurological diseases. Research on the benefits of IHT in other neurological diseases is still needed to be done.

References

Websites

Axilum Robotics [EN]. 2021. Axilum Robotics - Robot for transcranial magnetic stimulation. [online] Available at: <<https://www.axilumrobotics.com/en/?noredirect=en-US>> [Accessed 25 November 2021].

Brainbox. 2021. Brainsight TMS Navigation by Brainbox. [online] Available at: <<https://brainbox-neuro.com/products/brainsight-tms-navigation>> [Accessed 25 November 2021].

Oed.com. 2021. Home: Oxford English Dictionary. [online] Available at: <<https://www.oed.com/>> [Accessed 25 November 2021].

Reeve Foundation. (2020). Costs of Living with Spinal Cord Injury. [online] Reeve Foundation. Available at: <<https://www.christopherreeve.org/living-with-paralysis/costs-and-insurance/costs-of-living-with-spinal-cord-injury>> [Accessed 24 August 2020].

Seniam.org. (2021). Welcome to SENIAM. [online] Available at: <<http://www.seniam.org/>> [Accessed 20 March 2021].

Statista. 2021. Spinal cord injuries: common causes 2015 Statistic | Statista. [online] Available at: <<https://www.statista.com/statistics/448888/spinal-cord-injury-common-causes-united-kingdom-uk/>> [Accessed 24 November 2021].

Journals/ Books

Abboud, F. and Kumar, R. (2014). Obstructive sleep apnea and insight into mechanisms of sympathetic overactivity, *Journal of Clinical Investigation*, 124(4), pp. 1454–1457. doi: 10.1172/JCI70420.

Agosto-Marlin, I. M. and Mitchell, G. S. (2017). Spinal BDNF-induced phrenic motor facilitation requires PKC θ activity, *Journal of Neurophysiology*, 118(5), pp. 2755–2762. doi: 10.1152/jn.00945.2016.

Akselrod, S. et al. (1981). Power Spectrum Analysis of Heart Rate Fluctuation: A Quantitative Probe of Beat-to-Beat Cardiovascular Control, *American Association for the Advancement of Science*, 213, pp. 1–3.

Alexander, M. S. et al. (2010). Outcome Measures in Spinal Cord Injury, *Nature-Spinal cord*, 47(8), pp. 582–591. doi: 10.1038/sc.2009.18.

Al-Majed, A. A., Siu, L. T. and Gordon, T. (2004). Electrical stimulation accelerates and enhances expression of regeneration-associated genes in regenerating rat femoral motoneurons, *European Journal of Neuroscience*, 24(3), pp. 379–402. doi: 10.1023/B:CEMN.0000022770.66463.f7.

Ambrosini, E. et al. (2018). StimTrack: An open-source software for manual transcranial magnetic stimulation coil positioning, *Journal of Neuroscience Methods*. Elsevier B.V., 293, pp. 97–104. doi: 10.1016/j.jneumeth.2017.09.012.

Aminoff, M. J. (2012). *Electroencephalography: general principles and clinical applications*. 6th edn, Aminoff's *Electrodiagnosis in Clinical Neurology*. 6th edn. Elsevier Inc. doi: 10.1016/B978-1-4557-0308-1.00003-0.

Andrew, D. et al. (2015). Somatosensory evoked potentials show plastic changes following a novel motor training task with the thumb, *Clinical Neurophysiology*. International Federation of Clinical Neurophysiology, 126(3), pp. 575–580. doi: 10.1016/j.clinph.2014.05.020.

Arai, N. et al. (2005). Comparison between short train, monophasic and biphasic repetitive transcranial magnetic stimulation (rTMS) of the human motor cortex, *Clinical Neurophysiology*, 116(3), pp. 605–613. doi: 10.1016/j.clinph.2004.09.020.

Ashammakhi, N. et al. (2019). Regenerative Therapies for Spinal Cord Injury, *Tissue Engineering - Part B: Reviews*, 25(6), pp. 471–491. doi: 10.1089/ten.teb.2019.0182.

ATS statement: guidelines for the six-minute walk test. ATS Committee on Proficiency Standards for Clinical Pulmonary Function Laboratories. *Am J Respir Crit Care Med* 2002;166(1):111–117.

Bach, K. B. and Mitchell, G. S. (1996). Hypoxia-induced long-term facilitation of respiratory activity is serotonin dependent, *Respiration Physiology*, 104(2–3), pp. 251–260. doi: 10.1016/0034-5687(96)00017-5.

- Baker-Herman, T. L. et al. (2004). BDNF is necessary and sufficient for spinal respiratory plasticity following intermittent hypoxia, *Nature Neuroscience*, 7(1), pp. 48–55. doi: 10.1038/nn1166.
- Baker-Herman, T. L. and Mitchell, G. S. (2002). Phrenic long-term facilitation requires spinal serotonin receptor activation and protein synthesis, *Journal of Neuroscience*, 22(14), pp. 6239–6246. doi: 10.1523/jneurosci.22-14-06239.2002.
- Banala, S. K. et al. (2008). Robot assisted gait training with active leg exoskeleton (ALEX), *Proceedings of the 2nd Biennial IEEE/RAS-EMBS International Conference on Biomedical Robotics and Biomechanics, BioRob 2008*, 17(1), pp. 653–658. doi: 10.1109/BIOROB.2008.4762885.
- Bareyre, F. M. et al. (2004). The injured spinal cord spontaneously forms a new intraspinal circuit in adult rats, *Nature Neuroscience*, 7(3), pp. 269–277. doi: 10.1038/nn1195.
- Bassovitch, O. and Serebrovskaya, T. V. (2009). Equipment and regimes for intermittent hypoxia therapy, Chapter 30, pp. 589–601. From: Xi L., Serebrovskaya, T.V. (2009). *Intermittent Hypoxia: from molecular mechanisms to clinical applications*. Nova Publishers.
- Bastani, A. and Jaberzadeh, S. (2012). A Higher Number of TMS-Elicited MEP from a Combined Hotspot Improves Intra- and Inter-Session Reliability of the Upper Limb Muscles in Healthy Individuals, *PLoS ONE*, 7(10). doi: 10.1371/journal.pone.0047582.
- Béguin, P. C. et al. (2005). Acute intermittent hypoxia improves rat myocardium tolerance to ischemia, *Journal of Applied Physiology*, 99(3), pp. 1064–1069. doi: 10.1152/jappphysiol.00056.2005.
- Behan, M., Zabka, A. G. and Mitchell, G. S. (2002). Age and gender effects on serotonin-dependent plasticity in respiratory motor control, *Respiratory Physiology and Neurobiology*, 131(1–2), pp. 65–77. doi: 10.1016/S1569-9048(02)00038-1.
- Behrman, A. L. and Harkema, S. J. (2000). *Spinal Cord Injury : A Series of Case Studies*, *Physical Therapy-Spinal Cord Injury Special Series*, 80(7), pp. 688–700.
- Berry, H. R., Tate, R. J. and Conway, B. A. (2017). Transcutaneous spinal direct current stimulation induces lasting fatigue resistance and enhances explosive vertical jump performance, *PLoS ONE*, 12(4), pp. 1–16. doi: 10.1371/journal.pone.0173846.
- Bestmann, S. and Krakauer, J. W. (2015). The uses and interpretations of the motor-evoked potential for understanding behaviour, *Experimental Brain Research*, 233(3), pp. 679–689. doi: 10.1007/s00221-014-4183-7.
- Bisogni, V. et al. (2016). The sympathetic nervous system and catecholamines metabolism in obstructive sleep apnoea, *Journal of Thoracic Disease*, 8(2), pp. 243–254. doi: 10.3978/j.issn.2072-1439.2015.11.14.
- Bobet, J., Gossen, E. R. and Stein, R. B. (2005). A comparison of models of force production during stimulated isometric ankle dorsiflexion in humans, *IEEE Transactions on Neural Systems and Rehabilitation Engineering*, 13(4), pp. 444–451. doi: 10.1109/TNSRE.2005.858461.
- Bobyleva, O. V. and Glazachev, O. S. (2007). Changes in autonomic response and resistance to acute graded hypoxia during intermittent hypoxic training, *Human Physiology*, 33(2), pp. 199–206. doi: 10.1134/S0362119707020107.
- Bos, R. et al. (2013). Activation of 5-HT_{2A} receptors upregulates the function of the neuronal K-Cl cotransporter KCC2, *Proceedings of the National Academy of Sciences of the United States of America*, 110(1), pp. 348–353. doi: 10.1073/pnas.1213680110.
- Bracken, M. B. et al. (1992). Methylprednisolone or naloxone treatment after acute spinal cord injury: 1-year follow-up data: Results of the second National Acute Spinal Cord Injury Study, *Journal of Neurosurgery*, 76(1), pp. 23–31. doi: 10.3171/jns.1992.76.1.0023.
- Bruton, A., Conway, J. H. and Holgate, S. T. (2000). Reliability: What is it, and how is it measured?, *Physiotherapy*, 86(2), pp. 94–99. doi: 10.1016/S0031-9406(05)61211-4.
- Burns, A. S. et al. (2012). Clinical diagnosis and prognosis following spinal cord injury. 1st edn, *Handbook of Clinical Neurology*. 1st edn. Elsevier B.V. doi: 10.1016/B978-0-444-52137-8.00003-6.
- Burtscher, M. et al. (2004). Intermittent hypoxia increases exercise tolerance in elderly men with and without coronary artery disease, *International Journal of Cardiology*, 96(2), pp. 247–254. doi: 10.1016/j.ijcard.2003.07.021.

- Cacchio, A. et al. (2011). Reliability of TMS-related measures of tibialis anterior muscle in patients with chronic stroke and healthy subjects, *Journal of the Neurological Sciences*. Elsevier B.V., 303(1–2), pp. 90–94. doi: 10.1016/j.jns.2011.01.004.
- Caizhong, X. et al. (2014). The application of somatosensory evoked potentials in spinal cord injury rehabilitation, *NeuroRehabilitation*, 35(4), pp. 835–840. doi: 10.3233/NRE-141158.
- Carpino, G. et al. (2018). Assessing Effectiveness and Costs in Robot-Mediated Lower Limbs Rehabilitation: A Meta-Analysis and State of the Art, *Journal of Healthcare Engineering*. Hindawi, 2018. doi: 10.1155/2018/7492024.
- Carroll, T. J., Riek, S. and Carson, R. G. (2001). Reliability of the input-output properties of the cortico-spinal pathway obtained from transcranial magnetic and electrical stimulation, *Journal of Neuroscience Methods*, 112(2), pp. 193–202. doi: 10.1016/S0165-0270(01)00468-X.
- Casas, M. et al. (2000). Intermittent hypobaric hypoxia induces altitude acclimation and improves the lactate threshold, *Aviation Space and Environmental Medicine*, 71(2), pp. 125–130.
- Chacaroun, S. et al. (2017). Physiological responses to two hypoxic conditioning strategies in healthy subjects, *Frontiers in Physiology*, 7, pp. 1–20. doi: 10.3389/fphys.2016.00675.
- Chaillou, T. (2018). Skeletal muscle fiber type in hypoxia: Adaptation to high-altitude exposure and under conditions of pathological hypoxia, *Frontiers in Physiology*, 9, pp. 1–17. doi: 10.3389/fphys.2018.01450.
- Christiansen, L. et al. (2018). Acute intermittent hypoxia enhances corticospinal synaptic plasticity in humans, *eLife*, 7, pp. 1–17. doi: 10.7554/eLife.34304.
- Chung Tae, K. P. and T. E. L. (2014). Peripheral Neuropathy-Clinical and Electrophysiological Considerations, *National Institutes of Health*, 24(1), pp. 49–65. doi: 10.1016/j.nic.2013.03.023.Peripheral.
- Clanton, T. and Klawitter, P. F. (2001). Physiological and Genomic Consequences of Intermittent Hypoxia Invited Review: Adaptive responses of skeletal muscle to intermittent hypoxia: the known and the unknown, *Journal of Applied Physiology*, 90(2475–2487), pp. 1593–1599. Available at: <http://www.ncbi.nlm.nih.gov/pubmed/11007556>.
- Cohen, D. and Cuffin, B. N. (1991). Developing a More Focal Magnetic Stimulator.Part I: Some Basic Principles. *Journal of Clinical Neurophysiology*, pp. 102–111.
- Cohen, G., Riahi, Y. and Sasson, S. (2012). Free Radicals and Metabolic Disorders, *Encyclopedia of Radicals in Chemistry, Biology and Materials*. doi: 10.1002/9781119953678.rad057.
- Cowen, P. J. (2002). Cortisol, serotonin and depression: All stressed out?, *British Journal of Psychiatry*, 180, pp. 99–100. doi: 10.1192/bjp.180.2.99.
- Cramer, G., Darby, S. and Cramer, G. (2014). *Clinical Anatomy Of The Spine, Spinal Cord, And ANS*. St. Louis: Elsevier.
- Cruccu, G. et al. (2008). Recommendations for the clinical use of somatosensory-evoked potentials, *Clinical Neurophysiology*, 119(8), pp. 1705–1719. doi: 10.1016/j.clinph.2008.03.016.
- Cruse, R. et al. (1982). Paradoxical Lateralization of Cortical Potentials Evoked by Stimulation of Posterior Tibial Nerve, *Archives of Neurology*, 39(4), pp. 222–225. doi: 10.1001/archneur.1982.00510160028005.
- Curt, A., Schwab, M.E., Dietz, V.(2004). Review: Providing the clinical basis for new interventional therapies: refined diagnosis and assessment of recovery after spinal cord injury, *Spinal Cord*, 42, pp. 1-6. doi:10.1038/sj.sc.3101558
- Dale, E. A., Ben Mabrouk, F. and Mitchell, G. S. (2014). Unexpected benefits of intermittent hypoxia: Enhanced respiratory and nonrespiratory motor function, *Physiology*, 29(1), pp. 39–48. doi: 10.1152/physiol.00012.2013.
- Dale-Nagle, E. A. et al. (2010). Spinal plasticity following intermittent hypoxia: Implications for spinal injury, *Annals of the New York Academy of Sciences*, 1198, pp. 252–259. doi: 10.1111/j.1749-6632.2010.05499.x.
- Danner, N. et al. (2008). Navigated transcranial magnetic stimulation and computed electric field strength reduce stimulator-dependent differences in the motor threshold, *Journal of Neuroscience Methods*, 174(1), pp. 116–122. doi: 10.1016/j.jneumeth.2008.06.032.
- Darling, W. G., Wolf, S. L. and Butler, A. J. (2006). Variability of motor potentials evoked by transcranial

- magnetic stimulation depends on muscle activation, *Experimental Brain Research*, 174(2), pp. 376–385. doi: 10.1007/s00221-006-0468-9.
- Dasari, V. R. (2014). Mesenchymal stem cells in the treatment of spinal cord injuries: A review, *World Journal of Stem Cells*, 6(2), p. 120. doi: 10.4252/wjsc.v6.i2.120.
- Deldicque, L. and Francaux, M. (2013). Acute vs chronic hypoxia: what are the consequences for skeletal muscle mass?, *Cellular and Molecular Exercise Physiology*, 2(1). doi: 10.7457/cmep.v2i1.e5.
- Deng, J. et al. (2018). Cell Transplantation for Spinal Cord Injury: Tumorigenicity of Induced Pluripotent Stem Cell-Derived Neural Stem/Progenitor Cells, *Stem Cells International*. Hindawi, 2018. doi: 10.1155/2018/5653787.
- Deng, Z. De, Lisanby, S. H. and Peterchev, A. V. (2013). Electric field depth-focality tradeoff in transcranial magnetic stimulation: Simulation comparison of 50 coil designs, *Brain Stimulation*. Elsevier Ltd, 6(1), pp. 1–13. doi: 10.1016/j.brs.2012.02.005.
- Dey, D. D., Landrum, O. and Oaklander, A. L. (2005). Central neuropathic itch from spinal-cord cavernous hemangioma: A human case, a possible animal model, and hypotheses about pathogenesis, *Pain*, 113(1–2), pp. 233–237. doi: 10.1016/j.pain.2004.09.032.
- Di Lazzaro, V. et al. (2001). Descending spinal cord volleys evoked by transcranial magnetic and electrical stimulation of the motor cortex leg area in conscious humans', *Journal of Physiology*, 537(3), pp. 1047–1058. doi: 10.1113/jphysiol.2001.012572.
- Dietz, V. and Curt, A. (2006). Neurological aspects of spinal-cord repair: promises and challenges, *Lancet Neurology*, 5(8), pp. 688–694. doi: 10.1016/S1474-4422(06)70522-1.
- Duman, R. S. et al. (2016). Synaptic plasticity and depression: new insights from stress and rapid-acting antidepressants, *Nature Medicine*. Nature Publishing Group, 22(3), pp. 238–249. doi: 10.1038/nm.4050.
- Eldaief, M. C., Press, D. Z. and Pascual-Leone, A. (2013). Transcranial magnetic stimulation in neurology A review of established and prospective applications, *Neurology: Clinical Practice*, 3(6), pp. 519–526. doi: 10.1212/01.CPJ.0000436213.11132.8e.
- Ellapen, T. J. et al. (2018). The benefits of hydrotherapy to patients with spinal cord injuries, *African Journal of Disability*, 7. doi: 10.4102/ajod.v7i0.a450.
- Ellaway, P. H., Davey, N. J. and Ljubisavljevic, M. (1999). Modern Techniques in Neuroscience Research, *Modern Techniques in Neuroscience Research*. doi: 10.1007/978-3-642-58552-4.
- Erim, Z. et al. (1999). Effects of aging on motor-unit control properties, *Journal of Neurophysiology*. 82(5), pp. 2081–2091. doi: 10.1152/jn.1999.82.5.2081.
- Fang, X. et al. (2019). Current status and potential application of navigated transcranial magnetic stimulation in neurosurgery: A literature review, *Chinese Neurosurgical Journal*. Chinese Neurosurgical Journal, 5(1), pp. 1–7. doi: 10.1186/s41016-019-0159-6.
- Fawcett, J. W. (2007). Guidelines for the conduct of clinical trials for spinal cord injury as developed by the ICCP panel: spontaneous recovery after spinal cord injury and statistical power needed for therapeutic clinical trials, 45, pp. 190–205. doi: 10.1038/sj.sc.3102007
- Ferree, T. C. et al. (2001). Scalp Electrode Impedance and EEG Data Quality, *Clinical Neurophysiology*, 112, pp. 1–9.
- Ferrer, G. and Sanfeliu, A. (2015). Multi-objective cost-to-go functions on robot navigation in dynamic environments, *IEEE International Conference on Intelligent Robots and Systems*, pp. 3824–3829. doi: 10.1109/IROS.2015.7353914.
- Fields, D. P., Springborn, S. R. and Mitchell, G. S. (2015). Spinal 5-HT₇ receptors induce phrenic motor facilitation via EPAC-mTORC1 signaling, *Journal of Neurophysiology*, 114(3), pp. 2015–2022. doi: 10.1152/jn.00374.2015.
- Fisher RA. Oliver and Boyd. (1954). *Statistical methods for research workers*.
- Fisher, M. A. (2012). *H-Reflex and F-Response Studies*. 6th edn, Aminoff's *Electrodiagnosis in Clinical Neurology*. 6th edn. Elsevier Inc. doi: 10.1016/B978-1-4557-0308-1.00018-2.

- Frigon, A. et al. (2007). Ankle position and voluntary contraction alter maximal M waves in soleus and tibialis anterior, *Muscle and Nerve*, 35(6), pp. 756–766. doi: 10.1002/mus.20747.
- Fuller, D. D. et al. (2000). Long term facilitation of phrenic motor output, *Respiration Physiology*, 121(2–3), pp. 135–146. doi: 10.1016/S0034-5687(00)00124-9.
- Garraway, S. M. and Huie, J. R. (2016). Spinal Plasticity and Behavior: BDNF-Induced Neuromodulation in Uninjured and Injured Spinal Cord, *Neural Plasticity*, 2016. doi: 10.1155/2016/9857201.
- Genazzani, A. R. et al. (2000). Progesterone, progestagens and the central nervous system, *Human Reproduction*, 15(SUPPL. 1), pp. 14–27. doi: 10.1093/humrep/15.suppl_1.14.
- Gerasimenko, Y. et al. (2015). Transcutaneous electrical spinal-cord stimulation in humans, *Annals of Physical and Rehabilitation Medicine*. Elsevier Masson SAS, 58(4), pp. 225–231. doi: 10.1016/j.rehab.2015.05.003.
- Giannini, M. J. et al. (2010). Understanding suicide and disability through three major disabling conditions: Intellectual disability, spinal cord injury, and multiple sclerosis, *Disability and Health Journal*. Elsevier Inc, 3(2), pp. 74–78. doi: 10.1016/j.dhjo.2009.09.001.
- Gibbons, R. S. et al. (2016). The effect of FES-rowing training on cardiac structure and function: Pilot studies in people with spinal cord injury, *Spinal Cord*. Nature Publishing Group, 54(10), pp. 822–829. doi: 10.1038/sc.2015.228.
- Gibbons, R. S., Beaupre, G. S. and Kazakia, G. J. (2016). FES-rowing attenuates bone loss following spinal cord injury as assessed by HR-pQCT, *Spinal Cord Series and Cases*. International Spinal Cord Society, 2(1), pp. 1–4. doi: 10.1038/scsandc.2015.41.
- Giblin, D. R. (1964). Somatosensory Evoked Potentials in Healthy Subjects and in Patients With Lesions of the Nervous System, *Annals of the New York Academy of Sciences*, 112(1), pp. 93–142. doi: 10.1111/j.1749-6632.1964.tb26744.x.
- Ginhoux, R. et al. (2013). A custom robot for Transcranial Magnetic Stimulation: First assessment on healthy subjects, *Proceedings of the Annual International Conference of the IEEE Engineering in Medicine and Biology Society, EMBS*. IEEE, pp. 5352–5355. doi: 10.1109/EMBC.2013.6610758.
- Golder, F. J. et al. (2008). Spinal Adenosine A2a Receptor Activation Elicits Long-Lasting Phrenic Motor Facilitation, *Journal of Neuroscience*, 28(9), pp. 2033–2042. doi: 10.1523/JNEUROSCI.3570-07.2008.
- Golder, F. J. and Mitchell, G. S. (2005). Spinal synaptic enhancement with acute intermittent hypoxia improves respiratory function after chronic cervical spinal cord injury, *Journal of Neuroscience*, 25(11), pp. 2925–2932. doi: 10.1523/JNEUROSCI.0148-05.2005.
- Gómez-Pinilla, F. et al. (2002). Voluntary exercise induces a BDNF-mediated mechanism that promotes neuroplasticity, *Journal of Neurophysiology*, 88(5), pp. 2187–2195. doi: 10.1152/jn.00152.2002.
- Gregory, C. M. et al. (2007). Resistance training and locomotor recovery after incomplete spinal cord injury: A case series, *Spinal Cord*, 45(7), pp. 522–530. doi: 10.1038/sj.sc.3102002.
- Groppa, S. et al. (2012). A practical guide to diagnostic transcranial magnetic stimulation: Report of an IFCN committee, *Clinical Neurophysiology*, 123(5), pp. 858–882. doi: 10.1016/j.clinph.2012.01.010.
- Haavik Taylor, H. and Murphy, B. A. (2007) ‘Altered cortical integration of dual somatosensory input following the cessation of a 20 min period of repetitive muscle activity’, *Experimental Brain Research*, 178(4), pp. 488–498. doi: 10.1007/s00221-006-0755-5.
- Haghighi, S. S. et al. (1992). Effect of graded hypoxia on cortical and spinal somatosensory evoked potentials, *Surgical Neurology*, 37(5), pp. 350–355. doi: 10.1016/0090-3019(92)90002-5.
- Hallett, M. (2000). Transcranial magnetic stimulation and the human brain, *Nature*, 406(6792), pp. 147–150. doi: 10.1038/35018000.
- Hallett, M. (2007). Transcranial Magnetic Stimulation: A Primer, *Neuron*, 55(2), pp. 187–199. doi: 10.1016/j.neuron.2007.06.026.
- Halonen, J. P., Jones, S. and Shawkat, F. (1988). Contribution of cutaneous and muscle afferent fibres to cortical SEPs following median and radial nerve stimulation in man, *Electroencephalography and Clinical Neurophysiology/ Evoked Potentials*, 71(5), pp. 331–335. doi: 10.1016/0168-5597(88)90035-4.

- Hamada, M. et al. (2007). Median nerve somatosensory evoked potentials and their high-frequency oscillations in amyotrophic lateral sclerosis, *Clinical Neurophysiology*, 118(4), pp. 877–886. doi: 10.1016/j.clinph.2006.12.001.
- Hamid, S. and Hayek, R. (2008). Role of electrical stimulation for rehabilitation and regeneration after spinal cord injury: An overview, *European Spine Journal*, 17(9), pp. 1256–1269. doi: 10.1007/s00586-008-0729-3.
- Han, S. et al. (2015). The linear-ordered collagen scaffold-BDNF complex significantly promotes functional recovery after completely transected spinal cord injury in canine, *Biomaterials*. Elsevier Ltd, 41, pp. 89–96. doi: 10.1016/j.biomaterials.2014.11.031.
- Hannula, H. et al. (2005). Somatotopic blocking of sensation with navigated transcranial magnetic stimulation of the primary somatosensory cortex, *Human Brain Mapping*, 26(2), pp. 100–109. doi: 10.1002/hbm.20142.
- Harkema, S. et al. (2011). Effect of epidural stimulation of the lumbosacral spinal cord on voluntary movement, standing, and assisted stepping after motor complete paraplegia: a case study, *National Institutes of Health*, 377(9781), pp. 1938–1947. doi: 10.1016/S0140-6736(11)60547-3.Effect.
- Harkema, S. J., Schmidt-read, M., Lorenz, D. J., et al. (2012). Balance and ambulation improvements in individuals with chronic incomplete spinal cord injury using locomotor training – Based Rehabilitation, *YAPMR*. Elsevier Inc., 93(9), pp. 1508–1517. doi: 10.1016/j.apmr.2011.01.024.
- Harquel, S. et al. (2017). Automatized set-up procedure for transcranial magnetic stimulation protocols, *NeuroImage*, 153(November 2016), pp. 307–318. doi: 10.1016/j.neuroimage.2017.04.001.
- Hashemirad, F. et al. (2017). Reliability of motor evoked potentials induced by transcranial magnetic stimulation: The effects of initial motor evoked potentials removal, *Basic and Clinical Neuroscience*, 8(1), pp. 43–50. doi: 10.15412/J.BCN.03080106.
- Hatanpaa, K. J. and Kim, J. H. (2014). *Neuropathology of viral infections*. 1st edn, *Handbook of Clinical Neurology*. 1st edn. Elsevier B.V. doi: 10.1016/B978-0-444-53488-0.00008-0.
- Hayes, H. B. et al. (2014). Daily intermittent hypoxia enhances walking after chronic spinal cord injury A randomized trial, *Neurology*, 82(2), pp. 104–113. doi: 10.1212/01.WNL.0000437416.34298.43.
- Herbison, G. J. et al. (1992). Motor Power Differences Within the First Two Weeks Post-SCI in Cervical Spinal Cord-Injured Quadriplegic Subjects, *Journal of Neurotrauma*, 9(4), pp. 373–380. doi: 10.1089/neu.1992.9.373.
- Hirsch, M. A. et al. (2014). Reliability of the timed 10-metre walk test during inpatient rehabilitation in ambulatory adults with traumatic brain injury, *Brain Injury*, 28(8), pp. 1115–1120. doi: 10.3109/02699052.2014.910701.
- Hoffman, M. S. et al. (2010). Spinal adenosine A2A receptor inhibition enhances phrenic long term facilitation following acute intermittent hypoxia, *Journal of Physiology*, 588(1), pp. 255–266. doi: 10.1113/jphysiol.2009.180075.
- Hoffman, M. S. and Mitchell, G. S. (2013). Spinal 5-HT7 receptors and protein kinase A constrain intermittent hypoxia-induced phrenic long-term facilitation, *Neuroscience*. IBRO, 250, pp. 632–643. doi: 10.1016/j.neuroscience.2013.06.068.
- Iwayama, K. et al. (1986). Changes of somatosensory evoked potential accompanying ischaemia and hypoxia in cats, *Neurological Research*, 8(3), pp. 157–163. doi: 10.1080/01616412.1986.11739748.
- Jackson, A. B. et al. (2004). A demographic profile of new traumatic spinal cord injuries: Change and stability over 30 years, *Archives of Physical Medicine and Rehabilitation*, 85(11), pp. 1740–1748. doi: 10.1016/j.apmr.2004.04.035.
- Jelkmann, W. and Hellwig-bürgel, T. (2001). Chapter 12 Biology of erythropoietin, pp. 169–170.
- Jezernik, S. et al. (2003). Robotic Orthosis Lokomat: A Rehabilitation and Research Tool, *Neuromodulation*, 6(2), pp. 108–115. doi: 10.1046/j.1525-1403.2003.03017.x.
- Ji, X. C. et al. (2015). Local Injection of Lenti-BDNF at the Lesion Site Promotes M2 Macrophage Polarization and Inhibits Inflammatory Response After Spinal Cord Injury in Mice, *Cellular and Molecular Neurobiology*. Springer US, 35(6), pp. 881–890. doi: 10.1007/s10571-015-0182-x.
- Jiang, S. D., Dai, L. Y. and Jiang, L. S. (2006). Osteoporosis after spinal cord injury, *Osteoporosis International*, 17(2), pp. 180–192. doi: 10.1007/s00198-005-2028-8.

- Jones, L. L. et al. (2001). Neurotrophic factors, cellular bridges and gene therapy for spinal cord injury, *Journal of Physiology*, 533(1), pp. 83–89. doi: 10.1111/j.1469-7793.2001.0083b.x.
- Julkunen, P. et al. (2009). Comparison of navigated and non-navigated transcranial magnetic stimulation for motor cortex mapping, motor threshold and motor evoked potentials, *NeuroImage*. Elsevier Inc., 44(3), pp. 790–795. doi: 10.1016/j.neuroimage.2008.09.040.
- Kalogianni, K. et al. (2018). Disentangling somatosensory evoked potentials of the fingers: Limitations and clinical potential, *Brain Topography*. Springer US, 31(3), pp. 498–512. doi: 10.1007/s10548-017-0617-4.
- Kalsi-Ryan, S., Karadimas, S. K. and Fehlings, M. G. (2013). Cervical spondylotic myelopathy: The clinical phenomenon and the current pathobiology of an increasingly prevalent and devastating disorder, *Neuroscientist*, 19(4), pp. 409–421. doi: 10.1177/1073858412467377.
- Kamoda, M. et al. (2001). Changes of middle latency somatosensory evoked potentials (SEPs) and alpha rhythmicity associated with oculomotor processes, *Clinical Neurophysiology*, 112(12), pp. 2250–2254. doi: 10.1016/S1388-2457(01)00688-5.
- Karimi-Abdolrezaee, S. et al. (2010). Synergistic effects of transplanted adult neural stem/progenitor cells, chondroitinase, and growth factors promote functional repair and plasticity of the chronically injured spinal cord, *Journal of Neuroscience*, 30(5), pp. 1657–1676. doi: 10.1523/JNEUROSCI.3111-09.2010.
- Kasai, T. et al. (1997). Evidence for facilitation of motor evoked potentials (MEPs) induced by motor imagery, *Brain Research*, 744(1), pp. 147–150. doi: 10.1016/S0006-8993(96)01101-8.
- Kesar, T. M., Stinear, J. W. and Wolf, S. L. (2018). The use of transcranial magnetic stimulation to evaluate cortical excitability of lower limb musculature: Challenges and opportunities, *Restorative Neurology and Neuroscience*, 36(3), pp. 333–348. doi: 10.3233/RNN-170801.
- Kesiktas, N. et al. (2004). The use of hydrotherapy for the management of spasticity, *Neurorehabilitation and Neural Repair*, 18(4), pp. 268–273. doi: 10.1177/1545968304270002.
- Kiers, L. et al. (1993). Variability of motor potentials evoked by transcranial magnetic stimulation, electroencephalography and clinical neurophysiology/ evoked potentials, 89(6), pp. 415–423. doi: 10.1016/0168-5597(93)90115-6.
- Kim, S. J. et al. (2016). Intermittent hypoxia-induced cardiorespiratory long-term facilitation: A new role for microglia, respiratory physiology and neurobiology. Elsevier B.V., 226, pp. 30–38. doi: 10.1016/j.resp.2016.03.012.
- Kim, S. M. et al. (2009). Sjögren's syndrome myelopathy: Spinal cord involvement in Sjögren's syndrome might be a manifestation of neuromyelitis optica, *Multiple Sclerosis*, 15(9), pp. 1062–1068. doi: 10.1177/1352458509106636.
- King, J. C. and Dumitru, D. (1994). A new understanding of far-field potentials and their use in clinical diagnosis, 5, pp. 421–445.
- Kinthead, R. et al. (2001). Plasticity in respiratory motor control: Intermittent hypoxia and hypercapnia activate opposing serotonergic and noradrenergic modulatory systems, *Comparative Biochemistry and Physiology - A Molecular and Integrative Physiology*, 130(2), pp. 207–218. doi: 10.1016/S1095-6433(01)00393-2.
- Kirshblum, S. C. et al. (2011). The international standards for neurological classification of spinal cord injury, *Journal of Spinal Cord Medicine*, 34(6), pp. 547–554. doi: 10.1179/107902611X13186000420242.
- Klein, M. M. et al. (2015). Transcranial magnetic stimulation of the brain: Guidelines for pain treatment research, *Pain*, 156(9), pp. 1601–1614. doi: 10.1097/j.pain.0000000000000210.
- Klomjai, W., Katz, R. and Lackmy-Vallée, A. (2015). Basic principles of transcranial magnetic stimulation (TMS) and repetitive TMS (rTMS), *Annals of Physical and Rehabilitation Medicine*, 58(4), pp. 208–213. doi: 10.1016/j.rehab.2015.05.005.
- Knaupp, W. et al. (1992). Erythropoietin response to acute normobaric hypoxia in humans, *Journal of Applied Physiology*, 73(3), pp. 837–840. doi: 10.1152/jappl.1992.73.3.837.
- Knecht, S. et al. (2005). Scalp position and efficacy of transcranial magnetic stimulation, *Clinical Neurophysiology*, 116(8), pp. 1988–1993. doi: 10.1016/j.clinph.2005.04.016.
- Kolakowsky-Hayner, S. A. et al. (2002). Post-injury substance abuse among persons with brain injury and

- persons with spinal cord injury, *Brain Injury*, 16(7), pp. 583–592. doi: 10.1080/02699050110119475.
- Kon, M. et al. (2012). Effects of low-intensity resistance exercise under acute systemic hypoxia on hormonal responses, *Journal of strength and conditioning research*, 26(3), pp. 611–617.
- Koo, T. K. and Li, M. Y. (2016). A guideline of selecting and reporting intraclass correlation coefficients for reliability research, *Journal of Chiropractic Medicine*. Elsevier B.V., 15(2), pp. 155–163. doi: 10.1016/j.jcm.2016.02.012.
- Krassioukov, A. and Claydon, V. E. (2006). The clinical problems in cardiovascular control following spinal cord injury: An overview, *Progress in Brain Research*, 152(c), pp. 223–229. doi: 10.1016/S0079-6123(05)52014-4.
- Kremenic, I. J. et al. (2004). Transcutaneous magnetic stimulation of the quadriceps via the femoral nerve, *Muscle and Nerve*, 30(3), pp. 379–381. doi: 10.1002/mus.20091.
- Krings, T. et al. (2001). Introducing navigated transcranial magnetic stimulation as a refined brain mapping methodology, *Neurosurgical Review*, 24(4), pp. 171–179. doi: 10.1007/s101430100151.
- Kucera, P., Goldenberg, Z. and Kurca, E. (2004). Sympathetic skin response: review of the method and its clinical use, *Bratislavské lekárske listy*, 105(3), pp. 108–116.
- Kujirai, T. et al. (1992). Corticocortical inhibition in human motor cortex, *Journal of Physiology*, 471, pp. 501–519.
- Lam, T. et al. (2012). CIHR Author Manuscript A systematic review of the efficacy of gait rehabilitation strategies for spinal cord injury, 13(1), pp. 1–23. doi: 10.1310/sci1301-32.A.
- Lamy, J.-C. and Boakye, M. (2013). BDNF Val66Met polymorphism alters spinal DC stimulation-induced plasticity in humans, *Journal of Neurophysiology*, 110(1), pp. 109–116. doi: 10.1152/jn.00116.2013.
- Langhammer, B., Lindmark, B. and Stanghelle, J. K. (2014). Physiotherapy and physical functioning post-stroke: exercise habits and functioning 4 years later? Long-term follow-up after a 1-year long-term intervention period: A randomized controlled trial, *Brain Injury*, 28(11), pp. 1396–1405. doi: 10.3109/02699052.2014.919534.
- Laufer, Y. et al. (2001). Quadriceps femoris muscle torques and fatigue generated by neuromuscular electrical stimulation with three different waveforms, *Physical Therapy*, 81(7), pp. 1307–1316. doi: 10.1093/ptj/81.7.1307.
- Ledsome, J. R., Cole, C. and Sharp-Kehl, J. M. (1996). Somatosensory evoked potentials during hypoxia and hypocapnia in conscious humans, *Canadian Journal of Anaesthesia*, 43(10), pp. 1025–1029. doi: 10.1007/BF03011904.
- Leslie, K. et al. (1999). Common peroneal nerve stimulation for neuromuscular monitoring: Evaluation in awake volunteers and anesthetized patients, *Anesthesia and Analgesia*, 88(1), pp. 197–203. doi: 10.1097/00000539-199901000-00037.
- Levy, P. et al. (2015). Obstructive sleep apnoea syndrome, *Nature*, 1, pp. 1–20. doi: 10.1038/nrdp.2015.15.
- Li, J. and Lepski, G. (2013). Cell transplantation for spinal cord injury: A systematic review, *BioMed Research International*, 2013. doi: 10.1155/2013/786475.
- Liechti, M. et al. (2008). Vestibulospinal responses in motor incomplete spinal cord injury, *Clinical Neurophysiology*. International Federation of Clinical Neurophysiology, 119(12), pp. 2804–2812. doi: 10.1016/j.clinph.2008.05.033.
- Liljequist, D., Elfving, B. and Roaldsen, K. S. (2019). Intraclass correlation – A discussion and demonstration of basic features, *PLoS ONE*. doi: 10.1371/journal.pone.0219854.
- Lindvall, O. et al. (1992). Differential regulation of mRNAs for nerve growth factor, brain-derived neurotrophic factor, and neurotrophin 3 in the adult rat brain following cerebral ischemia and hypoglycemic coma, *Proceedings of the National Academy of Sciences of the United States of America*, 89(2), pp. 648–652. doi: 10.1073/pnas.89.2.648.
- Ling, L. et al. (2001). Chronic intermittent hypoxia elicits serotonin-dependent plasticity in the central neural control of breathing, *Journal of Neuroscience*, 21(14), pp. 5381–5388. doi: 10.1523/jneurosci.21-14-05381.2001.
- Liu, X. et al. (2017). Reduced cerebrovascular and cardioventilatory responses to intermittent hypoxia in elderly, *Respiratory Physiology and Neurobiology*, 271. doi: 10.1016/j.resp.2019.103306.
- Lizamore, C. A. et al. (2016). The effect of short-term intermittent hypoxic exposure on heart rate variability in a

- sedentary population, *Acta Physiologica Hungarica*, 103(1), pp. 75–85. doi: 10.1556/036.103.2016.1.7.
- Lommatzsch, M. *et al.* (2005) ‘The impact of age, weight and gender on BDNF levels in human platelets and plasma’, *Neurobiology of Aging*, 26(1), pp. 115–123. doi: 10.1016/j.neurobiolaging.2004.03.002.
- Long, J. B., Youngblood, W. W. and Kizer, J. S. (1983). Effects of castration and adrenalectomy on in vitro rates of tryptophan hydroxylation and levels of serotonin in microdissected brain nuclei of adult male rats, *Brain Research*, 277(2), pp. 289–297. doi: 10.1016/0006-8993(83)90936-8.
- Lovett-Barr, M. R. *et al.* (2012). Repetitive intermittent hypoxia induces respiratory and somatic motor recovery after chronic cervical spinal injury, *National Institute of Health*, 32(11), pp. 3591–3600. doi: 10.1021/nl061786n.Core-Shell.
- Lundby, C., Calbet, J. A. L. and Robach, P. (2009). The response of human skeletal muscle tissue to hypoxia, *Cellular and Molecular Life Sciences*, 66(22), pp. 3615–3623. doi: 10.1007/s00018-009-0146-8.
- Lynch, M. *et al.* (2016). Effect of acute intermittent hypoxia on motor function in individuals with chronic spinal cord injury following ibuprofen pretreatment: A pilot study, *Journal of Spinal Cord Medicine*, 40(3), pp. 295–303. doi: 10.1080/10790268.2016.1142137.
- Lynskey, J. V., Belanger, A. and Jung, R. (2008). Activity-dependent plasticity in spinal cord injury’, *National Institute of Health*, 45(2), pp. 229–240. doi: 10.1038/jid.2014.371.
- Macerollo, A. *et al.* (2018). Neurophysiological changes measured using somatosensory evoked potentials, *Trends in Neurosciences*. Elsevier Ltd, 41(5), pp. 294–310. doi: 10.1016/j.tins.2018.02.007.
- Mackenzie, R. *et al.* (2011). Acute hypoxia and exercise improve insulin sensitivity (SI2*) in individuals with type 2 diabetes, *Diabetes/Metabolism Research and Reviews*, 27, pp. 94–101. doi: 10.1002/dmrr.
- Mahamed, S. and Mitchell, G. S. (2007). Is there a link between intermittent hypoxia-induced respiratory plasticity and obstructive sleep apnoea?, *Experimental physiology*, 92(1), pp. 27–37. doi: 10.1113/expphysiol.2006.033720.
- Maier, I. C. and Schwab, M. E. (2006). Sprouting, regeneration and circuit formation in the injured spinal cord: Factors and activity, *Philosophical Transactions of the Royal Society B: Biological Sciences*, 361(1473), pp. 1611–1634. doi: 10.1098/rstb.2006.1890.
- Malcolm, M. P. *et al.* (2006). Reliability of motor cortex transcranial magnetic stimulation in four muscle representations, *Clinical Neurophysiology*, 117(5), pp. 1037–1046. doi: 10.1016/j.clinph.2006.02.005.
- Malhotra, A. and White, D. P. (2002). Obstructive sleep apnoea, *Lancet*, 360(9328), pp. 237–245. doi: 10.1016/S0140-6736(02)09464-3.
- Mallet, R. T. *et al.* (2018). Cardioprotection by intermittent hypoxia conditioning: Evidence, mechanisms, and therapeutic potential, *American Journal of Physiology - Heart and Circulatory Physiology*, 315(2), pp. H216–H232. doi: 10.1152/ajpheart.00060.2018.
- Manimmanakorn. *et al.* (2013a). Effects of low-load resistance training combined with blood flow restriction or hypoxia on muscle function and performance in netball athletes, *Journal of Science and Medicine in Sport*. *Sports Medicine Australia*, 16(4), pp. 337–342. doi: 10.1016/j.jsams.2012.08.009.
- Manimmanakorn, A. *et al.* (2013b). Effects of resistance training combined with vascular occlusion or hypoxia on neuromuscular function in athletes, *European Journal of Applied Physiology*, 113(7), pp. 1767–1774. doi: 10.1007/s00421-013-2605-z.
- Manini, T. M. *et al.* (2012). Growth hormone responses to acute resistance exercise with vascular restriction in young and old men, *National Institute of Health*, 22(5), pp. 167–172. doi: 10.1016/j.ghir.2012.05.002.Growth.
- Manini, T. M. and Clark, B. C. (2009). Blood flow restricted exercise and skeletal muscle health, *Exercise and Sport Sciences Reviews*, 37(2), pp. 78–85. doi: 10.1097/JES.0b013e31819c2e5c.
- Mantilla, C. B. *et al.* (2014). TrkB kinase activity is critical for recovery of respiratory function after cervical spinal cord hemisection, *Experimental Neurology*. Elsevier Inc., 261, pp. 190–195. doi: 10.1016/j.expneurol.2014.05.027.
- Manukhina, E. B. *et al.* (2013). Normobaric, intermittent hypoxia conditioning is cardio- and vasoprotective in rats, *Experimental Biology and Medicine*, 238(12), pp. 1413–1420. doi: 10.1177/1535370213508718.

- Marino, R. J. et al. (2003). International standards for neurological classification of spinal cord injury, *The journal of spinal cord medicine*, 26 Suppl 1(November). doi: 10.1080/10790268.2003.11754575.
- Markand, O. (2020). *Clinical Evoked Potentials*. Springer International PU.
- Martini, F., Nath, J. and Bartholomew, E. (2018). *Fundamentals of Anatomy and Physiology*. Global Edition. Harlow, United Kingdom: Pearson Education Canada.
- Mathewson, K. E., Harrison, T. J. L. and Kizuk, S. A. D. (2017). High and dry? Comparing active dry EEG electrodes to active and passive wet electrodes, *Psychophysiology*, 54(1), pp. 74–82. doi: 10.1111/psyp.12536.
- Mauguiere, F. et al. (1999). *Somatosensory evoked potentials*, Elsevier. doi: 10.1016/B978-0-444-64032-1.00035-7.
- McCaughey, E. J. et al. (2016). Changing demographics of spinal cord injury over a 20-year period: a longitudinal population-based study in Scotland, *Spinal Cord*. Nature Publishing Group, 54(4), pp. 270–276. doi: 10.1038/sc.2015.167.
- McGuire, M. and Ling, L. (2005). Ventilatory long-term facilitation is greater in 1- vs. 2-mo-old awake rats, *Journal of Applied Physiology*, 98(4), pp. 1195–1201. doi: 10.1152/jappphysiol.00996.2004.
- McHughen, S. A. et al. (2011). Intense training overcomes effects of the val 66met BDNF polymorphism on short-term plasticity, *Experimental Brain Research*, 213(4), pp. 415–422. doi: 10.1007/s00221-011-2791-z.
- McPherson, R. W., Zeger, S. and Traystman, R. J. (1986). Relationship of somatosensory evoked potentials and cerebral oxygen consumption during hypoxic hypoxia in dogs, *Stroke*, 17(1), pp. 30–36. doi: 10.1161/01.STR.17.1.30.
- Merletti, R. (1999). Standards for reporting EMG data, *Journal of Electromyography and Kinesiology*. doi: 10.1016/s1050-6411(15)00221-7.
- Merton, P. A. and Morton, H. B. (1980). Stimulation of the cerebral cortex in the intact human subject, *Nature*, p. 227. doi: 10.1038/285227a0.
- Millhorn, D. E. and Eldridge, F. L. (1986). Role of ventrolateral medulla in regulation of respiratory and cardiovascular systems, *Journal of Applied Physiology*, 61(4), pp. 1249–1263. doi: 10.1152/jappl.1986.61.4.1249.
- Millhorn, D. E. and Eldridge, F. L. (1986). Role of ventrolateral medulla in regulation of respiratory and cardiovascular systems, *Journal of Applied Physiology*, 61(4), pp. 1249–1263. doi: 10.1152/jappl.1986.61.4.1249.
- Millhorn, D. E., Eldridge, F. L. and Waldrop, R. G. (1980). Prolonged stimulation for respiration by endogenous central serotonin, *Respiration Physiology*, 42(3), pp. 171–188. doi: 10.1016/0034-5687(80)90113-9.
- Mitchell, G. S. and Terada, J. (2011). Should we standardize protocols and preparations used to study respiratory plasticity?, *Respiratory Physiology and Neurobiology*. Elsevier B.V., 177(2), pp. 93–97. doi: 10.1016/j.resp.2011.03.021.
- Razali, M. N. and Wah, B.Y. (2011). Power comparisons of Shapiro-Wilk, Kolmogorov-Smirnov, Lilliefors and Anderson-Darling tests, *Journal of Statistical Modeling and Analytics*, 2(1), pp. 21–33. Available at: <http://instatmy.org.my/downloads/e-jurnal/2/3.pdf%0Ahttps://www.nrc.gov/docs/ML1714/ML17143A100.pdf>.
- Mulcahey, M. J. et al. (2004). Implantation of the Freehand System® during initial rehabilitation using minimally invasive techniques, *Spinal Cord*, 42(3), pp. 146–155. doi: 10.1038/sj.sc.3101573.
- Müller-Dahlhaus, F., Ziemann, U. and Classen, J. (2010). Plasticity resembling spike-timing dependent synaptic plasticity: The evidence in human cortex, *Frontiers in Synaptic Neuroscience*, 2(JUL), pp. 1–11. doi: 10.3389/fnsyn.2010.00034.
- Multidisciplinary Association of Spinal Cord Injury Professionals (MASCIP). (2010). *Management of The Older Person with A New Spinal Cord Injury*. Stanmore, London: MASCIP.
- Muzyka, I. M. and Estephan, B. (2019). *Somatosensory evoked potentials*. 1st edn, *Handbook of Clinical Neurology*. 1st edn. Elsevier B.V. doi: 10.1016/B978-0-444-64032-1.00035-7.
- Myers, J., Lee, M. and Kiratli, J. (2007). Cardiovascular disease in spinal cord injury: An overview of prevalence, risk, evaluation, and management, *American Journal of Physical Medicine and Rehabilitation*, 86(2), pp. 142–

152. doi: 10.1097/PHM.0b013e31802f0247.

Naidu, A. et al. (2020). Daily acute intermittent hypoxia to improve walking function in persons with subacute spinal cord injury: a randomized clinical trial study protocol, *BMC Neurology*, 20(1), pp. 1–11. doi: 10.1186/s12883-020-01851-9.

Nakamura, H. et al. (1996). Direct and indirect activation of human corticospinal neurons by transcranial magnetic and electrical stimulation, *Neuroscience Letters*, 210(1), pp. 45–48. doi: 10.1016/0304-3940(96)12659-8.

Nakata, H. et al. (2017). Effects of acute hypoxia on human cognitive processing: A study using ERPs and SEPs, *Journal of Applied Physiology*, 123(5), pp. 1246–1255. doi: 10.1152/jappphysiol.00348.2017.

Nas, K. et al. (2015). Rehabilitation of spinal cord injuries, *World Journal of Orthopaedics*, 6(1), pp. 8–16. doi: 10.5312/wjo.v6.i1.8.

National Spinal Cord Injury Statistical Centre (NSCISC). (2019). Spinal cord injury facts and figures at a glance. Birmingham, Alabama, USA: Model Systems Knowledge Translation Centre.

Navarrete-Opazo, A., Alcayaga, J., Testa, D., et al. (2016a). Intermittent hypoxia does not elicit memory impairment in spinal cord injury patients, *Archives of Clinical Neuropsychology*, 31(4), pp. 332–342. doi: 10.1093/arclin/acw012.

Navarrete-Opazo, A., Alcayaga, J., Sepúlveda, O., et al. (2016b). Repetitive intermittent hypoxia and locomotor training enhances walking function in incomplete spinal cord injury subjects: A randomized, triple-blind, placebo-controlled clinical trial, *Journal of Neurotrauma*, 10, p. neu.2016.4478. doi: 10.1089/neu.2016.4478.

Navarrete-Opazo, A. et al. (2017). Intermittent hypoxia and locomotor training enhances dynamic but not standing balance in patients with incomplete spinal cord injury, *Archives of Physical Medicine and Rehabilitation*, 98(3), pp. 415–424. doi: 10.1016/j.apmr.2016.09.114.

Navid, M. S. et al. (2019). The effects of filter's class, cutoff frequencies, and independent component analysis on the amplitude of somatosensory evoked potentials recorded from healthy volunteers, *Sensors (Switzerland)*, 19(11), pp. 1–18. doi: 10.3390/s19112610.

Ngomo, S. et al. (2012). Comparison of transcranial magnetic stimulation measures obtained at rest and under active conditions and their reliability, *Journal of Neuroscience Methods*. Elsevier B.V., 205(1), pp. 65–71. doi: 10.1016/j.jneumeth.2011.12.012.

Numakawa, T. (2010). Functional interactions between steroid hormones and neurotrophin BDNF, *World Journal of Biological Chemistry*, 1(5), p. 133. doi: 10.4331/wjbc.v1.i5.133.

Nuwer, M. R. (1998). Fundamentals of evoked potentials and common clinical applications today, *Electroencephalography and clinical neurophysiology*, 106, pp. 142–148.

O'Reardon, J. P. et al. (2007). Efficacy and safety of transcranial magnetic stimulation in the acute treatment of major depression: A multisite randomized controlled trial, *Biological Psychiatry*, 62(11), pp. 1208–1216. doi: 10.1016/j.biopsych.2007.01.018.

Olejniczak, P. (2006). Neurophysiologic basis of EEG, *Journal of Clinical Neurophysiology*, 23(3), pp. 186–189. doi: 10.1097/01.wnp.0000220079.61973.6c.

Onifer, S. M., Smith, G. M. and Fouad, K. (2011). Plasticity after spinal cord injury: Relevance to recovery and approaches to facilitate it, *Neurotherapeutics*, 8(2), pp. 283–293. doi: 10.1007/s13311-011-0034-4.

Osborne, M. C., Verhovshek, T. and Sengelaub, D. (2007). Androgen regulates trkB immunolabeling in spinal motoneurons, *Journal of Neuroscience Research*, 3253(April), pp. 3244–3253. doi: 10.1002/jnr.

Oyinbo, C. A. (2011). Secondary injury mechanisms in traumatic spinal cord injury a nugget, *Acta Neurobiologiae Experimentalis*, 71(2), pp. 281–299.

Ozkul, Y. and Uckardes, A. (2002). Median nerve somatosensory evoked potentials in migraine, *European Journal of Neurology*, 9(3), pp. 227–232. doi: 10.1046/j.1468-1331.2002.00387.x.

Passmore, S. R., Murphy, B. and Lee, T. D. (2014). The origin, and application of somatosensory evoked potentials as a neurophysiological technique to investigate neuroplasticity, *Journal of the Canadian Chiropractic Association*, 58(2), pp. 170–183.

- Penfield, W. and Boldrey, E. (1937). Somatic motor and sensory representation in man, *Brain*, pp. 389–443. doi: 10.1093/brain/60.4.389.
- Penrod LE, Hegde SK, Ditunno JF. (1990). Age effect on prognosis for functional recovery in acute, traumatic central cord syndrome. *Arch Phys Med Rehabil*; 71:963–968.
- Peri, E. et al. (2017). Intra and inter-session reliability of rapid Transcranial Magnetic Stimulation stimulus-response curves of tibialis anterior muscle in healthy older adults, *PLoS ONE*, 12(9), pp. 1–17. doi: 10.1371/journal.pone.0184828.
- Peyssonaux, C., Nizet, V. and Johnson, R. S. (2008). Role of the hypoxia inducible factors in iron metabolism, *Cell Cycle*, 7(1), pp. 28–32. doi: 10.4161/cc.7.1.5145.
- Phillips, S. M. et al. (2004). Body-weight-support treadmill training improves blood glucose regulation in persons with incomplete spinal cord injury, 1, pp. 716–724.
- Piatt, J. A. et al. (2016). Problematic secondary health conditions among adults with spinal cord injury and its impact on social participation and daily life, *Journal of Spinal Cord Medicine*. Taylor & Francis, 39(6), pp. 693–698. doi: 10.1080/10790268.2015.1123845.
- Picht, T. et al. (2013). A comparison of language mapping by preoperative navigated transcranial magnetic stimulation and direct cortical stimulation during awake surgery, *Neurosurgery*, 72(5), pp. 808–819. doi: 10.1227/NEU.0b013e3182889e01.
- Pons, J., Raya, R. and González, J. (2016). *Emerging therapies in neurorehabilitation II*. Switzerland: Springer International PU.
- Poornima, S. et al. (2013). Median nerve somatosensory evoked potentials in medical students: Normative data, *Advanced Biomedical Research*, 2(1), p. 56. doi: 10.4103/2277-9175.115797.
- Prosser-Loose, E. J. et al. (2015). Delayed intervention with intermittent hypoxia and task training improves forelimb function in a rat model of cervical spinal injury, *Journal of Neurotrauma*, 32(18), pp. 1403–1412. doi: 10.1089/neu.2014.3789.
- Purves, D., and Williams, S.M. (2001). *Neuroscience*. 2nd ed. Sunderland, Mass.: Sinauer Associates.
- Quraishe, S., Forbes, L. H. and Andrews, M. R. (2018). The extracellular environment of the CNS: Influence on plasticity, sprouting, and axonal regeneration after spinal cord injury, *Neural Plasticity*. Hindawi, 2018(Figure 1). doi: 10.1155/2018/2952386.
- Raffa, G. et al. (2016). A novel technique for region and linguistic specific nTMS-based DTI fiber tracking of language pathways in brain tumor patients, *Frontiers in Neuroscience*, 10(DEC), pp. 1–17. doi: 10.3389/fnins.2016.00552.
- Rizzo, V. et al. (2014). Preoperative functional mapping for rolandic brain tumor surgery, *Neuroscience Letters*. Elsevier Ireland Ltd, 583, pp. 136–141. doi: 10.1016/j.neulet.2014.09.017.
- Rosenzweig, E. S. et al. (2019). Chondroitinase improves anatomical and functional outcomes after primate spinal cord injury, *Nature Neuroscience*. Springer US, 22(8), pp. 1269–1275. doi: 10.1038/s41593-019-0424-1.
- Rossi, S. et al. (2009). Safety, ethical considerations, and application guidelines for the use of transcranial magnetic stimulation in clinical practice and research, *Duke L. & Tech. Rev.*, 2216(2009), pp. 323–330. doi: 10.1016/j.clinph.2009.08.016.Rossi.
- Rossini, P. M. et al. (1994). Non-invasive electrical and magnetic stimulation of the brain, spinal cord, roots and peripheral nerves: Basic principles and procedures for routine clinical and research application: An updated report from an I.F.C.N. Committee, *Clinical Neurophysiology*, 91(2), pp. 79–92.
- Rossini, P. M. et al. (2015). Non-invasive electrical and magnetic stimulation of the brain, spinal cord, roots and peripheral nerves: Basic principles and procedures for routine clinical and research application: An updated report from an I.F.C.N. Committee, *Clinical Neurophysiology*. International Federation of Clinical Neurophysiology, 126(6), pp. 1071–1107. doi: 10.1016/j.clinph.2015.02.001.
- Rotenberg, A., Horvath, J.C., Pascual-Leone, A. (2014). *Transcranial magnetic stimulation*. New York: Springer International PU.
- Rothwell, J. et al. (1991). Stimulation of the human motor cortex through the scalp, *Experimental Physiology*, 76(2), pp. 159–200. doi: 10.1113/expphysiol.1991.sp003485.

- Ruitenbergh, M. J. et al. (2004). Adeno-associated viral vector-mediated gene transfer of brain-derived neurotrophic factor reverses atrophy of rubrospinal neurons following both acute and chronic spinal cord injury, *Neurobiology of Disease*, 15(2), pp. 394–406. doi: 10.1016/j.nbd.2003.11.018.
- Ruohonen, J. and Karhu, J. (2010). Navigated transcranial magnetic stimulation, *Clinical neurophysiology*. Elsevier Masson SAS, 40(1), pp. 7–17. doi: 10.1016/j.neucli.2010.01.006.
- Rushton, D. N. (2003). Functional Electrical Stimulation and rehabilitation-an hypothesis, *Elsevier*, 13, pp. 75–78. doi: 10.1016/S.
- Salahuddin, L. et al. (2007). Ultra short term analysis of heart rate variability for monitoring mental stress in mobile settings, *Annual International Conference of the IEEE Engineering in Medicine and Biology - Proceedings*, pp. 4656–4659. doi: 10.1109/IEMBS.2007.4353378.
- Samra, S. K. et al. (1987). Differential effects of isoflurane on human median nerve somatosensory evoked potentials, *Anesthesiology*, 66, pp. 29–35.
- Sandhu, M. S. et al. (2019). Prednisolone pretreatment enhances intermittent hypoxia-induced plasticity in persons with chronic incomplete spinal cord injury, *Neurorehabilitation and Neural Repair*, 33(11), pp. 911–921. doi: 10.1177/1545968319872992.
- Sandro, M. K. (2017). *Navigated Transcranial Magnetic Stimulation in Neurosurgery*, Springer, 1. doi: 10.1007/978-3-319-54918-7
- Sandrow-Feinberg, H. R. and Houlié, J. D. (2015). Exercise after spinal cord injury as an agent for neuroprotection, regeneration and rehabilitation, *Brain Research*. Elsevier, 1619, pp. 12–21. doi: 10.1016/j.brainres.2015.03.052.
- Santo, E. et al. (2015). Is body weight-support treadmill training effective in increasing muscle trophism after traumatic spinal cord injury? A systematic review, pp. 176–181. doi: 10.1038/sc.2014.198.
- Satriotomo, I. et al. (2016). Repetitive acute intermittent hypoxia increases growth/neurotrophic factor expression in non-respiratory motor neurons, *Neuroscience*, 322, pp. 479–488. doi: 10.1016/j.neuroscience.2016.02.060.
- Savic, G. et al. (2000). Stoke Mandeville Hospital employment following spinal cord injury – a British multicentre study, NHS.
- Sawaya, R. and Radwan, W. (2013). Sarcoidosis associated with neuromyelitis optica, *Journal of Clinical Neuroscience*. Elsevier Ltd, 20(8), pp. 1156–1158. doi: 10.1016/j.jocn.2012.09.030.
- Schega, L. et al. (2013). Effects of intermittent hypoxia on cognitive performance and quality of life in elderly adults: A pilot study, *Gerontology*, 59(4), pp. 316–323. doi: 10.1159/000350927.
- Schilero, G. J. et al. (2009). Pulmonary function and spinal cord injury, *Respiratory Physiology and Neurobiology*, 166(3), pp. 129–141. doi: 10.1016/j.resp.2009.04.002.
- Schulze, H. et al. (2018). Exercise restores chloride homeostasis and decreases spasticity through the BDNF-KCC2 pathway after chronic SCI, *bioRxiv*. doi: 10.1101/489740.
- Schumacher, R.N. *Linear and Nonlinear Approaches to the Analysis of R-R Interval Variability*. SAGE, 5(211), doi: 0.1177/1099800403260619
- Scivoletto, G. et al. (2008). Clinical factors that affect walking level and performance in chronic spinal cord lesion patients, *Spine*, 33(3), pp. 259–264. doi: 10.1097/BRS.0b013e3181626ab0.
- Scott, B. R. et al. (2015). Exercise with blood flow restriction: An updated evidence-based approach for enhanced muscular development, *Sports Medicine*, 45(3), pp. 313–325. doi: 10.1007/s40279-014-0288-1.
- Segal, J. L. and Brunnemann, S. R. (1998). 4-Aminopyridine alters gait characteristics and enhances locomotion in spinal cord injured humans, *Journal of Spinal Cord Medicine*, 21(3), pp. 200–204. doi: 10.1080/10790268.1998.11719527.
- Semenza, G. L. (2008) 'Reviews: regulation of oxygen homeostasis by Hypoxia-Inducible Factor-1', *Physiology*, 24, pp. 97–106. doi: 10.1152/physiol.00045.2008.
- Semenza, G. L. and Wang, G. L. (1992). A nuclear factor induced by hypoxia via de novo protein synthesis binds to the human erythropoietin gene enhancer at a site required for transcriptional activation, *Molecular and Cellular Biology*, 12(12), pp. 5447–5454. doi: 10.1128/mcb.12.12.5447.

- Sequeira, V. C. C., Bandeira, P. M. and Azevedo, J. C. M. (2019). Heart rate variability in adults with obstructive sleep apnea: A systematic review, *Sleep Science*, 12(3), pp. 214–221. doi: 10.5935/1984-0063.20190082.
- Serebrovskaya, T. V (2002). Intermittent hypoxia research in the former soviet union and the commonwealth of independent states: History and review of the concept and selected applications, *high altitude medicine & biology*, 3(2), pp. 205–221.
- Serebrovskaya, T. V. et al. (2008). Intermittent hypoxia: Cause of or therapy for systemic hypertension?, *Experimental Biology and Medicine*, 233(6), pp. 627–650. doi: 10.3181/0710-MR-267.
- Serebrovskaya, T. V. and Xi, L. (2016). Intermittent hypoxia training as non-pharmacologic therapy for cardiovascular diseases: Practical analysis on methods and equipment, 241, pp 1708-1723. doi: 10.1177//1535370216657614
- Shaffer, F. and Ginsberg, J. P. (2017). An overview of heart rate variability metrics and norms, *Frontiers in Public Health*, 5, pp. 1–17. doi: 10.3389/fpubh.2017.00258.
- Shin, J. C. et al. (2011). Comparison of lower extremity motor score parameters for patients with motor incomplete spinal cord injury using gait parameters, *Spinal Cord. Nature Publishing Group*, 49(4), pp. 529–533. doi: 10.1038/sc.2010.158.
- Shoukri, M. M., Asyali, M. H. and Donner, A. (2004). Sample size requirements for the design of reliability study: Review and new results, *statistical methods in medical research*, 13(4), pp. 251–271. doi: 10.1191/0962280204sm365ra.
- Sihle-Wissel, M., Scholz, M. and Cunitz, G. (2000). Transcranial magnetic-evoked potentials under total intravenous anaesthesia and nitrous oxide, *British Journal of Anaesthesia. British Journal of Anaesthesia*, 85(3), pp. 465–467. doi: 10.1093/bja/85.3.465.
- Sivaramakrishnan, A., Solomon, J. M. and Manikandan, N. (2018). Comparison of transcutaneous electrical nerve stimulation (TENS) and functional electrical stimulation (FES) for spasticity in spinal cord injury - A pilot randomized cross-over trial, *Journal of Spinal Cord Medicine. Taylor & Francis*, 41(4), pp. 397–406. doi: 10.1080/10790268.2017.1390930.
- Souza, V. H. et al. (2018). Development and characterization of the InVesalius navigator software for navigated transcranial magnetic stimulation, *Journal of Neuroscience Methods. Elsevier*, 309(August), pp. 109–120. doi: 10.1016/j.jneumeth.2018.08.023.
- Spungen, A. M. et al. (1997). Self-reported prevalence of pulmonary symptoms in subjects with spinal cord injury, *Spinal Cord*, 35(10), pp. 652–657. doi: 10.1038/sj.sc.3100489.
- Stevenson, C. M. et al. (2016). Traumatic central cord syndrome: Neurological and functional outcome at 3 years, *Spinal Cord. Nature Publishing Group*, 54(11), pp. 1010–1015. doi: 10.1038/sc.2016.34.
- Streiner, D., Norman, G. and Cairney, J. (2015). *Health measurement scales*. 5th ed. Oxford: Oxford University Press.
- Streeter, K. A. et al. (2017). Intermittent hypoxia enhances functional connectivity of midcervical spinal interneurons, *Journal of Neuroscience*, 37(35), pp. 8349–8362. doi: 10.1523/JNEUROSCI.0992-17.2017.
- Swinnen, E. et al. (2010). Effectiveness of robot-assisted gait training in persons with spinal cord injury: A systematic review, *Journal of Rehabilitation Medicine*, 42(6), pp. 520–526. doi: 10.2340/16501977-0538.
- Tadjalli, A. and Mitchell, G. S. (2019). Cervical spinal 5-HT_{2A} and 5-HT_{2B} receptors are both necessary for moderate acute intermittent hypoxia-induced phrenic long-term facilitation, *Journal of Applied Physiology*, 127(2), pp. 432–443. doi: 10.1152/jappphysiol.01113.2018.
- Taheri, B. A., Knight, R. T. and Smith, R. L. (1994). A dry electrode for EEG recording, *Electroencephalography and Clinical Neurophysiology*, 90(5), pp. 376–383. doi: 10.1016/0013-4694(94)90053-1.
- Tahrani, A. A., Ali, A. and Stevens, M. J. (2013). Obstructive sleep apnoea and diabetes: An update, *Current Opinion in Pulmonary Medicine*, 19(6), pp. 631–638. doi: 10.1097/MCP.0b013e3283659da5.
- Takarada, Y. et al. (2000). Effects of resistance exercise combined with moderate vascular occlusion on muscular function in humans, *Journal of Applied Physiology*, 88(6), pp. 2097–2106. doi: 10.1152/jappphysiol.2000.88.6.2097.
- Tan, A. Q., Barth, S. and Trumbower, R. D. (2020). Acute intermittent hypoxia as a potential adjuvant to improve walking following spinal cord injury: Evidence, challenges, and future directions', *Current Physical Medicine and*

- Rehabilitation Reports. *Current Physical Medicine and Rehabilitation Reports*, 8(3), pp. 188–198. doi: 10.1007/s40141-020-00270-8.
- Tang, W. et al. (2018). Surface electromyographic examination of poststroke neuromuscular changes in proximal and distal muscles using clustering index analysis, *Frontiers in Neurology*, 8, pp. 1–9. doi: 10.3389/fneur.2017.00731.
- Tashiro, S. et al. (2015). BDNF Induced by treadmill training contributes to the suppression of spasticity and allodynia after spinal cord injury via upregulation of KCC2, *Neurorehabilitation and Neural Repair*, 29(7), pp. 677–689. doi: 10.1177/1545968314562110.
- Task force of the Euro and Electrophysiology. (1996). Heart rate variability: Standards of measurement, physiological interpretation, and clinical use, *European Heart Journal*, 17, pp. 354–381. doi: 10.4324/9781315372921.
- Taylor, J. L. and Martin, P. G. (2009). Voluntary motor output is altered by spike-timing-dependent changes in the human corticospinal pathway, *Journal of Neuroscience*, 29(37), pp. 11708–11716. doi: 10.1523/JNEUROSCI.2217-09.2009.
- Terao, Y. and Ugawa, Y. (2002). Basic mechanisms of TMS, *Journal of Clinical Neurophysiology*, 19(4), pp. 322–343. doi: 10.1097/00004691-200208000-00006.
- Tester, N. J. et al. (2014). Long-term facilitation of ventilation in humans with chronic spinal cord injury, *American Journal of Respiratory and Critical Care Medicine*, 189(1), pp. 57–65. doi: 10.1164/rccm.201305-0848OC.
- Tica, J., Bradbury, E. J. and Didangelos, A. (2018). Combined transcriptomics, proteomics and bioinformatics identify drug targets in spinal cord injury, *International Journal of Molecular Sciences*, 19(5). doi: 10.3390/ijms19051461.
- Treede, R. D., Lorenz, J. and Baumgärtner, U. (2003). Clinical usefulness of laser-evoked potentials, *Neurophysiologie Clinique*, 33(6), pp. 303–314. doi: 10.1016/j.neucli.2003.10.009.
- Trumbower, R. D. et al. (2012). Exposure to acute intermittent hypoxia augments somatic motor function in humans with incomplete spinal cord injury, *Neurorehabilitation and Neural Repair*, 26(2), pp. 163–172. doi: 10.1177/1545968311412055.
- Trumbower, R. D. et al. (2017). Effects of acute intermittent hypoxia on hand use after spinal cord trauma: A preliminary study, *Neurology*, 89(18), pp. 1904–1907. doi: 10.1212/WNL.0000000000004596.
- Tzvetanov, P., Rousseff, R. T. and Milanov, I. (2003). Lower limb SSEP changes in stroke - Predictive values regarding functional recovery, *Clinical Neurology and Neurosurgery*, 105(2), pp. 121–127. doi: 10.1016/S0303-8467(02)00132-4.
- Ueno, S., Tashiro, T. and Harada, K. (1988). Localized stimulation of neural tissues in the brain by means of a paired configuration of time-varying magnetic fields, *Journal of Applied Physics*, 64(10), pp. 5862–5864. doi: 10.1063/1.342181.
- Valipour, S., Shaligram, A. D. and Kulkarni, G. R. (2014). Detection of an alpha rhythm of EEG signal based on EEGLAB, *International Journal of Engineering Research and Applications*, 4(1), pp. 154–159.
- Van Middendorp, J. J. et al. (2009). ASIA impairment scale conversion in traumatic SCI: Is it related with the ability to walk? A descriptive comparison with functional ambulation outcome measures in 273 patients, *Spinal Cord*. Nature Publishing Group, 47(7), pp. 555–560. doi: 10.1038/sc.2008.162.
- Vavrek, R. et al. (2006). BDNF promotes connections of corticospinal neurons onto spared descending interneurons in spinal cord injured rats, *Brain*, 129(6), pp. 1534–1545. doi: 10.1093/brain/awl087.
- Vivodtzev, I. et al. (2020). Mild to moderate sleep apnea is linked to hypoxia-induced motor recovery after spinal cord injury, *American Journal of Respiratory and Critical Care Medicine*, 202(6), pp. 887–890. doi: 10.1164/rccm.202002-0245LE.
- Vogtel, M. and Michels, A. (2010). Role of intermittent hypoxia in the treatment of bronchial asthma and chronic obstructive pulmonary disease, *Current Opinion in Allergy and Clinical Immunology*, 10(3), pp. 206–213. doi: 10.1097/ACI.0b013e32833903a6.
- Washabaugh, E. P. and Krishnan, C. K. (2016). A low-cost system for coil tracking during transcranial magnetic stimulation, *Physiology & Behavior*, 34(2), pp. 337–346. doi: 10.3233/RNN-150609.A.

- Weidemann, A. and Johnson, R. S. (2008). Biology of HIF-1 α , *Cell Death and Differentiation*, 15(4), pp. 621–627. doi: 10.1038/cdd.2008.12.
- Weidner, N., Rupp, R. and Tansey, K. (2017). *Neurological Aspects of Spinal Cord Injury*.
- Weishaupt, N. et al. (2013). Synergistic effects of BDNF and rehabilitative training on recovery after cervical spinal cord injury, *Behavioural Brain Research*, 239(1), pp. 31–42. doi: 10.1016/j.bbr.2012.10.047.
- Welch, J. F. et al. (2020). Synergy between acute intermittent hypoxia and task-specific training, *Exercise and Sport Sciences Reviews*, 48(3), pp. 125–132. doi: 10.1249/JES.0000000000000222.
- Wen Dong, J. et al. (2003). Intermittent hypoxia attenuates ischemia/reperfusion induced apoptosis in cardiac myocytes via regulating Bcl-2/Bax expression, *Cell Research*, 13(5), pp. 385–391. Available at: <http://www.cell-research.com>.
- Wessels, M. et al. (2010). Body weight-supported gait training for restoration of walking in people with an incomplete spinal cord injury a systematic review, *Journal of Rehabilitation Medicine*, 42(6), pp. 513–519. doi: 10.2340/16501977-0525.
- Wilkerson, J. E. R. and Mitchell, G. S. (2009). Daily intermittent hypoxia augments spinal BDNF levels, ERK phosphorylation and respiratory long-term facilitation, *Experimental Neurology*. Elsevier Inc., 217(1), pp. 116–123. doi: 10.1016/j.expneurol.2009.01.017.
- Wilson, M. T., Moezzi, B. and Rogasch, N. C. (2021). Modeling motor-evoked potentials from neural field simulations of transcranial magnetic stimulation, *Clinical Neurophysiology*, 132(2), pp. 412–428. doi: 10.1016/j.clinph.2020.10.032.
- Wirz, M. and Dietz, V. (2012). Concepts of aging with paralysis. Implications for recovery and treatment. 1st edn, *Handbook of Clinical Neurology*. Elsevier B.V. doi: 10.1016/B978-0-444-52137-8.00005-X.
- Wong, S., Shem, K. and Crew, J. (2012). Specialized respiratory management for acute cervical spinal cord injury: A retrospective analysis, *topics in spinal cord injury rehabilitation*, 18(4), pp. 283–290. doi: 10.1310/sci1804-283.
- Workman, C. and Basset, F. A. (2012). Post-metabolic response to passive normobaric hypoxic exposure in sedentary overweight males: A pilot study, *Nutrition and Metabolism*, 9, pp. 1–9. doi: 10.1186/1743-7075-9-103.
- World Health Organization. (2013). *International perspectives on spinal cord injury*. World Health Organization.
- Wu, M. J. et al. (2020) ‘5-HT7 Receptor Inhibition Transiently Improves Respiratory Function Following Daily Acute Intermittent Hypercapnic-Hypoxia in Rats With Chronic Midcervical Spinal Cord Contusion’, *Neurorehabilitation and Neural Repair*, 34(4), pp. 333–343. doi: 10.1177/1545968320905806.
- Xu, X. M. et al. (1995). A Combination of BDNF and NT-3 promotes supraspinal axonal regeneration into schwann cell grafts in adult rat thoracic spinal cord’, *Experimental Neurology*, 134, pp. 261–272.
- Yin, H., Paiva, A. and Billard, A. (2015). Learning cost function and trajectory for robotic writing motion, *IEEE-RAS International Conference on Humanoid Robots*, 2015-Febru, pp. 608–615. doi: 10.1109/HUMANOIDS.2014.7041425.
- Yunokuchi, K. and Cohen, D. (1991). Developing a More Focal Magnetic Stimulator. Part II: Fabricating Coils and Measuring Induced Current Distributions. *Journal of Clinical Neurophysiology*, pp. 112–120.
- Zabka, A. G., Mitchell, G. S. and Behan, M. (2005). Ageing and gonadectomy have similar effects on hypoglossal long-term facilitation in male Fischer rats, *Journal of Physiology*, 563(2), pp. 557–568. doi: 10.1113/jphysiol.2004.077511.
- Zakaria, N. A. et al. (2015). Quantitative analysis of fall risk using TUG test, *Computer Methods in Biomechanics and Biomedical Engineering*, 18(4), pp. 426–437. doi: 10.1080/10255842.2013.805211.
- Zamparo, P. and Pagliaro, P. (1998). The energy cost of level walking before and after hydro-kinesi therapy in patients with spastic paresis, *Scandinavian Journal of Medicine and Science in Sports*, 8(4), pp. 222–228. doi: 10.1111/j.1600-0838.1998.tb00196.x.
- Zimmer, M. B., Nantwi, K. and Goshgarian, H. G. (2007). Effect of spinal cord injury on the respiratory system: basic research and current clinical treatment options, *The journal of spinal cord medicine*, 30(4), pp. 319–30. doi: 10.1016/j.expneurol.2007.05.015.

Zong, P. et al. (2004). Intermittent hypoxic training protects canine myocardium from infarction, *Experimental Biology and Medicine*, 229(8), pp. 806–812. doi: 10.1177/153537020422900813.

Appendices

Appendix.I.(Capter.2.)

1) Activity and health questionnaire

Date	Investigator	Signature

ACTIVITY AND HEALTH QUESTIONNAIRE

Name _____ Age _____

Have you ever been told that you have had or have any of the following conditions? If yes, please mark with an X in the appropriate box:

Cardiorespiratory

- High blood pressure
- Blood clot
- Narrowing of arteries
- Angina/chest pain on exertion
- Congenital heart disease
- Asthma/exercise-induced asthma
- Chronic bronchitis
- Emphysema
- T.B
- Other/comments

Neurological

- Epilepsy
- Nerve damage
- Parkinson's
- Stroke
- Other/comments

Other conditions

- Diabetes (type 1 or 2)
- Inflammatory joint condition
- Orthopaedic surgery (musculo-skeletal)
- Metallic plates/implants
- Pacemaker
- Pregnant
- Tendon or ligament injury to the knee or ankle
- Other/comments

Physical Activity Status

This can be an accumulation of moderate to vigorous level activities including brisk walking, exercise, sports and housework

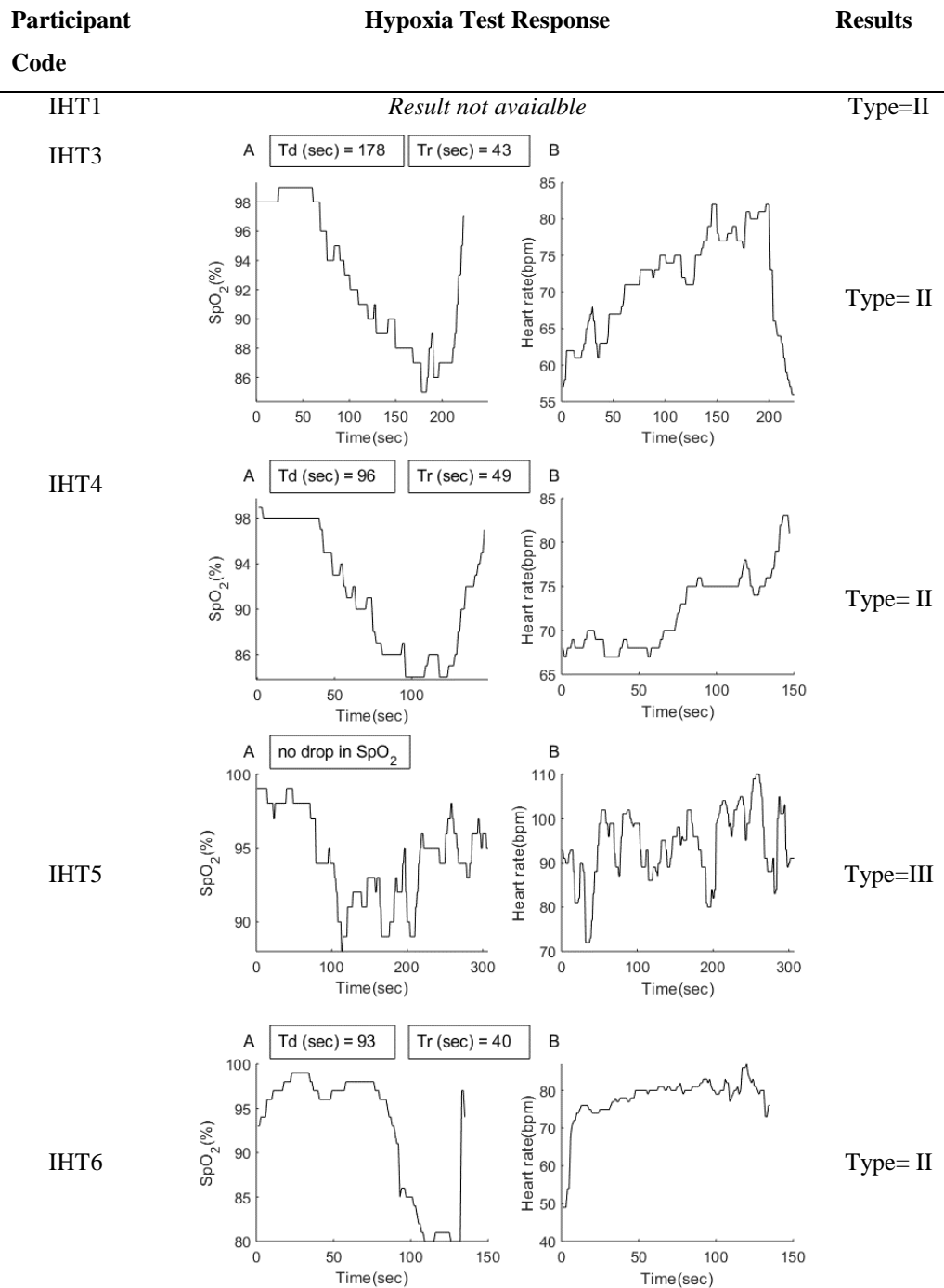
- Exercise/physically active less than 3 hours per week
- Exercise/physically active 3—7 hours per week
- Exercise/physically active over 7 hours per week

I have read, understood and completed this questionnaire to the best of my knowledge.

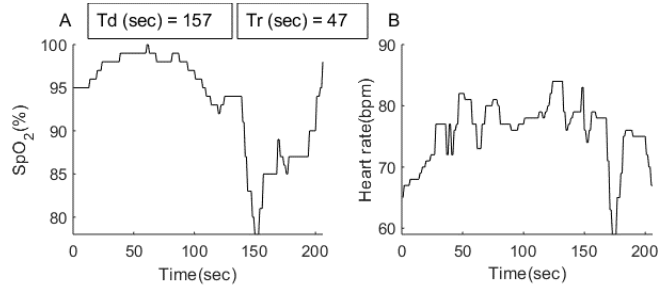
I will inform the investigators of any illness, injury or condition that occurs during the course of participation in the study.

Signed.....Date.....

2) Individual hypoxia test graphs

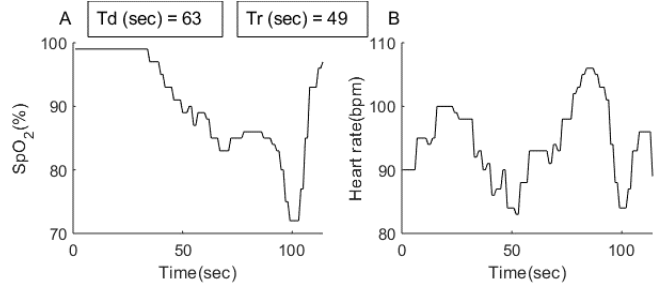


IHT7



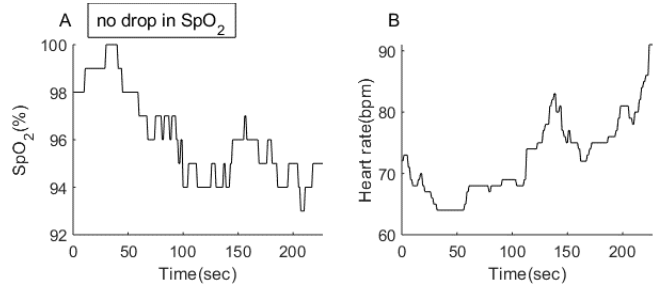
Type= II

IHT8



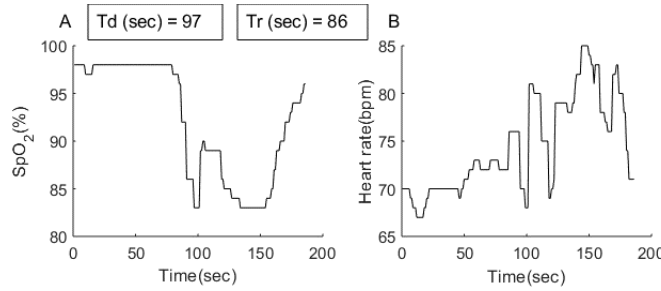
Type= II

IHT10



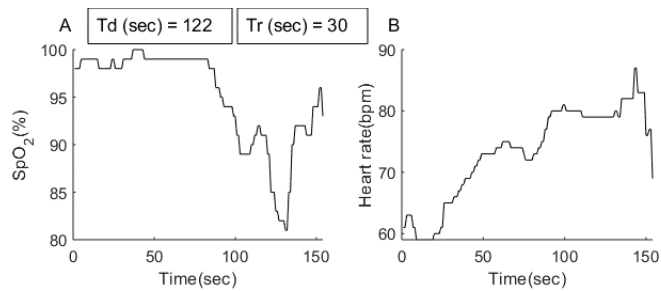
Type= III

IHT11

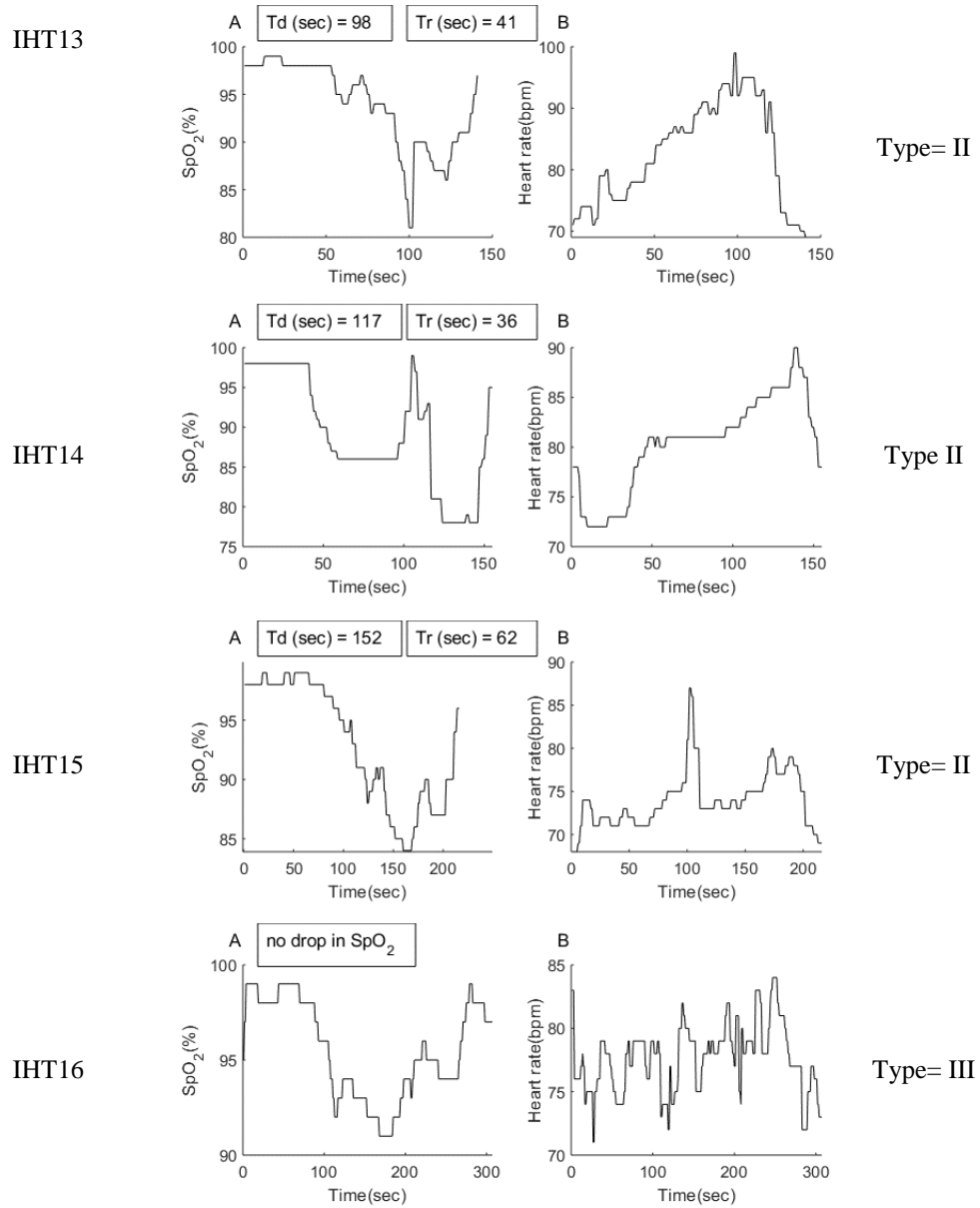


Type= II

IHT12



Type= II

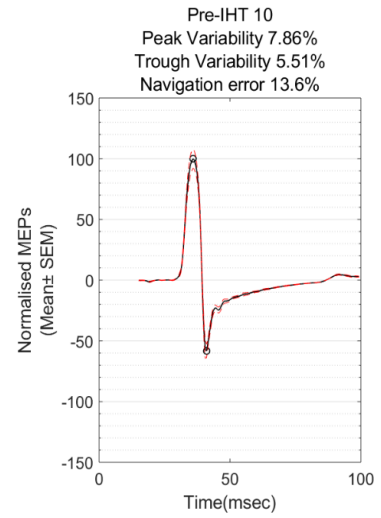
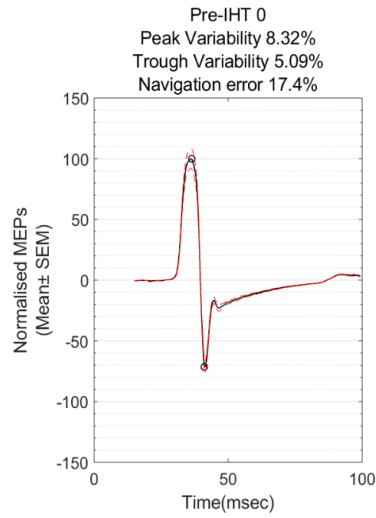


Td: time to descend; Tr: time to recover

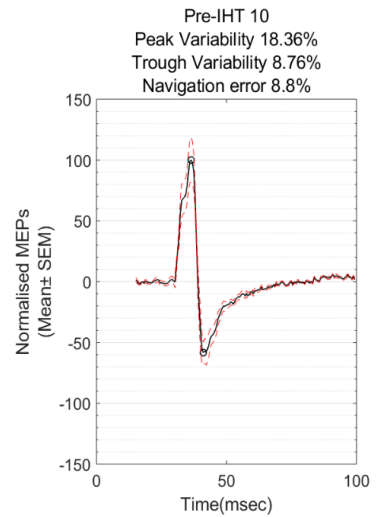
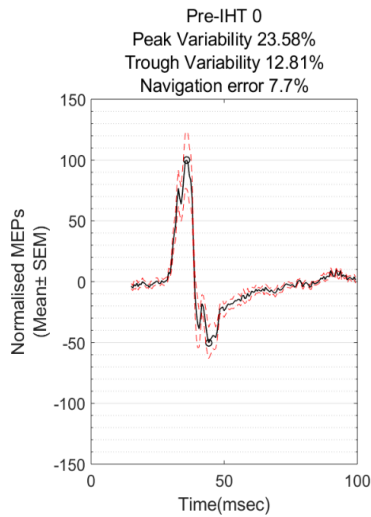
Appendix.II. (Chapter.5.)

1) Baseline peak and trough variability

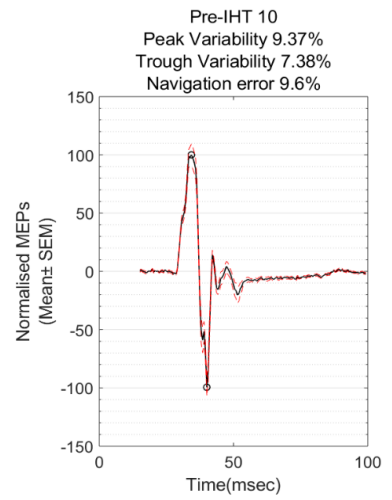
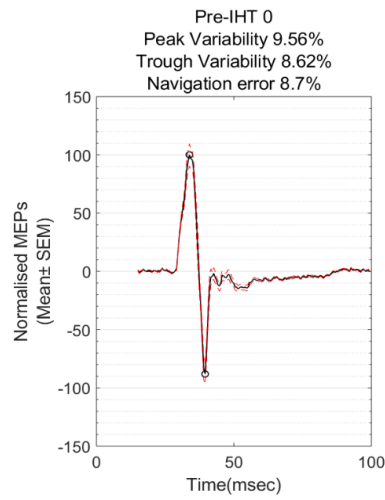
IHT2



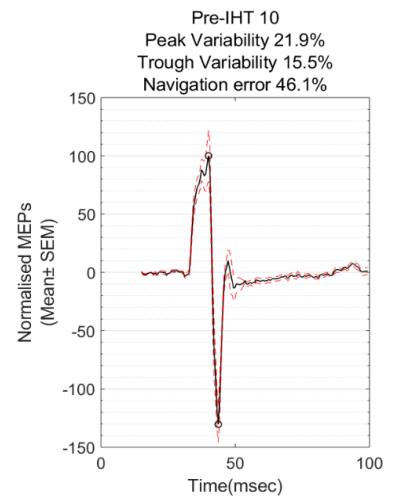
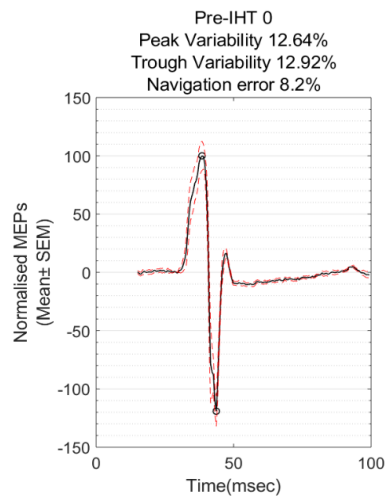
IHT6



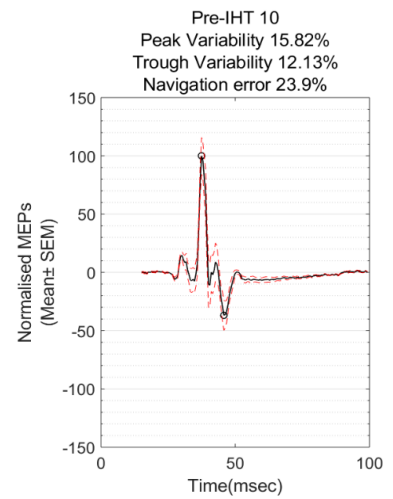
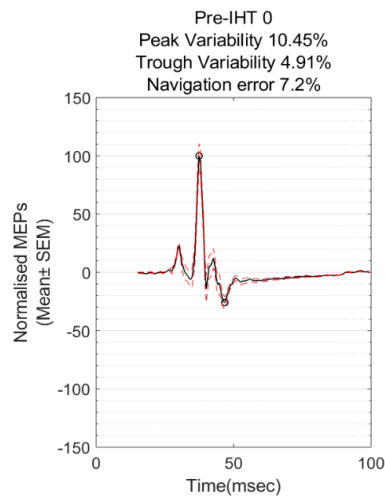
IHT10



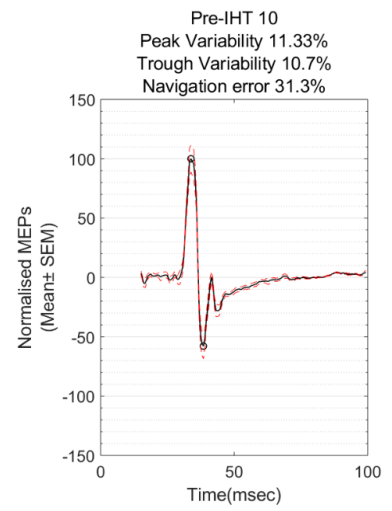
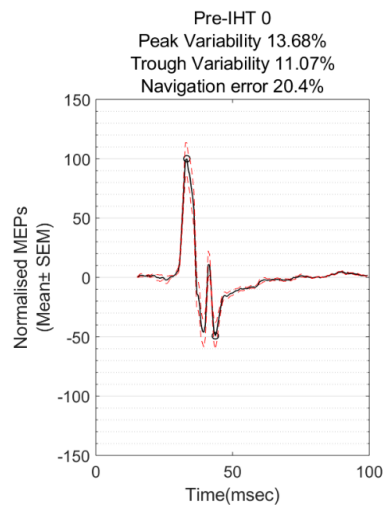
IHT11



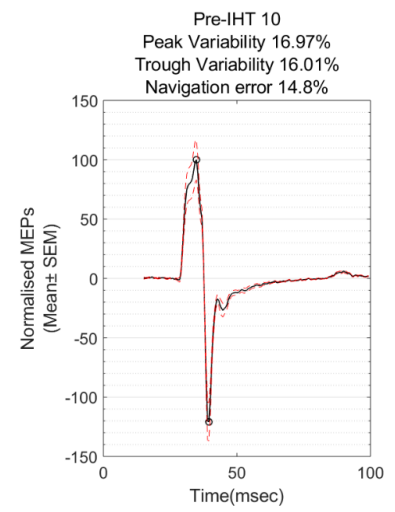
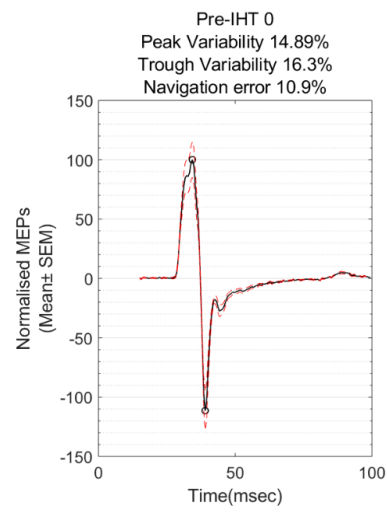
IHT12



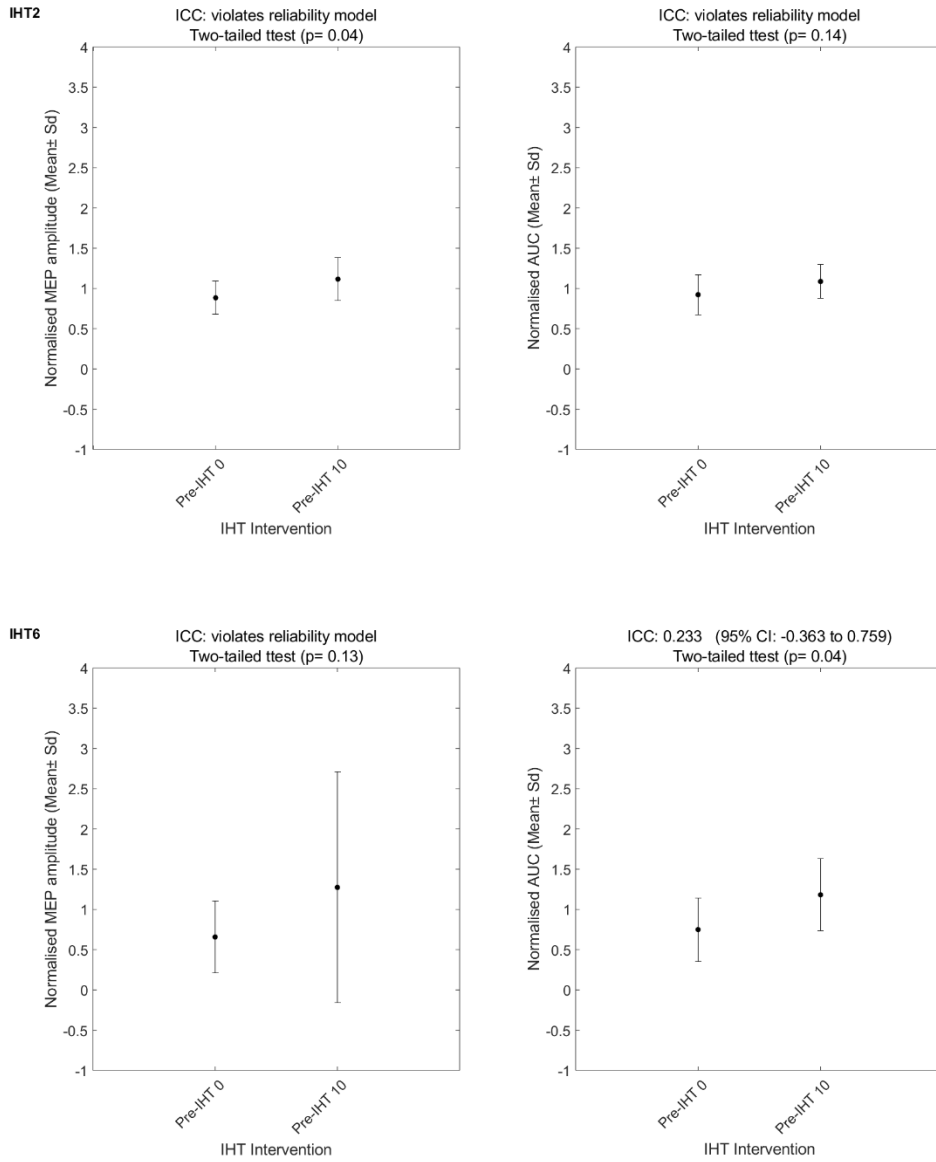
IHT14

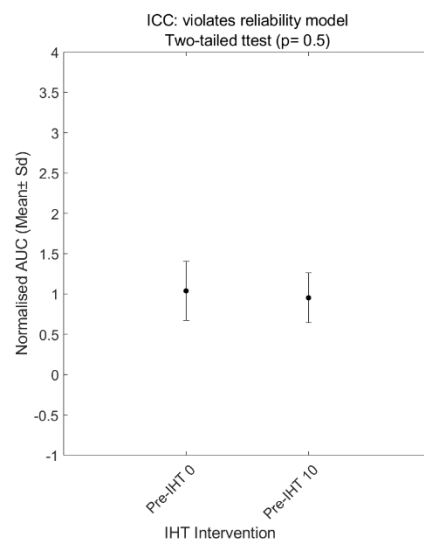
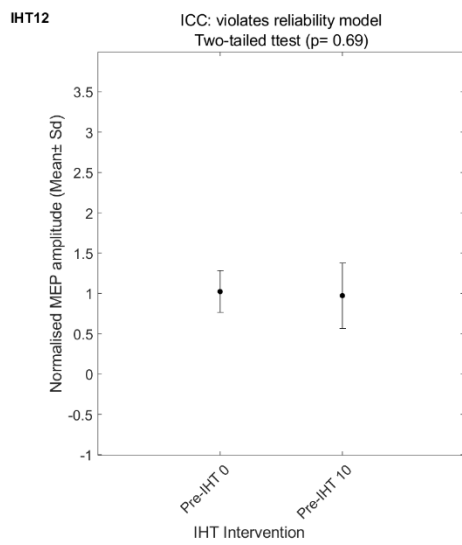
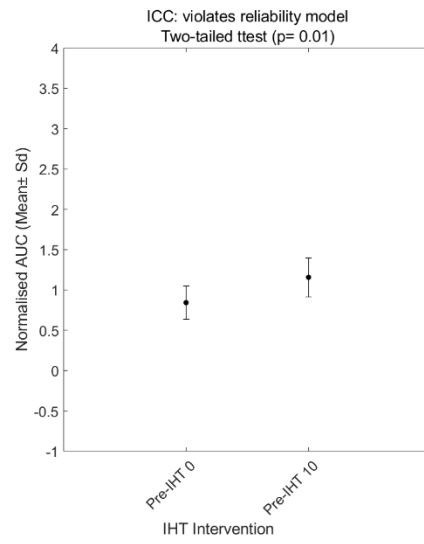
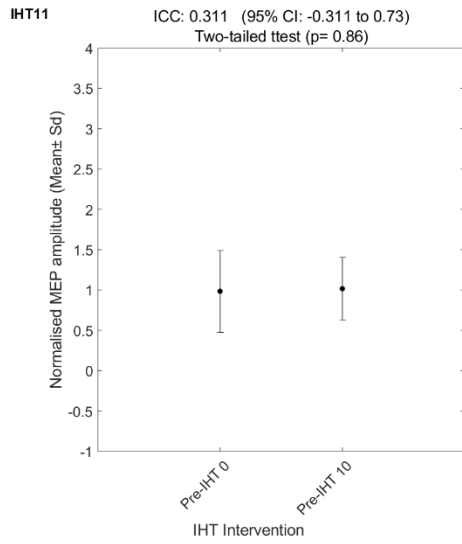
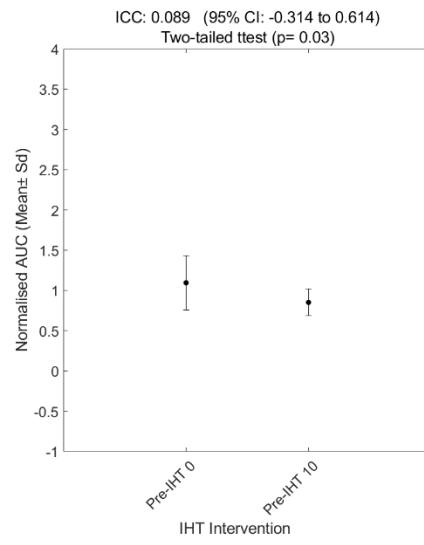
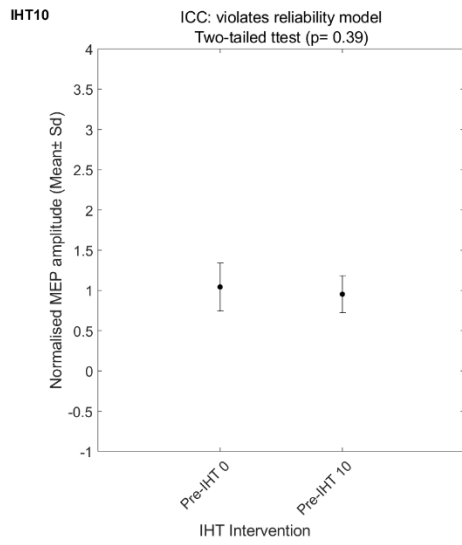


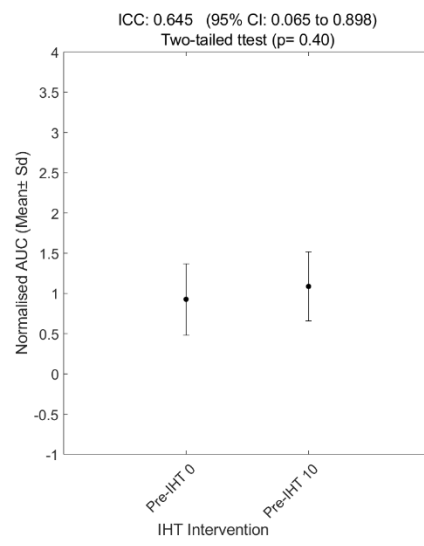
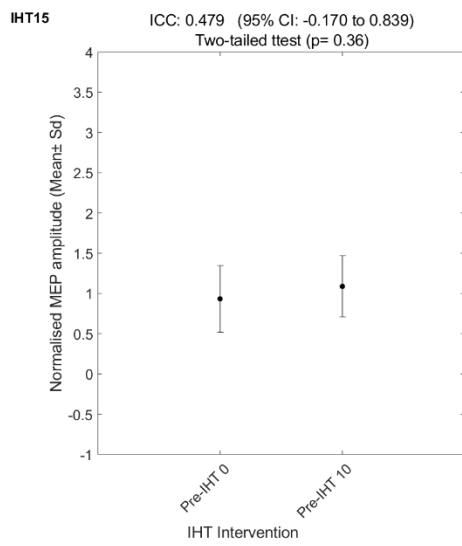
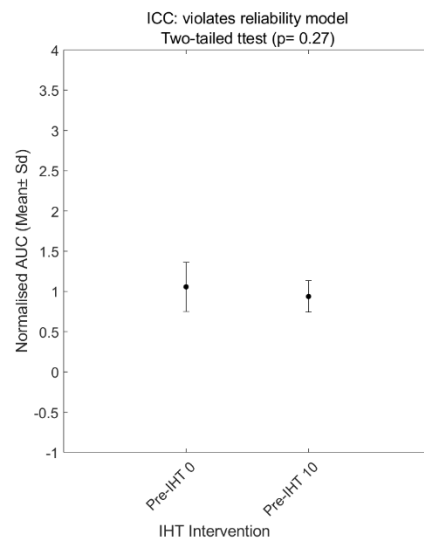
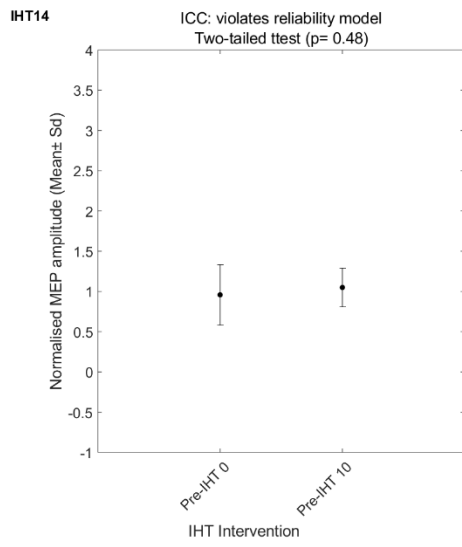
IHT15



2) ICC analysis and two-tailed t-test between baseline measurements

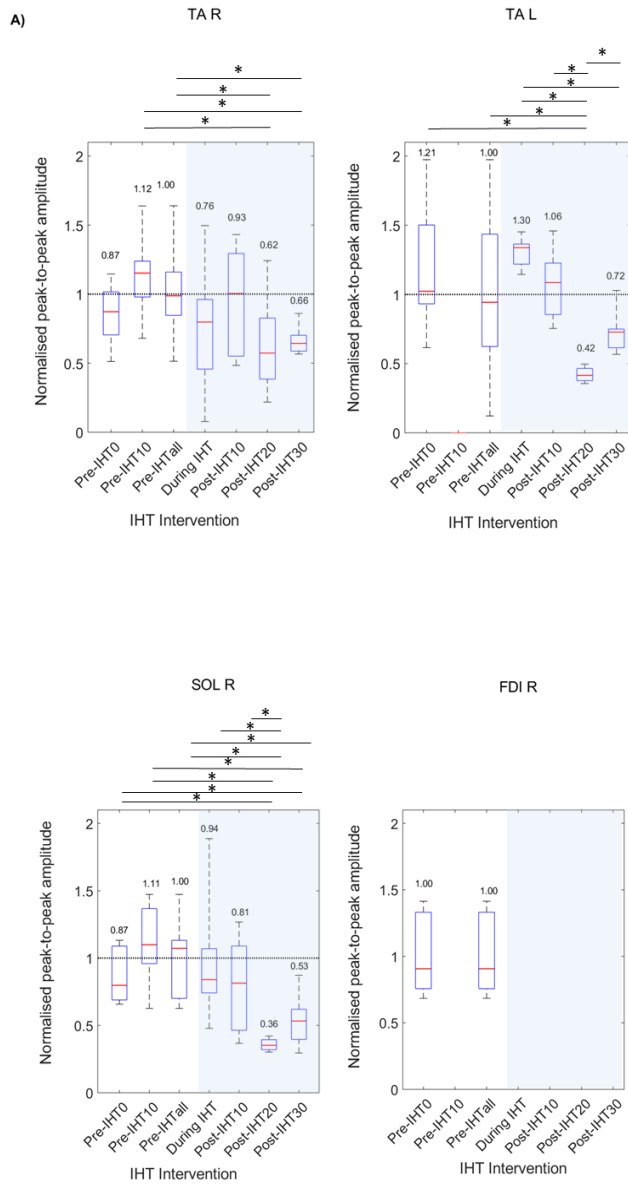






3) Peak-to-peak amplitude boxplots

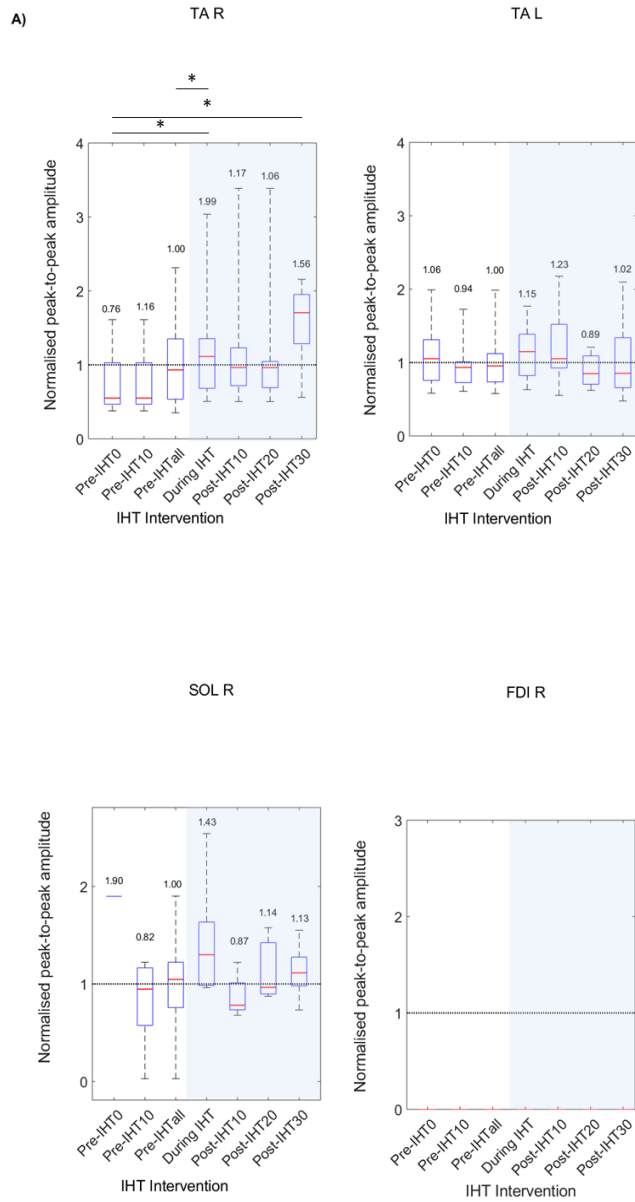
IHT2



B)

Navigation error (%)	
Pre-IHT 0	17.4
Pre-IHT10	13.6
During IHT	8.1
Post-IHT10	11.9
Post-IHT20	7.1
Post-IHT30	8.0

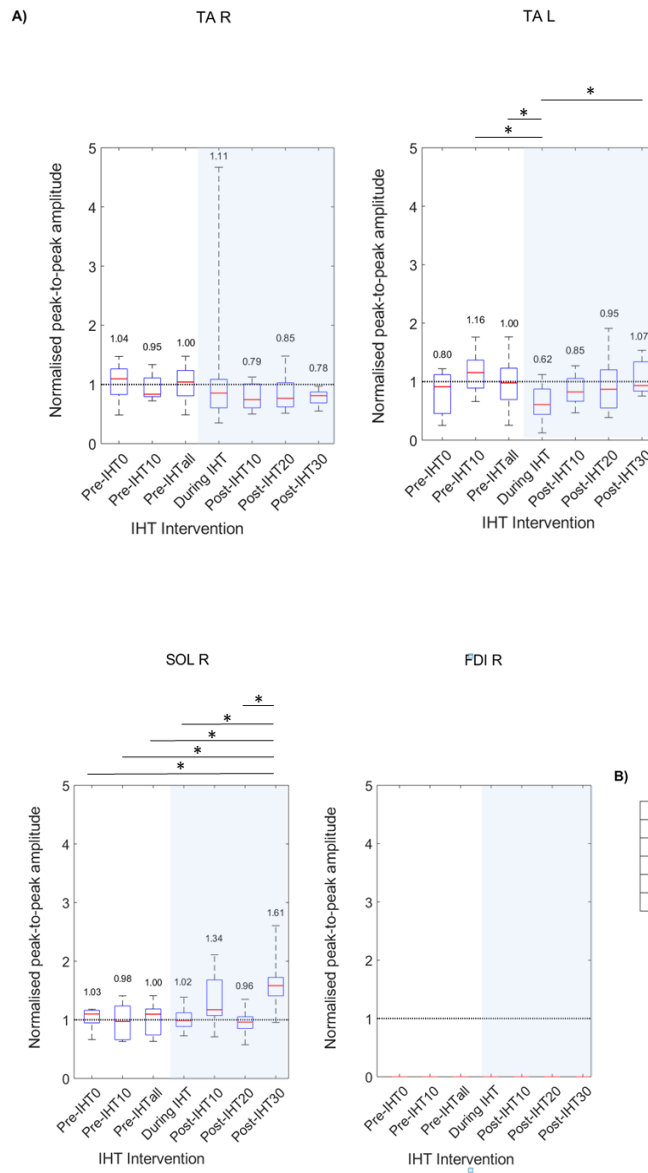
IHT6



B)

Navigation error (%)	
Pre-IHT 0	7.7
Pre-IHT10	7.8
During IHT	9.2
Post-IHT10	10.5
Post-IHT20	11.2
Post-IHT30	8.4

IHT10

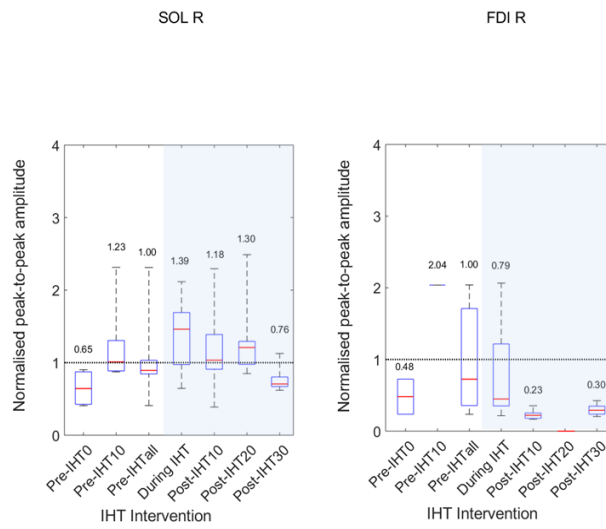
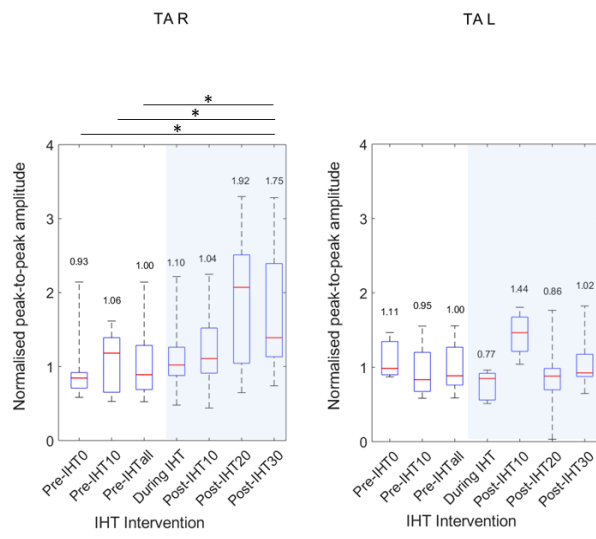


B)

Navigation error (%)	
Pre-IHT 0	8.7
Pre-IHT10	9.6
During IHT	6.9
Post-IHT10	9.4
Post-IHT20	11.2
Post-IHT30	13.1

IHT11

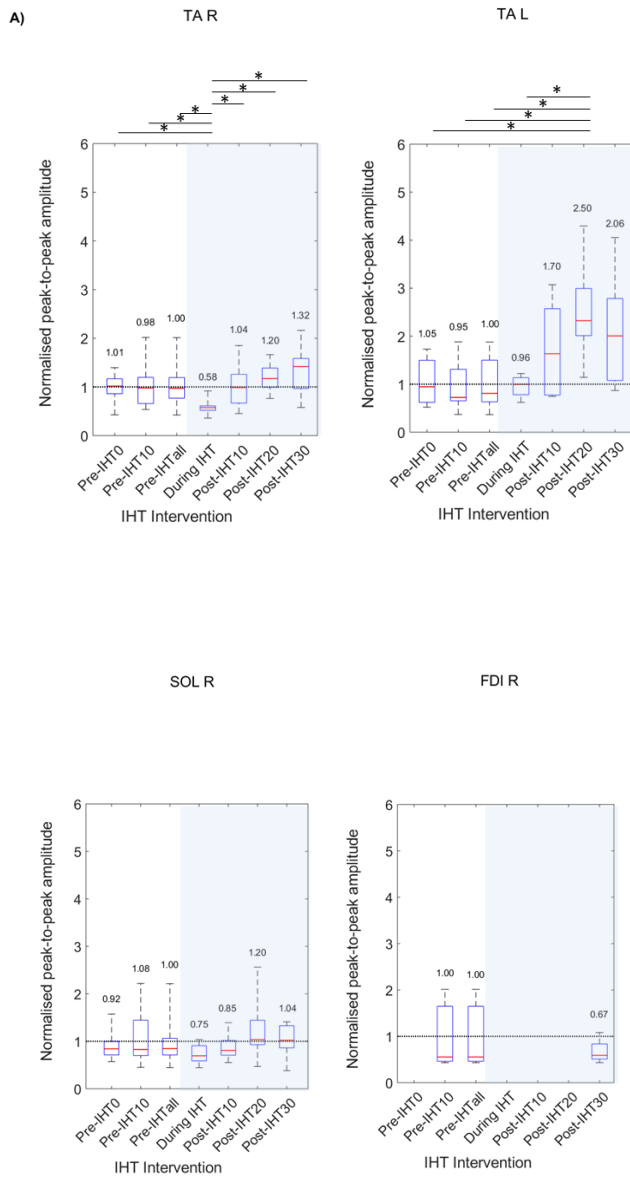
A)



B)

Navigation error (%)	
Pre-IHT 0	8.2
Pre-IHT10	46.1
During IHT	7.6
Post-IHT10	9.1
Post-IHT20	8.3
Post-IHT30	8.2

IHT12

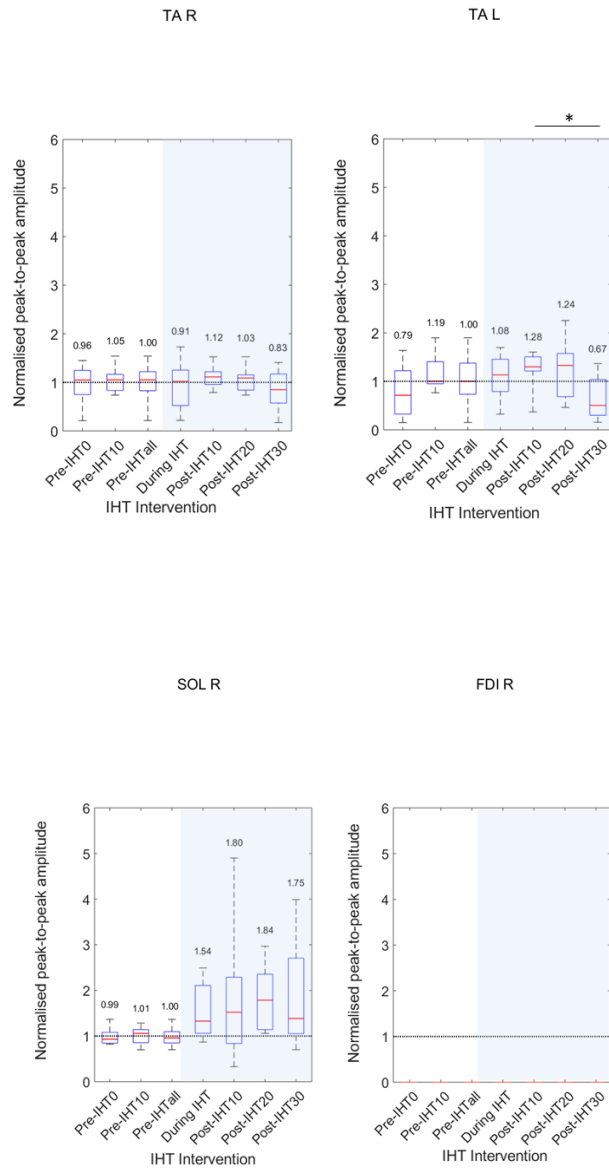


B)

Navigation error (%)	
Pre-IHT 0	7.2
Pre-IHT10	12.9
During IHT	13.9
Post-IHT10	8.0
Post-IHT20	9.9
Post-IHT30	12.0

IHT14

A)

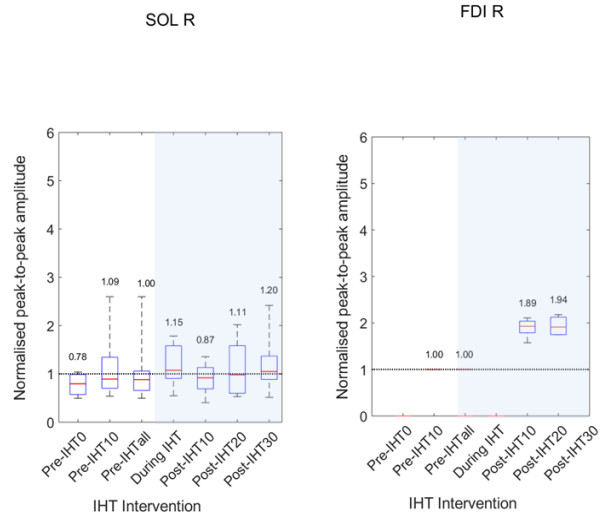
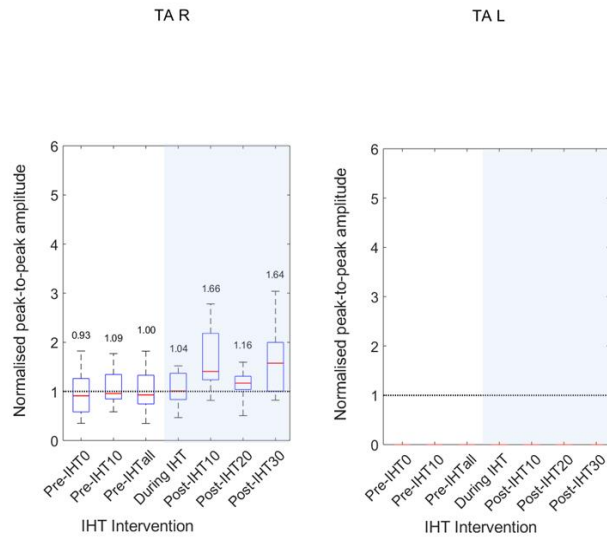


B)

Navigation error (%)	
Pre-IHT 0	20.4
Pre-IHT10	31.3
During IHT	23.0
Post-IHT10	33.7
Post-IHT20	30.5
Post-IHT30	33.6

IHT15

A)

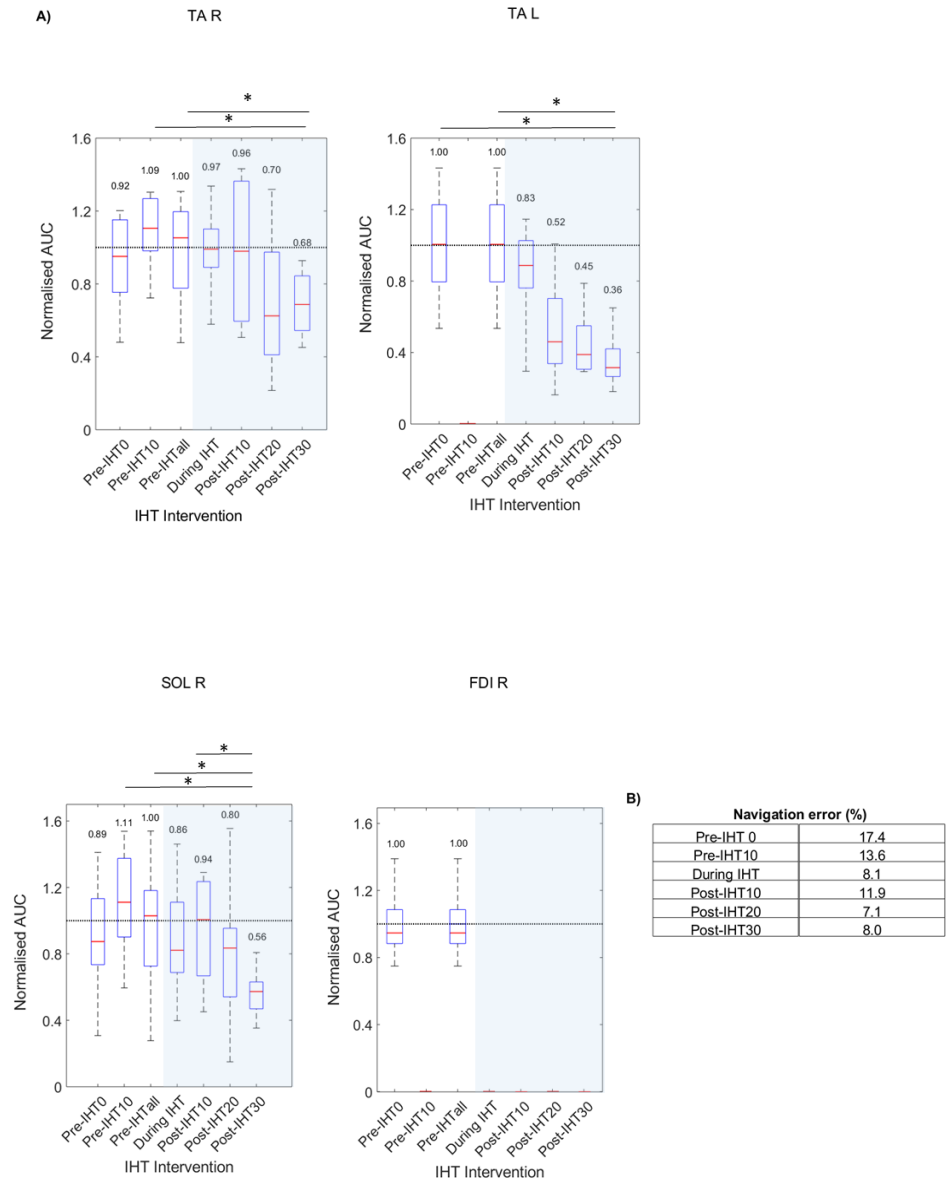


B)

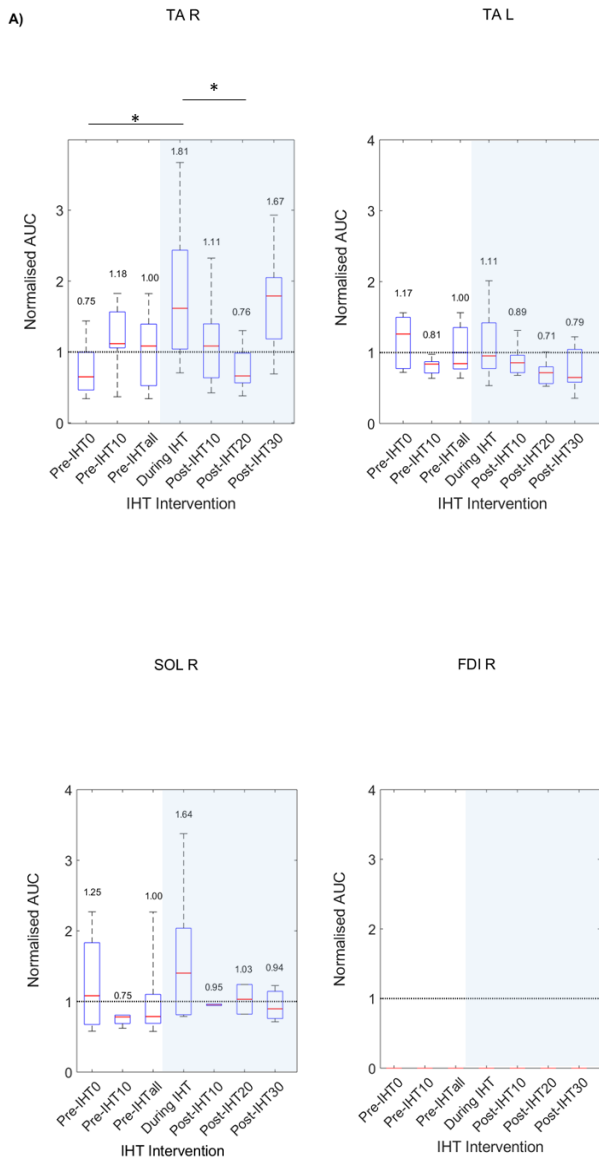
Navigation error (%)	
Pre-IHT 0	10.9
Pre-IHT10	14.8
During IHT	10.8
Post-IHT10	12
Post-IHT20	2.9
Post-IHT30	26.9

4) AUC boxplots

IHT2



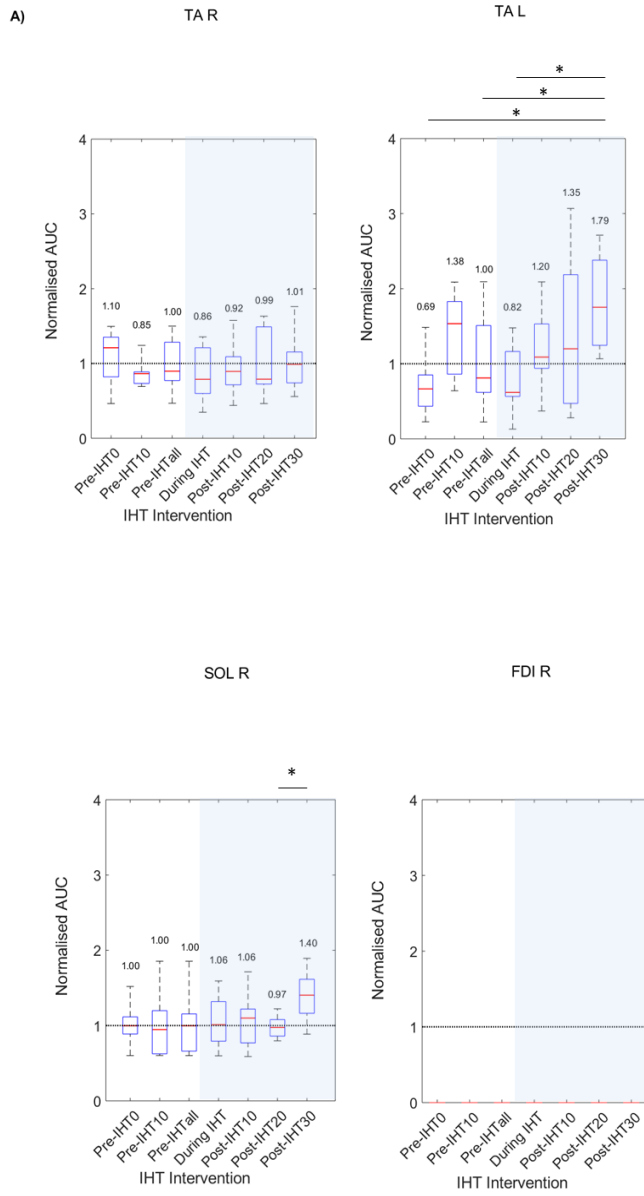
IHT6



B)

Navigation error (%)	
Pre-IHT0	7.7
Pre-IHT10	8.8
During IHT	9.2
Post-IHT10	10.5
Post-IHT20	11.2
Post-IHT30	8.4

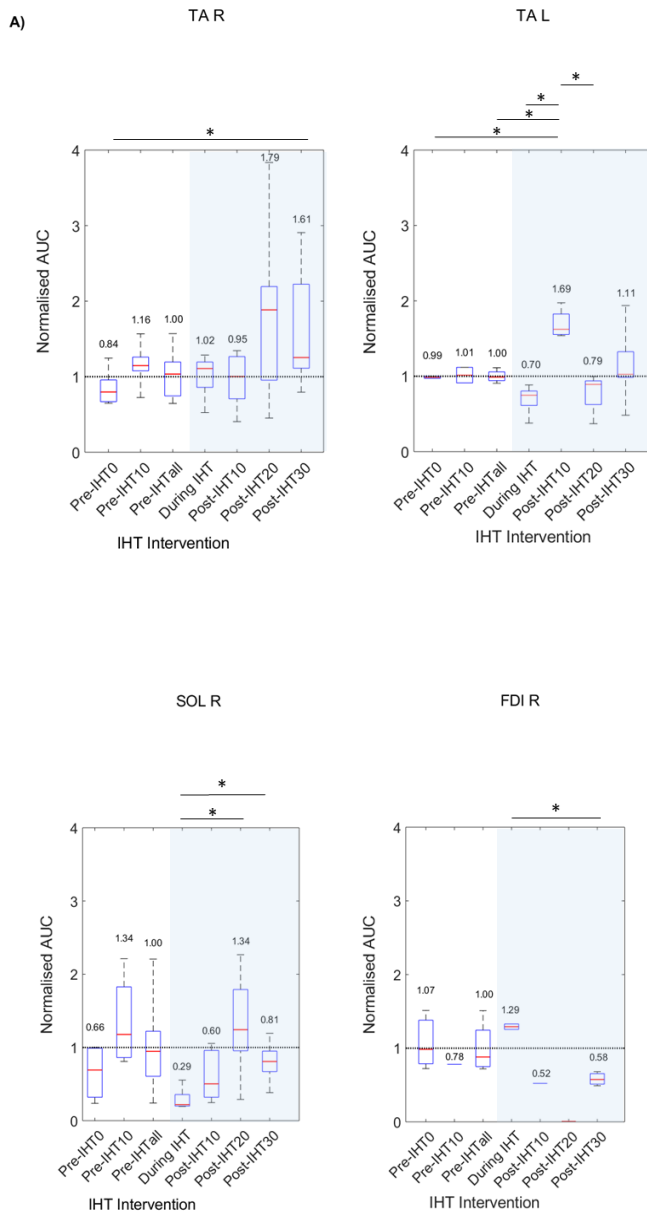
IHT10



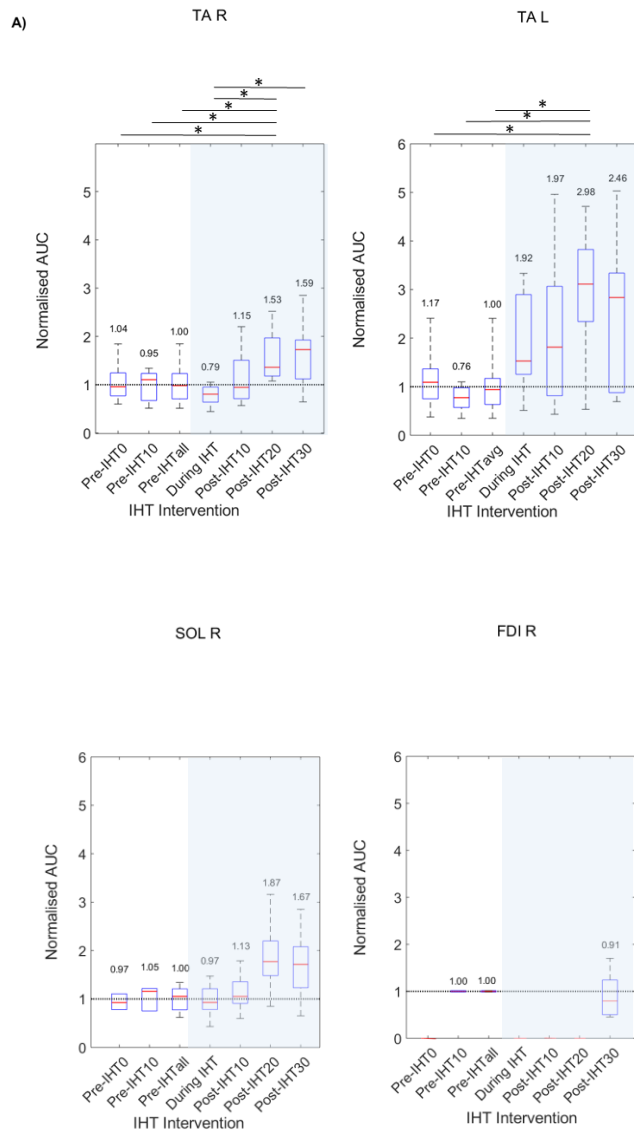
B)

Navigation error (%)	
Pre-IHT 0	8.7
Pre-IHT10	9.6
During IHT	6.9
Post-IHT10	9.4
Post-IHT20	11.2
Post-IHT30	13.1

IHT11



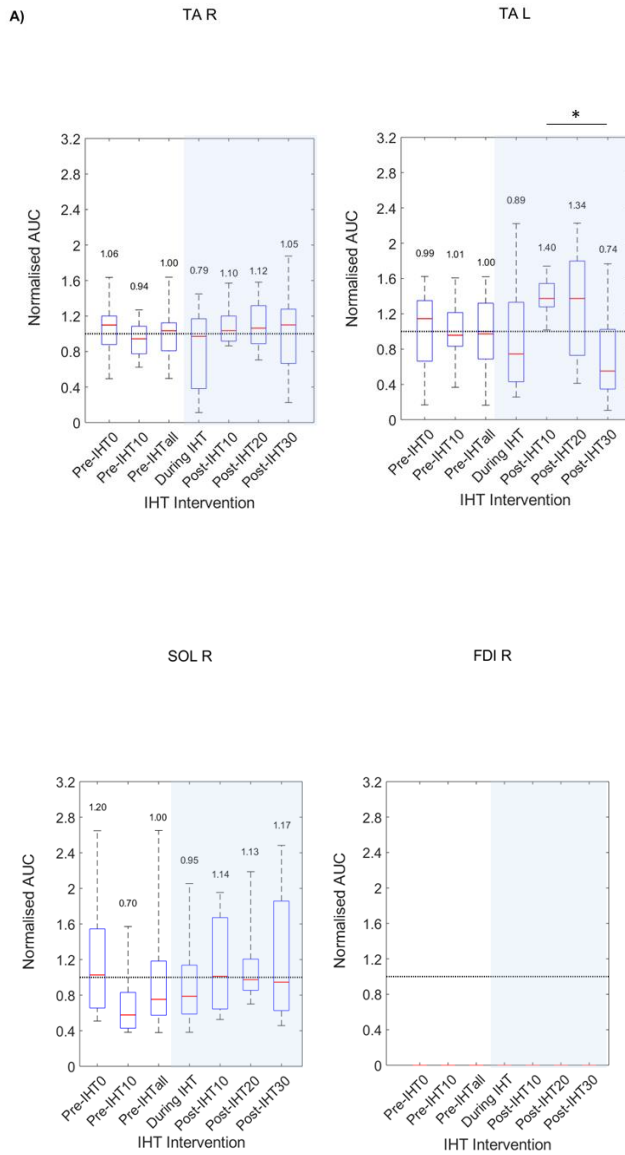
IHT12



B)

Navigation error (%)	
Pre-IHT 0	7.2
Pre-IHT10	12.9
During IHT	13.9
Post-IHT10	8.0
Post-IHT20	9.9
Post-IHT30	12.0

IHT14

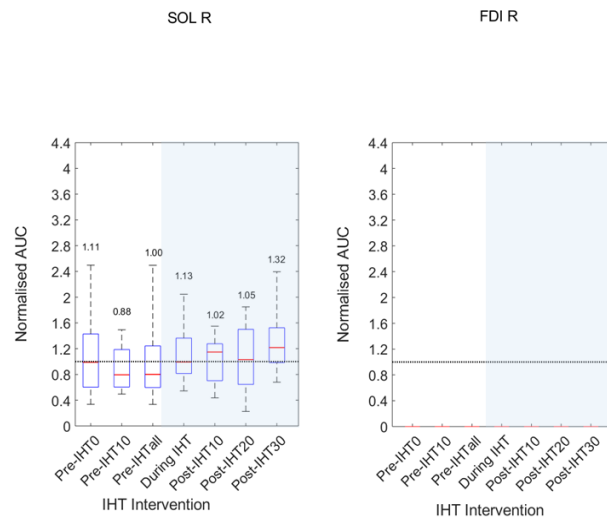
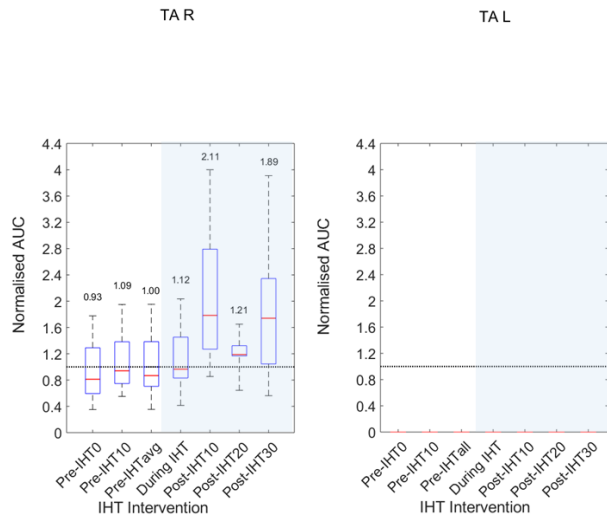


B)

Navigation error (%)	
Pre-IHT 0	20.4
Pre-IHT10	31.3
During IHT	23.0
Post-IHT10	33.7
Post-IHT20	30.5
Post-IHT30	33.6

IHT15

A)

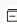


B)

Navigation error (%)	
Pre-IHT 0	10.9
Pre-IHT10	14.8
During IHT	10.8
Post-IHT10	12.0
Post-IHT20	2.9
Post-IHT30	26.9

Appendix.III. (Ethics Application)

1) Ethics Approval

Approval: **UEC17/29** Conway/Berry/Kahani: The influence of intermittent hypoxia training on sensory and motor pathways in healthy adults. 

Subject: Approval: **UEC17/29** Conway/Berry/Kahani: The influence of intermittent hypoxia training on sensory and motor pathways in healthy adults.

Dear Bernie

ETHICAL AND SPONSORSHIP APPROVAL
UEC17/29 Conway/Berry/Kahani: The influence of intermittent hypoxia training on sensory and motor pathways in healthy adults.

I can confirm that the University Ethics Committee (UEC) has approved this protocol and appropriate insurance cover and sponsorship have now also been confirmed.

I would remind you that the UEC must be informed of any changes you plan to make to the research project, so that it has the opportunity to consider them. Any change of staffing within the research team should be reported to UEC.

The UEC would also expect you to report back on the progress and outcome of your project, with an account of anything which may prompt ethical questions for any similar future project and with anything else that you feel the Committee should know.

Any adverse event that occurs during an investigation must be reported as quickly as possible to UEC and, within the required time frame, to any appropriate external agency.

The University agrees to act as sponsor of the above mentioned project subject to the following conditions:

1. That the project obtains/has and continues to have University/Departmental Ethics Committee approval.
2. That the project is carried out according to the project protocol.
3. That the project continues to be covered by the University's insurance cover.
4. That the Director of Research and Knowledge Exchange Services is immediately notified of any change to the project protocol or circumstances which may affect the University's risk assessment of the project.
5. That the project starts within 12 months of the date of this letter.

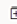
As sponsor of the project the University has responsibilities under the Scottish Executive's Research Governance Framework for Health and Community Care. You should ensure you are aware of those responsibilities and that the project is carried out according to the Research Governance Framework.


On behalf of the Committee, I wish you success with this project.







Kind regards
Angelique

Angelique Laverty
Research & Knowledge Exchange Services (RKES)

2) Amendment Approval

Amendment Approval: **UEC17/29** Conway/berry/Kahani; The influence of intermittent hypoxia training on sensory and motor pathways in healthy adults 

 Agioula Toli
Thank you very much Angelique for the quick response Best wishes, Yuly Tue 26/11/2019 16:07

 Ethics
Tue 26/11/2019 15:34     

To: Agioula Toli
Cc: Bernard Conway; Danial Kahani; Ethics
Dear Agioula

I can confirm that the University Ethics Committee has approved the **amendment** to this protocol and appropriate insurance cover and sponsorship are confirmed.

I remind you that the Committee must be informed of any changes that are made to the research project, so that they have the opportunity to consider them. The Committee also expects you to report back on the progress and outcome of your project, with an account of anything which may prompt ethical questions for any similar future project and with anything else that you feel the Committee should know.

The University agrees to act as sponsor of the above mentioned project subject to the following conditions:

1. That the project obtains/has and continues to have University/Departmental Ethics Committee approval.
2. That the project is carried out according to the project protocol.
3. That the project continues to be covered by the University's insurance cover.
4. That the Director of Research and Knowledge Exchange Services is immediately notified of any change to the project protocol or circumstances which may affect the University's risk assessment of the project.
5. That the project starts within 12 months of the date of this letter.

As sponsor of the project the University has responsibilities under the Scottish Executive's Research Governance Framework for Health and Community Care. You should ensure you are aware of those responsibilities and that the project is carried out according to the Research Governance Framework.

On behalf of the Committee, I wish you success with this project.
Kind regards
Angelique

Appendix. IV. (Participant Information Sheet and Consent form)

Participant Information Sheet

Name of department: Department of Biomedical Engineering

Title of the study: The influence of intermittent hypoxia training on sensory and motor pathways in healthy adults

Introduction.

We are a group of researchers at University of Strathclyde interested in central nervous system function and restoration after injury or disease. This particular project is led by Prof Bernard Conway who is a research scientist working in the Department of Biomedical Engineering. The work is supported by the following staff, Dr Danial Kahani and Dr Rothwelle Tate and the work will be performed by postgraduate research student Ms Agioula Anna Toli (agioula.toli@strath.ac.uk). All staff are trained in the research procedures this study will use.

The purpose of this information sheet is to invite you to take part in our research study and inform you on what that might entail.

Before you decide, we would like you to understand why the research is being done and what it would involve for you. Ms Toli will, together with a staff member, go through the information sheet with you and answer any questions you have. Talk to others about the study if you wish. Ask us if there is anything that is not clear.

What is Intermittent Hypoxia Training?

Intermittent Hypoxia Training is a method commonly used by elite athletes to simulate training at high altitudes. It is essentially a method where the oxygen content of the air you breathe is reduced and a machine switches between air with normal and low oxygen content every minute for 30 minutes. The low oxygen level you will be exposed to are set to be equivalent to breathing air at 19,000 feet (5800m).

What is the purpose of this investigation?

A growing body of evidence supports the idea that short periods of breathing low oxygen similar to that experienced during high altitude training can cause changes in central nervous system function (neuroplasticity) that are cumulative over time. Low oxygen or high altitude training has been popular with elite athletes for many decades but only now is this approach to training being considered as helpful for recovery from brain or spinal cord damage. The literature suggests that a method known as Intermittent Hypoxia Training (IHT) may therefore promote recovery of sensory function and movement when incorporated into intensive rehabilitation of patients with motor or sensory disability. It is believed that IHT has the potential to stimulate neuroplasticity by switching on genes that help form new connections within the nervous system and it is the ability of our nervous system to do this that allows us to learn new motor skills or recover those compromised by disease or injury.

In this study we would like to find out whether a single session of IHT can induce changes in sensory and/or motor pathways in the central nervous system of healthy individuals. We are also interested to observe if IHT leads to any changes in muscle function. The aim of these experiments is to understand whether IHT effects are central and/or peripheral.

We are also interested in learning if gene variations might contribute to any effects we observe. The results of this work will provide us with valuable data on what parts of the central nervous system IHT affects and this, together with any insight into role different gene variants make to this process will allow us to design research studies that will explore how to deliver and assess rehabilitation programmes that incorporated IHT for patients with stroke or spinal cord injury.

In most studies of the type we are undertaking it is common to observe marked variation in how individuals respond. Traditionally one of the ways to address this variability is to recruit large numbers of subjects. Recent research looking at how brains create new connections suggests that some of the variability between individuals may relate to which forms of particular genes they possess. The types of gene we are interested in are those that help your body repair and promote new nerve cell connections. An example is a gene linked to the production of a compound called brain derived neurotrophic factor (BDNF). BDNF is a protein that provides a chemical message that enables these connections to become established during activity. The gene that is linked to the production of this protein can exist in different forms in different people. Accordingly, we are interested to know if our subjects carry different forms of this type of gene and others involved in neural repair and connection formation as this will help us understand why one person's data can dramatically differ from another.

University ethical approval has been granted for this study.

Do you have to take part?

Whether you take part or not is entirely your own decision and is voluntary.

If you do decide to take part but later change your mind or withdraw part way through the study this is entirely up to you and this decision will not have any negative consequences for you, your work or study here. We would like to recruit 50 participants.

This study will investigate the effects of 30 minutes of IHT. IHT is delivered via a face mask that you breath from. The face mask is connected to a machine that will control the level of O₂ in the air you breath. During IHT you will breath an oxygen level that is comparable to being at very high altitude. This will make you breath more deeply and faster. After the 30 minutes are over you will breath normal room air again. We will monitor how you respond to the IHT by measuring your blood pressure, level of O₂ in your blood, your breathing rate and electrocardiogram. These physiological measurements are made to ensure that you remain safe and well during the IHT session.

To understand how IHT affects sensory and motor function we will use simple tests of your central nervous system before, during and after IHT. These tests use specialised equipment that allows us to test your motor and sensory pathways. The tests are safe and pain free. To test your sensory pathways small electrical stimuli that excite the nerves supplying your skin are stimulated and this results in a signal being generated in your brain. We can detect this signal via small recording electrodes placed on your head. This recording technique is known as electroencephalography and the sensory test is known as the Somatosensory Evoked Potential (SEP). To test the motor system we do something similar, but here we use a device to stimulate the areas of your brain that command your muscles to move. This is a technique known as transcranial magnetic stimulation (TMS) and this is also a pain free procedure. The response to TMS is a small twitch in your muscles and we can record this using electrodes similar to those previously described but which are placed on the skin lying over muscles of the lower leg. Changes in the signals we record before, during and after IHT will tell us a lot about how IHT affects the important sensory and motor pathways of the central nervous system.

To understand whether IHT directly affects how much force muscle produces we will undertake a simple safe test to measure muscle force output before, during and after IHT. This procedure uses short pulses of electricity on the skin surface that will cause your muscle to contract. This procedure may cause a slight discomfort as we will use electrical stimulation on the leg which may excite the small nerves that respond to painful events. If you find the stimulation causes discomfort, we will not continue with the test. For this experiment your lower leg needs to be uncovered. Accordingly, you will be asked to bring a pair of shorts on the day of the session or use suitable clothing that we have available. You will be asked to sit comfortably with your

foot placed on a foot rest. Following stimulation, the force generated by the contracting muscle will be measured using sensors built into the foot rest your foot will rest upon.

What will you do in the project?

If you decide to take part in the study and after providing us with your fully informed consent, you will attend for an initial familiarisation session where you will be required to complete an activity and health questionnaire and will be familiarised with the study protocols. We will also ask you to participate in a hypoxia tolerance test and take a swab of your cheek saliva (about 10--15 min). This initial session will last no longer than one hour (Visit 1).

To complete the study, you will be asked to attend our lab on a further 3 occasions (Visits 2,3 and 4). These sessions are longer and will require approximately 2 hours of your time.

Test sessions for Visits 2,3 and 4 will be a minimum of 7 days apart and you will be asked to refrain from any form of heavy, intensive or unaccustomed exercise in the days prior to testing and will be asked to avoid consuming any food or caffeinated beverages within the preceding two hours of the test beginning. During Visit 2 we will test SEPs, during Visit 3 we will test TMS and during Visit 4 we will test FES. Unfortunately, we are not able to provide payments for your time or reimburse any expenses you may have incurred using public transport or your own car.

You may withdraw from the study at any time if you wish.

A summary of what will happen in each of the 4 visits follows from here.

We also request that you do remove any clear or coloured nail varnish before participating in the experiments as nail varnish affects our ability to non-invasively measure the amount of oxygen in your blood by a technique known as pulse oximetry. Furthermore, for Visit 4 we will request that you bring a pair of shorts you can change to as we will require to place stimulating electrodes near the knee area.

Visit 1: Hypoxia Tolerance Test and health questionnaire.

During the first visit we will show you the various tests you will be required to undertake. At the time of the first visit we will also ask you to take a hypoxia tolerance test. This test lets us check that IHT will not make you feel unwell. On satisfactory completion of the hypoxia tolerance test we will also ask you to complete an activity and health questionnaire.

At the end of Visit 1 we will identify three dates (a week apart) when you are free to come to the lab and complete the SEP, TMS and FES testing.

Visit 2 SEP testing

This test involves the following procedures and we estimate that it will take approximately two hours of your time

- 1) Monitoring your ECG, blood O₂ levels, breathing rate and blood pressure throughout the investigation
- 2) Measuring the SEP before IHT.
- 3) Participation in a 30 minute IHT session where O₂ levels are reduced to 50% of normal air values.
- 4) Measuring heart rate and saturation of oxygen in the blood during IHT
- 5) Measuring the SEP at intervals over a 60-minute period following IHT

Visit 3 TMS testing

This test involves the following procedures and we estimate that it will take approximately two hours of your time

- 1) Monitoring your ECG, blood O₂ levels, breathing rate and blood pressure throughout the investigation
- 2) Measuring the response to TMS before IHT.
- 3) Participation in a 30 minute IHT session where O₂ levels are reduced to 50% of normal air values.
- 4) Measuring heart rate and saturation of oxygen in the blood during IHT
- 5) Measuring the response to TMS at intervals over a 30-minute period following IHT

Visit 4 FES testing

This test involves the following procedures and we estimate that it will take approximately two hours of your time

- 1) Monitoring your ECG, blood O₂ levels, breathing rate and blood pressure throughout the investigation
- 2) Measuring FES before IHT
- 3) Participation in a 30 minute IHT session where O₂ levels are reduced to 50% of normal air values.
- 4) Measuring heart rate and saturation of oxygen in the blood during IHT
- 5) Measuring the response to FES at intervals over a 30-minute period following IHT

Why have you been invited to take part?

You have been invited because you are a normally healthy adult with a BMI of under 30 and aged between 18—60. You are definitely not pregnant and have no history of respiratory, cardiovascular, epilepsy, neurological condition, neuromuscular damage, implanted metallic device or plate in the spine or lower limbs, current health problems or illness.

What are the potential risks to you in taking part?

The IHT procedure is considered safe as are the various tests we will perform that measure sensory and motor function and together your participation in this study poses very little risk to your wellbeing. There are some potential risks, including:

- Poor tolerance to hypoxia resulting in a sense of breathlessness and palpitations. If high levels of breathlessness are encountered IHT will be stopped and the investigation ended. This is not expected to happen in people of moderate health.
- A tingling sensation at the site where we use electrical pulses to generate SEP responses. If this is perceived as painful the intensity will be reduced to comfortable levels.
- Rarely, slight redness under the stimulating or recording electrodes. This is temporary and recovers very quickly after stimulation.
- Transient headache following repeated TMS. Here, the number of pulses and frequency of stimulation will be kept to a minimum.
- The activation of facial muscles by TMS. This may cause some discomfort, but similarly as above, the number of pulses and frequency of stimulation will be kept to a minimum.
- Stimulating the skin surface lying over nerves can cause temporary discomfort and if the stimulation is perceived as painful the intensity will be reduced.

You should not take part if any of the following apply.

These are our exclusion criteria for this study.

- Age below 18 or over 60
- BMI over 30
- Any history of epilepsy,
- Any neurological condition affecting movement or mood
- Any history of head or brain injury
- Any previous brain operation or treatment for aneurysm
- Any history of migraine or debilitating headaches.
- Any recent musculoskeletal injury or disease,
- Any recent tendon or ligament injury to the knee or ankle
- Any implanted metallic device or plate in the spine, head or lower limbs.
- Any implanted medical device
- Any current respiratory illness or injury
- Currently or recently completed a course of antibiotic medication
- Any history of heart or cardiovascular disease
- Any history of hypertension or its treatment
- Prescription of any medication for a blood, heart or respiratory disorder
- Any history of asthma
- Currently experiencing hay fever or similar allergy
- Currently taking prescribed or non-prescribed anti-hayfever medication
- Any skin condition or disease
- Possible, suspected or confirmed pregnancy
- Poor exercise tolerance
- Knowledge of becoming breathless during flying
- Current health problems or illness, as revealed by a health questionnaire completed on Visit 1.

What happens to the information in the project?

We will use a unique code for each individual who participates in the study so all the information you provide and the results of the test, will be kept pseudo-anonymous. We will ask you for information regarding your age, health and activity levels. We may also record electrode position on the skin by digital camera. This information will be stored in a locked cabinet in the department of Biomedical Engineering. Test data files will be initially stored on a password protected laboratory laptop and backed up to a secure archive housed on the University's Strathcloud server.

The University of Strathclyde is registered with the Information Commissioner's Office who implements the Data Protection Act 1998. All personal data on participants will be processed in accordance with the provisions of the Data Protection Act 1998.

Thank you for reading this information – please ask any questions if you are unsure about what is written here.

What happens next?

If you are interested in participating in the study please contact either

Yuly Toli: agioula.toli@strath.ac.uk

or

Dr Danial Kahani: danial.kahani@strath.ac.uk

and we will arrange a suitable time for you to come for a familiarisation appointment at the University as well as answer any questions you may have. If you have decided not to participate we would like to thank you for reading this information sheet and considering our research.

When we have finished collecting all the information we will analyse the results and send each participant a short summary of what we have found and will let colleagues from other universities know about our results during scientific conferences, the details of which may be published in scientific journals.

Researcher contact details:

- Agioula Anna Toli or Dr Danial Kahani, Department of Biomedical Engineering, Graham Hills, 16 Scotland Rd, Richmond St, Glasgow, G1 1XQ. Email: danial.kahani@strath.ac.uk
- Dr Rothwelle Tate, Strathclyde Institute of Pharmacy and Biomedical Science, Hamnett Wing John Arbuthnott Building, 161 Cathedral St, Glasgow G4 0RE. E-mail: r.j.tate@strath.ac.uk

Chief Investigator details:

Professor Bernard Conway, Agioula Anna Toli. E-mail: b.a.conway@strath.ac.uk

This investigation was granted ethical approval by the University of Strathclyde Ethics Committee. If you have any questions/concerns, during or after the investigation, or wish to contact an independent person to whom any questions may be directed or further information may be sought from, please contact:

Secretary to the University Ethics Committee
Research & Knowledge Exchange Services
University of Strathclyde
Graham Hills Building
50 George Street Glasgow, G1 1QE. Telephone: 0141 548 3707 Email:
ethics@strath.ac.uk

Consent Form

Name of department: Biomedical Engineering

Title of the study: The influence of intermittent hypoxia training on sensory and motor pathways in healthy adults.

- I confirm that I have read and understood the information sheet for the above project and the researcher has answered any queries to my satisfaction.
- I consent to being a participant in the project
- I consent to being photographed in order to have electrode positions recorded.
- I understand that my participation is voluntary and that I am free to withdraw from the project at any time, without having to give a reason and without any consequences
- I understand that I can withdraw my data from the study at any time before it becomes pseudo-anonymous.
- I understand that any information recorded in the investigation will remain confidential and no information that identifies me will be made publicly available.

Intermittent Hypoxia Training Study

(PRINT NAME)	
Signature of Participant:	Date:

Appendix.V. (Hashemirad et al. 2017 Figure)

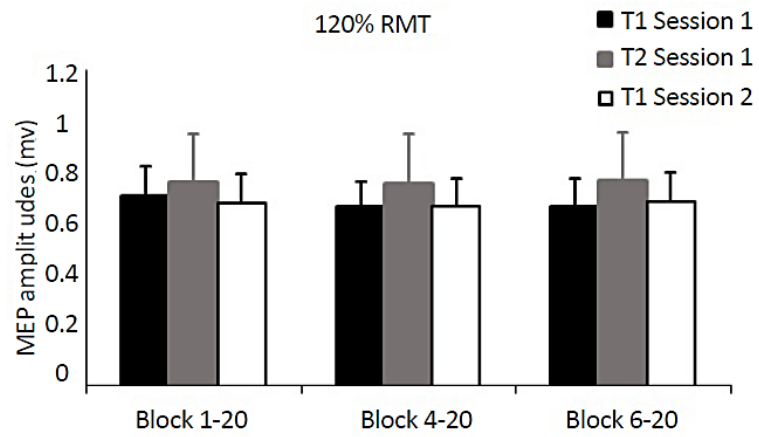


Figure.1. MEP amplitude in block 1(stimulation 1 to 20), block 2 (stimulations 5 to 20) and block 3 (stimulations 6 to 20). T1, T2 and T3 refers to 3 time points were 20 MEPs were recorded.